Design, synthesis and evaluation of quinazolinone analogues as monoamine oxidase inhibitors

MA Qhobosheane

orcid.org 0000-0003-3005-0028

Dissertation submitted in partial fulfilment of the requirements for the degree Magister of Science in Pharmaceutical Chemistry at the North-West University

Promoter:	Prof LJ Legoabe
Co-promoter:	Prof JP Petzer
Assistant promoter:	Prof A Petzer

Graduation May 2018

Student number: 27836576

This work is based on the research supported by National Research Foundation of South Africa (Grant specific unique reference numbers (UID) 96135). The Grant holders acknowledge that opinions, findings and conclusions or recommendations expressed in any publication generated by the NRF supported research are that of the authors, and that the NRF accepts no liability whatsoever in this regard.

PREFACE

This dissertation is submitted in an article format in accordance with the General Academic Rules (A.13.7.3) of the North-West University. This dissertation includes two articles which were compiled for submission to Bioorganic & Medicinal Chemistry. The author guidelines have been included (Appendix C). All scientific research (synthesis, biology and documentation of the dissertation and articles) for the purpose of this dissertation was conducted by Miss M.A. Qhobosheane at the North-West University, Potchefstroom campus.

ACKNOWLEDGEMENTS

First and foremost I would like to thank the Almighty God for granting me the strength and courage to finish this dissertation.

I would like to express my sincere appreciation to the following people for all the support they showed me throughout the course of my study:

- My supervisor Prof L.J. Legoabe for your constant encouragement, guidance and patience. Words cannot describe how grateful I am to have had you as my mentor. It was a great honour to be in your group.
- My co-supervisor Prof J.P. Petzer for your expertise.
- My assistant supervisor Prof A. Petzer for your advice and assistance with the biological studies.
- All Pharmaceutical Chemistry personnel for your co-operation and creating a friendly and enabling environment.
- My mother Maagatha, my brother Nkeeane and my sister Mabohlokoa Qhobosheane for your constant love, support and encouragement.
- My best friend Teboho Khofu for your love and support in difficult times during my study.
- All my friends and family for your love and support.
- Reformed Church Potchefstroom, die Bult bible study group for your spiritual support and constant encouragement.

I would also like to thank the following institutions for their assistance during this study:

- The North-West University for granting me an opportunity to study at this institution and for the financial support.
- Dr J. Jordaan and Mr A. Joubert of the SASOL Centre for Chemistry for your help with NMR and MS analyses.
- Prof Jan du Preez for your help with the HPLC analyses.

"No discipline seems pleasant at the time, but painful. Later on, however, it produces a harvest of righteousness and peace for those who have been trained by it"

Hebrews 12:11

ABSTRACT

Parkinson's disease (PD) is the second most common neurodegenerative disease after Alzheimer's disease, and it is estimated to affect approximately 1% of the population over the age of 65. PD is characterised by non-motor and motor symptoms such as resting tremor, bradykinesia and muscle rigidity, which are a result of neuronal dopamine deficiency due to the progressive loss of the dopaminergic pathway that leads from the substantia nigra pars compacta (SNpc) to the striatum. Non-motor symptoms of PD include sleep disturbances, depression and anxiety.

There is presently no cure for PD, and the present treatment can neither reverse nor stop the disease progression. However, PD can be treated symptomatically with a variety of therapies which include L-dopa, dopamine agonists, aromatic L-amino acid decarboxylase (AADC) inhibitors, catechol-O-methyltransferase (COMT) inhibitors and monoamine oxidase (MAO) B inhibitors. L-dopa has been the mainstay of PD treatment for over 30 years, and it remains the most effective treatment to date. However, L-dopa should be combined with a peripheral AADC inhibitor to ensure its neuronal bioavailability and to avoid its peripheral side-effects. MAO-B inhibitors have also been found effective in PD treatment because they enhance brain dopamine levels in PD, and thus alleviate the symptoms.

The MAO-A and MAO-B enzymes are mitochondrial outer membrane-bound flavoproteins that catalyse the oxidative deamination of monoamine neurotransmitters dopamine, norepinephrine and epinephrine. The MAOs are differently distributed in the body, with MAO-A dominating in the intestines, heart and placenta, while MAO-B dominates in the brain, glial cells in the brain and liver. Oxidation of dopamine by MAO generates hydrogen peroxide and aldehyde derivatives, by-products which are potentially neurotoxic. MAO-B inhibitors increase brain dopamine levels and also reduce levels of hydrogen peroxide and aldehyde derivatives in the brain, and therefore are neuroprotective in this respect. MAO-A inhibitors are used clinically in treatment of depression, while MAO-B inhibitors are used as therapy for PD. Selective and reversible MAO inhibitors are more clinically acceptable because they do not cause the side-effects that are associated with irreversible and non-selective MAO inhibition.

The aim of the present study was to explore 4(3*H*)-quinazolinone as a scaffold for design of potent and selective MAO-B inhibitors.

The MAO inhibitory potential of quinazolinones has been illustrated in several studies. A study conducted by Bahadur (1982) revealed that quinazolinones can inhibit MAO activity by as much as 80%. In their study, Bahadur (1982) discovered that the increase or decrease in MAO inhibitory activity of quinazolinones depends on the type of substituent, as well as the position at which it is attached. This is in agreement with similar studies carried out by Rastogi *et al.* (1972)

and Lata *et al.* (1982). A number of studies have been conducted to evaluate quinazolinones as potential MAO inhibitors, but none have been done to study the structure-activity relationships (SARs) with respect to thiobenzyl and benzyloxy substitution. This study expanded on the SARs of MAO inhibition by quinazolinone derivatives to enable the design of novel potent MAO inhibitors of this chemical class. Particular attention was given to the benzyloxy and thiobenzyl derivatives of 4(3*H*)-quinazolinone.

Chemistry: Two series of compounds were synthesised and evaluated as potential MAO inhibitors. The thioether (14 compounds), C6 mono- (12 compounds) and N3/C6 disubstituted (9 compounds) derivatives of 4(3*H*)-quinazolinone were synthesised using standard chemical procedures. The reactants were suspended in either ethanol or N,N-dimethylformamide (DMF) in the presence of a base. The products were precipitated with ice-cold water and were subsequently dried or recrystallised from appropriate solvents. The structures and purities were confirmed by NMR, MS and HPLC.

MAO inhibition studies: To determine the 50% inhibitory concentration (IC_{50}) values and selectivity index (SI), a fluorometric assay was carried out employing recombinant human MAO-A and MAO-B as enzyme sources, and kynuramine as substrate. The first series consisted of 14 compounds, 12 of which exhibited good MAO-B inhibition properties, with IC_{50} values in the micromolar to sub-micromolar range. The most potent compound in this series (**3k**) exhibited an IC_{50} value of 0.142 μM. Interesting trends were observed through the SAR analyses of the compounds in this series. For example, *meta*-halogen substitution of the thioether derivatives dramatically increased the inhibitor potencies. A number of derivatives (5 of 21) in the second series showed selective inhibition of MAO-B. The disubstituted compounds **2b** and **2h** are notable as the most potent inhibitors in this series with IC_{50} values of 0.685 μM and 0.847 μM, respectively. However, meaningful SARs for MAO inhibition could not be derived because most compounds in this series did not inhibit the MAOs.

The 4(3*H*)-quinazolinone derivatives were successfully synthesised in this study, and it may be concluded that they are potent and selective MAO-B inhibitors, thus promising leads for the future design of PD therapies.

Keywords: Parkinson’s disease, monoamine oxidase, quinazolinone

TABLE OF CONTENTS

LIST OF TABLES

LIST OF FIGURES

List of abbreviations

5-HIAA	5-Hydroxyindole acetic acid
5-HT	Serotonin
6-OHDA	6-Hydroxydopamine
AADC	Aromatic L-amino acid decarboxylase
ACh	Acetylcholine
ADH	Alcohol dehydrogenase
ALDH	Aldehyde dehydrogenase
APCI	Atmospheric pressure chemical ionisation
ATP	Adenosine triphosphate
BBB	Blood-brain barrier
BDNF	Brain-derived neurotrophic factor
BH_4	Tetrahydrobiopterin
ChE	Cholinesterase
CNS	Central nervous system
COMT	Catechol-O-methyl transferase
COX	Cyclooxygenase
CSC	(*E*)-8-(Chlorostyryl)caffeine
CSF	Cerebrospinal fluid
DA	Dopamine
DARPP	Dopamine- and cAMP- regulated phosphoprotein
DAT	Dopamine transporter
DATATOP	Tocopherol and deprenyl antioxidative therapy of parkinsonism
DMD	Dimethylformamide
DMSO	Dimethyl sulfoxide
DNA	Deoxyribonucleic acid
DOPAC	3,4-Dihydroxyphenylacetic acid
DOPAL	3,4-Dihydroxyphenylacetaldehyde
DOPET	3,4-Dihydroxyphenylethanol
FAD	Flavin adenine dinucleotide
GABA	γ-Aminobutyric acid
GAPDH	Glyceraldehyde-3-phospjate dehydrogenase
GBA	Glucocerebrocidase
GDNF	Glial-derived neurotrophic factor
GI	Gastrointestinal

GPO	Glutathione peroxidase
GSH	Glutathione
GTP	Guanosine triphosphate
GTPCH	GTP cyclohydrolate
H_2O_2	Hydrogen peroxide
HPLC	High performance liquid chromatography
HRMS	High resolution mass spectra
IC_{50}	50% inhibitory concentration
IL	Interleukin
JEV	Japanese encephalitis virus
JNK	c-Jun N-terminal kinase
LB	Lewi body
L-dopa	Levodopa
LRRK-2	Leucine rich repeat kinase-2
MAO	Monoamine oxidase
MAPK	Mitogen-activated protein kinase
MHz	Megahertz
mp	Melting point
$MPDP^+$	1-Methyl-4-phenyl-2,3-dihydropyridine
MPP^+	1-Methyl-4-phenylpyridinium
MPPP	1-Methyl-4-phenyl-4-propionoxipiperidine
MPTP	1-Methyl-4-phenyl-1,2,3,6-tetrahydropyridine
mRNA	Messenger ribonucleic acid
NADH	Nicotinamide adenine dinucleotide
NADPH	Nicotinamide adenine dinucleotide phosphate
NGF	Nerve growth factor
NMDA	N-Methyl-D-aspartate
NMR	Nuclear magnetic resonance
NO	Nitric oxide
NOS	Nitric oxide synthase
NSAIDs	Non-steroidal anti-inflammatory drugs
$ONOO^-$	Peroxynitrite
PD	Parkinson’s disease
PINK1	PTEN-induced putative kinase 1

PNS	Peripheral nervous system
PTEN	Phosphatase and tensin homologue
RNA	Ribonucleic acid
ROS	Reactive oxygen species
SARs	Structure-activity relationships
SD	Standard deviation
SI	Selectivity index
SNpc	Substantia nigra pars compacta
SOD	Superoxide dismutase
SSRIs	Selective serotonin reuptake inhibitors
$t_{1/2}$	Half-life
TB	Tuberculosis
TCAs	Tricyclic antidepressants
TH	Tyrosine hydroxylase
TLC	Thin layer chromatography
TNF	Tumour necrosis factor
UCH-L1	Ubiquitin carboxyl terminal hydrolase L1
VMAT2	Vesicular monoamine transporter 2
VTA	Ventral tegmental

Kinetics

EI	Enzyme-inhibitor complex
ES	Enzyme-substrate complex
I	Inhibitor
K_i	Inhibition constant
K_m	Michaelis constant
[S]	Substrate concentration
V_i	Initial velocity
V_{max}	Maximal velocity

CHAPTER 1
INTRODUCTION

1.1 Introduction

James Parkinson initially described Parkinson's disease (PD) as involuntary tremulous motion, with decreased muscle power at rest (Parkinson, 2002), which diminishes during voluntary activity (Rang *et al.*, 2007) and is accompanied by slowness of movement and impairment of postural balance with a tendency to bent the trunk forward and to pass from a walking to a running pace. The senses and intellect remain unharmed in PD (Parkinson, 2002). PD is a progressive disorder whose symptoms worsen with time (Roach & Scherer, 2004), and the symptoms usually begin on one side of the body and gradually spread to the other side (Fahn, 2003).

PD is the second most common age-related neurodegenerative disorder after Alzheimer's disease, and it affects approximately 1% of the population over the age of 65 (Gibrat *et al.*, 2009). According to Rang *et al.* (2007) this disease has no known underlying cause, but is the result of a deficiency of dopamine (DA) and an excess of acetylcholine (Ach) in the central nervous system (CNS) (Roach & Scherer, 2004). Today, PD is characterised by resting tremor which decreases with voluntary movement, increased resistance to passive movement of the limbs (rigidity), slowness of movement (bradykinesia), reduction in movement amplitude (hypokinesia) and absence of normal unconscious movements such as arm swing in walking (akinesia) (Dauer & Przedborski, 2003).

Pathologically, PD is characterised by the progressive loss of dopaminergic neurons projecting from the substantia nigra pars compacta (SNpc) to the striatal motor loci (Gibrat *et al.*, 2009). Cell loss in the locus ceruleus, dorsal nuclei of the vagus, raphe nuclei, nucleus basalis of the Meynert and some other catecholaminergic brain stem structures, including the ventral tegmental area, also exist (Lees *et al.*, 2009). According to Vila and Przedborski (2004), the presence of intraneuronal inclusions called Lewi bodies (LBs) is one of the hallmarks of PD. Susceptible genes such as α-synuclein, leucin rich repeat kinase 2 (LRRK-2) and glucocerebrocidase (GBA) have shown that genetic predisposition is another important causal factor (Lees *et al.*, 2009).

Age is the major risk factor for PD (Lees *et al.*, 2009). The mean age of onset is 55 years (Dauer & Przedborski, 2003), although 10% of people with the disease are younger than 45 years of age (Lees *et al.*, 2009). The incidence of PD increases significantly with age, from 200/100 000 overall to 200/10 000 at age 70, and it seems to decrease in the ninth decade of life (Dauer & Przedborski, 2003; Lees *et al.*, 2009). There is no apparent genetic cause in

about 95% of PD cases, but the disease is inherited in the remaining cases (Dauer & Przedborski, 2003).

1.2 Monoamine oxidase

Monoamine oxidase (MAO) is an enzyme that is found in all tissues and almost all cells of the body, bound to the outer mitochondrial membrane. Its active site contains flavin adenine dinucleotide (FAD), which is bound to the cysteine of a –Ser-Gly-Gly-Cys-Tyr– sequence (Prisinzano, 2006). MAO catalyses the oxidative deamination of catecholamines such as norepinephrine, epinephrine and DA, as well as the monoamines serotonin and histamine, to the corresponding aldehyde and free amine, with the generation of hydrogen peroxide (H_2O_2) (Youdim *et al.*, 2006).

MAO is not a single enzyme, but it exists in two forms, MAO-A and MAO-B (Youdim *et al.*, 2006). These isoforms are differently distributed in the body. MAO-B is found predominantly in the brain and platelets, whereas MAO-A is found predominantly in the intestinal tract. MAO-A and MAO-B differ in their substrate preferences, immunological properties, molecular weight and anatomical locations, and they are inhibited by different inhibitors (Victor & Waters, 2003).

During development, MAO-A appears before MAO-B, with the level of MAO-B increasing greatly in the brain after birth (Youdim *et al.*, 2006). The distribution of the two MAO isoforms also differs in the human brain; the highest MAO-A concentrations are in the catecholaminergic neurons of the locus ceruleus, whereas the highest MAO-B concentrations are in the serotonergic and histaminergic neurons of the raphe and posterior hypothalamus (Foley *et al.*, 2000; Youdim *et al.*, 2006). Foley *et al.* (2000) notes that there are high concentrations of both forms of the MAO enzyme in the human basal ganglia.

Youdim *et al.* (2006) indicates that MAO in peripheral tissues oxidise amines and prevent their entry into the systemic circulation, and thus serve as protective barriers. For example, MAO-B in the microvessels of the blood-brain barrier (BBB) metabolises amines thereby preventing their entry into the CNS (Youdim *et al.*, 2006; Legoabe *et al.*, 2012a). Another example of the protective effect of MAO is found with the “cheese reaction”. Tyramine, an indirectly acting sympathomimetic amine which is present in fermented foods, is metabolised by intestinal MAO-A. This reduces the amount of tyramine that enters the systemic circulation and prevents the tyramine induced release of norepinephrine from peripheral neurons known as the “cheese reaction” (Legoabe *et al.*, 2012a). In addition, intraneuronal MAO-A and MAO-B in the CNS and peripheral nervous system (PNS) protect neurons from

exogenous amines, terminate the actions of amine neurotransmitters, and regulate the contents of intracellular amine stores (Youdim *et al.*, 2006).

Oxidant stress may occur via the formation of H_2O_2 and oxygen derived free radicals in the MAO catalytic cycle (Fahn & Cohen, 1992). Because the substantia nigra is rich in DA, which can undergo both enzymatic oxidation via MAO and non-enzymatic autoxidation, H_2O_2 and oxyradicals are generated in the midbrain nucleus (Fahn & Cohen, 1992). Oxidant stress may cause loss of monoaminergic neurons in patients with PD. Neurotoxins that selectively destroy dopaminergic neurons in the nigra, such as 6-hydroxydopamine (6-OHDA) and 1-methyl-4-phenyl-1,2,3,6-tetrahydropyridine (MPTP) appear to act by generating oxidant stress (Fahn & Cohen, 1992).

MAO inhibition interrupts the metabolism of catecholamines leading to an increase in endogenous and exogenous substrates as well as trace amines (tyramine, tryptamine etc.). MAO inhibition thus increases the levels of biogenic amine neurotransmitters (Volz & Gleiter, 1998). MAO inhibitors are primarily used for the treatment of depression and neurological disorders such as PD (Volz & Gleiter, 1998). These inhibitors belong to the earliest drugs used in PD, and they have been used for many years alone or in combination with L-dopa, the metabolic precursor of DA (Riederer & Laux, 2011). However, earlier use of non-selective irreversible MAO inhibitors was terminated due to their ability to cause fatal drug-food interactions (e.g. the “cheese reaction”) (Kumar *et al.*, 2016; Schatzberg & Nemeroff, 2017). When MAO-A is inhibited in the PNS, tyramine enters the blood stream (Robakis & Fahn, 2015) and acts as a false neurotransmitter at nerve terminals, triggering the release of norepinephrine which results in hypertensive crisis.

It is worth noting that selective irreversible MAO inhibitors lose their selectivity at high concentrations (Foley *et al.*, 2000). For example, when given at high doses, selegiline, an irreversible selective MAO-B inhibitor, also inhibits MAO-A and potentiates the sympathomimetic action of tyramine (Youdim & Weinstock, 2004). The development of selective MAO inhibitors which are reversible in nature emerged in recent years (Schatzberg & Nemeroff, 2017). At normal doses, MAO-B inhibitors do not act on tyramine metabolism in the gut, while possessing the ability to increase striatal neuronal responses to DA. Therefore MAO-B inhibitors are useful in the treatment of PD (Robakis & Fahn, 2015). Selegiline was the first synthesised selective MAO-B inhibitor, and because of its inability to cause the cheese reaction (at normal doses), it has served as the benchmark against which new MAO-B inhibitors are measured (Foley *et al.*, 2000).

There is evidence that if MAO-B inhibitors are used in the very early stages of PD, they may delay the need to start L-dopa therapy (Youdim & Weinstock, 2004), and delay the onset of more severe disability (Rossiter *et al.*, 2012). Based on the clinical utility of MAO inhibitors, the discovery of new classes of MAO inhibitors is merited. The current study is focused on exploring the quinazolinone scaffold for the design and synthesis of potent reversible MAO inhibitors.

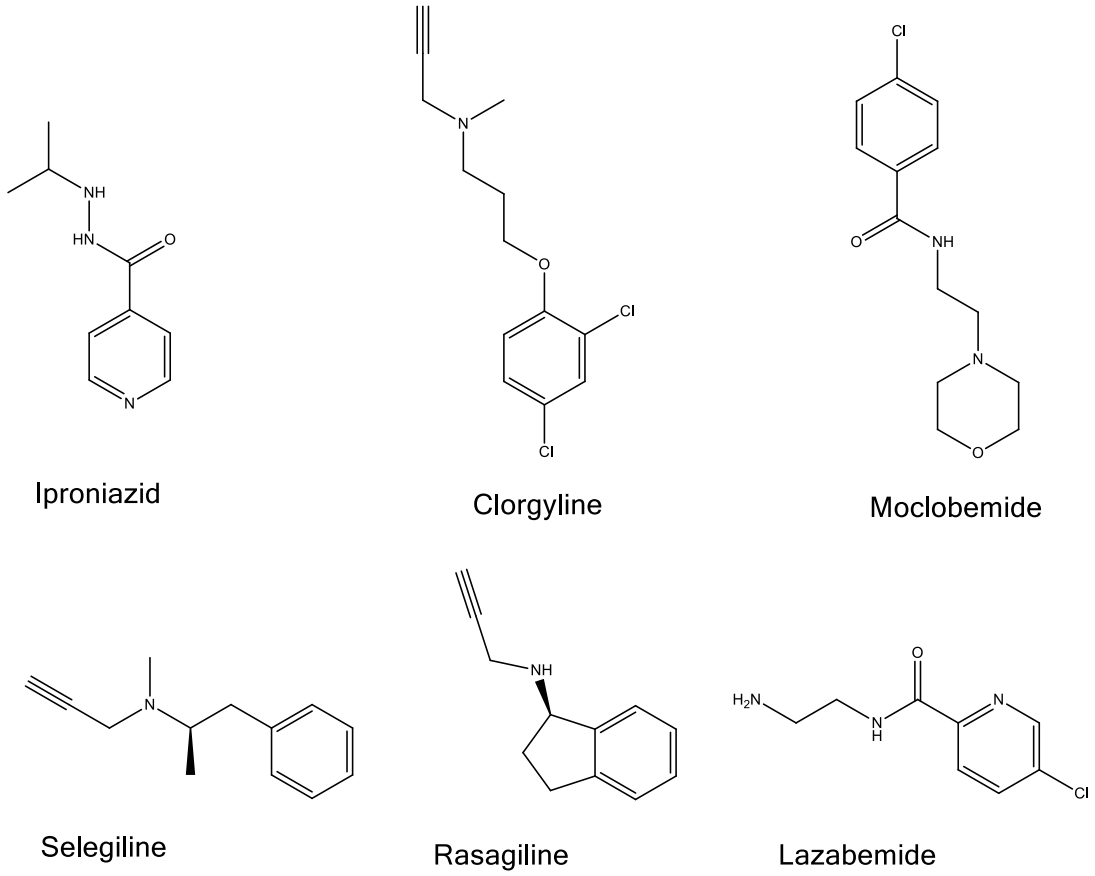

Figure 1.1: Some common MAO inhibitors used in the treatment of depression and Parkinson's disease.

1.3 Rationale

Quinazolinone is a class of fused heterocycles that are found in approximately 150 naturally occurring alkaloids isolated from a number of families of the plant kingdom. Quinazolinones are also found in microorganisms and animals (Arora *et al.*, 2011; Rajput & Mishra, 2012; Banu *et al.*, 2015). Due to their diverse range of biological properties, synthetic methods have been explored to develop quinazoline and quinazolinone derivatives (Khan *et al.*, 2016). The MAO inhibitory profiles of quinazolinones have previously been reported by various researchers (Lata *et al.*, 1982; Gökhan-Kelekçi *et al.*, 2009; Khattab *et al.*, 2015).

A study carried out by Khattab *et al.* (2015) revealed that selected amino acid derivatives of quinazolinones (compounds **1**, **2** and **3**) inhibit MAO competitively, with the majority of tested compounds exhibiting selectivity for MAO-A over MAO-B. Compounds with shorter linkers between the hydrophobic head and the terminal functional group displayed better inhibition activities. This observation was attributed to differing orientations of the inhibitors in the binding side and the formation of hydrogen bonds with the MAO-A backbone (Khattab *et al.*, 2015). A study conducted by Bahadur (1983) revealed that MAO inhibition potency increases when quinazolinones are substituted with a phenyl at position 2 and an optimum substituent at position 6 and/or position 8. The most potent inhibitors (compounds **4** and **5**) were substituted with a halogen on C6 and these compounds inhibited MAO to a level of more than 80%. This is in agreement with results reported by Rastogi *et al.* (1972), where the introduction of a halogen substituent on position 6 of the quinazolinone nucleus enhanced the inhibitor potency.

Lata *et al.* (1982) synthesised and screened 16 quinazolinone derivatives as MAO inhibitors and discovered that their potencies are dependent on the position of attachment of the substituent and on the type of substituent attached. In addition, Srivastava *et al.* (1980) reported that the potency of MAO inhibition increases when quinazolinones are substituted with halogens on the C6 and C8 positions of the quinazolinone backbone. In summary, the above discussions show that attachment of suitable substituents on the appropriate positions of the quinazolinone moiety is a prerequisite for the development of potent MAO inhibitors of this class.

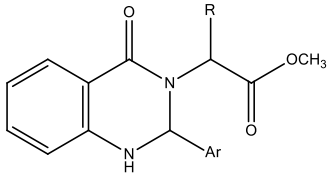

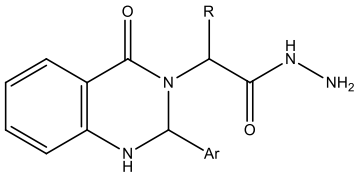

1, R = H, Ar = 4-Cl-C_6H_4

3, R = H, Ar = 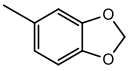

2, R = CH_3, Ar = 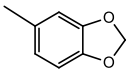

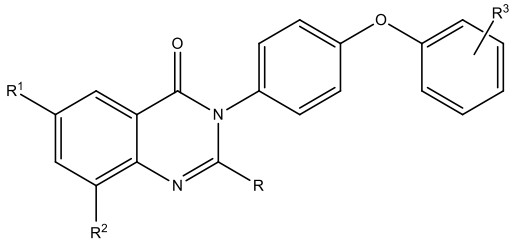

4, R = C_6H_5, R^1 = Br, R^2 = H, R^3 = H

5, R = C_6H_5, R^1 = Br, R^2 = H, R^3 =4-F

Figure 1.2: Quinazolinone derivatives found to actively inhibit MAO in previous studies (Bahadur, 1983; Khattab *et al.*, 2015).

Based on these discussions, this study will examine the MAO inhibitory properties of a series of 4(3*H*)-quinazolinone derivatives. A total of 35 compounds will be synthesised, with the first series comprising of fourteen different thioether derivatives (**3a**-**m**) of 4(3*H*)-quinazolinone, and the second series consisting of twelve C6 mono- (**1a**-**l**) and nine N3/C6 di-substituted (**2a**-**i**) derivatives of 4(3*H*)-quinazolinone.

1.4 Hypothesis of this study

As discussed above, the MAO inhibitory activity of the quinazolinone scaffold has been reported in a number of studies. However, the effect of benzyloxy and thiobenzyl substitution of the quinazolinone moiety has not yet been explored. Based on the observation that benzyloxy substitution enhances the MAO-B inhibition potency and selectivity of heterocyclic compounds (Legoabe *et al.*, 2012a; Legoabe *et al.*, 2012b), we predict that benzyloxy substituted 4(3*H*)-quinazolinones will exhibit similar properties. A previous study carried out on a structurally similar bicyclic scaffold, coumarin, reported that thiobenzyl substitution of the coumarin backbone markedly increases affinity and selectivity for the MAO-B isoenzyme (Catto *et al.*, 2006). We envisage that a similar trend will be observed in thioether-containing 4(3*H*)-quinazolinone derivatives. It is also hypothesised that further substitution of the phenyl

ring with halogen (F, Cl, Br, I) and alkyl (CN, CF_3) substituents will significantly enhance the inhibition potency of the quinazolinone derivatives.

1.5 Objectives of this study

The main aim of this study is to explore 4(3*H*)-quinazolinone as a scaffold for design of potent and selective MAO-B inhibitors.

The primary objectives of this study are;

- To design, synthesise and characterise novel quinazolinone derivatives.
- To evaluate the synthesised compounds as recombinant human MAO-A and MAO-B inhibitors by determination of the IC_{50} values.
- To determine the reversibility of inhibition by the selected active compounds. The recovery of the enzymatic activity after dialysis of enzyme-inhibitor complexes will be evaluated.
- To determine if a selected inhibitor's mode of inhibition is competitive or non-competitive.
- To determine the structure-activity relationships of the synthesised compounds as inhibitors of the MAO enzymes.

Table 1.1: Proposed compounds to be synthesised in this study

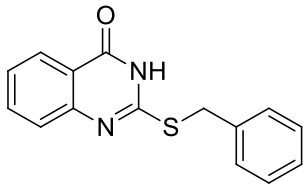 **3a**	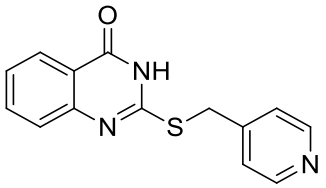 **3b**	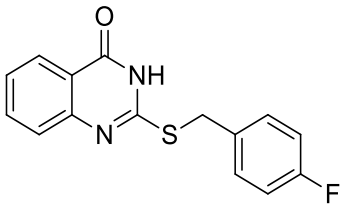 **3c**
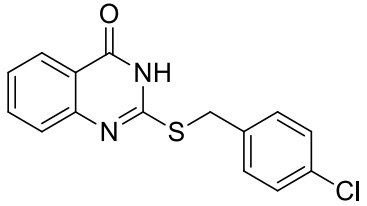 **3d**	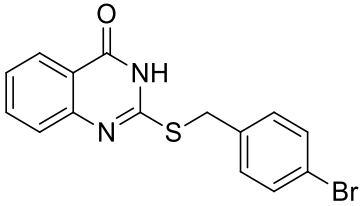 **3e**	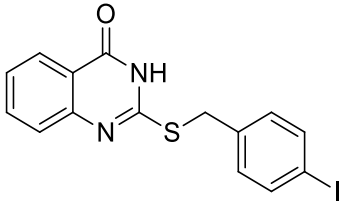 **3f**
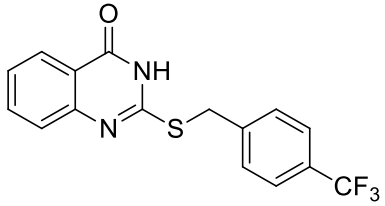 **3g**	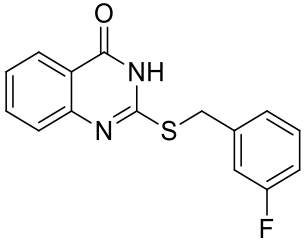 **3h**	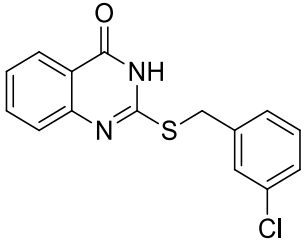 **3i**
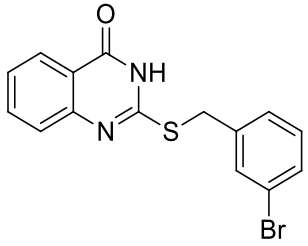 **3j**	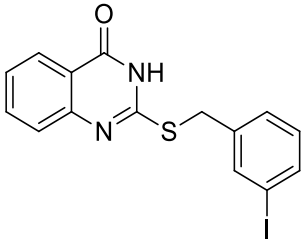 **3k**	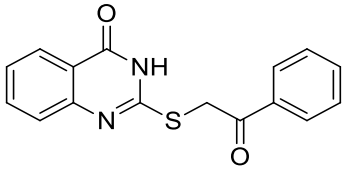 **3l**

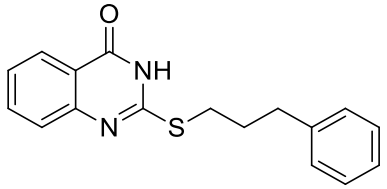 **3m**	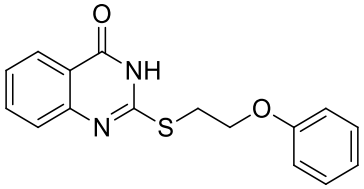 **3n**	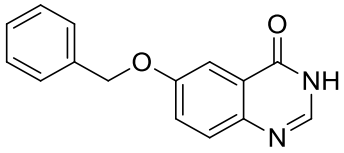 **1a**
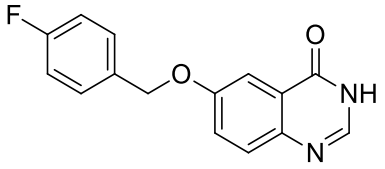 **1b**	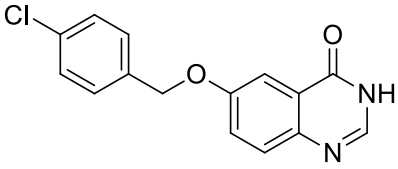 **1c**	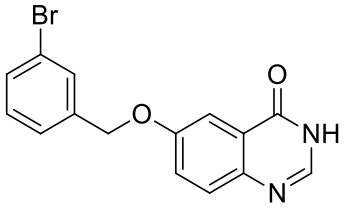 **1d**
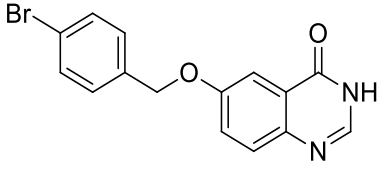 **1e**	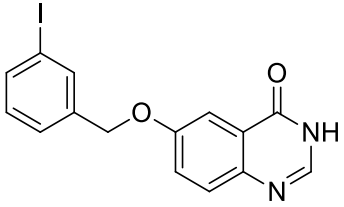 **1f**	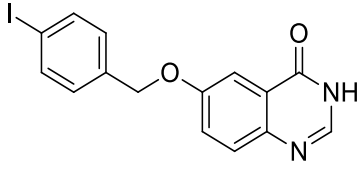 **1g**
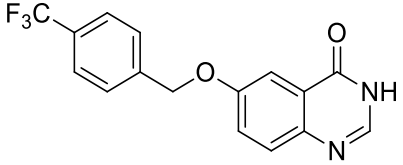 **1h**	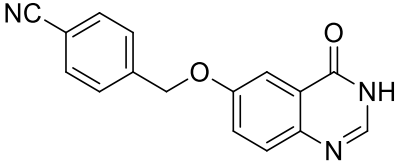 **1i**	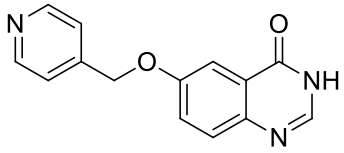 **1j**
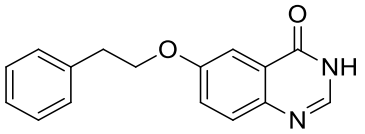 **1k**	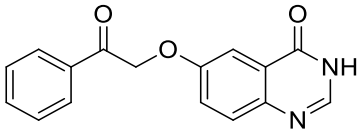 **1l**	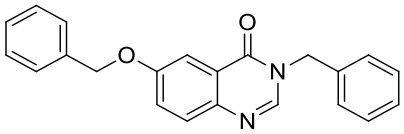 **2a**

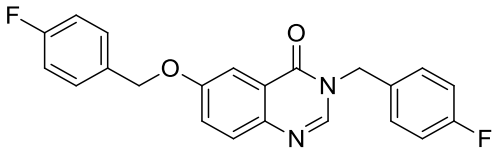 **2b**	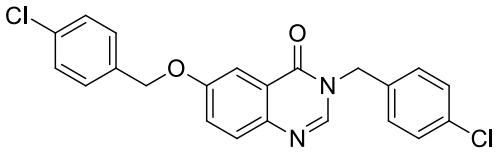 **2c**	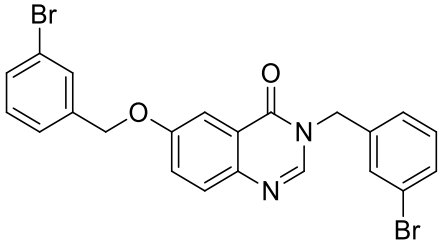 **2d**
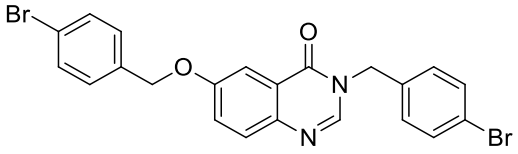 **2e**	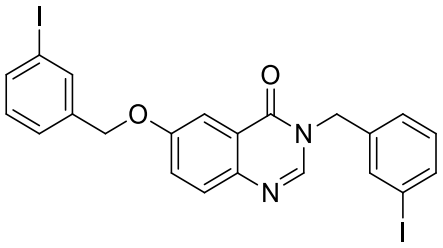 **2f**	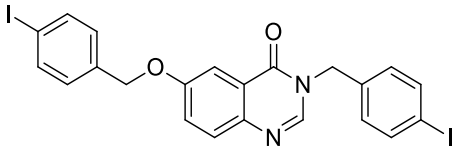 **2g**
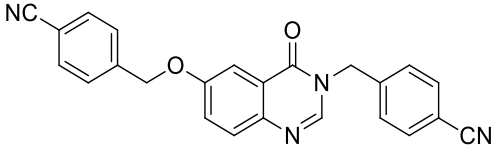 **2h**	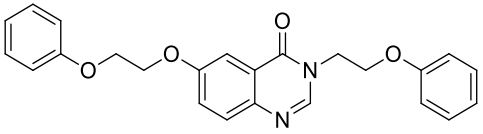 **2i**	

REFERENCES

Arora, R., Kapoor, A., Gill, N. & Rana, A. 2011. Quinazolinone: an overview. *International research journal of pharmacy*, 2:21-28.

Bahadur, S. 1983. Syntheses and biological activities of some new 4 (3*H*)-quinazolinones. *Archiv der pharmazie*, 316(11):964-968.

Banu, H.B., Prasad, K.V.S.R. & Bharathi, K. 2015. Biological importance of quinazolin-4-one scaffold and its derivatives- a brief update. *International journal of pharmacy and pharmaceutical sciences*, 7(6):1-7.

Catto, M., Nicolotti, O., Leonetti, F., Carotti, A., Favia, A.D., Soto-Otero, R., Méndez-Álvarez, E. & Carotti, A. 2006. Structural insights into monoamine oxidase inhibitory potency and selectivity of 7-substituted coumarins from ligand- and target-based approaches. *Journal of medicinal chemistry*, 49(16):4912-4925.

Dauer, W. & Przedborski, S. 2003. Parkinson's disease: mechanisms and models. *Neuron*, 39(6):889-909.

Fahn, S. 2003. Description of Parkinson's disease as a clinical syndrome. *Annals of the New York academy of sciences*, 991(1):1-14.

Fahn, S. & Cohen, G. 1992. The oxidant stress hypothesis in Parkinson's disease: evidence supporting it. *Annals of neurology*, 32(6):804-812.

Foley, P., Gerlach, M., Youdim, M.B. & Riederer, P. 2000. MAO-B inhibitors: multiple roles in the therapy of neurodegenerative disorders? *Parkinsonism & related disorders*, 6(1):25-47.

Gibrat, C., Saint-Pierre, M., Bousquet, M., Lévesque, D., Rouillard, C. & Cicchetti, F. 2009. Differences between subacute and chronic MPTP mice models: investigation of dopaminergic neuronal degeneration and α-synuclein inclusions. *Journal of neurochemistry*, 109(5):1469-1482.

Gökhan-Kelekçi, N., Koyunoğlu, S., Yabanoğlu, S., Yelekçi, K., Özgen, Ö., Uçar, G., Erol, K., Kendi, E. & Yeşilada, A. 2009. New pyrazoline bearing 4(3*H*)-quinazolinone inhibitors of

monoamine oxidase: synthesis, biological evaluation, and structural determinants of MAO-A and MAO-B selectivity. *Bioorganic & medicinal chemistry*, 17(2):675-689.

Khan, I., Zaib, S., Batool, S., Abbas, N., Ashraf, Z., Iqbal, J. & Saeed, A. 2016. Quinazolines and quinazolinones as ubiquitous structural fragments in medicinal chemistry: an update on the development of synthetic methods and pharmacological diversification. *Bioorganic & medicicnal chemistry*, 24(11):2361-2381.

Khattab, S.N., Haiba, N.S., Asal, A.M., Bekhit, A.A., Amer, A., Abdel-Rahman, H.M. & El-Faham, A. 2015. Synthesis and evaluation of quinazoline amino acid derivatives as monoamine oxidase (MAO) inhibitors. *Bioorganic & medicinal chemistry*, 23(13):3574-3585.

Kumar, B., Mantha, A.K. & Kumar, V. 2016. Recent developments on the structure–activity relationship studies of MAO inhibitors and their role in different neurological disorders. *Royal Society of chemistry advances*, 6(48):42660-42683.

Lata, A., Satsangi, R.K., Srivastava, V.K. & Kishor, K. 1982. Monoamine oxidase inhibitory and CNS activities of some quinazolinones. *Arzneimittelforschung*, 32(1):24-27.

Lees, A.J., Hardy, J. & Revesz, T. 2009. Parkinson's disease. *Lancet*, 373(9680):2055-2066.

Legoabe, L.J., Petzer, A. & Petzer, J.P. 2012a. Inhibition of monoamine oxidase by selected C6-substituted chromone derivatives. *European journal of medicinal chemistry*, 49:343-353.

Legoabe, L.J., Petzer, A. & Petzer, J.P. 2012b. Selected C7-substituted chromone derivatives as monoamine oxidase inhibitors. *Bioorganic chemistry*, 45:1-11.

Parkinson, J. 2002. An essay on the shaking palsy. *The journal of neuropsychiatry & clinical neurosciences*, 14(2):223-236.

Prisinzano, T.E. 2006. Medicinal chemistry: a molecular and biochemical approach. Nogrady T. and Weaver D.F. New York: Oxford University Press. *Journal of medicinal chemistry*, 49:3428.

Rajput, R. & Mishra, A.P. 2012. A review on biological activity of quinazolinones. *International journal of pharmacy and pharmaceutical sciences*, 4(2):66-70.

Rang, H.P., Dale, M.M., Ritter, J.M., Flower, R.J. & Henderson, G. 2007. Rang and Dale's pharmacology. 6th ed. London: Churchill Livingstone.

Rastogi, V., Barthwal, J. & Parmar, S.S. 1972. Synthesis of substituted 2-methyl-3 (4′-hydrazinocarbonyl-methylene-oxy-phenyl)-4-quinazolones as monoamine oxidase inhibitors. *Journal für praktische chemie*, 314(1):187-192.

Riederer, P. & Laux, G. 2011. MAO-inhibitors in Parkinson's disease. *Experimental neurobiology*, 20(1):1-17.

Roach, S.S. & Scherer, J.C. 2004. Introductory clinical pharmacology. 7th ed. Philadelphia: Lippincott Williams & Wilkins.

Robakis, D. & Fahn, S. 2015. Defining the role of the monoamine oxidase-B inhibitors for Parkinson's disease. *CNS drugs*, 29(6):433-441.

Rossiter, D., Blockman, M., Barnes, K.I., Cohen, K., Decloedt, E., Waal, R., Maartens, G., McIlleron, H. & Sixanda, P.Z. 2012. South African medicines formulary. 10th ed. Cape Town: Health and Medical Publishing Group.

Schatzberg, A.F. & Nemeroff, C.B. 2017. Textbook of psychopharmacology. 5th ed. Virginia: American Psychiatric Publishing.

Srivastava, V.K., Satsangi, R.K., Kumar, P. & Kishor, K. 1980. Monoamine oxidase inhibitory activity of 2-aryl-3-(5'-chlorobenzophenon-2'-yl)-quinazolin-4-(3*H*)-ones. *Indian journal of physiology and pharmacology*, 24(4):361-363.

Victor, D. & Waters, C. 2003. Monoamine oxidase inhibitors in Parkinson's disease. *Neurological disease and therapy*, 59:425-436.

Vila, M. & Przedborski, S. 2004. Genetic clues to the pathogenesis of Parkinson's disease. *Nature medicine*, 10:S58-62.

Volz, H.-P. & Gleiter, C.H. 1998. Monoamine oxidase inhibitors. *Drugs & aging*, 13(5):341-355.

Youdim, M.B., Edmondson, D. & Tipton, K.F. 2006. The therapeutic potential of monoamine oxidase inhibitors. *Nature reviews neuroscience*, 7(4):295-309.

Youdim, M.B. & Weinstock, M. 2004. Therapeutic applications of selective and non-selective inhibitors of monoamine oxidase A and B that do not cause significant tyramine potentiation. *Neurotoxicology*, 25(1-2):243-250.

CHAPTER 2
LITERATURE OVERVIEW

2.1 Parkinson's disease

2.1.1 General background

Parkinson's disease (PD) is a slowly progressive CNS disorder characterised by involuntary contraction of skeletal muscles at rest, with a tendency to bend forward and to pass from a walking to a running pace (Parkinson, 2002). The major clinical signs and symptoms for diagnosis of PD are dyskinesia (slowness and poverty of movement), muscular rigidity, resting tremor (which subsides with voluntary movement) and impaired postural movement, leading to tendency to fall forward or backwards when the centre of gravity is displaced (Bruton *et al.*, 2008).

The earliest physical signs of PD occur gradually and may be unnoticed for a long time, and include slight dragging of one foot, fatigue and stiffness, stooped posture, flexion of one arm with lack of swing and poor quality of speech (Lees *et al.*, 2009). As time and disease progress, difficulties increase. For example a change in a patient's writing occurs, with a tendency to slope usually in an upward direction, and then get smaller and more cramped after a line or two (Parkinson, 2002; Lees *et al.*, 2009). Other symptoms include early loss of smell and sleep disturbances (Lees *et al.*, 2009). Lees *et al.* (2009) indicates that in the late stages of PD, the face becomes mask-like and open mouthed with a wide-eyed, unblinking stare. All dextrous movements become increasingly difficult and a patient may need help in getting out of bed, bathing, dressing and eating (Lees *et al.*, 2009).

2.1.1.1 Neurochemical and neuropathological features

The pathological hallmark of PD is loss of pigmented dopaminergic neurons in the SNpc that provide dopaminergic innervation to the striatum (caudate and putamen) (Bruton *et al.*, 2008) and the presence of LBs (Dauer & Przedborski, 2003). LBs are intracytoplasmic inclusions that are composed of a variety of proteins such as α-synuclein, parkin, ubiquitin and neurofilaments. They can be found in every affected brain region (Przedborski, 2005), and they are a result of defective response to oxidative neuronal injury (Tugwell, 2008). According to Uhl *et al.* (1994), the pattern of SNpc cell loss coincides with the level of DA transporter (DAT) messenger ribonucleic acid (mRNA) expression, and it is consistent with the finding that DA depletion is most pronounced in the dorsolateral putamen.

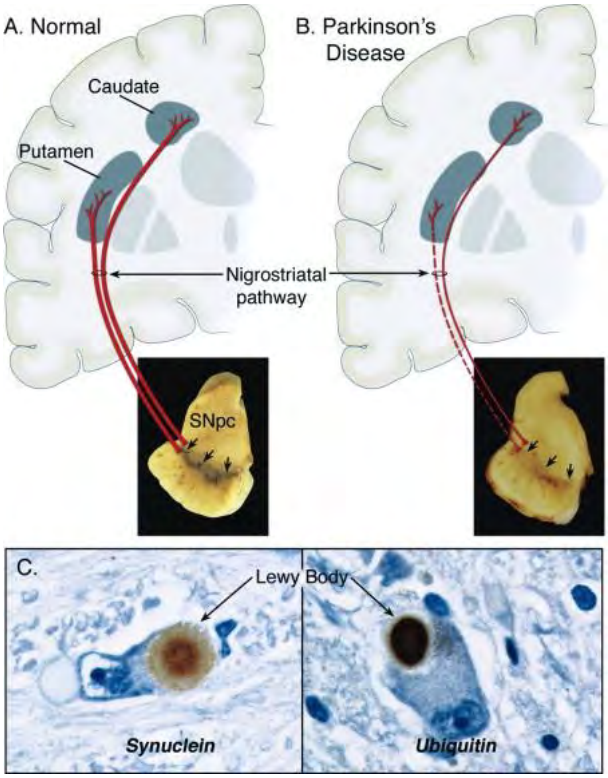

Figure 2.1: Neuropathology of PD (Dauer & Przedborski, 2003).

The cell bodies of the mesolimbic dopaminergic neurons that reside adjacent to the SNpc in the ventral tegmental (VTA) area are less affected in PD (Dauer & Przedborski, 2003). Research indicates that there is less depletion of DA in the caudate, the main site of projection of these neurons (Dauer & Przedborski, 2003). Cell loss in PD is concentrated in the ventrolateral and caudal portions of SNpc, and the degree of terminal loss in the striatum is more pronounced than the extent of SNpc dopaminergic neuron loss, suggesting that the striatal dopaminergic nerve terminals are the major targets for the degenerative process (Dauer & Przedborski, 2003).

2.1.1.2 Aetiology

Environmental factors

Several studies have identified that some environmental influences play an important role in the cause of PD (Warner & Schapira, 2003). Rural living is associated with the agricultural industry, and as a result it has been identified as one of the factors that increase the risk of developing PD. For example, paraquat is structurally similar to the N-methyl-4-phenyl-2,3-dihydropyridinium ion (MPP^+), the active metabolite of MPTP, and it has been used as a herbicide (Dauer & Przedborski, 2003). High PD incidence has also been shown in people who drink well water (Tugwell, 2008).

Genetic factors

Genetic mutation is one of the causes of PD aetiology. A greater percentage of PD cases is not inherited, but it has been estimated that a parent with PD increases the child's lifetime risk of developing the disease from 2% to 6% (Tugwell, 2008). Mutations in the SNpc gene are rare and highly penetrant, and they cause early onset autosomal dominant inherited forms of PD (Polito *et al.*, 2016). On the other hand, mutations in the LRRK-2 gene are rare and have incomplete and age-dependant penetrance. These mutations cause late onset autosomal dominant inherited forms of PD (Polito *et al.*, 2016).

2.1.1.3 Pathogenesis

The symptoms of PD result from the degeneration of the dopaminergic pathway that projects from the substantia nigra to the corpus striatum (Tugwell, 2008). Dauer and Przedborski (2003) propose that there are two major hypotheses for the pathogenesis of PD. One hypothesis suggests that misfolding and aggregation of proteins are key in the death of SNpc dopaminergic neurons, whereas the other hypothesis proposes that mitochondrial dysfunction and oxidative stress, including toxic oxidised DA species, are the main cause.

According to Dauer and Przedborski (2003), available data argues that the mechanism of neuronal death in PD starts with a healthy dopaminergic neuron being affected by an aetiological factor such as mutant α-synuclein. On the other hand, there may be a cascade of deleterious factors within the neuron, that is made up of multiple factors such as free radicals, mitochondrial dysfunction, excitotoxicity, neuroinflammation and apoptosis (Przedborski, 2005).

2.1.1.4 Genetics

According to Lees *et al.* (2009), several mutations in several genes are linked with L-dopa-responsive parkinsonism. Six pathogenic mutations in LRRK-2, a kinase encoding the protein dardarin, have been reported, and the most common of these is Gly2019Ser with a world-wide frequency of 1% in sporadic cases and 4% in patients with hereditary parkinsonism (Lees *et al.*, 2009). Lees *et al.* (2009) suggests that loss-of-function mutations in four genes, parkin, DJ-1, phosphatase and tensin homolog (PTEN)-induced putative kinase 1 (PINK1) and adenosine triphosphate (ATP) 13A2 cause recessive early onset parkinsonism (age of onset < 40 years). Heterozygous loss of function of GBA increases the risk of developing PD more than fivefold, thus the risk of developing PD is increased thirteen times if one carries a severe GBA mutation, which reduces mean age of disease onset from 60 to 55 years (Lees *et al.*, 2009). Parkin mutations are the second most common genetic causes of L-dopa-responsive parkinsonism (Lees *et al.*, 2009).

2.1.2 Symptomatic treatment

2.1.2.1 L-Dopa

L-Dopa, the metabolic precursor of DA is the most effective medication for PD and it should always be the initial treatment option regardless of the age of the patient (Lees *et al.*, 2009). Oral L-dopa is absorbed rapidly from the small intestines and into the CNS through an aromatic amino acid membrane transporter, and it competes with dietary protein at this level (Bruton *et al.*, 2008). In the CNS, dopa decarboxylase converts L-dopa to DA, mainly within the presynaptic terminals of dopaminergic neurons in the striatum (Bruton *et al.*, 2008).

According to Bruton *et al.* (2008), L-dopa is primarily decarboxylated in the intestinal mucosa and at other peripheral sites so that little of the parent drug reaches the cerebral circulation, and probably <1% penetrates the CNS. Therefore L-dopa should not be administered alone, but together with a peripherally acting inhibitor of aromatic L-amino acid decarboxylase (AADC), that does not penetrate well into the CNS. Bruton *et al.* (2008) states that inhibition of peripheral decarboxylase significantly increases the fraction of administered L-dopa that remains unmetabolised and available to cross the BBB, and reduces the incidence of nausea and other gastrointestinal (GI) side-effects due to peripheral conversion of the drug to DA.

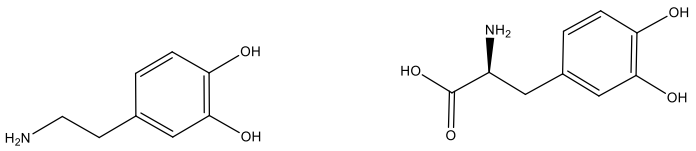

Dopamine L-dopa

Figure 2.2: Structures of dopamine and L-dopa.

Although L-dopa is the most effective agent for symptomatic treatment of PD, it loses its efficiency with long term use, and the patient's motor state may fluctuate severely with each dose, resulting in the so-called "on/off phenomenon" in which each dose of L-dopa effectively improves mobility for a period of time, perhaps 1 to 2 hours, but rigidity and akinesia return rapidly at the end of the dosing interval (Bruton *et al.*, 2008).

2.1.2.2 DA agonists

DA agonists provide effective relief either as first line therapy or in early PD as an adjunct to L-dopa (Fernandez & Chen, 2007). These drugs are a common first-line treatment in patients younger than 55 years of age (Lees *et al.*, 2009). According to Bruton *et al.* (2008), most DA receptor agonists have a substantially longer duration of action than L-dopa, and they are particularly effective in the treatment of patients that have developed the on/off

phenomena. However, DA agonists are less potent than L-dopa and they do not target all symptoms of PD (Fernandez & Chen, 2007) .There are four orally administered DA agonists available for PD treatment: older ergot agents such as bromocriptine and pergolide, and two newer more selective compounds ropinirole and pramipexole (Bruton *et al.*, 2008).

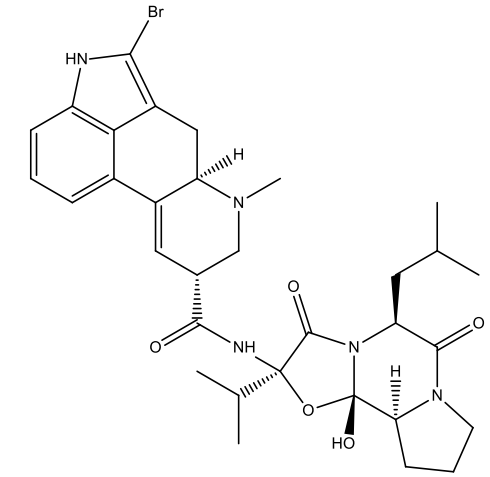

Bromocriptine

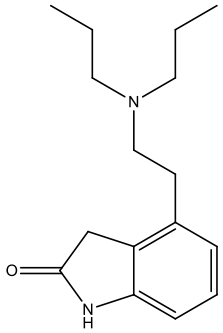

Ropinirole

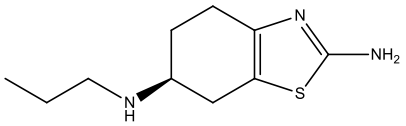

Pramipexole

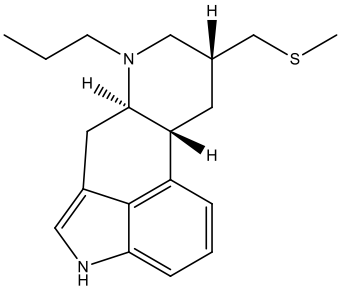

Pergolide

Figure 2.3 Structures of bromocriptine, ropinirole, pramipexole and pergolide.

Bromocriptine is a D_2 receptor agonist and a partial D_1 receptor antagonist while pergolide is an agonist of both receptor types (Bruton *et al.*, 2008). Ropinirole and pramipexole have selective activity at D_2 and D_3 receptors, with little or no activity at receptors of the D_1 class (Bruton *et al.*, 2008). Bruton *et al.* (2008) states that initial treatment with bromocriptine or pergolide may cause nausea, fatigue and severe hypotension and should be initiated at a lower dose which can gradually be titrated over a period of weeks to months. On the other hand, ropinirole and pramipexole can be initiated more quickly, achieving therapeutically useful doses in a week or less. In addition to that, non-ergot DA receptor agonists cause lesser GI disturbances than ergot derivatives, but they can cause nausea and sleepiness (Bruton *et al.*, 2008).

Apomorphine

Apomorphine is a potent DA agonist which stimulates both the D_1 and D_2 receptors (Tugwell, 2008; Rossiter *et al.*, 2012). It is administered subcutaneously and has high affinity for D_2, D_3, D_5, and adrenergic $\alpha_{1D,}$ α_{2B} and α_{2C} receptors. Apomorphine has low affinity for D_1 receptors (Bruton *et al.*, 2008). Apomorphine has a rapid onset of action and is used as "rescue therapy" for the acute treatment of the "off" response to dopaminergic therapy (Bruton *et al.*, 2008; Tugwell, 2008; Rossiter *et al.*, 2012). This drug has similar side effects to those of oral DA agonists. It is highly emetogenic and requires pre- and post-antiemetic therapy, starting 3 days prior to the initial dose of apomorphine, and continued at least during the first 2 months of therapy (Bruton *et al.*, 2008).

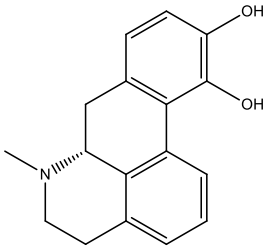

Figure 2.4: Structure of apomorphine.

2.1.2.3 Carbidopa and benserazide

Carbidopa and benserazide are inhibitors of peripheral AADC that do not penetrate well into the CNS. AADC is an enzyme that decarboxylates L-dopa, thus decreasing its conversion to DA in the peripheral tissues, and resulting in a decrease in its CNS bioavailability (Bruton *et al.*, 2008). Inhibition of this enzyme markedly increases the fraction of administered L-dopa that remains unmetabolized and available to cross the BBB (Dhall & Kreitzman, 2016). Formulations of L-dopa with AADC inhibitors allows administration of lower doses of L-dopa, thus reducing peripheral side-effects (Carvey, 2010).

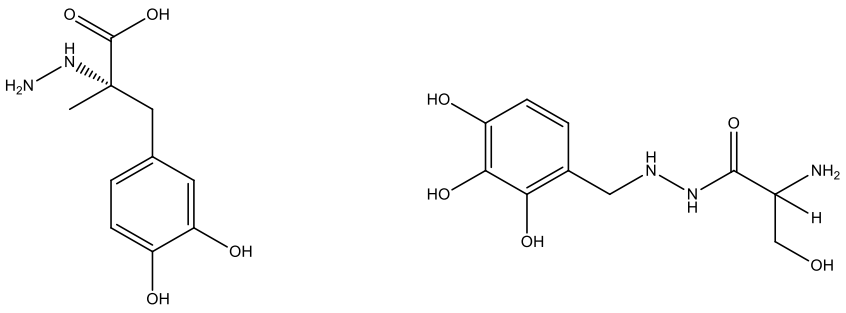

Carbidopa Benserazide

Figure 2.5: Structures of carbidopa and benserazide

2.1.2.4 COMT inhibitors

Catechol-O-methyltransferase (COMT) metabolises L-dopa as well as DA, resulting in the pharmacologically inactive compounds 3-*O*-methyl dopa (from L-dopa) and 3-methoxytyramine (from DA) (Bruton *et al.*, 2008). COMT inhibitors block this peripheral conversion of L-dopa to 3-*O*-methyl dopa, increasing both plasma half-life ($t_{1/2}$) of L-dopa as well as the fraction that reaches the CNS (Bruton *et al.*, 2008). COMT inhibitors can be used adjunctively with L-dopa in late phases of PD, reducing both the "off" time experience, and the end-of-dose deterioration (Tugwell, 2008; Rossiter *et al.*, 2012).

There are two COMT inhibitors currently available for the treatment of PD namely entacapone and tolcapone. Entacapone increases bioavailability of L-dopa by inhibiting COMT peripherally and does not cross the BBB (Tugwell, 2008). Several studies have shown that entacapone reduces motor fluctuations in patients with PD. Tugwell (2008) adds that there is a possibility that co-administration of entacapone with L-dopa may delay the development of motor fluctuations.

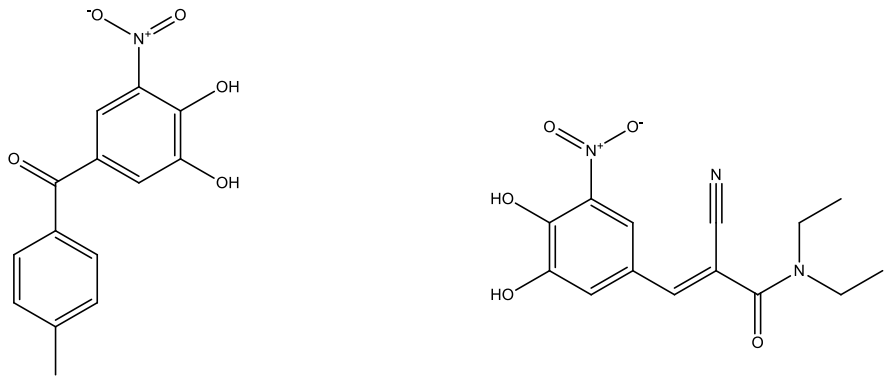

Tolcapone Entacapone

Figure 2.6: Structures of tolcapone and entacapone

2.1.2.5 MAO-B inhibitors

MAO-B inhibitors block the B isoform of the MAO enzyme that is found in the human brain (Fernandez & Chen, 2007). Selectively inhibiting this enzyme enhances striatal dopaminergic activity by inhibiting the oxidative metabolism of DA, thus improving the motor symptoms of PD (Fernandez & Chen, 2007). Two drugs, selegiline [(R)-deprenyl] and rasagiline, are currently the most used inhibitors of MAO-B (Tugwell, 2008). Selegiline is used as an adjunct to L-dopa in the management of PD, whereas rasagiline is used as mono- or adjunct therapy (Rossiter *et al.*, 2012).

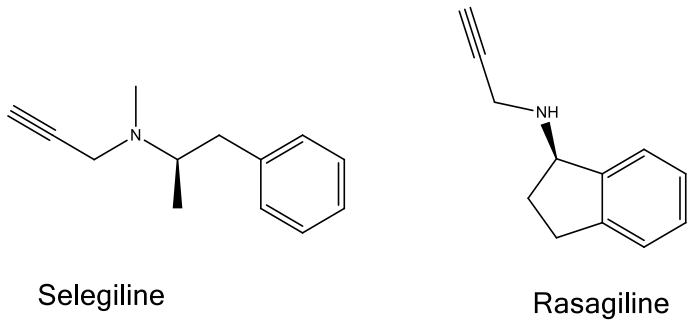

Selegiline Rasagiline

Figure 2.7: Structures of selegiline and rasagiline

2.1.2.6 Anticholinergic drugs

Before the discovery of L-dopa, antagonists of muscarinic ACh receptors were widely used for treatment of PD (Bruton *et al.*, 2008). Anticholinergics were first used when it was discovered that dopaminergic deficiency resulted in increased striatal cholinergic activity and a subsequent imbalance between these neurotransmitters (DeMaagd & Philip, 2015). Anticholinergic drugs can be used as adjuncts to L-dopa as well as monotherapy early in the course of the disease (Brocks, 1999).

Bruton *et al.* (2008) suggests that anticholinergic drugs act in the neostriatum through the receptors that mediate the response to intrinsic cholinergic innervation. The agents acting as muscarinic antagonists that are currently used in treatment of PD include trihexyphenidyl, benztropine and diphenhydramine (Bruton *et al.*, 2008). Trihexyphenidyl is a synthetic tertiary amine anticholinergic that is used as an adjunct to L-dopa therapy. This drug decreases striatal levels of Ach without increasing its turnover rate (Meltzer, 1991). Benztropine acts with a similar mechanism to trihexyphenidyl (Meltzer, 1991).

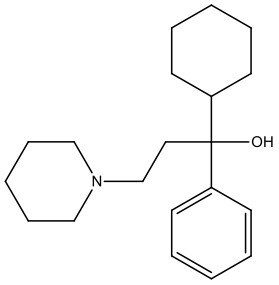

Trihexyphenidyl

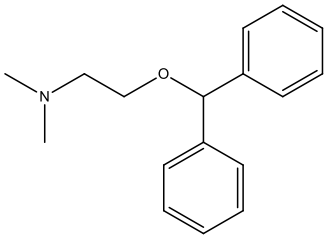

Diphenhydramine

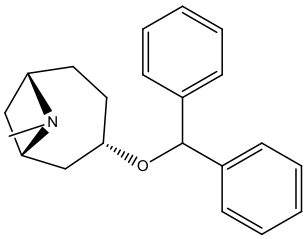

Benztropine

Figure 2.8: Structures of trihexyphenidyl, diphenhydramine, and benztropine.

2.1.2.7 Adenosine A_{2A} receptor antagonists

Hauser and Schwarzschild (2005) state that specific adenosine A_{2A} receptor antagonists reverse motor deficits or enhance dopaminergic treatments in animal models of PD. A_{2A} blockade has been found to improve abnormalities of muscle tone and tremors in rodents, extending the potential benefits of A_{2A} blockade for PD symptoms. Hauser and Schwarzschild (2005) state that co-administration of an A_{2A} receptor antagonist with L-dopa produces a synergistic antiparkinsonian effect. A selective adenosine A_{2A} antagonist istradefylline remediates PD by blocking A_{2A} receptor-mediated striatopallidal medium spiny neuron modulation, thus facilitating nigral neurotransmitter release (Dungo & Deeks, 2013). A_{2A} antagonists also have the potential for improving motor activity while showing a low potential for inducing or exacerbating dyskinesia. In addition, laboratory studies have raised the possibility that prolonged A_{2A} blockade may prevent the development of dyskinesia (Hauser & Schwarzschild, 2005).

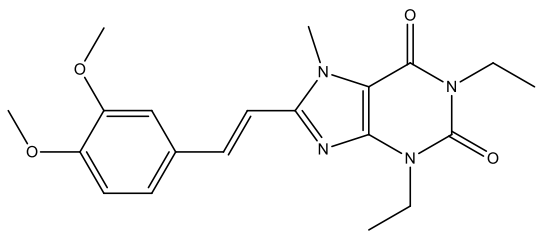

Figure 2.9: Structure of istradefylline (KW-6002)

2.1.2.8 Amantadine

Amantadine was originally used as an antiviral drug and its antiparkinson effects were discovered in the late 1990s (Tugwell, 2008). Amantadine has anticholinergic properties, but more importantly, it can activate DA release from nerve terminals (Fahn, 2003; Bruton *et al.*, 2008). In addition, amantadine interferes with transmission at glutamatergic N-methyl-D-aspartate (NMDA) receptors, and in turn inhibits NMDA-evoked release of ACh in striatal tissue (Tugwell, 2008). It has been suggested that amantadine may be useful as an adjunct to L-dopa. Its glutamate-antagonist properties may reduce overactivity of the subthalamic nucleus which may be the cause of dyskinesia, thus reducing the severity of L-dopa-induced dyskinesia (Fahn, 2003; Bruton *et al.*, 2008; Tugwell, 2008).

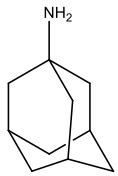

Figure 2.10: Structure of amantadine

2.1.3 Drugs for neuroprotection

2.1.3.1 MAO-B inhibitors: Selegiline, lazabemide and L-dopa

The tocopherol and deprenyl antioxidative therapy of parkinsonism (DATATOP) study conducted with selegiline can delay the emergence of disability that require treatment with L-dopa (Fernandez-Espejo, 2004). In contrast to L-dopa monotherapy, co-administration of selegiline with L-dopa prolongs chances of survival and lessens disability (Koller, 1997). Clinical trials have led to a hypothesis that chronic selegiline would lessen oxidative stress generated from DA turnover, and afford neuroprotection (Koller, 1997; LeWitt & Taylor, 2008).

Studies have demonstrated that selegiline limits MPTP-induced nigral damage and reduces PC12 cell apoptosis in doses that do not inhibit MAO-B (Koller, 1997). It has been proposed that selegiline rescues nigral neurons by inducing selective changes in transcription, protein synthesis and alterations in gene expression. Research has also shown that selegiline, in

doses that do not inhibit MAO-B, limits free radical formation and prevents nigral damage due to direct administration of MPP^+ (Koller, 1997). Selegiline may influence the rate of neuronal degeneration through mechanisms that are not dependent on MAO-B inhibition (Koller, 1997). In addition, treatment with selegiline lowers the risk for eventually developing freezing of gait (Koller, 1997).

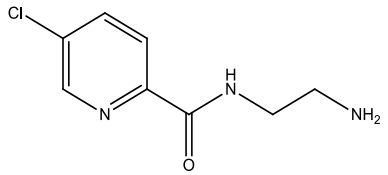

Figure 2.11: Structure of lazabemide.

Lazabemide is a selective reversible MAO-B inhibitor and undergoes rapid clearance after administration. It has been demonstrated that lazabemide has similar symptomatic effects compared to selegiline (LeWitt & Taylor, 2008). Rasagiline, a highly selective MAO-B inhibitor, enhances release of DA in addition to retarding its catabolism and antagonises three cellular processes that are involved in the cascade of events leading to apoptosis. These events are intracellular translocation of glycolytic enzyme glyceraldehyde-3-phosphate, induction of bcl-2 and activation of mitochondrial permeability transition (LeWitt & Taylor, 2008). Rasagiline also blocks actions of N-methyl-R-salsolinol, an endogenous neurotoxin that is a condensation product of oxidised DA (LeWitt & Taylor, 2008).

2.1.3.2 Dopaminergic drugs: Pramipexole, ropinirole and rasagiline

Studies have shown that initial treatment of PD patients with DA agonists, pramipexole or ropinirole, reduces the decline of nigrostriatal function compared to patients on L-dopa alone (Fernandez-Espejo, 2004). DA agonists such as pramipexole have been demonstrated to exert a direct antioxidant effect and they scavenge hydroxyl radicals as a result of their hydroxylated benzyl ring structure, thus rendering them neuroprotective (Fernandez-Espejo, 2004). DA receptor agonists have been hypothesised as potentially neuroprotective by acting at D_2 autoreceptors, found in dopaminergic substantia nigra terminals, to supress DA release and thus reduce oxidative stress (Yacoubian & Standaert, 2009). According to Yacoubian and Standaert (2009) *in vitro* and animal studies have shown that DA receptor agonists reduce dopaminergic cell death.

Studies with pramipexole have demonstrated potentially protective actions against oxidative stress and the neurotoxic effect on dopaminergic neurons of various experimental toxins including methamphetamine, 3-acetylpyridine, 6-OHDA and MPTP (LeWitt & Taylor, 2008). However, the mechanisms contributing to the protective actions of pramipexole have not

been defined, although activation of the D_3 receptor agonist was suggested in one study, and blocking the cascade of apoptosis in others (LeWitt & Taylor, 2008).

Ropinirole was shown to enhance mechanisms against oxidative stress and exerts protective action against 6-OHDA-induced loss of nigrostriatal dopaminergic projections in mice (LeWitt & Taylor, 2008).

2.1.3.3 Antioxidant therapy

Studies have shown that selegiline significantly delays the time of onset of L-dopa treatment (Yacoubian & Standaert, 2009). On the other hand, rasagiline is more potent than selegiline and has metabolites with potential antioxidant properties. The antioxidant, coenzyme Q10, is a cofactor in the electron transport chain in mitochondria and it has been shown to reduce dopaminergic neurodegeneration in PD mouse models (Yacoubian & Standaert, 2009).

Yacoubian and Standaert (2009) state that uric acid is a potential neuroprotective agent in PD. Uric acid acts as an antioxidant by scavenging reactive oxygen and nitrogen species. A decreased incidence of PD among patients with high serum urate levels and among subjects with gout has been reported in previous studies (Yacoubian & Standaert, 2009). Slower disease progression is attributed to high plasma urate levels in patients with early PD (Yacoubian & Standaert, 2009).

2.1.3.4 Mitochondrial energy enhancement drugs: Coenzyme Q10 and creatine

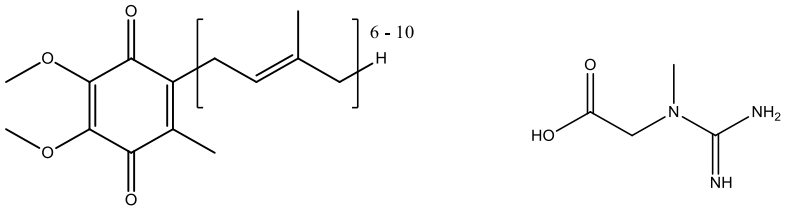

Coenzyme Q10 Creatine

Figure 2.12: Structures of coenzyme Q10 and creatine

Mitochondria of the substantia nigra, platelets and skeletal muscle in PD possess reduced activity of the first step of the mitochondrial electron transport chain, complex I (LeWitt & Taylor, 2008). Coenzyme Q10 (also known as ubiquinone) is an essential co-factor serving as an electron acceptor for mitochondrial complex I (LeWitt & Taylor, 2008). Several studies have shown that coenzyme Q10 is also a potent antioxidant in lipid membranes and mitochondria as it has a potential of slowing PD progression. LeWitt and Taylor (2008) state that augmenting brain creatine concentration is another strategy for targeting the defects in mitochondrial complex I.

According to LeWitt and Taylor (2008), creatine serves as a precursor for conversion to phosphocreatine, an energy intermediate which transfers phosphoryl groups for ATP synthesis in mitochondria. Increasing creatine intake enhances formation of phosphocreatine, ultimately resulting in the reduction of oxidative stress though stabilisation of mitochondrial creatine kinase (LeWitt & Taylor, 2008). In addition, creatine kinase inhibits the opening of the mitochondrial transition pore, hence improving mitochondrial metabolism and down regulating a putative neurodegenerative mechanism (LeWitt & Taylor, 2008).

2.1.3.5 Anti-inflammatory drugs

Activation of microglia, increased cytokine production, and increased complement protein levels suggestive of neuroinflammation have been demonstrated in PD (Yacoubian & Standaert, 2009). According to Yacoubian and Standaert (2009), anti-inflammatory agents, including non-steroidal anti-inflammatory drugs (NSAIDs) and minocycline, have been pursued as potential disease modifying treatments for PD in order to slow down disease progression. Certain NSAIDs, such as aspirin, have shown neuroprotective properties in studies done in culture and animal models (Yacoubian & Standaert, 2009). However, there is conflicting data regarding which NSAID, what dosing and what timing provides the best neuroprotection (Yacoubian & Standaert, 2009). Research has indicated that the use of NSAIDs lowers the risk of PD by 45%, but ibuprofen is the only NSAID with proven neuroprotective effect (Yacoubian & Standaert, 2009).

2.1.3.6 Antiapoptotic drugs: Minocycline, TCH346 and Cep-1347

There is evidence that activation of apoptosis is a possible mechanism for neurodegeneration in PD. Studies show that pre-treatment with minocycline improves survival of dopaminergic substantia nigra neurons in rodent models of 6-OHDA and MPTP-induced parkinsonism (LeWitt & Taylor, 2008). According to LeWitt and Taylor (2008), minocycline inhibits the activation of microglia, which is a prominent feature in the brain of PD patients and in experimental neurotoxin models. Minocycline also lessens factors that mediate apoptosis, such as caspase-I (LeWitt & Taylor, 2008).

Glyceraldehyde-3-phosphate dehydrogenase (GAPDH), an enzyme that can initiate apoptosis, is inhibited by the propagylamine TCH346, which has antiapoptotic activity (Yacoubian & Standaert, 2009). TCH346 has a similar structure to selegiline, however, it does not inhibit MAO-B and it is not metabolised to amphetamine compounds (LeWitt & Taylor, 2008). Histological analysis has revealed that TCH346 treatment lessens MPTP induced dopaminergic neuron loss (LeWitt & Taylor, 2008).

Another antiapoptotic agent that has shown promise in clinical studies is CEP-1347 (Yacoubian & Standaert, 2009). This compound is an inhibitor of mixed lineage kinase-3, a kinase that can activate the c-Jun N-terminal kinase (JNK) pathway involved in cell death (LeWitt & Taylor, 2008; Yacoubian & Standaert, 2009).

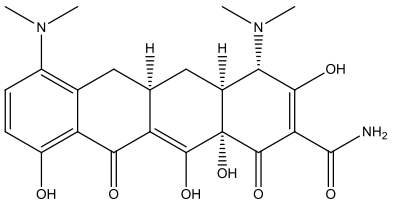

Minocycline

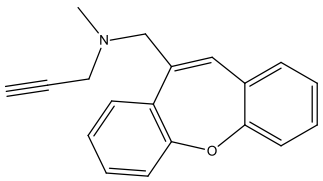

TCH346

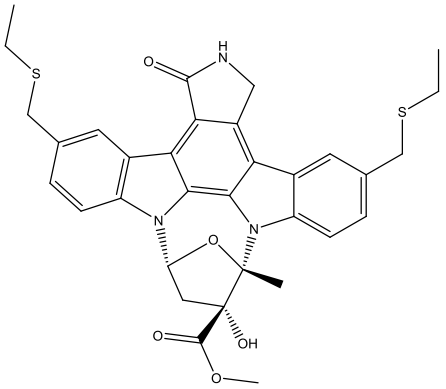

Cep-1347

Figure 2.13: Structures of minocycline, TCH346 and Cep-1347

2.1.3.7 NMDA antagonists/ Antiglutamatergic drugs

One rationale for PD neuroprotection has been to block glutamate neurotransmission in the substantia nigra because glutamate can act as an excitotoxin contributing to neuronal damage (Tugwell, 2008). Amantadine has been claimed to slow progression of PD by reducing the extent of cell death caused by excess glutamate activity. However, there is no good evidence to support this claim (Tugwell, 2008). On the other hand, riluzole, a drug used to treat amyotropic lateral sclerosis, blocks the presynaptic release of glutamate (LeWitt & Taylor, 2008; Tugwell, 2008). However, the results of a trial with riluzole in early PD showed no evidence for a neuroprotective effect (LeWitt & Taylor, 2008; Tugwell, 2008).

2.1.3.8 Adenosine A_{2A} receptor antagonists

Epidemiological studies have indicated that caffeine, an adenosine A_{2A} antagonist, may reduce the incidence of PD at least in men (Hauser & Schwarzschild, 2005). Caffeine mediates its action by antagonising adenosine receptors when administered to mice in

doses corresponding to typical human doses, and it reverses the loss of striatal DA in a dose-dependent manner (Hauser & Schwarzschild, 2005; Yacoubian & Standaert, 2009). Caffeine also prevents MPTP- or 6-OHDA-induced loss of dopaminergic nerve terminals and DA cell bodies in the striatum (Hauser & Schwarzschild, 2005). More recent research has suggested that A_{2A} receptor antagonists not only improve symptomatic function in PD, but may also be neuroprotective (Yacoubian & Standaert, 2009). Yacoubian and Standaert (2009) state that A_{2A} antagonists may also be neuroprotective in non-dopaminergic brain areas in animal models.

2.1.4 Mechanisms of neurodegeneration

2.1.4.1 Oxidative stress and mitochondrial dysfunction

In normal physiology, reactive oxygen species (ROS) are generated which are normally scavenged by cells. In this respect superoxide ions are converted to H_2O_2 by superoxide dismutase, while H_2O_2 is converted to water by the action of glutathione peroxidase (GPO) (Fernandez-Espejo, 2004). Oxidative stress occurs from overproduction of reactive radicals as a result of either an overproduction of reactive species or a failure of cell buffering mechanisms that normally limit their accumulation (Yacoubian & Standaert, 2009). Schapira and Jenner (2011) state that deficiencies in the major oxidant enzyme systems in the brain, catalase, superoxide dismutase and GPO, along with a reduction in levels of reduced glutathione (GSH) lead to oxidative stress and contributes to PD neurodegeneration.

Increased levels of iron found in the substantia nigra act as a catalyst for oxidative reactions, which result in the production of free radicals, that in turn cause neuronal damage (Tugwell, 2008). On the other hand, DA metabolism promotes oxidative stress because it gives rise to DA-quinone species, molecules that damage proteins by reacting with cysteine residues (Fernandez-Espejo, 2004; Yacoubian & Standaert, 2009).

A strong decrease in GSH increases the cells' sensitivity to toxins and potentiates the toxic effects of glial cell activation such as the enhancement of nitric oxide synthase (NOS) activity. Increased NOS activity leads to excess nitric oxide (NO) as well as the oxidising agents, peroxynitrite ($ONOO^-$) and the hydroxyl radical (Fernandez-Espejo, 2004). In addition, excessive formation of reactive oxygen and nitrogen species in PD increases oxidative damage to proteins, lipids and deoxyribonucleic acid (DNA) (Fernandez-Espejo, 2004). Fernandez-Espejo (2004) suggests that strong oxidative stress in the substantia nigra can lead to misfolding of proteins such as α-synuclein and parkin. Loss of normal function of α-synuclein alters normal vesicle function, thus enhancing intracellular levels of DA, which enhance oxidative stress (Fernandez-Espejo, 2004).

Iron-mediated free radical production can inhibit complex I activity. There exists an interaction between oxidative stress and mitochondrial dysfunction, enhancing each other in a cycle of toxicity (Fernandez-Espejo, 2004). Schapira and Jenner (2011) suggest that PD patients with mitochondrial dysfunction have a deficiency of complex I within the brain, which is confined to the substantia nigra. According to Schapira and Jenner (2011), specific gene mutations that induce dopaminergic cell death contribute to mitochondrial dysfunction in PD. Researchers have discovered that fibroblasts from patients with parkin mutations exhibit decreased complex I activity and complex I linked ATP production (Schapira & Jenner, 2011).

2.1.4.2 Protein aggregation and misfolding

Alpha-synuclein is the primary aggregation protein in PD, and is a major component of LBs and Lewy neutrites (Yacoubian & Standaert, 2009). Researchers have hypothesised that poor protein degradation and accumulation of misfolded proteins are the primary factors linking genetic alterations to dopaminergic neurodegeneration in PD (Vila & Przedborski, 2004). This suggests that α-synuclein and DJ-1 mutations cause abnormal protein conformations, overwhelming the protein degradation systems, the proteosomal and lysosomal pathways. Parkin and ubiquitin carboxyl-terminal hydrolase L1 (UCH-L1) mutations, in turn, undermine the cells' ability to detect and degrade misfolded proteins (Vila & Przedborski, 2004).

Research suggests that point mutations, overexpression, and oxidative damage of α-synuclein may promote self-aggregation (Yacoubian & Standaert, 2009). However, it is unclear how overabundance or aggregation of α-synuclein causes neuronal injury (Yacoubian & Standaert, 2009). Yacoubian and Standaert (2009) state that possible mechanisms are toxic effects of oligomers on cell membranes or proteosomal function, effects of α-synuclein on gene transcription or regulation, interactions of α-synuclein with cell signalling and cell death cascades, alterations in DA storage and release, and α-synuclein-mediated activation of inflammatory mechanisms.

Parkin and UCH-L1 have also been associated with protein aggregation in PD (Yacoubian & Standaert, 2009). Ubiquitin is an E3 protein ligase involved in targeting misfolded proteins for degradation, and mutations of parkin found in genetic forms of PD disrupt its E3 ubiquitin activity (Yacoubian & Standaert, 2009). In addition, UCH-L1 serves as ubiquitin recycling enzyme in neurons, and its dysfunction promotes aggregation of damaged proteins, including α-synuclein (Yacoubian & Standaert, 2009). Dauer and Przedborski (2003) state that protein aggregates can directly cause damage, perhaps by deforming the cell or

interfering with intracellular trafficking in neurons. Oxidative stress may also trigger dysfunctional protein metabolism (Dauer & Przedborski, 2003).

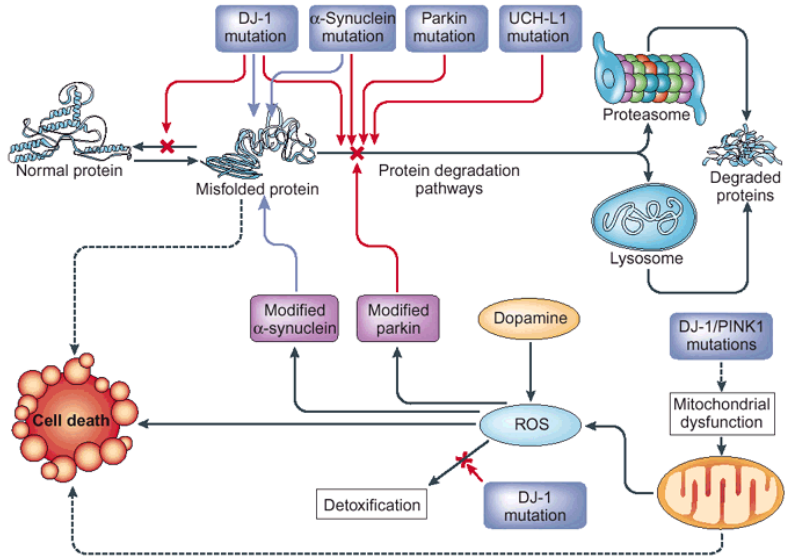

Figure 2.14: Genetic mutations and pathogenesis of PD (Vila & Przedborski, 2004).

2.1.4.3 Neuroinflammation

Increased levels of cytokines in the striatum and cerebrospinal fluid (CSF), including proinflammatory cytokines such as tumour necrosis factor (TNF)-α, interleukin (IL)-1β and IL-6, suggest neuroinflammatory reactions in PD (Fernandez-Espejo, 2004). In addition, there is upregulation of inflammatory-associated factors such as cyclooxygenase(COX)-2, and inducible NOS (Fernandez-Espejo, 2004).

Aggregated and nitrated forms of α-synuclein can directly trigger a microglial response and release of cytotoxic factors *in vitro* (Yacoubian & Standaert, 2009). It has been reported that α-synuclein or modified forms of the protein can trigger microglial and humoral responses in mouse models (Yacoubian & Standaert, 2009). According to Yacoubian and Standaert (2009), there is evidence that NSAIDs reduce dopaminergic cell death in animal and culture PD models. These compounds are thus neuroprotective and epidemiology studies have suggested that NSAIDs and statins may reduce the risk of PD.

2.1.4.4 Excitotoxicity

One of the factors involved in PD pathogenesis is excitotoxicity. The subthlamic nucleus becomes hyperactive once substantia nigra degeneration is advanced, leading to enhanced glutamatergic release within the nigra (Fernandez-Espejo, 2004). According to Yacoubian and Standaert (2009), glutamate is the primary excitatory transmitter in the mammalian

CNS, and a primary driver of excitotoxic processes. Excess NMDA receptor activation by glutamate can damage dopaminergic cells of the substantia nigra because glutamate enhances permeability to calcium through NMDA receptors located on these neurons (Fernandez-Espejo, 2004; Yacoubian & Standaert, 2009).

Enhancement of intracellular calcium can induce cell degeneration by promoting the production of $ONOO^-$ through activation of NOS. This further aggravates progression of the disease leading to accelerated nigral neurodegeneration (Fernandez-Espejo, 2004; Yacoubian & Standaert, 2009). Dopaminergic neurons in the substantia nigra have a large number of glutamate receptors and receive glutamatergic innervation from the subthalamic nucleus and cortex (Yacoubian & Standaert, 2009). Yacoubian and Standaert (2009) state that NMDA receptor antagonists protect against dopaminergic cell loss in MPTP models, but a major limitation to clinical application is low potency and poor tolerability of currently available agents.

2.1.4.5 Apoptosis

Apoptosis is a programmed cell death that is characterised by morphological changes including cell shrinkage and DNA degradation (Lev *et al.*, 2003). The apoptotic process is caused by a cascade of events in which a family of cysteine proteases known as caspases leads to cleavage of multiple cellular substrates (Lev *et al.*, 2003; Yacoubian & Standaert, 2009). According to Schulz and Gerhardt (2001), condensation and fragmentation of nuclear chromatin, compaction of organelles, a decrease in cell volumes and alterations to the cell membrane are evidence of apoptosis. Lev *et al.* (2003) states that apoptotic cell death is characterised by factors that enhance the apoptotic process (i.e., *bax, bcl-x*) and others that inhibit the death process (e.g., *bcl-2,bcl-xL*). Research has revealed signs of both apoptotic and autophagic cell death in the substantia nigra of PD patients. However, alterations in cell death pathways are unlikely to be the primary cause of PD, but both apoptotic and autophagic cell death pathways are hypothesised to become activated in PD through oxidative stress, protein aggregation, excitotoxicity or inflammatory processes (Yacoubian & Standaert, 2009).

2.1.4.6 Loss of trophic factors

The brain-derived neurotrophic factor (BDNF), glial derived neurotrophic factor (GDNF) and nerve growth factor (NGF) have all been demonstrated to be reduced in the nigra in PD (Yacoubian & Standaert, 2009). *In vitro* studies have shown that neurotrophic factors support survival of embryonic dopaminergic neurons with varying degrees of specificity and potency (Siegel & Chauhan, 2000). Yacoubian and Standaert (2009) suggest that treatment with growth factors could constitute potential neuroprotective therapy in PD. The potent ability of

these agents to stimulate growth and arborisation of dopaminergic neurons suggests that they may be useful neuroprotective treatments, even if deficiency of factors is not the primary cause of the disease process (Yacoubian & Standaert, 2009).

2.2 Monoamine oxidase

2.2.1 General background and tissue distribution

In 1928, Mary Hare-Bernheim characterised an enzyme catalysing the oxidative deamination of tyramine, which she named tyramine oxidase. A few years later Hugh Blaschko found that tyramine oxidase, norepinephrine oxidase and aliphatic oxidase are the same enzyme, capable of metabolising primary, secondary and tertiary amines, but not diamines (Youdim & Bakhle, 2006). It was Zeller who eventually named it MAO. MAO catalyses the oxidative deamination of monoamines including 5-hydroxytryptamine (5-HT/serotonin), histamine, and the catecholamines DA, epinephrine and norepinephrine (Youdim *et al.*, 2006).

The isoforms of MAO, MAO-A and MAO-B have different pH optima and sensitivity to heat inactivation (Youdim & Bakhle, 2006). These isoforms were originally distinguished by their sensitivities to acetylinic inhibitors clorgyline and selegiline (Youdim & Bakhle, 2006). MAO is located in the outer mitochondrial membrane, although a small proportion of each of the MAO isoenzymes is associated with the microsomal fraction (Youdim *et al.*, 2006). The active site of MAO contains FAD, a cofactor at which irreversible inhibitors of MAO are covalently linked (Prisinzano, 2006; Youdim *et al.*, 2006).

Table 2.1: Distribution of MAO-A and MAO-B in man and in the brains of selected species

Tissue	% of total activity	
	MAO-A	MAO-B
Liver	45	55
Gastrointestinal tract	<80	>20
Kidneys	25	75
Lungs	55	45
Platelets	<5	>95
Brain		
Human	<20	>80
Guinea pig	20	80
Cat	25	75
Pig	40	60
Rat	55	45

(Foley *et al.*, 2000)

2.2.2 Biological function of MAO-B

According to Youdim *et al.* (2006) MAO in peripheral tissues such as the intestines, the liver and the placenta protect the body by oxidising amines from the blood or preventing entry into circulation. Research suggests that intraneuronal MAO in the PNS and CNS protect neurons from exogenous amines, terminate actions of amine neurotransmitters and regulate the contents of intracellular amine stores (Youdim *et al.*, 2006). MAO-B in serotonergic neurons eliminates exogenous amines and minimise their access to synaptic vesicles, thus contributing to the purity of serotonin delivered to the synaptic cleft (Youdim *et al.*, 2006). However, recent studies have shown that elevated MAO-B levels induce apoptosis in neuronal and kidney cells (Binda *et al.*, 2002).

2.2.3 Substrate specificities

MAO-A is irreversibly inhibited by low concentrations of clorgyline and it metabolises serotonin and norepinephrine, whereas MAO-B is inhibited by low concentrations of selegiline, and is active towards benzylamine and 2-phenylethylamine as substrates (Youdim & Bakhle, 2006; Youdim *et al.*, 2006). On the other hand, DA, norepinephrine,

epinephrine, tryptamine and tyramine are equally well metabolised by both forms of the enzyme (Youdim & Bakhle, 2006; Youdim *et al.*, 2006).

Table 2.2: Substrate specificities of MAO in the cerebral cortex.

Substrate	MAO-A			MAO-B		
	K_m (µM)	V_{max} (pmol min^{-1} mg $protein^{-1}$)	V_{max}/K_m (µmol M^{-1} min^{-1} mg $protein^{-1}$)	K_m (µM)	V_{max} (pmol min^{-1} mg $protein^{-1}$)	V_{max}/K_m (µmol M^{-1} min^{-1} mg $protein^{-1}$)
Epinephrine	125 ± 42	379 ± 54	3.03 ± 1.11	266 ± 9	456 ± 61	1.75 ± 0.23
Dopamine	212 ± 33	680 ± 123	3.21 ± 0.77	229 ± 33	702 ± 158	3.07 ± 0.82
Serotonin	137 ± 24	228 ± 31	1.66 ± 0.37	1093 ± 20	6.6 ± 1.3	0.006 ± 0.001
Norepinephrine	284 ± 17	561 ± 42	1.98 ± 0.19	238 ± 30	321 ± 13	1.35 ± 0.18
2-Phenylethylamine	140 ± 22	20 ± 8	0.14 ± 0.06	4 ± 2	309 ± 24	77.3 ± 39.1
Tryptamine	35 ± 6	58 ± 5	1.66 ± 0.32	35 ± 8	108 ± 2	2.84 ± 0.60
Tyramine	127 ± 18	182 ± 28	1.43 ± 0.30	107 ± 21	343 ± 48	3.21 ± 0.77

(Youdim *et al.*, 2006)

2.2.3.1 Genes and MAO

The genes encoding MAO-A and MAO-B are approximately 70% identical. They are located on the X-chromosome (Xp 11.23), each comprising 15 exons with identical intron-exon organisation, which suggests that they are derived from the same ancestral gene (Shih *et al.*, 1999; Youdim *et al.*, 2006). According to Youdim *et al.* (2006), MAO-B expression is regulated by the mitogen-activated protein kinase (MAPK) pathway.

Youdim *et al.* (2006) indicates that progesterone, testosterone, corticosteroids and glucocorticoids increase levels of MAO-A, but they have little effect on MAO-B. In addition, MAO-A is elevated in the endometrium, reproductive tissue and the brain when the levels of progesterone are high during the oestrus cycle (Youdim *et al.*, 2006). Shih *et al.* (1999) reports that MAO-A knockout mice have elevated brain levels of serotonin, norepinephrine, and DA, and manifest aggressive behaviour similar to human males with MAO-A gene

deletion. In contrast, MAO-B knockout mice do not exhibit aggression, and only levels of phenylethylamine are increased (Shih *et al.*, 1999).

2.2.4 Biological function of MAO-A

In rodents, MAO-A is present in the extraneuronal compartment and within the dopaminergic terminals, where it metabolises both intraneuronal and released DA (Youdim & Bakhle, 2006). The intraneuronal enzyme acts to maintain low concentrations of DA, norepinephrine and serotonin (Foley *et al.*, 2000; Youdim & Bakhle, 2006). Youdim and Bakhle (2006) note that MAO-A inhibition is a practical means of controlling DA levels in the brain, although DA is equally metabolised by both MAO-A and MAO-B.

2.2.4.1 The cheese reaction

MAO inhibitors, notably tranylcypromine induce an important adverse effect known as the cheese reaction (Youdim & Bakhle, 2006). Cheese reaction is the potentiation of sympathomimetic activity due to the presence of tyramine in cheese and fermented drinks such as beer and wine (Youdim & Weinstock, 2004; Youdim & Bakhle, 2006; Youdim *et al.*, 2006). Youdim and Bakhle (2006) state that under normal circumstances, dietary amines are extensively metabolised by MAO in the gut wall and the liver, and are thus prevented from entering the systemic circulation. Inhibition of peripheral MAO permits entry of unmetabolised tyramine and other monoamines into the circulatory system, and result in the release of norepinephrine from peripheral adrenergic neurons (Youdim & Bakhle, 2006).

The consequence of this release is a severe hypertensive reaction, which can be fatal (Youdim & Weinstock, 2004; Youdim & Bakhle, 2006). In contrast, selective MAO-B inhibitors do not cause the cheese effect because tyramine is effectively metabolised by intestinal MAO-A (Youdim *et al.*, 2006). Youdim *et al.* (2006) note that MAO-B inhibitors do not promote the cheese reaction unless administered at concentrations high enough to inhibit MAO-A.

2.2.4.2 MAO-A in depression

Norepinephrine and epinephrine are substrates of MAO-A that are implicated in depression. Youdim and Bakhle (2006) state that non-selective, irreversible inhibitors of MAO-A (clorgyline, tranylcypromine) have antidepressant effects, however, the major disadvantage of these early inhibitors was the incidence of the cheese reaction (Youdim & Bakhle, 2006). In contrast, reversible MAO-A inhibitors (e.g. moclobemide) also exhibit desirable antidepressant effects (Youdim & Weinstock, 2004). Reversible MAO-A inhibitors can be displaced by tyramine from the active site of the enzyme, thereby enabling the amine to be

metabolised, and thus preventing its entrance into the circulation (Youdim & Weinstock, 2004).

The combination of reversible MAO-A and MAO-B inhibitors may be useful in the treatment of therapy-resistant depression (Youdim & Bakhle, 2006). However, the combination of MAO inhibitors with uptake inhibitors, either tricyclic antidepressants (TCAs) or selective serotonin reuptake inhibitors (SSRIs), should be avoided because such combinations may provoke the serotonin syndrome (Youdim & Bakhle, 2006).

2.2.4.3 The serotonin syndrome

The serotonin syndrome is a potentially life-threatening drug reaction that occurs as a result of overstimulation of intrasynaptic 5-HT_{1A} receptors by SSRIs, TCAs, MAO inhibitors and other serotonergic agents in central grey nuclei and the medulla (Gillman, 1999; Birmes *et al.*, 2003). Symptoms of the serotonin syndrome include akinesia-like restlessness, muscle twitches and myoclonus, hyperreflexia, sweating, penile erection, shivering and coma, and the onset of symptoms is observed within 24 hours following administration or overdose of the serotonergic agent (Birmes *et al.*, 2003; Bruton *et al.*, 2008).

2.2.5 The role of MAO-B in PD

MAO-B is implicated in the pathogenesis of PD because of its ability to oxidise DA and produce H_2O_2 (Kurth *et al.*, 1993). According to Youdim *et al.* (2006), the aldehyde and H_2O_2 products of MAO catalysis are neurotoxic, and have been shown to cause lesions of midbrain neurons *in vivo*. MAO-B also produces MPP^+, the active neurotoxin of MPTP metabolism (Kurth *et al.*, 1993). Inhibition of mitochondrial electron transport by MPP^+ results in impaired Ca^{2+} homeostasis and increased production of ROS such as superoxide (Youdim *et al.*, 2006). In addition, elevated production of superoxide may lead to formation of toxic hydroxyl radicals, or react with NO to form $ONOO^-$ (Dauer & Przedborski, 2003). These species may cause cellular damage by reacting with nucleic acids, proteins and lipids (Dauer & Przedborski, 2003).

2.2.5.1 Metabolism of DA

Oxidative stress is strongly associated with DA metabolism because degradation of DA generates ROS and its oxidation can lead to endogenous neurotoxins (Meiser *et al.*, 2013). DA is synthesised in the cytosol of catecholaminergic neurons, where L-tyrosine is hydroxylated at the phenol ring by tyrosine hydroxylase (TH), to yield L-dopa. This oxidation is regulated by tetrahydrobiopterin (BH_4), a cofactor which is synthesised from guanosine triphosphate (GTP), by GTP cyclohydrolate (GTPCH) (Meiser *et al.*, 2013). According to Meiser *et al.* (2013), the next step is decarboxylation of L-dopa to DA by AADC (also known

as dopa decarboxylase). Meiser *et al.* (2013) states that the synaptic vesicles are emptied into the synaptic cleft to interact with the post-synaptic DA receptors or the pre-synaptic DA autoreceptors upon excitation of the dopaminergic neurons.

Furthermore, DA is sequestered into the synaptic storage vesicles by vesicular monoamine transporter 2 (VMAT2) after neuronal uptake by DAT (Meiser *et al.*, 2013). MAO degrades DA in the cytosol due to leakage from the synaptic vesicle, leading to the production of H_2O_2 and the reactive 3,4-dihydroxyphenylacetaldehyde (DOPAL) (Meiser *et al.*, 2013). According to Meiser *et al.* (2013), DOPAL can be inactivated by either reduction to the corresponding alcohol 3,4-dihydroxyphenylethanol (DOPET), or by further oxidation to the carboxylic acid 3,4-dihydroxyphenylacetic acid (DOPAC), by alcohol dehydrogenase (ADH) or aldehyde dehydrogenase (ALDH), respectively. DA in the synaptic cleft is also taken up by surrounding glial cells, which readily degrade it by the action of MAO and COMT (Meiser *et al.*, 2013).

2.2.5.2 Generation of toxic by-products

MAO catalyses the oxidative deamination of catecholamines norepinephrine, epinephrine, DA, as well as monoamines serotonin and histamine to the corresponding aldehyde, H_2O_2 and either ammonia or a substituted amine (Youdim *et al.*, 2006). Studies have shown that DA is mainly oxidised by MAO-B in the human and by MAO-A in rats (Meiser *et al.*, 2013). On the other hand, the neurotoxin MPTP is metabolised selectively by MAO-B to the active toxin MPP^+ in both rats and primates (Youdim & Bakhle, 2006; Meiser *et al.*, 2013).

Meiser *et al.* (2013) suggest that L-dopa and DA are oxidised enzymatically, by metals (Fe^{3+}) or even spontaneously yielding highly reactive electron-poor ortho-quinones such as dopa-quinone and DA-quinone. According to Meiser *et al.* (2013), DA can also be enzymatically oxidised by COX, tyrosine and other enzymes. In addition, DA-quinone can react further to form the neurotoxin 6-OHDA in the presence of iron (Meiser *et al.*, 2013). DA-quinones are also precursors for the enzymatic formation of tetrahydroquinolines such as salsinol, an endogenous neurotoxin which causes oxidative stress and mitochondrial damage by inhibition of the electron transport chain (Meiser *et al.*, 2013).

2.2.5.3 MAO levels in the brain and aging

Analyses of human brain post-mortem samples report that MAO-B activity increases with age and in neurodegenerative diseases, and it has been proposed that this increase reflects age-associated increases in glial cells (Fowler *et al.*, 1997; Nicotra *et al.*, 2004). However, there is little or no variation in MAO-A activity (Nicotra *et al.*, 2004). Nicotra *et al.* (2004) reported that MAO-A activity is high at birth, it decreases rapidly during the first 2 years and

remains constant thereafter. In contrast, MAO-B remains constant during early childhood and rises during advanced age (Nicotra *et al.*, 2004). According to Fowler *et al.* (1997), the age related increase in MAO-B is consistent with the compartmentalisation of MAO-B within the cell bodies of serotonergic neurons and in glial cells. Studies propose that age-related increases in brain MAO-B increase oxidative stress, thus contributing to an increase in susceptibility to neurodegeneration (Fowler *et al.*, 1997; Nicotra *et al.*, 2004).

2.2.5.4 The role of aldehyde dehydrogenase and GPO

The aldehyde produced from the oxidative deamination of catecholamines is rapidly metabolised by aldehyde dehydrogenase to acidic metabolites such as 5-hydroxyindole acetic acid (5-HIAA) from serotonin, or DOPAC from DA. These products are commonly used as the measure of MAO activity *in vitro* and *in vivo* (Youdim & Bakhle, 2006). The main by-product of monoamine oxidation by MAO is H_2O_2. This is inactivated in the brain mainly by GPO, which uses GSH as a cofactor (Youdim & Bakhle, 2006). According to Youdim and Bakhle (2006) deficiency of GSH in addition to an increase in MAO and iron may lead to generation of the highly reactive free hydroxyl radical from H_2O_2 via the Fenton reaction. The hydroxyl radical depletes cellular antioxidants and reacts with and damages lipids, proteins and DNA, thus increasing oxidative damage to neurons (Youdim & Bakhle, 2006).

2.2.6 The potential role of MAO-A in PD

MAO-A is present in the extraneuronal compartment and within the dopaminergic terminals, where it is involved in metabolism of both neuronal and released DA (Youdim & Weinstock, 2004; Youdim & Bakhle, 2006). However, little attention is paid to the inhibition of MAO-A in PD, even though DA is as well metabolised by MAO-A as it is by MAO-B in the striatum (Youdim & Bakhle, 2006). Numerous studies in rats have shown that inhibition of MAO-A with either reversible (moclobemide) or irreversible (clorgyline) inhibitors increases brain norepinephrine and serotonin levels but has little effect on DA levels (Youdim & Weinstock, 2004). However, striatal microdyalisis in rats showed that moclobemide significantly increases DA release (Youdim & Weinstock, 2004). Youdim and Weinstock (2004), indicate that intraneuronal inhibition of MAO-A by moclobemide may account for prolonged duration of the motor response to L-dopa.

2.2.7 Irreversible MAO-B inhibitors

Two currently available selective, irreversible MAO-B inhibitors for the treatment of PD, selegiline and rasagiline, are used as monotherapy in early PD and as adjunctive therapy to L-dopa and DA agonists in late stage PD (Fernandez & Chen, 2007; Robakis & Fahn, 2015).

2.2.7.1 Selegiline

Selegiline is an irreversible selective MAO-B inhibitor that delays the progression of PD inhibiting the oxidative deamination of DA, phenylethylamine and benzylamine, but not that of norepinephrine and serotonin at lower doses (Youdim & Bakhle, 2006; Robakis & Fahn, 2015). However, selegiline loses its selectivity at higher doses (Youdim & Bakhle, 2006). Selegiline also prevents apoptosis by altering gene expression for pro- and antiapoptotic proteins, resulting in the preservation of mitochondrial integrity during oxidative stress (Fernandez & Chen, 2007).

2.2.7.2 Pargyline

Research has shown that pargyline irreversibly binds to MAO-B and prevents both clinical and neuropathological evidence of the neurotoxic effects of MPTP by inhibiting conversion of MPTP to MPP^+ (Langston *et al.*, 1984).

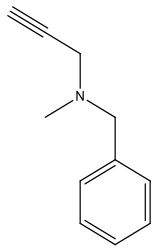

Figure 2.15: Structure of pargyline

2.2.7.3 Rasagiline

Rasagiline is a selective irreversible MAO-B inhibitor that can be used alone or in combination with other PD medications from early to late stages of the disease (Robakis & Fahn, 2015). According to Youdim *et al.* (2005), rasagiline activates the antiapoptotic pathways involved in the collapse of the mitochondrial membrane potential by activation of Bcl-2, Bcl-X1 and downregulation of Bad and Bax at the level of the mitochondria. In animal models of MPTP-induced parkinsonism, pretreatment with rasagiline inhibits degeneration of dopaminergic nigral cells (Fernandez & Chen, 2007). Rasagiline also protects dopaminergic cells and cerebellar granule cells from challenges with 6-OHDA, N-methyl-(R)-salsolinol and N-morpholinosydonimine in experimental models of PD (Fernandez & Chen, 2007).

2.2.7.4 Ladostigil

According to Youdim and Bakhle (2006), ladostigil is a cholinesterase (ChE) inhibitor that is structurally related to rasagiline, which possesses neither MAO-A or MAO-B inhibition properties *in vitro* or acutely *in vivo* (Youdim & Bakhle, 2006). However, chronic treatment with ladostigil irreversibly inhibits both brain MAO isoforms (Youdim & Bakhle, 2006).

Studies have demonstrated that non-selective inhibition of MAO by ladostigil increases the levels of norepinephrine, serotonin and DA in the hipoccampus and striatum of rats and mice (Youdim & Bakhle, 2006). Furthermore, ladostigil prevented striatal neurodegeneration and DA depletion induced by neurotoxin MPTP in the mouse model of PD (Youdim & Bakhle, 2006). By inhibiting both isoforms of MAO, ladostigil markedly increases brain DA in MPTP-mouse models. (Youdim & Bakhle, 2006).

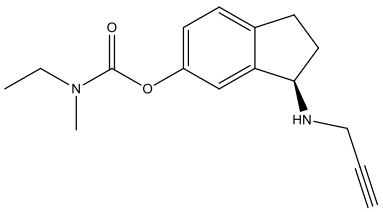

Figure 2.16: Structure of ladostigil

2.2.8 Reversible inhibitors of MAO-B

2.2.8.1 Lazabemide

In mouse models, lazabemide prevents striatal neurodegeneration and DA depletion caused by MPTP (Youdim & Bakhle, 2006). Lazabemide can be combined with a reversible MAO-A inhibitor (moclobemide) in the treatment of therapy resistant depression and it potentiates the effect of L-dopa and prevents the production of MPP^+ from MPTP (Berlin *et al.*, 2002; Youdim & Bakhle, 2006).

2.2.8.2 Isatin

Isatin is an endogenous competitive inhibitor of MAO which binds with similar affinities to both MAO-A and MAO-B (Hubalek *et al.*, 2005). Studies have demonstrated that isatin significantly increases striatal DA in the brain tissue of a rat model of PD (Minami *et al.*, 1999). Isatin also improves bradykinesia in Japanese encephalitis virus (JEV)-induced parkinsonism in rats. These findings suggest that isatin could be a possible treatment for PD (Ogata *et al.*, 2003).

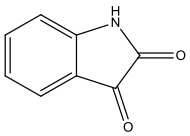

Figure 2.17: Structure of isatin

2.2.8.3 (E)-8-(Chlorostyryl)caffeine

(E)-8-(Chlorostyryl)caffeine (CSC) is a specific adenosine A_{2A} antagonist that possesses MAO-B inhibitory properties *in vitro* (Chen *et al.*, 2002). Research has demonstrated that

CSC blocks the MAO-B catalysed oxidation of MPTP to the active neurotoxin, MPP^+ *in vivo* (Chen *et al.*, 2002). According to Chen *et al.* (2002) pre-treatment of mice with CSC lessens MPTP-induced loss of striatal DA. Because of its ability to inhibit both MAO-B and A_{2A} receptors, CSC also has enhanced neuroprotective potential (Chen *et al.*, 2002).

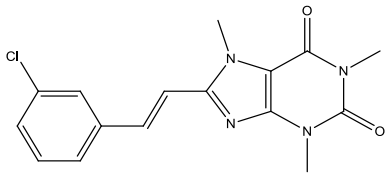

Figure 2.18: Structure of (E)-8-(chlorostyryl)caffeine

2.2.8.4 1,4-Diphenylbutene

1,4-Diphenylbutene is a reversible inhibitor of MAO-B which occupies both the entrance and the substrate cavity space in the enzyme. These findings provide a rationale for development of MAO-B specific inhibitors (Binda *et al.*, 2003).

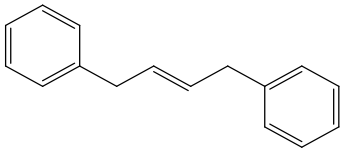

Figure 2.19: Structure of 1,4-diphenylbutene

2.2.8.5 Trans,trans-farnesol

The inhibitory activity of *trans,trans*-farnesol evaluated on human placental mitochondrial MAO-A and human liver mitochondrial MAO-B revealed that this compound is a potent inhibitor of human liver MAO-B activity, but is inactive against human placenta MAO-A (Khalil *et al.*, 2006).

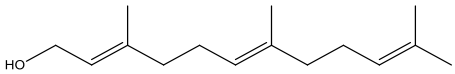

Figure 2.20: Structure of trans,trans-farnesol

2.2.8.6 Safinamide

Safinamide is used as an adjunct to L-dopa and can be used in combination with other PD medications in mid- to late-stage PD (Robakis & Fahn, 2015). However, unlike selegiline and rasagiline, safinamide blocks voltage dependant sodium channels and also inhibits glutamate release (Robakis & Fahn, 2015). In addition, safinamide possesses an antidyskinetic effect due to its anti-glutamate activity (Robakis & Fahn, 2015). Like other MAO-B inhibitors, safinamide has neuroprotective properties *in vitro* and *in vivo*, and it has

been shown to prevent neuronal cell death in animal and tissue culture models (Robakis & Fahn, 2015).

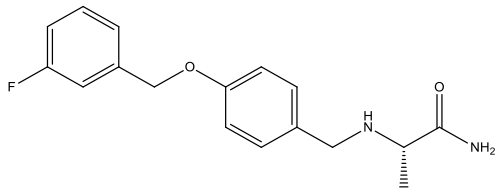

Figure 2.21: Structure of safinamide

2.2.9 Inhibitors of MAO-A

2.2.9.1 Clorgyline

Finberg (2014) indicates that clorgyline is an irreversible MAO inhibitor that has high potency for MAO-A, but not for MAO-B. Early studies defined a dosage range for effective inhibition of MAO-A in rats and showed that clorgyline has a similar degree of efficacy for inhibition of MAO in the CNS and peripheral tissues when administered by subcutaneous injection (Finberg, 2014). Although clorgyline increased brain levels of norepinephrine and serotonin, and showed antidepressant activity in a series of clinical trials, it was abandoned as an antidepressant due to the cheese-reaction, caused by this drug (Youdim & Bakhle, 2006).

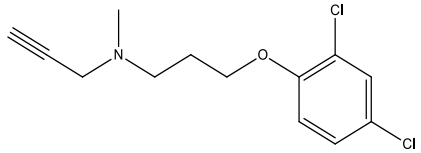

Figure 2.22: Structure of clorgiline

2.2.9.2 Tranylcypromine and phenelzine

Tranylcypromine is the currently used cyclopropamine that was developed for inhibition of MAO in the treatment of depression (Finberg, 2014). According to Finberg (2014), tranylcypromine is a highly effective and rapidly acting irreversible inhibitor of both MAO isoforms. Studies performed on rat brain demonstrated that different doses of tranylcypromine inhibited the MAO oxidation of serotonin, phenylethylamine and DA as measured *in vitro,* and produced a similar effect *in vivo* (Green & Youdim, 1975). However, tranylcypromine is not commonly used today because of the possible danger of the cheese effect (Finberg, 2014). On the other hand, phenelzine is one of the first MAO inhibitors that was discovered accidentally after chemical modification of the anti-tuberculosis (TB) drug, isoniazid (Finberg, 2014).

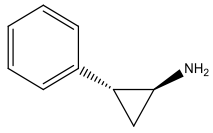

Tranylcypromine

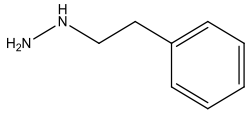

Phenelzine

Figure 2.23: Structures of tranylcypromine and phenelzine

According to Finberg (2014), phenelzine was in clinical use for treatment of depression until it was discovered that it causes the cheese reaction. Studies show that MAO-B metabolises phenelzine to yield phenylacetic acid and p-hydroxyphenylacetic acid as major metabolites, and N-acetylphenelzine as a minor metabolite (Finberg, 2014). The latter was found to be an active MAO inhibitor in rat brain (Finberg, 2014). It has recently been discovered that phenelzine is also converted to N2-phenylethylidenehydrazine by MAO-B, but inhibition of this metabolite does not increase brain neurotransmitter levels as does phenelzine (Finberg, 2014). Finberg (2014) reports that phenelzine also increases brain levels of γ-Aminobutyric acid (GABA) and alanine in rats by inhibiting GABA and alanine transaminases.

2.2.9.3 Moclobemide and brofaromine

Moclobemide is somewhat less effective, although better tolerated than other MAO inhibitors such as phenelzine or tranylcypromine (Lotufo-Neto *et al.*, 1999). Moclobemide is a reversible MAO-A inhibitor that is devoid of the cheese reaction because it is readily displaced from its MAO-A binding site by tyramine (Lotufo-Neto *et al.*, 1999). Brofaromine is a reversible MAO-A inhibitor that is used in treatment of depression (Lotufo-Neto *et al.*, 1999). Lotufo-Neto *et al.* (1999) states that both moclobemide and brofaromine have short durations of MAO-A inhibition and they are reversibly displaced from the enzymatic site by substrates such as tyramine, DA and serotonin. In conclusion, both moclobemide and brofaromine are effective antidepressants and they are safer and better tolerated than the older, non-selective, and irreversible MAO inhibitors (Lotufo-Neto *et al.*, 1999).

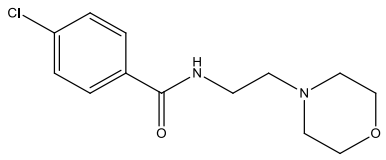

Moclobemide

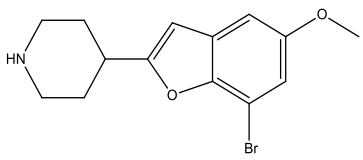

Brofaramine

Figure 2.24: Structures of moclobemide and brofaromine

2.2.9.4 Iproniazid

The MAO inhibitory activity of an anti-TB drug, isoniazid, was discovered by chance, and this led to production of a related compound iproniazid, which became the first MAO inhibitor to

be used successfully in the treatment of depression (Youdim & Bakhle, 2006). Although iproniazid demonstrated remarkable antidepressant activity, it caused liver toxicity because of its hydrazine structure (Youdim & Bakhle, 2006).

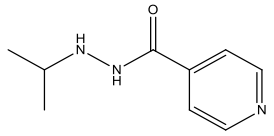

Figure 2.25: Structure of iproniazid

2.2.10 The three dimensional structure of MAO-B

Human MAO-B crystallises as a dimer and it is divided into three domains, the flavin binding domain, substrate binding domain and the membrane binding domain (Edmondson *et al.*, 2004). The active site consists of two cavities. The first cavity, termed the entrance cavity, is very hydrophobic in nature, and it exhibits a volume of 290 $Å^3$ (Youdim *et al.*, 2006). Edmondson *et al.* (2007) states that the substrate cavity is flat, similarly hydrophobic to the entrance cavity and exhibits a volume of 390 $Å^3$, with the covalently bound FAD coenzyme at the distal end (Youdim *et al.*, 2006; Edmondson *et al.*, 2007). According to Edmondson *et al.* (2007), the entrance and the substrate cavities are separated by an Ile199 side chain which serves as a gate between the two cavities. The FAD coenzyme at the end of the substrate cavity is covalently bound in an 8α-thioether linkage to Cys397. In addition, when analysed using the computer program GRID, both active sites cavities are very hydrophobic, with sites for favourable amine binding close to the flavin involving two near parallel tyrosyl (398 and 435) residues that form the aromatic cage (Edmondson *et al.*, 2007).

The covalently bound FAD is shown to be in a hydrophobic environment within the enzyme with specific interactions dominated by H-bonding to either side chains or peptide bonds in the protein (Edmondson *et al.*, 2004). Edmondson *et al.* (2004) note that the only electrostatic interaction is between the amino pyrophosphate of the FAD and the positively charged guanidine group of Arg42. Furthermore, the ribose ring of the FAD adenosine moiety is specifically H-bound to the carboxylate of Glu34, to the guanidine group of Arg36 and to a water molecule (Edmondson *et al.*, 2004). Mutations of Glu34 to Ala, Asp or Gln results in over 90% loss in catalytic activity of the mutant MAO-B (Edmondson *et al.*, 2004).

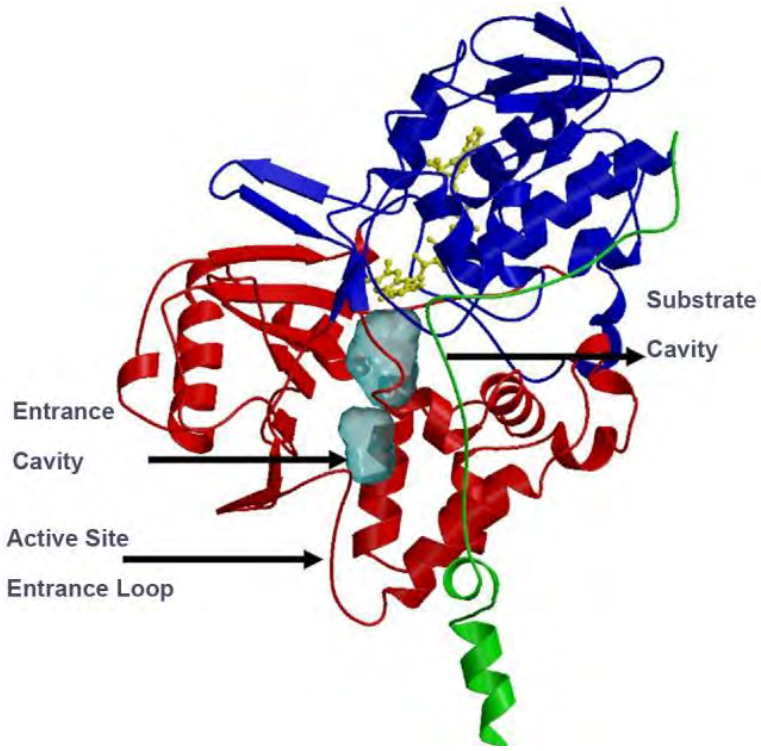

Figure 2.26: **Structure of human MAO-B. The covalent flavin moiety is shown in a ball and stick model in yellow. The flavin binding domain is in blue, the substrate domain is in red and the membrane binding domain is in green (Edmondson *et al.*, 2007).**

2.2.11 The three dimensional structure of MAO-A

The overall structure of human MAO-A is similar to that of human MAO-B, but MAO-A crystallises as a monomer and has a single substrate binding cavity, with a protein loop at the entrance of the cavity (De Colibus *et al.*, 2005; Edmondson *et al.*, 2007). According to De Colibus *et al.* (2005), the inhibitor binding site is formed by a single cavity that extents from the flavin ring to the cavity-shaping loop consisting of residues 210-216. The cavity size of MAO-A is 550 $Å^3$ and is lined by 11 aliphatic and 5 aromatic residues, demonstrating that it is very hydrophobic (De Colibus *et al.*, 2005; Edmondson *et al.*, 2007). Like MAO-B, the *re* face of the covalent FAD is situated at the back of the active site with the two parallel tyrosyl residues (407 and 444) forming an aromatic cage in front of the flavin (Edmondson *et al.*, 2007).

Unlike MAO-B, the substrate cavity of MAO-A is shorter in length and wider (De Colibus *et al.*, 2005). Substrate entry into MAO- B involves entrance and substrate cavities that become fused with certain inhibitors bound, however, the active cavity of MAO-A does not have such a dipartite nature (De Colibus *et al.*, 2005).

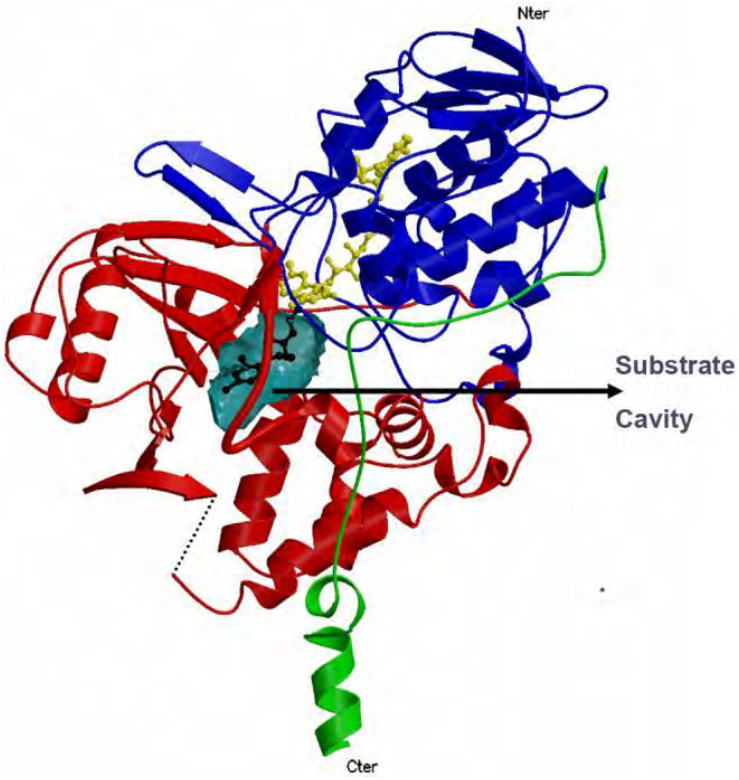

Figure 2.27: **Ribbon diagram of the human MAO A structure. The covalent flavin moiety is shown in a ball and stick model in yellow. The flavin binding domain is in blue, the substrate domain is in red and the membrane binding domain is in green (Edmondson *et al.*, 2007).**

2.2.12 *In vitro* measurements of MAO activity

There are numerous methods by which MAO activity can be determined, for example, monitoring disappearance of substrates or formation of products such as H_2O_2 and aldehydes (Yan *et al.*, 2004). H_2O_2 formed by MAO can be determined using either fluorometric or luminometric assays, whereas aldehydes generated by deamination can be measured by spectrophotometry, fluorometry, liquid chromatography and radiometry (Yan *et al.*, 2004).

However, most of these methods have many disadvantages including low sensitivity, non-specificity for substrates and requirement of high enzyme concentrations (Yan *et al.*, 2004). The use of oxygen by the MAO enzymes and the formation of H_2O_2 are the only methods for the measurement of enzyme activity that are independent of the nature of the substrate. In this respect is the polarographic determination of oxygen consumption, an accurate method of measuring MAO activity (Holt *et al.*, 1997).

Alternatively, kynuramine can be used as a non-selective *in vitro* MAO substrate (Yan *et al.*, 2004). Deamination catalysed by MAO converts kynuramine to 3-(2-aminophenyl)-3-

oxopropionaldehyde as an intermediate that can be intramolecularly condensed to yield 4-hydroxyquinoline (Yan *et al.*, 2004). According to Yan *et al.* (2004), conversion of 3-(2-aminophenyl)-3-oxopropionaldehyde to 4-hydroxyquinoline is rapid and complete, thus, MAO activity can be measured by specifically determining the formation of 4-hydroxyquinoline.

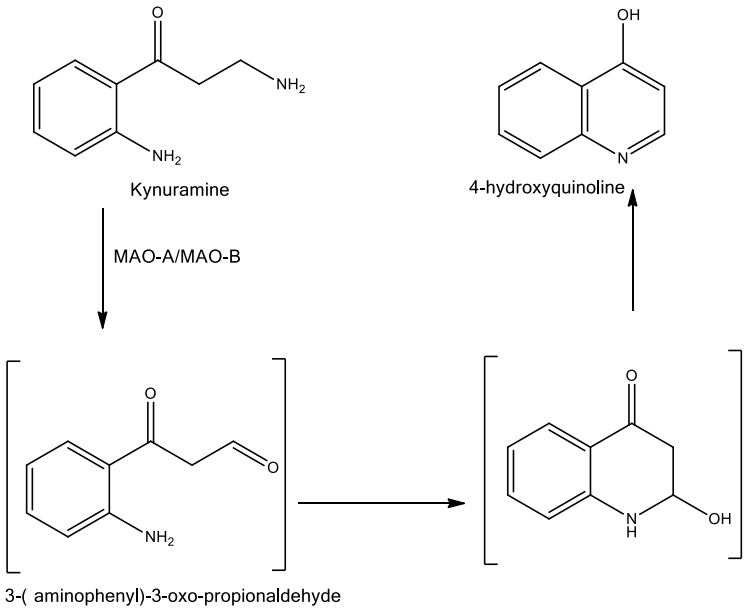

Figure 2.28: Conversion of kynuramine to 4-hydroxyquinoline by MAO (Yan *et al.*, 2004).

2.3 Enzyme kinetics

2.3.1 Michaelis-Menten kinetics

Enzymatic reactions obeying Michaelis-Menten kinetics in the presence of varying concentrations of single inhibitors have been described in terms of types of inhibitors, the inhibitor may be competitive, uncompetitive or non-competitive (Chou & Talaly, 1977). For a given enzymatic reaction and inhibition mechanism, rate equations specific for each circumstance can be derived with steady state or rapid equilibrium analysis. According to Chou and Talaly (1977), these rate equations always contain the maximum velocity term as well as kinetic constants and concentration factors for each of the substrates and inhibitors. The Michaelis-Menten equation mathematically illustrates the relationship between initial velocity (V_i) and substrate concentration [S] (Bender *et al.*, 2003).

$$V_{\mathrm{i}} = \frac{Vmax[S]}{Km + [S]}$$

In this equation, K_m (Michaelis constant) is the substrate concentration at which V_i is half the maximal velocity ($V_{max}/2$) attainable at a particular concentration of the enzyme. According to

Bender *et al.* (2003), the Michaelis-Menten equation may be evaluated under three conditions to illustrate the dependence of initial reaction velocity on [S] and K_m:

1. When [S] is much less than K_m, the term K_m + [S] is essentially equal to K_m.

$$V_i = \frac{Vmax[S]}{Km + [S]} \approx \frac{Vmax[S]}{Km} \approx (\frac{Vmax}{Km})[S]$$

V_{max} and K_m are both constants and their ratio is constant, therefore when [S] is considerably less than K_m, V_i is directly proportional to K[S], and the initial reaction velocity is directly proportional to [S] (Bender *et al.*, 2003)

2. When [S] is much greater than K_m, the term K_m + [S] is essentially equal to [S].

$$V_i = \frac{Vmax[S]}{Km + [S]} \approx \frac{Vmax[S]}{[S]} \approx Vmax$$

Thus, when [S] greatly exceeds K_m, the reaction velocity is maximal (V_{max}) and unaffected by further increase in substrate concentration.

3. When [S] = K_m.

$$V_i = \frac{Vmax[S]}{Km + [S]} = \frac{Vmax}{2}$$

2.3.1.1 K_m and V_{max} determinations

K_m and V_{max} are determined using a linear form of Michaelis-Menten equation, where the numeric value of V_{max} is directly measured. The linear form of the Michaelis-Menten equation permits extrapolation of V_{max} and K_m from initial velocity data obtained at less than saturating conditions of the substrate.

Starting with:

$$V_i = \frac{Vmax[S]}{Km + [S]}$$

When inverted,

$$\frac{1}{V_i} = \frac{Km + [S]}{Vmax[S]}$$

When factored,

$$\frac{1}{V_i} = \frac{Km}{Vmax} + \frac{[S]}{Vmax[S]}$$

And when simplified:

$$\frac{1}{V_i} = \left(\frac{Km}{Vmax}\right)\frac{1}{[S]} - \frac{1}{Vmax}$$

The above equation is the equation for a straight line, y = ax + b, where y = $1/V_i$ and x = 1/[S]. A plot of $1/V_i$ as a function of 1/[S] gives a straight line whose y-intercept is equal to $1/V_{max}$, and whose slope is equal to K_m/V_{max}. This plot is called a double reciprocal or Linweaver-Burke plot (Bender *et al.*, 2003). Setting the y term of the equation equal to zero and solving for x reveals that the x-intercept is equal to $-1/K_m$. Thus K_m is easily calculated from the x-intercept.

2.3.1.2 K_i determination and competitive inhibition

According to Bender *et al.* (2003), most classic competitive inhibitors are structurally similar to substrates, and thus they are termed substrate analogues. In competitive inhibition, the inhibitor (I) frequently binds to the substrate binding site of the active site of the enzyme and blocks access of the substrate. Binding of the substrate and the inhibitor to the active site of the enzyme forms an enzyme-substrate complex (ES) and an enzyme-inhibitor complex (EI), respectively (Bender *et al.*, 2003). The formation and dissociation of the EI complex is a dynamic process described by:

$$EI \underset{K_{-1}}{\overset{K_1}{\rightleftharpoons}} E + I$$

For this process, the equilibrium constant K_i is:

$$K_i = \frac{[E][I]}{[EI]} = \frac{K_1}{K_{-1}}$$

K_i can be determined graphically using a method described by Dixon (1953). Plotting $1/V_i$ against [I] when [S] is constant results in a straight line (Dixon, 1953). If plots are made at two different substrate concentrations $[S]_1$ and $[S]_2$, the lines will intersect at a point on the left of the y-axis, which lies at $-K_i$ and can be read off directly (Dixon, 1953).

2.3.1.3 IC_{50} determination

IC_{50} is the inhibitory concentration of a drug that gives half-maximal response and its value depends on concentration of the enzyme, the inhibitor and the substrate (Cer *et al.*, 2009).

$$IC_{50} = K_i(1 + \frac{[S]}{Km})$$

When the [S] used in the assay is much lower than K_m, IC_{50} values approximate K_i. When [S] is significantly smaller than K_m, [S]/K_m approaches zero, and IC_{50} approaches K_i. IC_{50} is always higher than K_i in competitive inhibition (Burlingham & Widlanski, 2003). Similar to competitive inhibition, IC_{50} values for uncompetitive inhibitors also are always higher than K_i. However, for uncompetitive inhibitors, IC_{50} values approximate K_i when the [S] used in the assay is much higher than K_m. At large values of [S], the ratio K_m/[S] approaches zero, and IC_{50} approaches K_i (Burlingham & Widlanski, 2003).

Mathematically, the relationship between K_i and IC_{50} for uncompetitive inhibition is represented as follows:

$$IC_{50} = K_i(1 + \frac{Km}{[S]})$$

2.4 Animal models of PD

2.4.1 MPTP

2.4.1.1 General background

Researchers have discovered that inadvertent injection with MPTP results in clinical symptoms similar to sporadic PD in humans (Betarbet *et al.*, 2002). In 1982, young drug users developed a rapidly progressive parkinsonian syndrome traced to intravenous use of street preparation of 1-methyl-4-phenyl-4-propionoxipiperidine (MPPP), an analogue of the narcotic meperidine (Dauer & Przedborski, 2003). Illicit synthesis of MPPP led to the production of a neurotoxic contaminant, MPTP. According to Betarbet *et al.* (2002), MPTP crosses the BBB and is metabolised by MAO-B in astrocytes to MPP^+. Exposure to MPTP results in nigrostriatal dopaminergic degeneration in a number of species including mice, cats and primates (Betarbet *et al.*, 2002). Betarbet *et al.* (2002) states that acute MPTP exposure results in specific degeneration of nigrostriatal dopaminergic pathway with 50% to 90% loss of DA in the striatum. MPTP exposure in primates mimics behavioural characteristics of PD including bradykinesia and rigidity (Betarbet *et al.*, 2002).

2.4.1.2 Mechanism of action

After administration, MPTP crosses the BBB and is first metabolised in astrocytes by MAO-B to yield 1-methyl-4-phenyl-2,3-dihydropyridine ($MPDP^+$). $MPDP^+$ then disproportionates to generate the corresponding pyridium species MPP^+ (Betarbet *et al.*, 2002; Smeyne &

Jackson-Lewis, 2005). Once converted to MPP^+ in the astrocytes, MPP^+ stimulates the up-regulation of TNF-α, IL-1β and IL-6, and these in turn up-regulate inducible NOS (Smeyne & Jackson-Lewis, 2005). According to Smeyne and Jackson-Lewis (2005), inducible NOS is minimally expressed in the normal brain and is upregulated in the substantia nigra's microglia in both PD and mice following MPTP treatment.

According to Smeyne and Jackson-Lewis (2005), inducible NOS produces large amounts of the uncharged and lipophilic molecule, NO, which can freely pass through membranes and travel distances greater than the length of a neuron. Since MPP^+ cannot freely exit from the glial environment, because of its high degree of polarity, it has been suggested that there may be a specific transporter that actively moves it out of the glia (Smeyne & Jackson-Lewis, 2005). Furthermore, once in the mitochondria, MPP^+ inhibits cellular respiration through blockade of the electron transport enzyme, nicotinamide adenine dinucleotide (NADH):ubiquinone oxidoreductase (Complex I), resulting in reduction of cellular ATP and neuronal toxicity (Smeyne & Jackson-Lewis, 2005).

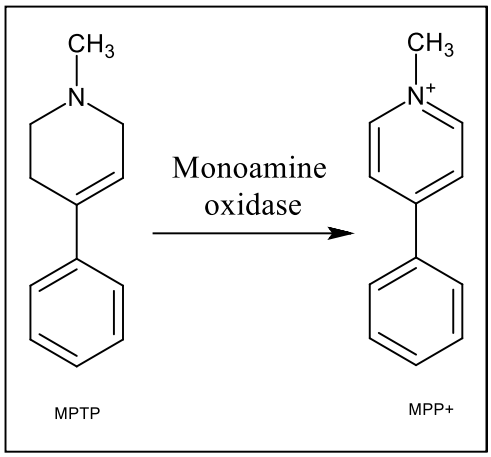

Figure 2.29: The conversion of MPTP to MPP^+

MPP^+ may also inhibit complexes III (ubiquinol:ferrocytochrome c oxidoreductase) and IV (ferrocytochrome *c*:oxygen oxidoreductase or cytochrome *c* oxidase) of the electron transport chain (Smeyne & Jackson-Lewis, 2005). NO produced and released by glial cells can enter the cytosol and react with the superoxide radical to form $ONOO^-$, one of the most destructive oxidising molecules (Smeyne & Jackson-Lewis, 2005).

2.4.2 6-OHDA

According to Betarbet *et al.* (2002), 6-OHDA was the first chemical agent discovered that had specific neurotoxic effects on catecholaminergic pathways. 6-OHDA does not cross the BBB, therefore it must be injected stereotactically into the substantia nigra, the nigrostriatal tract or striatum to specifically target the nigrostriatal pathway (Betarbet *et al.*, 2002;

Jackson-Lewis *et al.*, 2012). According to Jackson-Lewis *et al.* (2012), injection of 6-OHDA into the SNpc destroys approximately 60% of the TH-containing neurons in rat and mouse brains, with the subsequent loss of TH-positive terminals in the striatum.

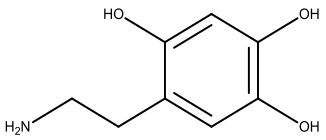

Figure 2.30: Structure of 6-OHDA

Jackson-Lewis *et al.* (2012) states that 6-OHDA uses the DAT to access the cytosol, where it can auto-oxidise, and hence generate intracellular oxidative stress. Researchers have reported that 6-OHDA-induced degeneration involves the generation of H_2O_2 and hydroxyl radicals in the presence of iron (Betarbet *et al.*, 2002). In addition, 6-OHDA leads to a reduction in GSH and superoxide dismutase (SOD) activity, and an increase in malondialdehyde levels in the striatum (Jackson-Lewis *et al.*, 2012). It has also been shown that 6-OHDA is toxic to mitochondrial complex I and DA produces lesions in the nigrostriatal pathway (Jackson-Lewis *et al.*, 2012).

2.4.3 Rotenone

Rotenone, a commonly used organic herbicide and insecticide, is highly lipophilic and readily crosses the BBB (Betarbet *et al.*, 2002; Dauer & Przedborski, 2003; Jackson-Lewis *et al.*, 2012). Studies have reported that chronic exposure to low doses of rotenone results in uniform inhibition of complex I throughout the rat brain (Betarbet *et al.*, 2002). According to Betarbet *et al.* (2002), rotenone also causes selective degeneration of the dopaminergic nigrostriatal pathway, selective striatal oxidative damage and formation of ubiquitin- and α-synuclein-positive inclusions in the nigral cells, which were similar to Lewy bodies of PD.

Betarbet *et al.* (2002) remarks that rotenone-exposed rats are hypokinetic with a flexed posture similar to the stooped posture of PD patients, while some animals developed severe rigidity and a few spontaneously shaking paws resembling resting tremor in PD. Another study of rats chronically infused with rotenone showed significant reductions in striatal dopamine- and cAMP-regulated phosphoprotein (DARPP)-32-positive, cholinergic, and nicotinamide adenine dinucleotide phosphate (NADPH) diaphorase-positive neurons (Dauer & Przedborski, 2003).

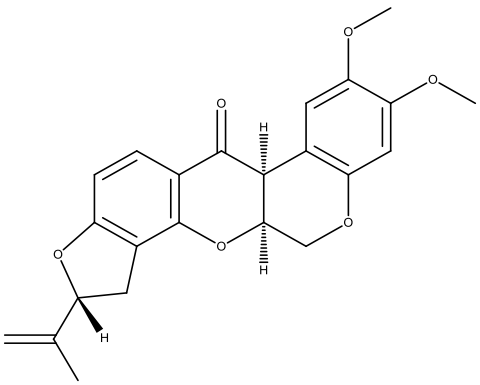

Figure 2.31: Structure of rotenone

2.4.4 Paraquat

1,1'-Dimethyl-4,4'-bipyridinium or paraquat is a widely used herbicide that exhibits structural similarity to MPP^+ (Betarbet *et al.*, 2002; Dauer & Przedborski, 2003; Jackson-Lewis *et al.*, 2012). Paraquat crosses the BBB slowly and to a limited extent, but unlike MPP^+, it exerts its toxicity through oxidative stress mediated by redox cycling. Paraquat thus generates ROS, particularly the superoxide radical, H_2O_2 and hydroxyl radicals that lead to the damage of lipids, proteins, DNA and ribonucleic acid (RNA) (Betarbet *et al.*, 2002; Dauer & Przedborski, 2003; Jackson-Lewis *et al.*, 2012).

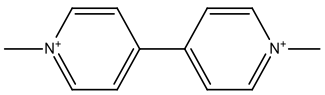

Figure 2.32: Structure of paraquat

Systemic paraquat administration to mice causes a dose-dependent decrease in dopaminergic nigral neurons and striatal dopaminergic innervation, accompanied by α-synuclein-containing inclusions as well as increases in α-synuclien immunostaining in the frontal cortex (Betarbet *et al.*, 2002; Dauer & Przedborski, 2003)

2.4.5 Gene-based models

Genetic mutations in PD are rare, and the majority of PD cases are sporadic and do not result from obvious genetic defects (Betarbet *et al.*, 2002; Jackson-Lewis *et al.*, 2012). Mutation in three genes, α-synuclein, parkin and UCHL-1, which appear to participate in the ubiquitin-proteasome pathway is often implicated in familial PD (Betarbet *et al.*, 2002; Dauer & Przedborski, 2003). Dauer and Przedborski (2003) remark that PD-causing mutations in the gene DJ-1 have recently been identified, and this protein also appears to have a potential link to the ubiquitin-proteasome pathway. On the other hand, transgenic mice expressing human α-synuclein demonstrate a number of PD features, including loss of

nigrostriatal dopaminergic terminals in the striatum, development of α-synuclein and ubiquitin-positive cytoplasmic inclusions and motor impairments (Betarbet *et al.*, 2002).

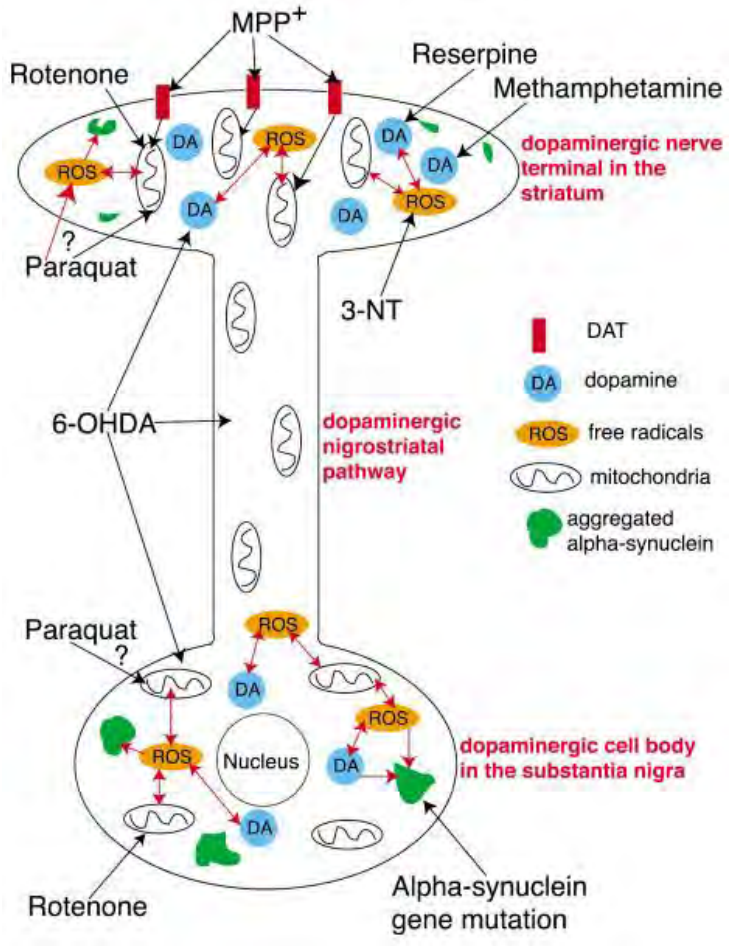

Figure 2.33: Schematic representation of the site of action of pharmacological agents or genetic manipulations resulting in nigrostriatal degeneration and striatal DA depletion. (Betarbet *et al.*, 2002).

2.5 Quinazolinones

2.5.1 General background

It has been reported that heterocyclic chemistry comprises at least half of all organic chemistry research worldwide (Connolly *et al.*, 2005; Chawla & Batra, 2013). Notably, heterocyclic compounds form the basis of many pharmaceutical, chemical and veterinary products (Connolly *et al.*, 2005; Banu *et al.*, 2015). Heterocyclic compounds are ring structures that have atoms of at least two different elements as members of the ring (Chawla & Batra, 2013), some of which are inorganic.

Quinazolines belong to the N-containing heterocyclic compounds, and have been shown to exhibit a broad spectrum of biological activities (Wang & Gao, 2013; Asif, 2014). Evolving

synthetic methods are being used to synthesise a variety of quinazoline compounds with different biological activities (Wang & Gao, 2013). The addition of various active groups to the quinazoline moiety alters the properties of the quinazoline ring considerably, thus modifying its activity (Wang & Gao, 2013; Asif, 2014). Quinazolinones result from introduction of a keto group to the pyrimidine ring of quinazolines (Tiwary *et al.*, 2015). According to Chawla and Batra (2013), quinazolinones are heterocyclic compounds with two fused aromatic rings, comprising of two nitrogen atoms and one keto group.

2.5.2 Biological activities

Quinazolinone derivatives are found in more than 100 naturally occurring alkaloids (He *et al.*, 2014; Khan *et al.*, 2014), and are known to possess a wide variety of biological activities including anti-inflammatory, antipsychotic, antihypertensive (Chawla & Batra, 2013), antimalarial, anticonvulsant (Banu *et al.*, 2015), diuretic (Rajput & Mishra, 2012), anti-HIV, anticancer, antimutagenic, antidepressant (Asif, 2014), analgesic, CNS depressant, antihistaminic and antiparkinsonian activities (Tiwary *et al.*, 2015).

Quinazolinones have two structural isomers depending on the position of the keto group, 2(1*H*)-quinazolinones and 4(3*H*)-quinazolinones (Banu *et al.*, 2015), with the 4-isomer being more common (Chawla & Batra, 2013).

4(3*H*)-quinazolinone 2(1*H*)-quinazolinone

Figure 2.34: Isomers of quinazolinones

The 4(3*H*)-quinazolinones are the most prevalent, either as intermediates, or as natural products in various biosynthetic pathways. The 4(3*H*)-quinazolinones are derived from anthranilates (anthranilic acid or various esters, isatoic anhydride, anthranilamide and anthranilonitrile) (Rajput & Mishra, 2012). On the other hand, the 2(1*H*)-quinazolinone isomer is predominately a product of the reaction of anthranilonitrile or benzamides with nitriles (Rajput & Mishra, 2012).

Medicinal chemists have been inspired by the stability of the quinazolinone nucleus, and to synthesise new potential medicinal agents, have introduced many bioactive moieties to this nucleus (Banu *et al.*, 2015; Tiwary *et al.*, 2015). According to Gokhan-Kelekci *et al.* (2009), a

number of quinazolinones and their analogues have been shown to exhibit MAO inhibitory activity.

Gokhan-Kelekci *et al.* (2009) evaluated the MAO inhibitory activity of a series of 4(3*H*)-quinazolinone derivatives using MAO from rat liver, and revealed that substitution on the 2nd and 3rd positions on the ring system of this quinazolinone isomer with different heterocyclic moieties results in high potency MAO inhibitors. Among the evaluated compounds were inhibitors that were selective for MAO-A as well as MAO-B. The most potent inhibitors exhibited IC_{50} values of 1.03 μM and 0.16 μM for MAO-A and MAO-B, respectively.

Khattab *et al.* (2015) evaluated amino acid derivatives of quinazolinones as inhibitors of bovine brain MAO. The evaluated compounds however showed selective inhibition of MAO-A over MAO-B, with IC_{50} values ranging from 0.016 μM to 0.196 μM. A few of the test compounds possessed inhibitory profiles similar to that of the reference MAO-A inhibitor, clorgyline.

2.5.3 Synthetic methods

The first quinazolinone derivative, 2-cyano-3,4-dihydro-4-oxoquinazoline, was synthesised in the late 1860s by using cyanogens and anthranilic acid as starting materials (Chawla & Batra, 2013; Asif, 2014). Inspired by the wide range of biological activities exhibited by quinazolinone derivatives, many useful procedures have been developed for their syntheses.

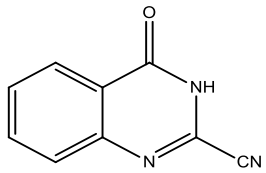

Figure 2.35: Structure of 2-cyano-3,4-dihydro-4-oxoquinazoline

The Niementowski synthesis is the most common method for synthesis of 4(3*H*)-quinazolinones. It involves heating anthranilic acid or one of its functional derivatives in an open container containing excess formamide at 120-150 °C for at least 6 hours (He *et al.*, 2014; Tiwary *et al.*, 2015). During this procedure, water is eliminated and the reaction proceeds via an *o*-amidobenzamide intermediate. This method of quinazolinone synthesis is known to be variable and sometimes gives impure products in low yields (He *et al.*, 2014).

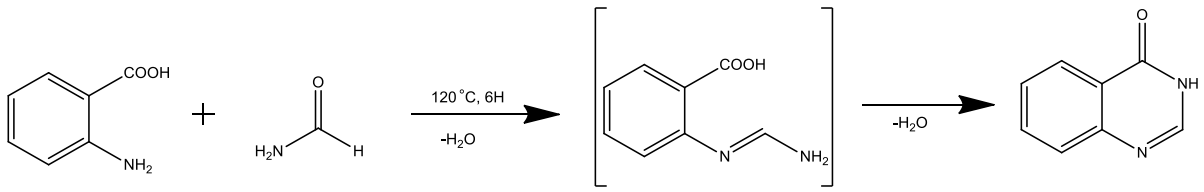

Figure 2.36: The Niementowski reaction (Tiwary *et al.*, 2015)

Alexandre *et al.* (2002) re-investigated and improved the Niementowski synthesis by using microwave irradiation, improving the yield and purity, and reducing reaction time for the synthesis of 4(3*H*)-quinazolinones.

Because of their wide range of biological activities, and their proven MAO inhibitory potential, quinazolinones have attracted attention for further investigation as MAO inhibitors.

2.6 Conclusion

This chapter discussed PD as a progressive neurodegenerative disorder which has no cure, but can be treated symptomatically. The aetiology and symptomatic treatment of PD were briefly discussed in this chapter. The metabolic precursor of dopamine, L-dopa still remains the most effective treatment option for PD. L-dopa should however be given together with a peripheral dopa decarboxylase inhibitor to reduce any side-effects that result from its peripheral activation, and to increase its cerebral bioavailability. This chapter also discussed the three dimensional structures of the MAO isoenzymes and their importance as therapeutic targets for neurological diseases, particularly PD. Inhibition of MAO-B enhances brain DA levels in PD, and it is one of the pharmacological approaches to treating PD. MAO-B inhibitors have been used alone or in combination with L-dopa to combat the symptoms of PD. MAO-B inhibitors also protect against neuronal damage caused by the products of MAO catalysis. As discussed earlier, quinazolinones possess a wide range of biological properties, including antiparkinsonian activity. This study will thus explore quinazolinones as potential inhibitors of MAO-B.

REFERENCES

Alexandre, F.-R., Berecibar, A. & Besson, T. 2002. Microwave-assisted niementowski reaction. back to the roots. *Tetrahedron letters*, 43(21):3911-3913.

Asif, M. 2014. Chemical characteristics, synthetic methods, and biological potential of quinazoline and quinazolinone derivatives. *International journal of medicinal chemistry*, 2014:1-27.

Banu, H.B., Prasad, K.V.S.R. & Bharathi, K. 2015. Biological importance of quinazolin-4-one scaffold and its derivatives- a brief update. *International journal of pharmacy and pharmaceutical sciences*, 7(6):1-7.

Bender, D.A., Botham, K.M., Granner, D.K., Keeley, F.W., Kenelly, P.J., Mayes, P.A., Murray, R.K., Rand, M.L., Rodwell, V.W. & Weil, A.P. 2003. Harper's illustrated biochemistry. 26th ed. New York: McGraw-Hill.

Berlin, I., Aubin, H.J., Pedarriosse, A.M., Rames, A. & Lancrenon, S. 2002. Lazabemide, a selective, reversible monoamine oxidase B inhibitor, as an aid to smoking cessation. *Addiction*, 97(10):1347-1354.

Betarbet, R., Sherer, T.B. & Greenamyre, J.T. 2002. Animal models of Parkinson's disease. *Bioessays*, 24(4):308-318.

Binda, C., Li, M., Hubalek, F., Restelli, N., Edmondson, D.E. & Mattevi, A. 2003. Insights into the mode of inhibition of human mitochondrial monoamine oxidase B from high-resolution crystal structures. *Proceedings of the national academy of sciences*, 100(17):9750-9755.

Binda, C., Newton-Vinson, P., Hubálek, F., Edmondson, D.E. & Mattevi, A. 2002. Structure of human monoamine oxidase B, a drug target for the treatment of neurological disorders. *Nature structural & molecular biology*, 9(1):22-26.

Birmes, P., Coppin, D., Schmitt, L. & Lauque, D. 2003. Serotonin syndrome: a brief review. *Canadian medical association journal*, 168(11):1439-1442.

Brocks, D.R. 1999. Anticholinergic drugs used in Parkinson's disease: an overlooked class of drugs from a pharmacokinetic perspective. *Journal of pharmacy and pharmaceutical sciences*, 2(2):39-46.

Bruton, L., Parker, K., Blumenthal, D. & Buxton, I. 2008. Goodman and Gilman's manual of pharmacology and therapeutics. New York: McGraw Hill.

Burlingham, B.T. & Widlanski, T.S. 2003. An intuitive look at the relationship of Ki and IC50: A more general use for the Dixon plot. *Journal of chemical education*, 80(2):214.

Carvey, P.M. 2010. Dopa-decarboxylase inhibitors. (*In* Encyclopedia of movement disorders:313-316).

Cer, R.Z., Mudunuri, U., Stephens, R. & Lebeda, F.J. 2009. IC_{50}-to-K_i: a web-based tool for converting IC_{50} to K_i values for inhibitors of enzyme activity and ligand binding. *Nucleic acids research*, 37:W441-W445.

Chawla, A. & Batra, C. 2013. Recent advances of quinazolinone derivatives as marker for various biological activities. *International research journal of pharmacy*, 4(3):49-58.

Chen, J.-F., Steyn, S., Staal, R., Petzer, J.P., Xu, K., Van der Schyf, C.J., Castagnoli, K., Sonsalla, P.K., Castagnoli, N. & Schwarzschild, M.A. 2002. 8-(3-Chlorostyryl) caffeine may attenuate MPTP neurotoxicity through dual actions of monoamine oxidase inhibition and A_{2A} receptor antagonism. *Journal of biological chemistry*, 277(39):36040-36044.

Chou, T. & Talaly, P. 1977. A simple generalized equation for the analysis of multiple inhibitions of Michaelis-Menten kinetic systems. *Journal of biological chemistry*, 252(18):6438-6442.

Connolly, D.J., Cusack, D., O'Sullivan, T.P. & Guiry, P.J. 2005. Synthesis of quinazolinones and quinazolines. *Tetrahedron*, 61(43):10153-10202.

Dauer, W. & Przedborski, S. 2003. Parkinson's disease: mechanisms and models. *Neuron*, 39(6):889-909.

De Colibus, L., Li, M., Binda, C., Lustig, A., Edmondson, D.E. & Mattevi, A. 2005. Three-dimensional structure of human monoamine oxidase A (MAO A): relation to the structures of

rat MAO A and human MAO B. *Proceedings of the national academy of sciences*, 102(36):12684-12689.

DeMaagd, G. & Philip, A. 2015. Parkinson's disease and its management: part 3: nondopaminergic and nonpharmacological treatment options. *Pharmacy and therapeutics*, 40:668.

Dhall, R. & Kreitzman, D.L. 2016. Advances in levodopa therapy for Parkinson disease Review of RYTARY (carbidopa and levodopa) clinical efficacy and safety. *Neurology*, 86(14):S13-S24.

Dixon, M. 1953. The determination of enzyme inhibitor constants. *Biochemical journal*, 55:170-171.

Dungo, R. & Deeks, E.D. 2013. Istradefylline: first global approval. *Drugs*, 73:875-882.
Edmondson, D.E., Binda, C. & Mattevi, A. 2004. The FAD binding sites of human monoamine oxidases A and B. *Neurotoxicology*, 25(1-2):63-72.

Edmondson, D.E., Binda, C. & Mattevi, A. 2007. Structural insights into the mechanism of amine oxidation by monoamine oxidases A and B. *Archives of biochemistry and biophysics*, 464(2):269-276.

Fahn, S. 2003. Description of Parkinson's disease as a clinical syndrome. *Annals of the New York academy of sciences*, 991(1):1-14.

Fernandez-Espejo, E. 2004. Pathogenesis of Parkinson's disease. *Molecular neurobiology*, 29(1):15-30.

Fernandez, H.H. & Chen, J.J. 2007. Monoamine oxidase-B inhibition in the treatment of Parkinson's disease. *Pharmacotherapy*, 27(12):174s-185s.

Finberg, J.P.M. 2014. Update on the pharmacology of selective inhibitors of MAO-A and MAO-B: focus on modulation of CNS monoamine neurotransmitter release. *Pharmacology & therapeutics*, 143(2):133-152.

Foley, P., Gerlach, M., Youdim, M.B. & Riederer, P. 2000. MAO-B inhibitors: multiple roles in the therapy of neurodegenerative disorders? *Parkinsonism & related disorders*, 6(1):25-47.

Fowler, J.S., Volkow, N.D., Wang, G.J., Logan, J., Pappas, N., Shea, C. & MacGregor, R. 1997. Age-related increases in brain monoamine oxidase B in living healthy human subjects. *Neurobiology of aging*, 18(4):431-435.

Gillman, P. 1999. The serotonin syndrome and its treatment. *Journal of psychopharmacology*, 13(1):100-109.

Gokhan-Kelekci, N., Koyunoglu, S., Yabanoglu, S., Yelekci, K., Ozgen, O., Ucar, G., Erol, K., Kendi, E. & Yesilada, A. 2009. New pyrazoline bearing 4(3H)-quinazolinone inhibitors of monoamine oxidase: synthesis, biological evaluation, and structural determinants of MAO-A and MAO-B selectivity. *Bioorganic & medicinal chemistry*, 17(2):675-689.

Green, A.R. & Youdim, M.B. 1975. Effects of monoamine oxidase inhibition by clorgyline, deprenil or tranylcypromine on 5-hydroxytryptamine concentrations in rat brain and hyperactivity following subsequent tryptophan administration. *British journal of pharmacology*, 55(3):415-422.

Hauser, R.A. & Schwarzschild, M.A. 2005. Adenosine A2A receptor antagonists for Parkinson's disease. *Drugs & aging*, 22(6):471-482.

He, L., Li, H., Chen, J. & Wu, X.-F. 2014. Recent advances in 4 (3*H*)-quinazolinone syntheses. *Royal Society of chemistry advances*, 4(24):12065-12077.

Holt, A., Sharman, D.F., Baker, G.B. & Palcic, M.M. 1997. A continuous spectrophotometric assay for monoamine oxidase and related enzymes in tissue homogenates. *Analytical biochemistry*, 244(2):384-392.

Hubalek, F., Binda, C., Khalil, A., Li, M., Mattevi, A., Castagnoli, N. & Edmondson, D.E. 2005. Demonstration of isoleucine 199 as a structural determinant for the selective inhibition of human monoamine oxidase B by specific reversible inhibitors. *Journal of biological chemistry*, 280(16):15761-15766.

Jackson-Lewis, V., Blesa, J. & Przedborski, S. 2012. Animal models of Parkinson's disease. *Parkinsonism & related disorders*, 18:S183-S185.

Khalil, A.A., Davies, B. & Castagnoli, N., Jr. 2006. Isolation and characterization of a monoamine oxidase B selective inhibitor from tobacco smoke. *Bioorganic & medicinal chemistry*, 14(10):3392-3398.

Khan, I., Ibrar, A., Abbas, N. & Saeed, A. 2014. Recent advances in the structural library of functionalized quinazoline and quinazolinone scaffolds: synthetic approaches and multifarious applications. *European journal of medicinal chemistry*, 76:193-244.

Khattab, S.N., Haiba, N.S., Asal, A.M., Bekhit, A.A., Amer, A., Abdel-Rahman, H.M. & El-Faham, A. 2015. Synthesis and evaluation of quinazoline amino acid derivatives as monoamine oxidase (MAO) inhibitors. *Bioorganic & medicinal chemistry*, 23(13):3574-3585.

Koller, W.C. 1997. Neuroprotective therapy for Parkinson's disease. *Experimental neurology*, 144(1):24-28.

Kurth, J.H., Kurth, M.C., Poduslo, S.E. & Schwankhaus, J.D. 1993. Association of a monoamine oxidase B allele with Parkinson's disease. *Annals of neurology*, 33(4):368-372.

Langston, J.W., Irwin, I., Langston, E.B. & Forno, L.S. 1984. Pargyline prevents MPTP-induced parkinsonism in primates. *Science*, 225(4669):1480-1482.

Lees, A.J., Hardy, J. & Revesz, T. 2009. Parkinson's disease. *Lancet*, 373(9680):2055-2066.

Lev, N., Melamed, E. & Offen, D. 2003. Apoptosis and Parkinson's disease. *Progress in neuro-psychopharmacology and biological psychiatry*, 27(2):245-250.

LeWitt, P.A. & Taylor, D.C. 2008. Protection against Parkinson's disease progression: clinical experience. *Neurotherapeutics*, 5(2):210-225.

Lotufo-Neto, F., Trivedi, M. & Thase, M.E. 1999. Meta-analysis of the reversible inhibitors of monoamine oxidase type A moclobemide and brofaromine for the treatment of depression. *Neuropsychopharmacology*, 20(3):226-247.

Meiser, J., Weindl, D. & Hiller, K. 2013. Complexity of dopamine metabolism. *Cell communication and signaling*, 11(1):34.

Meltzer, H.Y. 1991. The mechanism of action of novel antipsychotic drugs. *Schizophrenia bulletin*, 17:263-287.

Minami, M., Hamaue, N., Endo, T., Hirafuji, M., Terado, M., Ide, H., Yamazaki, N., Yoshioka, M., Ogata, A. & Tashiro, K. 1999. Effects of isatin, an endogenous MAO inhibitor, on dopamine (DA) and acetylcholine (ACh) concentrations in rats. *Nihon yakurigaku zasshi. Folia pharmacologica Japonica*, 114:186P-191P.

Nicotra, A., Pierucci, F., Parvez, H. & Senatori, O. 2004. Monoamine oxidase expression during development and aging. *Neurotoxicology*, 25(1-2):155-165.

Ogata, A., Hamaue, N., Terado, M., Minami, M., Nagashima, K. & Tashiro, K. 2003. Isatin, an endogenous MAO inhibitor, improves bradykinesia and dopamine levels in a rat model of Parkinson's disease induced by Japanese encephalitis virus. *Journal of the neurological sciences*, 206(1):79-83.

Parkinson, J. 2002. An essay on the shaking palsy. *The journal of neuropsychiatry & clinical neurosciences*, 14(2):223-236.

Polito, L., Greco, A. & Seripa, D. 2016. Genetic profile, environmental exposure, and their interaction in Parkinson’s disease. *Parkinson’s disease*, 2016:1-9.

Prisinzano, T.E. 2006. Medicinal chemistry: A molecular and biochemical approach. New York: Oxford University Press.

Przedborski, S. 2005. Pathogenesis of nigral cell death in Parkinson's disease. *Parkinsonism & related disorders*, 11:S3-S7.

Rajput, R. & Mishra, A.P. 2012. A review on biological activity of quinazolinones. *International journal of pharmacy and pharmaceutical sciences*, 4(2):66-70.

Robakis, D. & Fahn, S. 2015. Defining the role of the monoamine oxidase-B inhibitors for Parkinson's disease. *CNS drugs*, 29(6):433-441.

Rossiter, D., Blockman, M., Barnes, K.I., Cohen, K., Decloedt, E., Waal, R., Maartens, G., McIlleron, H. & Sixanda, P.Z. 2012. South African medicines formulary. 10th ed. Cape Town: Health and Medical Publishing Group.

Schapira, A.H. & Jenner, P. 2011. Etiology and pathogenesis of Parkinson's disease. *Movement disorders*, 26(6):1049-1055.

Schulz, J.B. & Gerhardt, E. 2001. Apoptosis: its relevance to Parkinson's disease. *Clinical neuroscience research*, 1:427-433.

Shih, J.C., Chen, K. & Ridd, M.J. 1999. Monoamine oxidase: from genes to behavior. *Annual review of neuroscience*, 22:197-217.

Siegel, G.J. & Chauhan, N.B. 2000. Neurotrophic factors in Alzheimer's and Parkinson's disease brain. *Brain research reviews*, 33(2):199-227.

Smeyne, R.J. & Jackson-Lewis, V. 2005. The MPTP model of Parkinson's disease. *Molecular brain research*, 134(1):57-66.

Tiwary, B., Pradhan, K., Nanda, A. & Chakraborty, R. 2015. Implication of quinazoline-4 (3*H*)-ones in medicinal chemistry: a brief review. *Journal of chemical biology & therapeutics*, 1.

Tugwell, C. 2008. Parkinson's disease in focus. London: Pharmaceutical Press.

Uhl, G.R., Walther, D., Mash, D., Faucheux, B. & Javoy-Agid, F. 1994. Dopamine transporter messenger RNA in Parkinson's disease and control substantia nigra neurons. *Annals of neurology*, 35(4):494-498.

Vila, M. & Przedborski, S. 2004. Genetic clues to the pathogenesis of Parkinson's disease. *Nature medicine*, 10:S58-62.

Wang, D. & Gao, F. 2013. Quinazoline derivatives: synthesis and bioactivities. *Chemistry central journal*, 7(1):95.

Warner, T.T. & Schapira, A.H. 2003. Genetic and environmental factors in the cause of Parkinson's disease. *Annals of neurology*, 53:S16-S23.

Yacoubian, T.A. & Standaert, D.G. 2009. Targets for neuroprotection in Parkinson's disease. *Biochimica et biophysica acta*, 1792(7):676-687.

Yan, Z., Caldwell, G.W., Zhao, B. & Reitz, A.B. 2004. A high-throughput monoamine oxidase inhibition assay using liquid chromatography with tandem mass spectrometry. *Rapid communications in mass spectrometry*, 18(8):834-840.

Youdim, M., Maruyama, W. & Naoi, M. 2005. Neuropharmacological, neuroprotective and amyloid precursor processing properties of selective MAO-B inhibitor antiparkinsonian drug, rasagiline. *Drugs today*, 41(6):369-391.

Youdim, M.B. & Bakhle, Y. 2006. Monoamine oxidase: isoforms and inhibitors in Parkinson's disease and depressive illness. *British journal of pharmacology*, 147(S1):S287-S296.

Youdim, M.B., Edmondson, D. & Tipton, K.F. 2006. The therapeutic potential of monoamine oxidase inhibitors. *Nature reviews neuroscience*, 7(4):295-309.

Youdim, M.B. & Weinstock, M. 2004. Therapeutic applications of selective and non-selective inhibitors of monoamine oxidase A and B that do not cause significant tyramine potentiation. *Neurotoxicology*, 25(1-2):243-250.

CHAPTER 3: ARTICLE 1

Synthesis and evaluation of 2-substituted 4(3*H*)-quinazolinone thioether derivatives as monoamine oxidase inhibitors.

Malikotsi A. Qhobosheane[1], Lesetja J. Legoabe[2,*], Jacobus P. Petzer[1,2], and Anél Petzer[1,2]

[1]*Pharmaceutical Chemistry, School of Pharmacy, North-West University, Private Bag X6001, Potchefstroom 2520, South Africa*

[2]*Centre of Excellence for Pharmaceutical Sciences, North-West University, Private Bag X6001, Potchefstroom 2520, South Africa*

Abstract

In the present study, a series of fourteen 2-mercapto-4(3*H*)-quinazolinone derivatives was synthesised and evaluated as potential inhibitors of the human monoamine oxidase (MAO) enzymes. Quinazolinone is the oxidised form of quinazolines, and although this class has not yet been extensively explored as MAO inhibitors, it has been shown to possess a wide variety of biological activities. Among the quinazolinone derivatives investigated, twelve compounds proved to be potent and selective MAO-B inhibitors, with the most potent inhibitor, 2-[(3-iodobenzyl)thio]quinazolin-4(3*H*)-one, exhibiting an IC_{50} value of 0.142 µM. None of the synthesised compounds were MAO-A inhibitors. Analyses of structure-activity relationships (SARs) for MAO-B inhibition show that substitution on the thiol of the quinazolinone moiety with a benzyl bearing a halogen (F, Cl, Br, I) on the *meta* and *para* positions yields high potency inhibitors. In contrast, substitution with an unsubstituted benzyl moiety showed little inhibition activity towards MAO-B. This study suggests that quinazolinones are promising leads for the development of selective MAO-B inhibitors which may be used for the treatment of neurodegenerative disorders such as Parkinson's disease.

Keywords: monoamine oxidase, MAO, quinazolinone, SAR, Parkinson's disease

Introduction

The human MAOs are mitochondrial bound flavin-dependent enzymes that catalyse the oxidative deamination of neurotransmitters such as serotonin (5-HT), dopamine, epinephrine and norepinephrine (Hassan *et al.*, 2006; Khattab *et al.*, 2010; Khattab *et al.*, 2015). The MAO enzyme exists in two isoforms, MAO-A and MAO-B, which are approximately 70% similar on the amino acid level (Kumar *et al.*, 2016). In spite of this, the MAOs differ in

substrate specificity, inhibitor selectivity and tissue distribution (Hassan *et al.*, 2006; Kumar *et al.*, 2016). For example, MAO-B is selectively and irreversibly inhibited by (R)-deprenyl and rasagiline, and preferentially metabolises benzylamine and phenylethylamine (Khattab *et al.*, 2010; Carradori & Silvestri, 2015). On the other hand, the MAO-A isoform has specificity for bulkier endogenous amines such as serotonin and is irreversibly inhibited by clorgyline and reversibly by moclobemide (Carradori & Silvestri, 2015). Dopamine, tyramine and tryptamine are common substrates for both forms of the enzyme (Srivastav *et al.*, 2013; Kumar *et al.*, 2016). The MAO enzymes are found in most tissues including the brain, gut, liver, platelets, and lymphocytes (Kumar *et al.*, 2016). In the brain, the two MAOs are not evenly distributed with MAO-B being the main form in the basal ganglia (Youdim *et al.*, 2006). Furthermore, MAO-B is mostly found in serotonergic neurons and astrocytes, whereas MAO-A is found predominantly in catecholaminergic neurons (Youdim *et al.*, 2006). In the peripheral tissues, the MAOs function as metabolic barriers, with MAO-A preventing the entry of biogenic amines such as tyramine into the systemic circulation. Similarly, MAO-B in the microvessels of the blood-brain barrier (BBB) prevents entry of certain amines such as phenylethylamine into the central nervous system (CNS) (Youdim *et al.*, 2006; Legoabe *et al.*, 2012).

The imbalance in the concentrations of monoamine neurotransmitters in the brain is associated with the chemical pathophysiology of various neurological disorders including depression, Parkinson's disease and Alzheimer's disease (Kumar *et al.*, 2016). In this respect, selective MAO-A inhibitors are used clinically as antidepressants and anxiolytics, whereas MAO-B inhibitors are used for the treatment of Parkinson's disease (Khattab *et al.*, 2015). However, the clinical use of certain MAO inhibitors is restricted because of their ability to cause an abnormal increase in blood pressure known as the cheese reaction (Khattab *et al.*, 2010; Kumar *et al.*, 2016). Normally, intestinal MAO-A metabolises tyramine, an indirectly acting sympathomimetic amine which is present in cheese and fermented drinks, and thus serves as a metabolic barrier for the entry of tyramine into the circulation (Legoabe *et al.*, 2012). In the presence of an irreversible non-selective MAO or selective MAO-A inhibitor, systemic tyramine concentrations increase, leading to the release of norepinephrine from the peripheral adrenergic neurons and a rapid blood pressure elevation (Legoabe *et al.*, 2012; Meiring *et al.*, 2013; Kumar *et al.*, 2016). This drug-food interaction may be fatal and is termed the "cheese reaction". Selective MAO-B inhibitors are devoid of the cheese reaction and possess good safety profiles (Carradori & Silvestri, 2015).

As mentioned, MAO-B inhibitors are used for the treatment of Parkinson's disease and are combined with L-dopa, the metabolic precursor of dopamine. By inhibiting dopamine metabolism in the brain, MAO-B inhibitors increase the therapeutic efficacy of L-dopa

(Mostert *et al.*, 2015; Nel *et al.*, 2016). MAO-B inhibitors may also be neuroprotective by reducing levels of hydrogen peroxide and aldehyde derivatives, potentially harmful by-products formed as a result of MAO-B catalysis (Mostert *et al.*, 2015; Nel *et al.*, 2016). These by-products may cause neuronal cell damage if not adequately inactivated. Because brain MAO-B activity increases with age, the contribution of hydrogen peroxide and aldehyde derivatives to neurodegeneration in Parkinson's disease may be particularly relevant (Legoabe *et al.*, 2012; Nel *et al.*, 2016). Based on these considerations, a number of research groups pursue the discovery of new MAO-B inhibitors in search of improved antiparkinsonian therapies.

Numerous scaffolds have been explored as leads for the design of potent MAO inhibitors. Among these is the quinazolinone moiety. Gökhan-Kelekçi *et al.* (2009) demonstrated that compounds bearing a phenyl on position 3 and a substituted phenyl on position 5 of quinazolinone hydrazine derivatives are highly potent MAO inhibitors. On the other hand, compounds bearing a substituted phenyl on position 3 and furyl/thienyl on position 5 are the least potent (Gökhan-Kelekçi *et al.*, 2009). The inhibition activities of these compounds are dependent on the nature and position of the substituent on the phenyl ring. Rastogi *et al.* (1972) and Srivastava *et al.* (1980), in turn, demonstrated that substitution with a halogen (F, Cl, Br, I) on positions 6 and 8 of the quinazolinone significantly enhances MAO inhibition. Srivastava *et al.* (1980) reported that potency of the inhibitor decreases as the electronegativity of the halogen substituent decreases (Cl > Br > I). Substitution on C2 of the 4(3*H*)-quinazolinone was considered in the present study. The unsubstituted and substituted benzyl moieties were linked, via a thiol ether, to 4(3*H*)-quinazolinone to yield **3a**–**k**. Since halogen substitution was shown to increase MAO inhibitory potency in previous studies, the 4(3*H*)-quinazolinone thioether derivatives were substituted with halogens at the *meta* and *para* positions of the benzyl ring. For the purpose of this study, the 2-oxo-2-phenylethyl (**3l**), 3-phenylpropyl (**3m**) and 2-phenoxyethyl (**3n**) substituents were also explored. Based on the previous studies, these 4(3*H*)-quinazolinone derivatives may act as potential MAO inhibitors.

Results and discussion

Chemistry

The 4(3*H*)-quinazolinone thioether derivatives (**3a**–**n**) were synthesised in poor to excellent yields (5-95%) by employing the nucleophilic substitution reaction (scheme 1). Commercially available 2-mercapto-4(3*H*)-quinazolinone and an appropriate arylalkyl bromide or chloride were suspended in ethanol (10 mL) in the presence of K_2CO_3 or NaOH, and stirred for 2 h. With the exception of **3n**, the target products were precipitated with the addition of ice-cold water, collected by filtration and dried. Compound **3n** was isolated by extraction with ethyl

acetate. The crude products obtained were purified by recrystallisation from appropriate solvents, and the structures and purities of the target compounds were verified by ^{1}H NMR, ^{13}C NMR, mass spectrometry and HPLC analyses as cited in the experimental section.

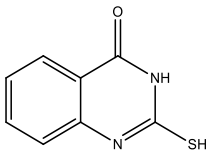

Figure 1: The structure of 2-mercapto-4(3*H*)-quinazolinone

IC_{50} values for the inhibition of MAO

Recombinant human MAO-A and MAO-B were employed to evaluate the MAO inhibitory properties of the newly synthesised compounds (Legoabe *et al.*, 2012; Mostert *et al.*, 2015; Nel *et al.*, 2016). Kynuramine served as enzyme substrate for both MAO-A and MAO-B. Kynuramine is oxidised to yield 4-hydroxyquinoline as ultimate product, a metabolite that fluoresces (λ_{ex} = 310 nm; λ_{em} = 400 nm) in alkaline media and can thus be readily measured by fluorescence spectrophotometry (Legoabe *et al.*, 2012; Meiring *et al.*, 2013; Petzer *et al.*, 2013). A typical enzyme reaction contained the substrate (50 µM) and the test inhibitors (at concentrations of 0.003-100 µM), and were initiated with addition of enzymes. As negative control samples, enzyme reactions were also carried out in absence of inhibitor. The reactions were subsequently incubated at 37 °C for 20 min and terminated by the addition of NaOH (2N). The rate of formation of 4-hydroxyquinoline in each incubation was measured by fluorescence spectrometry and the data were fitted to a sigmoidal curve of rate versus the logarithm of inhibitor concentration from which the IC_{50} values were estimated.

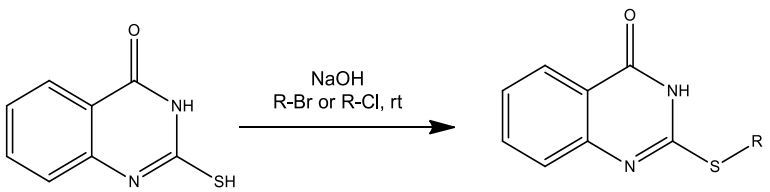

Scheme 1: Synthetic route for the synthesis of 4(3*H*)-quinazolinone thioether derivatives, **3a**–**n**.

The IC_{50} values for the inhibition of MAO by the 2-substituted 4(3*H*)-quinazolinone thioether derivatives are reported in **table 1**. The results show that 2-substituted 4(3*H*)-quinazolinones are indeed MAO inhibitors, with IC_{50} ranging from 0.142 to 31.8 µM for the MAO-B isoform. The results further demonstrate that the majority of the test inhibitors (12 of 14) are selective for MAO-B, with no compounds displaying inhibition towards the MAO-A isoform. With the exception of **3c** and **3h**, those derivatives bearing a halogen on the *meta*-position of the

benzyl ring (**3i, 3k** and **3j**) are more potent than the corresponding *para*-substituted derivatives. **3k**, the *meta*-iodobenzyl derivative is the most potent inhibitor among the evaluated compounds (IC_{50} = 0.142 μM). However, its *para*-iodo substituted isomer, **3f**, is devoid of inhibition activity for MAO-B. Since the *meta* and the *para* isomers can be considered as having similar lipophilicities (cLogP= 4.55 ± 0.66) and very similar electronic properties, the loss of activity of the *para*-iodo compound may be attributed to steric effects.

It is interesting to note that substitution on the benzyl ring with both halogens (F, Cl, Br, I) and alkyl (CF_3) substituents enhances MAO-B inhibitory potency relative to the derivative bearing an unsubstituted benzyl ring. In fact, with the exception of **3f**, all halogen-substituted derivatives act as potent MAO-B inhibitors. Also of note is that the 3-phenylpropyl (**3m**) and 2-phenoxyethyl (**3n**) substituted compounds exhibited similar MAO-B inhibition potencies compared to **3a**, which may be attributed to the absence of substituents (e.g. halogens) on the side chain phenyl rings. The pyridine substituted compound, **3b**, did not inhibit either MAO isoforms, which suggests that non-polar, lipophilic phenyl-containing substituents are more appropriate for MAO-B inhibition compared to the pyridine ring. The 2-oxo-2-phenylethyl substituted derivative **3l** also displayed relatively poor MAO-B inhibition, which shows that introduction of an oxo group to the side chain linker reduced MAO-B inhibition. These results demonstrate the appropriate substitution of 4(3*H*)-quinazolinones via thioether linkage for the design of MAO-B inhibitors.

Table 1: The IC_{50} values for the inhibition of MAO-A and MAO-B by 4(3*H*)-quinazolinone thioether derivatives.

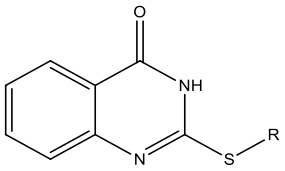

	R	IC_{50} (μM)[a]		SI[b]	cLogP
		MAO-A	MAO-B		
3a	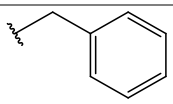	No inh[c]	3.028 ± 0.131	>33	3.52 ± 0.64
3b	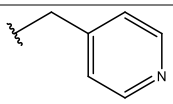	No inh[c]	No inh[c]	>1	2.03 ± 0.64
3c	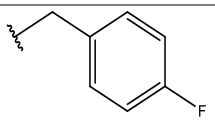	No inh[c]	0.566 ± 0.024	>177	3.57 ± 0.66
3d	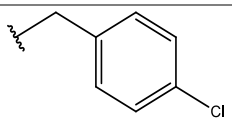	No inh[c]	0.482 ± 0.036	>207	4.12 ± 0.64
3e	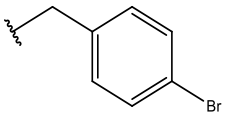	No inh[c]	0.779 ± 0.188	>128	4.29 ± 0.66
3f	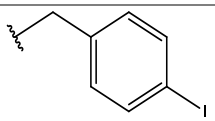	No inh[c]	No inh[c]	>1	4.55 ± 0.66
3g	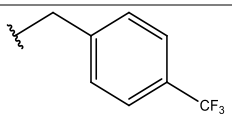	No inh[c]	0.700 ± 0.005	>143	4.09 ± 0.65
3h	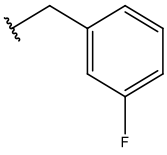	No inh[c]	2.504 ± 0.112	>40	3.57 ± 0.66
3i	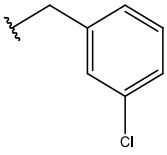	No inh[c]	0.230 ± 0.020	>435	4.12 ± 0.64

3j	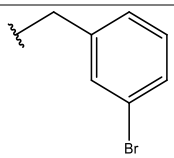	No inh[c]	0.208 ± 0.015	>481	4.29 ± 0.66
3k	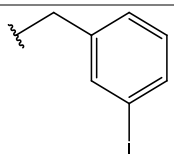	No inh[c]	0.142 ± 0.011	>704	4.55 ± 0.66
3l	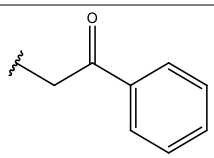	No inh[c]	31.82 ± 0.707	>3	3.22 ± 0.65
3m	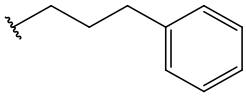	No inh[c]	5.986 ± 1.604	>17	4.37 ± 0.63
3n	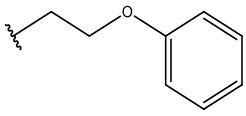	No inh[c]	1.241 ± 0.053	>81	3.66 ± 0.64

[a] All values are expressed as the mean ± standard deviation (SD) of triplicate determinations.

[b] Selectivity index (SI) = IC_{50}(MAO-A)/IC_{50}(MAO-B).

[c] No inhibition observed at a maximal tested concentration of 100 µM.

Reversibility of MAO-B inhibition

To examine the reversibility of MAO inhibition by the 4(3*H*)-quinazolinone thioether derivatives, recoveries of enzymatic activities after dialysis of enzyme-inhibitor mixtures were measured (Mostert *et al.*, 2016). MAO-B and a selected test inhibitor, compound **3k**, at a concentration equal to 4 x IC_{50} were combined for 15 min and subsequently dialysed for 24 h. As negative control, MAO-B was similarly dialysed in the absence of the inhibitor, and as positive control in the presence of the irreversible inhibitor (R)-deprenyl. Enzymatic activity is expected to recover to 100% of the negative control value following dialysis for reversible inhibitors. In contrast, for irreversible inhibition, enzyme activity is not expected to recover after dialysis. In this experiment, MAO-B activity was recovered to 108% of the control value after dialysis of mixtures containing MAO-B and **3k**. Enzyme activity of undialysed mixtures of MAO-B and **3k** are 46% of the control value, while only 3% of the control value was recovered after dialysis of mixtures containing MAO-B and (R)-deprenyl. The results are given in figure 2, and thus indicate that **3k** is a reversible inhibitor of MAO-B.

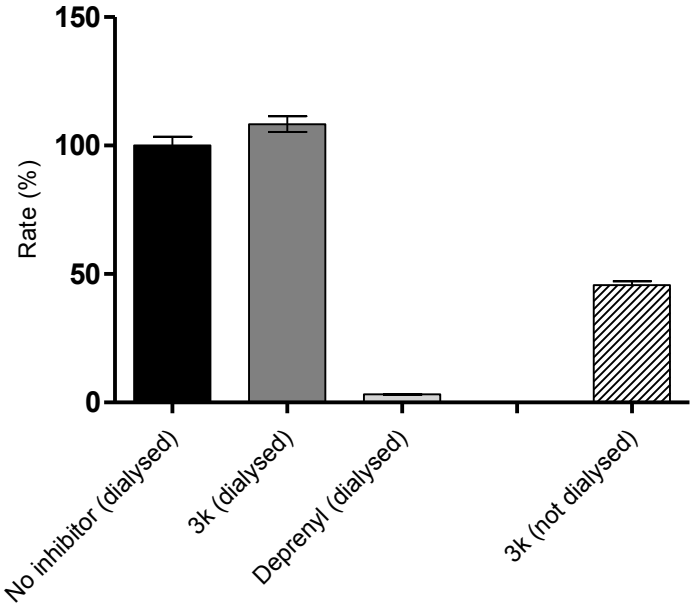

Figure 2: Reversibility of MAO-B inhibition by **3k**. MAO-B was pre-incubated with **3k** (at 4 x IC_{50}) for 15 min and dialysed for 24 h. Similarly, the enzyme was pre-incubated in the absence of the inhibitor and in the presence of the irreversible MAO-B inhibitor (R)-deprenyl. These mixtures were also dialysed for 24 h and the residual enzyme activities were measured. The residual activity of undialysed mixtures of MAO-B and **3k** are also shown (**3k** not dialysed) for comparison.

To investigate the mode of MAO-B inhibition by **3k**, a set of Lineweaver-Burke plots (figure 3) was constructed. A set comprising of 6 plots was constructed by measuring enzyme activities in the absence and presence of different inhibitor concentrations (0 µM, $^1/_4$ x IC_{50}, ½ x IC_{50}, ¾ x IC_{50}, 1 x IC_{50}, $1^1/_4$ x IC_{50}). Eight different substrate (kynuramine) concentrations ranging from 15 to 250 µM were used for each plot. The results show that the plots are linear and intersect on the y-axis. This indicates that **3k** inhibits MAO-B competitively. For MAO-B inhibition, the K_i value was estimated by plotting the slopes of the Lineweaver-Burke plots versus the inhibitor concentration, with the K_i equal to 0.092 µM.

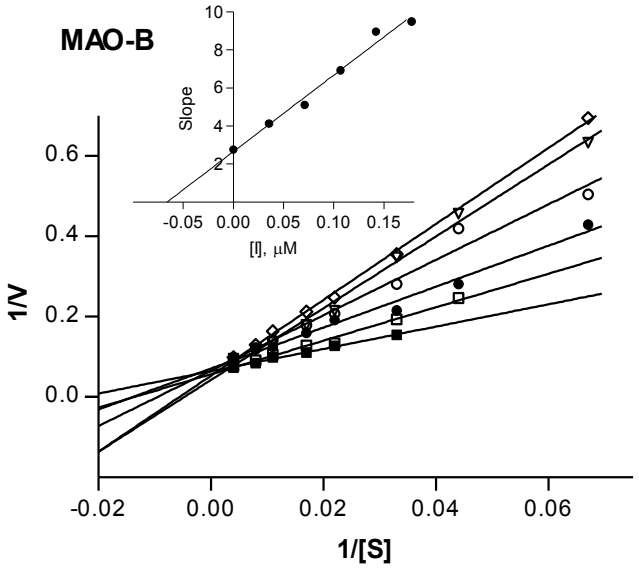

Figure 3: Lineweaver-Burke plots of human MAO-B catalytic activities in the absence (filled squares) and presence of various concentrations of **3k**.

Conclusion

The present study shows that C2-substituted 4(3*H*)-quinazolinone thioether derivatives are potent and selective inhibitors of human MAO-B, with compound **3k** being the most potent inhibitor (IC_{50} = 0.142 μM). An analysis of the SARs for MAO-B inhibition shows that substitution with a benzyl ring bearing a halogen on the *meta* or *para* positions is more favourable for MAO-B inhibition than substitution with an unsubstituted benzyl moiety. Of note is the finding that none of the derivatives inhibited MAO-A up to a maximal tested concentration of 100 μM. Based on their good selectivity profile for MAO-B, this series of 4(3*H*)-quinazolinone thioether derivatives represents promising leads for future development of novel selective MAO-B inhibitors, which have potential in the treatment of Parkinson's disease.

Acknowledgements

The NMR and MS spectra were recorded by André Joubert and Johan Jordaan of the SASOL Centre of Chemistry, North-West University. This work is based on the research supported by National Research Foundation of South Africa (Grant specific unique reference number (UID) 96135). The Grant holders acknowledge that opinions, findings and conclusions or recommendations expressed in any publication generated by the NRF supported research are that of the authors, and that the NRF accepts no liability whatsoever in this regard.

Experimental section

Chemicals and instrumentation

Unless otherwise noted, all starting materials and reagents were obtained from Sigma-Aldrich and used without further purification. Proton (^{1}H) and carbon (^{13}C) NMR spectra were recorded on a Bruker Avance III 600 spectrometer at frequencies of 600 MHz and 151 MHz, respectively, with DMSO-*d*6 serving as NMR solvent. All chemical shifts are reported in parts per million (δ). Spin multiplicities are given as s (singlet), d (doublet), dd (doublet of doublets), ddd (doublet of doublet of doublets), t (triplet) and m (multiplet). High resolution mass spectra (HRMS) were recorded on a Bruker micrOTOF-Q II mass spectrometer in atmospheric-pressure chemical ionisation (APCI) mode. The melting points (mp) were determined with a Buchi B-545 melting point apparatus and are uncorrected. Thin layer chromatography (TLC) was carried out using silica gel 60 (Merck) with UV254 fluorescent indicator. Microsomes from insect cells containing recombinant human MAO-A and MAO-B (5 mg protein/mL), and kynuramine dihydrobromide were obtained from Sigma-Aldrich. Fluorescence spectrophotometry was carried out with a Varian Cary Eclipse fluorescence spectrophotometer.

General procedure for synthesis of 4-(3*H*) quinazolinone analogues

A mixture of commercially available 2-mercapto-4(3*H*)-quinazolinone (0.3 g, 1.683 mmol), ethanol (10 mL) and an appropriately substituted arylalkyl halide was stirred in the presence of K_2CO_3 (0.465 g, 3.37 mmol) or NaOH (0.135 g, 3.37 mmol) for 2 h at room temperature. The reaction products were precipitated with the addition of ice-cold water (15 mL), collected by filtration and dried. Water soluble products were extracted to ethyl acetate (60 mL), dried over magnesium sulfate and the solvent was removed *in vacuo*. The target products were purified by recrystallisation from appropriate solvents. To monitor the progress of the reactions, silica gel TLC was performed with a mobile phase that consisted of petroleum ether:ethyl acetate (3:1).

2-(Benzylthio)quinazolin-4(3*H*)-one (3a)

The title compound was prepared in a yield of 93%: mp 212.4-213.1 °C (ethanol) ^{1}H NMR (600 MHz, DMSO) δ 12.59 (s, 1H), 8.04 (dd, *J* = 7.9, 1.3 Hz, 1H), 7.78 (ddd, *J* = 8.5, 7.3, 1.6 Hz, 1H), 7.61 (d, *J* = 7.9 Hz, 1H), 7.51 – 7.46 (m, 2H), 7.46 – 7.40 (m, 1H), 7.33 (dd, *J* = 10.3, 4.7 Hz, 2H), 7.28 – 7.22 (m, 1H), 4.50 (s, 2H). ^{13}C NMR (151 MHz, DMSO) δ 161.83, 155.91, 148.76, 137.87, 135.10, 129.67, 128.92, 127.75, 126.53, 126.38, 126.14, 120.49, 34.01. APCI-HRMS m/z: calcd for $C_{15}H_{13}N_2OS$, 269.0743, found 269.0755. Purity (HPLC): 99.2%.

2-[(Pyridin-4-ylmethyl)thio]quinazolin-4(3*H*)-one (3b)

The title compound was prepared in a yield of 5%: mp 336.6-336.7 °C. ^{1}H NMR (600 MHz, DMSO) δ 12.65 (s, 1H), 8.49 (d, *J* = 5.9 Hz, 2H), 8.01 (dd, *J* = 7.9, 1.3 Hz, 1H), 7.78 – 7.72 (m, 1H), 7.57 (d, *J* = 8.0 Hz, 1H), 7.51 – 7.47 (m, 2H), 7.44 – 7.38 (m, 1H), 4.47 (s, 2H). ^{13}C NMR (151 MHz, DMSO) δ 161.37, 154.84, 149.60, 148.16, 147.02, 134.61, 126.05, 125.89, 125.75, 124.19, 120.01, 32.13. APCI-HRMS m/z: calcd for $C_{14}H_{12}N_3OS$ (MH^+), 270.0696, found 270.0705. Purity (HPLC): 97.1%.

2-[(4-Fluorobenzyl)thio]quinazolin-4(3*H*)-one (3c)

The title compound was prepared in a yield of 67%: mp 200.4-202.5 °C (ethanol) ^{1}H NMR (600 MHz, DMSO) δ 8.04 – 7.98 (m, 1H), 7.78 – 7.70 (m, 1H), 7.57 (d, *J* = 8.1 Hz, 1H), 7.51 (dd, *J* = 8.4, 5.7 Hz, 2H), 7.43 – 7.35 (m, 1H), 7.12 (t, *J* = 8.8 Hz, 2H), 4.46 (s, 2H), 2.49 (s, 1H). ^{13}C NMR (151 MHz, DMSO) δ 162.16, 161.73, 160.54, 155.83, 148.41, 134.48, 133.97, 133.95, 131.22, 131.17, 126.07, 125.84, 125.53, 120.08, 115.25, 115.11, 32.69. APCI-HRMS m/z: calcd for $C_{15}H_{12}FN_2OS$ (MH^+), 287.0649, found 287.0660. Purity (HPLC): 99.1%.

2-[(4-Chlorobenzyl)thio]quinazoline-4(3*H*)-one (3d)

The title compound was prepared in a yield of 90%: mp 228.7-232.3 °C. ^{1}H NMR (600 MHz, DMSO) δ 12.58 (s, 1H), 8.04 – 7.98 (m, 1H), 7.79 – 7.72 (m, 1H), 7.59 (d, *J* = 8.1 Hz, 1H), 7.50 (d, *J* = 8.4 Hz, 2H), 7.41 (dd, *J* = 11.1, 4.0 Hz, 1H), 7.35 (d, *J* = 8.4 Hz, 2H), 4.46 (s, 2H). ^{13}C NMR (151 MHz, DMSO) δ 161.28, 155.08, 148.28, 136.81, 134.69, 131.86, 131.09, 128.36, 126.07, 125.78, 120.00, 105.03, 32.69. APCI-HRMS m/z: calcd for $C_{15}H_{12}ClN_2OS$ (MH^+), 303.0353, found 303.0384. Purity (HPLC): 96.5%.

2-[(4-Bromobenzyl)thio]quinazolin-4(3*H*)-one (3e)

The title compound was prepared in a yield of 95%: mp 242.6-245.0 °C. ^{1}H NMR (600 MHz, DMSO) δ 12.60 (s, 1H), 8.04 – 7.98 (m, 1H), 7.75 (s, 1H), 7.57 (d, *J* = 8.1 Hz, 1H), 7.49 (d, *J* = 8.4 Hz, 2H), 7.45 – 7.37 (m, 3H), 4.44 (s, 2H). ^{13}C NMR (151 MHz, DMSO) δ 161.54, 155.51, 148.31, 137.34, 134.59, 131.44, 131.28, 126.07, 125.89, 125.66, 120.35, 120.04, 32.75. APCI-HRMS m/z: calcd for $C_{15}H_{12}BrN_2OS$ ($M+2H^+$), 346.9848, found 348.9869. Purity (HPLC): 100.0%.

2-[(4-Iodobenzyl)thio]quinazolin-4(3*H*)-one (3f)

The title compound was prepared in a yield of 93%: mp 251.3-261.3 °C. ^{1}H NMR (600 MHz, DMSO) δ 12.59 (s, 1H), 8.01 (d, *J* = 7.8 Hz, 1H), 7.76 (s, 1H), 7.65 (d, *J* = 8.3 Hz, 2H), 7.58 (d, *J* = 8.1 Hz, 1H), 7.41 (s, 1H), 7.29 (d, *J* = 8.2 Hz, 2H), 4.42 (s, 2H). ^{13}C NMR (151 MHz, DMSO) δ 161.18, 154.96, 148.28, 137.56, 137.15, 134.72, 131.57, 126.05, 125.80, 121.95,

120.01, 93.27, 32.91. APCI-HRMS m/z: calcd for $C_{15}H_{12}IN_2OS$ (MH^+), 394.9698, found 394.9710. Purity (HPLC): 96.2%.

2-[(4-Trifluoromethyl)thio]quinazolin-4(3*H*)-one (3g)

The title compound was prepared in a yield of 82%: mp 217.3-219.7 °C. ^{1}H NMR (600 MHz, DMSO) δ 12.61 (s, 1H), 8.03 – 7.97 (m, 1H), 7.77 – 7.69 (m, 3H), 7.66 (d, *J* = 8.2 Hz, 2H), 7.57 (d, *J* = 8.1 Hz, 1H), 7.39 (s, 1H), 4.54 (s, 2H). ^{13}C NMR (151 MHz, DMSO) δ 161.87, 155.76, 148.42, 143.08, 134.43, 130.00, 127.82, 127.61, 126.07, 125.82, 125.52, 125.23, 125.21, 123.36, 120.11, 32.82. APCI-HRMS m/z: calcd for $C_{16}H_{12}F_3N_2SO$ (MH^+), 337.0617, found 337.0626. Purity (HPLC): 98.1%.

2-[(3-Fluorobenzyl)thio]quinazolin-4(3*H*)-one (3h)

The title compound was prepared in a yield of 63%: mp 193.7-266.1 °C (ethanol) ^{1}H NMR (600 MHz, DMSO) δ 12.60 (s, 1H), 8.01 (dd, *J* = 7.9, 0.9 Hz, 1H), 7.76 (s, 1H), 7.58 (d, *J* = 8.0 Hz, 1H), 7.44 – 7.38 (m, 1H), 7.33 (dd, *J* = 12.2, 6.9 Hz, 3H), 7.06 (s, 1H), 4.48 (s, 2H). ^{13}C NMR (151 MHz, DMSO) δ 162.77, 161.16, 148.28, 140.68, 140.63, 134.62, 130.36, 130.31, 126.09, 125.85, 125.68, 125.35, 125.33, 120.05, 116.02, 115.88, 114.15, 114.02, 39.92, 39.78, 39.64, 39.50, 39.36, 39.22, 39.08, 32.86. APCI-HRMS m/z: calcd for $C_{15}H_{12}FN_2OS$ (MH^+), 287.0649, found 287.0650. Purity (HPLC): 98.2%.

2-[(3-Chlorobenzyl)thio]quinazolin-4(3*H*)-one (3i)

The title compound was prepared in a yield of 86%: mp 209.6-212.7 °C. ^{1}H NMR (600 MHz, DMSO) δ 12.60 (s, 1H), 8.02 (dd, *J* = 7.9, 1.1 Hz, 1H), 7.79 – 7.73 (m, 1H), 7.61 – 7.54 (m, 2H), 7.48 – 7.37 (m, 2H), 7.36 – 7.25 (m, 2H), 4.47 (s, 2H). ^{13}C NMR (151 MHz, DMSO) δ 161.36, 155.17, 148.22, 140.39, 134.69, 132.82, 130.26, 129.11, 127.96, 127.20, 126.09, 125.84, 125.76, 120.03, 32.77. APCI-HRMS m/z: calcd for $C_{15}H_{12}ClN_2OS$ (MH^+), 303.0353, found 303.0367. Purity (HPLC): 97.8%.

2-[(3-Bromobenzyl)thio]quinazoline-4(3*H*)-one (3j)

The title compound was prepared in a yield of 79%: mp 218.9-219.9 °C. ^{1}H NMR (600 MHz, DMSO) δ 12.58 (s, 1H), 8.01 (dd, *J* = 7.9, 0.9 Hz, 1H), 7.76 (s, 1H), 7.71 (s, 1H), 7.58 (d, *J* = 8.1 Hz, 1H), 7.49 (d, *J* = 7.7 Hz, 1H), 7.42 (dd, *J* = 5.4, 4.1 Hz, 2H), 7.27 (d, *J* = 7.8 Hz, 1H), 4.46 (s, 2H). ^{13}C NMR (151 MHz, DMSO) δ 161.46, 155.25, 148.26, 140.72, 134.72, 132.05, 130.59, 130.10, 128.38, 126.13, 125.86, 125.79, 121.45, 120.05, 32.75. APCI-HRMS m/z: calcd for $C_{15}H_{12}BrN_2OS$ (M+2H$^+$), 346.9848, found 348.9825. Purity (HPLC): 98.2%.

2-[(3-Iodobenzyl)thio]quinazolin-4(3*H*)-one (3k)

The title compound was prepared in a yield of 87%: mp 227.0-262.1 °C. ^{1}H NMR (600 MHz, DMSO) δ 12.59 (s, 1H), 8.02 (dd, *J* = 7.9, 1.0 Hz, 1H), 7.90 (s, 1H), 7.77 (s, 1H), 7.62 – 7.55

(m, 2H), 7.51 (d, *J* = 7.8 Hz, 1H), 7.45 – 7.39 (m, 1H), 7.11 (t, *J* = 7.8 Hz, 1H), 4.42 (s, 2H). ^{13}C NMR (151 MHz, DMSO) δ 161.23, 140.47, 137.93, 135.89, 134.72, 130.56, 128.72, 127.26, 126.09, 125.81, 120.01, 118.40, 94.61, 77.42, 32.62. APCI-HRMS m/z: calcd for $C_{15}H_{12}IN_2OS$ (MH^+), 394.9709, found 394.9704. Purity (HPLC): 98.8%.

2-[(2-Oxo-2-phenylethyl)thio]quinazolin-4(3*H*)-one (3l)

The title compound was prepared in a yield of 6%: mp 263.7-265.9 °C (ethanol). ^{1}H NMR (600 MHz, DMSO) δ 12.71 (s, 1H), 8.09 (d, *J* = 7.7 Hz, 2H), 7.99 (d, *J* = 7.8 Hz, 1H), 7.72 – 7.61 (m, 2H), 7.58 (t, *J* = 7.7 Hz, 2H), 7.36 (t, *J* = 7.5 Hz, 1H), 7.11 (d, *J* = 8.2 Hz, 1H), 4.84 (s, 2H). ^{13}C NMR (151 MHz, DMSO) δ 193.76, 161.15, 155.02, 148.05, 136.22, 134.56, 133.50, 128.79, 128.32, 126.03, 125.66, 124.61, 119.79, 37.50. APCI-HRMS m/z: calcd for $C_{16}H_{13}N_2O_2S$ (MH^+), 297.0692, found 297.0723. Purity (HPLC): 99.2%.

2-[(3-Phenylpropyl)thio]quinazolin-4(3*H*)-one (3m)

The title compound was prepared in a yield of 39%: mp 152.1-245.7 °C ^{1}H NMR (600 MHz, DMSO) δ 12.54 (s, 1H), 8.00 (d, *J* = 7.9 Hz, 1H), 7.72 (dd, *J* = 11.2, 4.1 Hz, 1H), 7.43 (d, *J* = 8.1 Hz, 1H), 7.38 (t, *J* = 7.5 Hz, 1H), 7.28 (t, *J* = 7.5 Hz, 2H), 7.24 – 7.13 (m, 3H), 3.18 (t, *J* = 7.3 Hz, 2H), 2.71 (t, *J* = 7.5 Hz, 2H), 2.05 – 1.92 (m, 2H). ^{13}C NMR (151 MHz, DMSO) δ 161.67, 156.29, 148.50, 141.14, 134.44, 128.40, 128.36, 126.04, 125.92, 125.78, 125.41, 120.02, 34.19, 30.50, 29.12. APCI-HRMS m/z: calcd for $C_{17}H_{17}N_2OS$ (MH^+), 297.1056, found 297.1080. Purity (HPLC): 98.4%.

2-[(Phenoxyethyl)thio]quinazolin-4(3*H*)-one (3n)

The title compound was prepared in a yield of 32%: mp 176.0-178.7 °C (ethyl acetate). ^{1}H NMR (600 MHz, DMSO) δ 12.64 (s, 1H), 8.03 (dd, *J* = 7.9, 1.3 Hz, 1H), 7.79 – 7.73 (m, 1H), 7.52 (d, *J* = 8.1 Hz, 1H), 7.44 – 7.38 (m, 1H), 7.32 – 7.26 (m, 2H), 7.01 (d, *J* = 7.9 Hz, 2H), 6.94 (t, *J* = 7.3 Hz, 1H), 4.27 (t, *J* = 6.6 Hz, 2H), 3.60 (t, *J* = 6.6 Hz, 2H). ^{13}C NMR (151 MHz, DMSO) δ 161.23, 158.03, 153.27, 134.67, 129.56, 126.07, 125.87, 125.72, 120.85, 120.02, 114.52, 65.87, 30.69, 28.56. APCI-HRMS m/z: calcd for $C_{16}H_{15}N_2O_2S$ (MH^+), 299.0849, found, 299.0884. Purity (HPLC): 96.3%.

Protocol for the measurement of IC_{50} values

The IC_{50} values for inhibition of MAO-A and MAO-B were measured according to a method described by Mostert *et al.* (2015). The recombinant human MAOs served as enzyme sources in this study. The enzyme reactions were carried out in white 96-well plates (Eppendorf) in potassium phosphate buffer (100 mM, made isotonic with KCl) at pH 7.4. The final volume of the reactions was 200 µL and contained the MAO-A/B mixed substrate kynuramine (50 µM) and the test inhibitors at concentrations of 0.003–100 µM. Stock

solutions of the inhibitors were prepared in DMSO and added to the reactions to yield a final DMSO concentration of 4%. The reactions were initiated with addition of MAO-A (0.0075 mg protein/mL) or MAO-B (0.015 mg protein/mL), incubated for 20 min at 37 °C in a convection oven, and terminated with 80 µL NaOH (2N). The formation of 4-hydroxyquinoline was measured by fluorescence spectrophotometry (λ_{ex} = 310 nm; λ_{em} = 400 nm). A linear calibration curve containing authentic 4-hydroxyquinoline (0.047–1.56 µM) was constructed and used for these measurements. The inhibition data were fitted to the one site competition model incorporated into the Prism 5 software package (GraphPad) and the IC_{50} values were determined from the resulting sigmoidal plots (rate versus the logarithm of inhibitor concentration). IC_{50} values are expressed as mean ± standard deviation (SD) of triplicate measurements.

Dialysis of enzyme-inhibitor mixtures

The reversibility of MAO-B inhibition by 4(3*H*)-quinazolinone thioether derivatives was examined by dialysis. For this purpose, a procedure reported by Mostert *et al.* (2015) and Mostert *et al.* (2016) was followed and Slide-A-Lyzer® dialysis cassettes (Thermo Scientific) with a molecular weight cut-off of 10 000 and sample volume capacity of 0.3-5 mL were used. A mixture of MAO-B (0.03 mg/ml) and the test inhibitor (**3k**), at a concentration equal to 4-fold the IC_{50}, was prepared in potassium phosphate buffer (100 mM, pH 7.4, 5% sucrose) to a final volume of 0.8 mL and placed in the dialysis cassettes. DMSO (4%) was added to the mixtures as co-solvent. These mixtures were pre-incubated for 15 min at 37 °C and subsequently dialysed at 4 °C in 80 mL dialysis buffer (100 mM potassium phosphate, pH 7.4, 5% sucrose). The dialysis buffer was replaced at 3 h and 7 h after the start of dialysis. As controls, MAO-B was similarly pre-incubated and dialysed in the presence of the irreversible MAO-B inhibitor (R)-deprenyl (IC_{50} = 0.079 µM), as well as in the absence of the inhibitor. After 24 h of dialysis, the dialysed samples (250 µL) were diluted 2-fold with the addition of kynuramine to yield a final inhibitor concentration of 2 x IC_{50} and a final kynuramine concentration of 50 µM. These enzyme reactions were incubated for 20 min at 37 °C, after which they were terminated with addition of 400 µL NaOH (2N) and 1000 µL of water. The residual MAO activities were measured by fluorescence spectrophotometry as described for the IC_{50} determinations. For comparison, undialysed mixtures of MAO-B and **3k** were maintained at 4 °C for 24 h and thereafter diluted and assayed as above. All reactions were carried out in triplicate, and the residual enzyme catalytic rates were expressed as mean ± SD.

Construction of Lineweaver-Burk plots and K_i determination

The mode of MAO-B inhibition by **3k** was investigated by constructing six Lineweaver-Burke plots using a method described in literature (Mostert *et al.*, 2015; Mostert *et al.*, 2016). The first plot was constructed in the absence of inhibitor, while the remaining plots were constructed in the presence of five different inhibitor concentrations ($^1/_4$ x IC_{50}, ½ x IC_{50}, ¾ x IC_{50}, 1 x IC_{50}, $1^1/_4$ x IC_{50}). The substrate, kynuramine, was used at concentrations ranging from 15-250 µM, while the final concentration of MAO-B was 0.015 mg/mL. All enzyme reactions and catalytic activity measurements were carried out as described above. Linear regression analysis was performed using the Prism version 5.0 software package.

REFERENCES

Carradori, S. & Silvestri, R. 2015. New frontiers in selective human MAO-B inhibitors: miniperspective. *Journal of medicinal chemistry*, 58(17):6717-6732.

Gökhan-Kelekçi, N., Koyunoğlu, S., Yabanoğlu, S., Yelekçi, K., Özgen, Ö., Uçar, G., Erol, K., Kendi, E. & Yeşilada, A. 2009. New pyrazoline bearing 4(3*H*)-quinazolinone inhibitors of monoamine oxidase: synthesis, biological evaluation, and structural determinants of MAO-A and MAO-B selectivity. *Bioorganic & medicinal chemistry*, 17(2):675-689.

Hassan, S.Y., Khattab, S.N., Bekhit, A.A. & Amer, A. 2006. Synthesis of 3-benzyl-2-substituted quinoxalines as novel monoamine oxidase A inhibitors. *Bioorganic & medicinal chemistry letters*, 16(6):1753-1756.

Khattab, S.N., Haiba, N.S., Asal, A.M., Bekhit, A.A., Amer, A., Abdel-Rahman, H.M. & El-Faham, A. 2015. Synthesis and evaluation of quinazoline amino acid derivatives as monoamine oxidase (MAO) inhibitors. *Bioorganic & medicinal chemistry*, 23(13):3574-3585.

Khattab, S.N., Hassan, S.Y., Bekhit, A.A., El Massry, A.M., Langer, V. & Amer, A. 2010. Synthesis of new series of quinoxaline based MAO-inhibitors and docking studies. *European journal of medicinal chemistry*, 45(10):4479-4489.

Kumar, B., Mantha, A.K. & Kumar, V. 2016. Recent developments on the structure–activity relationship studies of MAO inhibitors and their role in different neurological disorders. *Royal Society of chemistry advances*, 6(48):42660-42683.

Legoabe, L.J., Petzer, A. & Petzer, J.P. 2012. Inhibition of monoamine oxidase by selected C6-substituted chromone derivatives. *European journal of medicinal chemistry*, 49:343-353.

Legoabe, L.J., Petzer, A. & Petzer, J.P. 2015. 2-acetylphenol analogs as potent reversible monoamine oxidase inhibitors. *Drug design, development and therapy*, 9:3635.

Meiring, L., Petzer, J.P. & Petzer, A. 2013. Inhibition of monoamine oxidase by 3, 4-dihydro-2 (1*H*)-quinolinone derivatives. *Bioorganic & medicinal chemistry letters*, 23(20):5498-5502.

Mostert, S., Petzer, A. & Petzer, J.P. 2015. Indanones as high-potency reversible inhibitors of monoamine oxidase. *ChemMedChem*, 10(5):862-873.

Mostert, S., Petzer, A. & Petzer, J.P. 2016. Inhibition of monoamine oxidase by benzoxathiolone analogues. *Bioorganic & medicinal chemistry letters*, 26(4):1200-1204.

Nel, M.S., Petzer, A., Petzer, J.P. & Legoabe, L.J. 2016. 2-Heteroarylidene-1-indanone derivatives as inhibitors of monoamine oxidase. *Bioorganic chemistry*, 69:20-28.

Petzer, A., Pienaar, A. & Petzer, J.P. 2013. The inhibition of monoamine oxidase by esomeprazole. *Drug research*, 63:462-467.

Rastogi, V., Barthwal, J. & Parmar, S.S. 1972. Synthesis of substituted 2-methyl-3 (4′-hydrazinocarbonyl-methylene-oxy-phenyl)-4-quinazolones as monoamine oxidase inhibitors. *Journal für praktische chemie*, 314(1):187-192.

Srivastav, M.K., Shamshuddin, M. & Shantakumar, S. 2013. Design, synthesis and characterization of novel 6, 7-dimethoxy-N 2-(substituted benzyl)-N 2-propylquinazoline-2, 4-diamine derivatives as anxiolytic and antidepressant agents. *American journal of chemistry*, 3(1):14-22.

Srivastava, V.K., Satsangi, R.K., Kumar, P. & Kishor, K. 1980. Monoamine oxidase inhibitory activity of 2-aryl-3-(5'-chlorobenzophenon-2'-yl)-quinazolin-4-(3*H*)-ones. *Indian journal of physiology and pharmacology*, 24(4):361-363.

Youdim, M.B., Edmondson, D. & Tipton, K.F. 2006. The therapeutic potential of monoamine oxidase inhibitors. *Nature reviews neuroscience*, 7(4):295-309.

APPENDIX A: SPECTRA

^{1}H NMR, ^{13}C NMR, MS and HPLC

Malikotsi A. Qhobosheane[1], Lesetja J. Legoabe[2,*], Jacobus P. Petzer[1,2], and Anél Petzer[1,2]

[1]Pharmaceutical Chemistry, School of Pharmacy, North-West University, Private Bag X6001, Potchefstroom 2520, South Africa

[2]Centre of Excellence for Pharmaceutical Sciences, North-West University, Private Bag X6001, Potchefstroom 2520, South Africa

2-(Benzylthio)quinazolin-4(3*H*)-one (3a)

^{1}H NMR

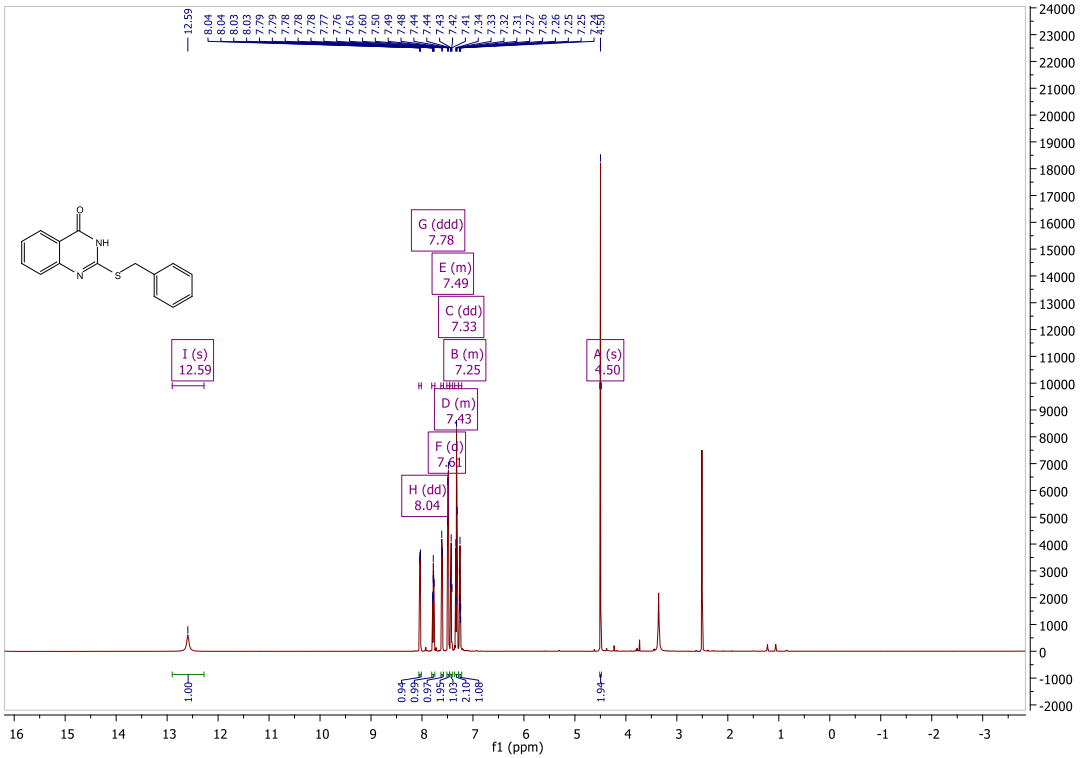

^{13}C NMR

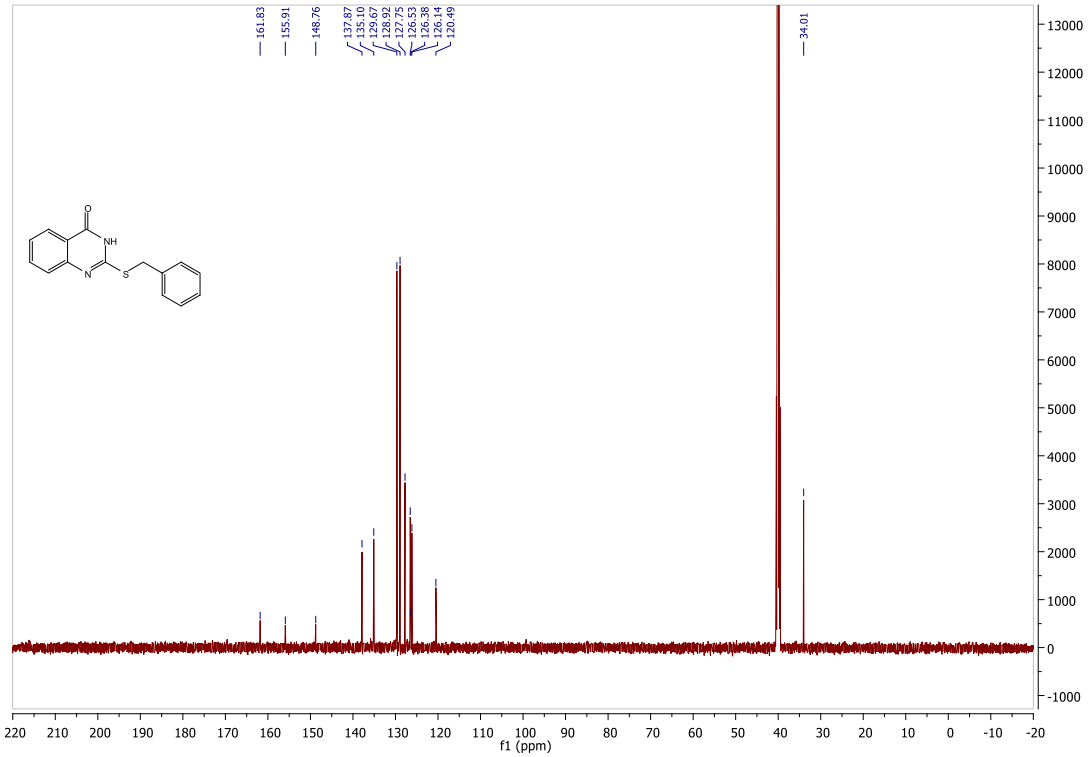

MS

Acquisition Parameter

Source Type	APCI	Ion Polarity	Positive	Set Nebulizer	1.6 Bar
Focus	Not active	Set Capillary	4500 V	Set Dry Heater	200 °C
Scan Begin	50 m/z	Set End Plate Offset	-500 V	Set Dry Gas	8.0 l/min
Scan End	1500 m/z	Set Collision Cell RF	100.0 Vpp	Set Divert Valve	Waste

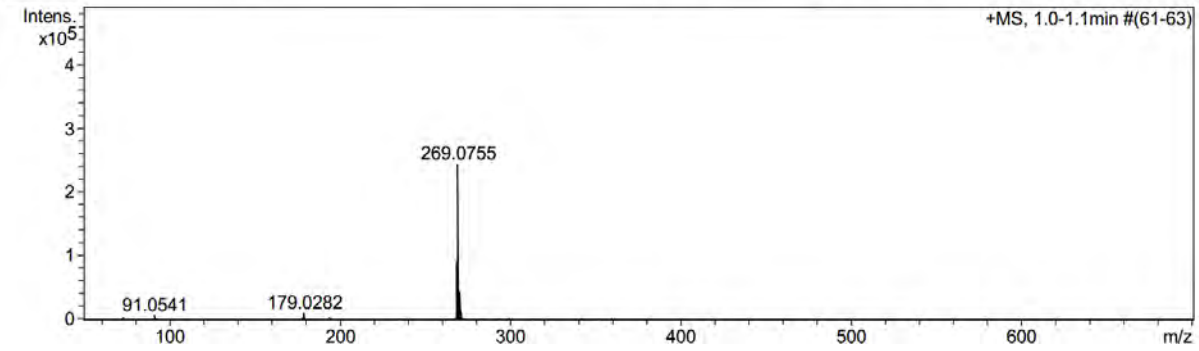

HPLC

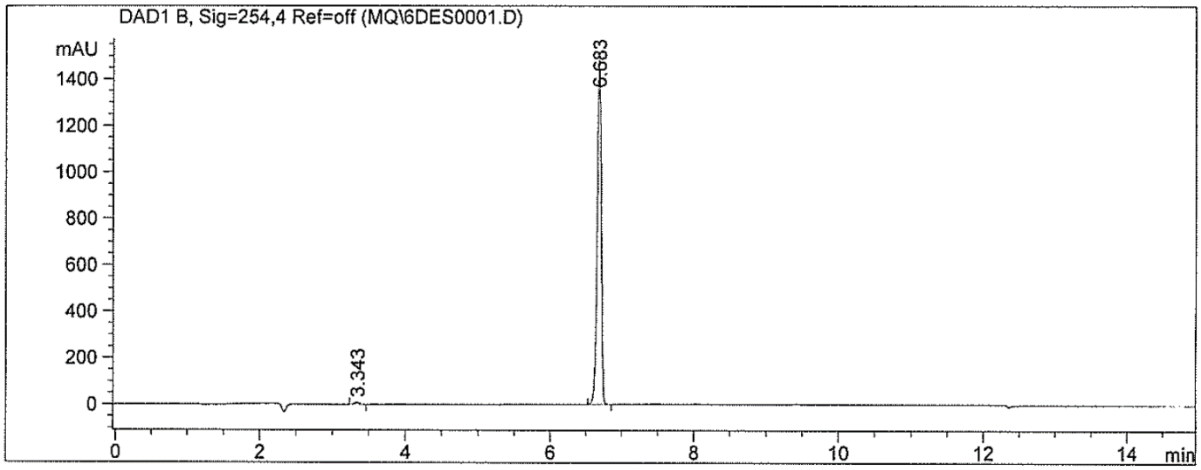

2-[(Pyridin-4-ylmethyl)thio]quinazolin-4(3*H*)-one (3b)

^{1}H NMR

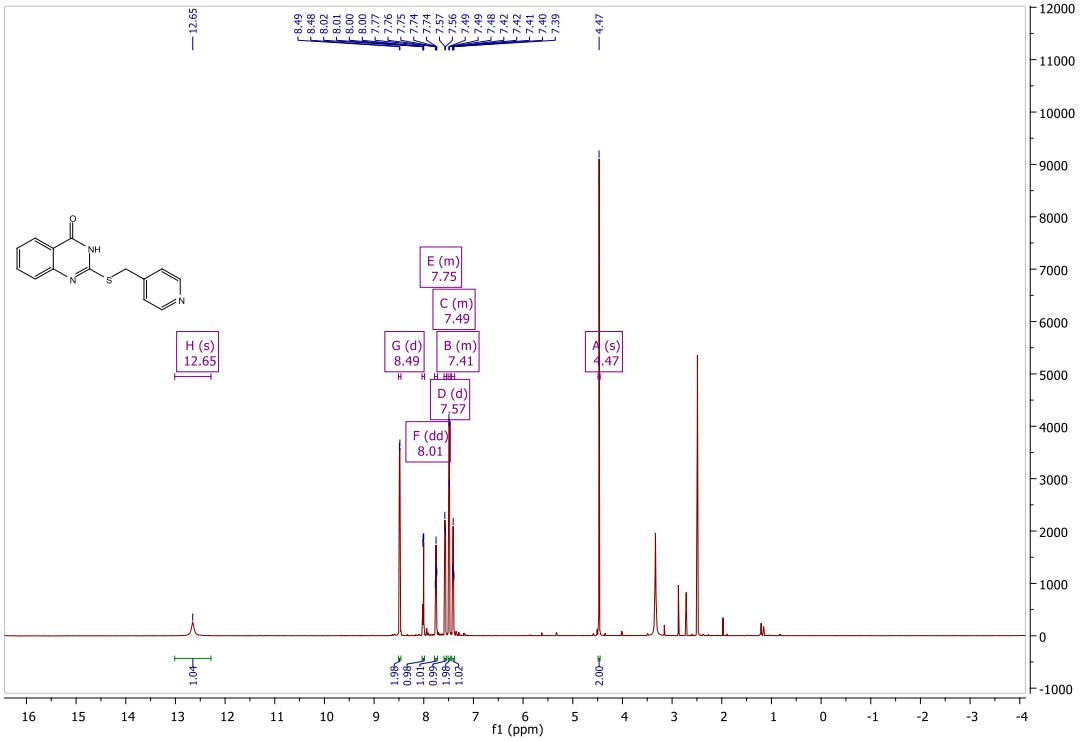

^{13}C NMR

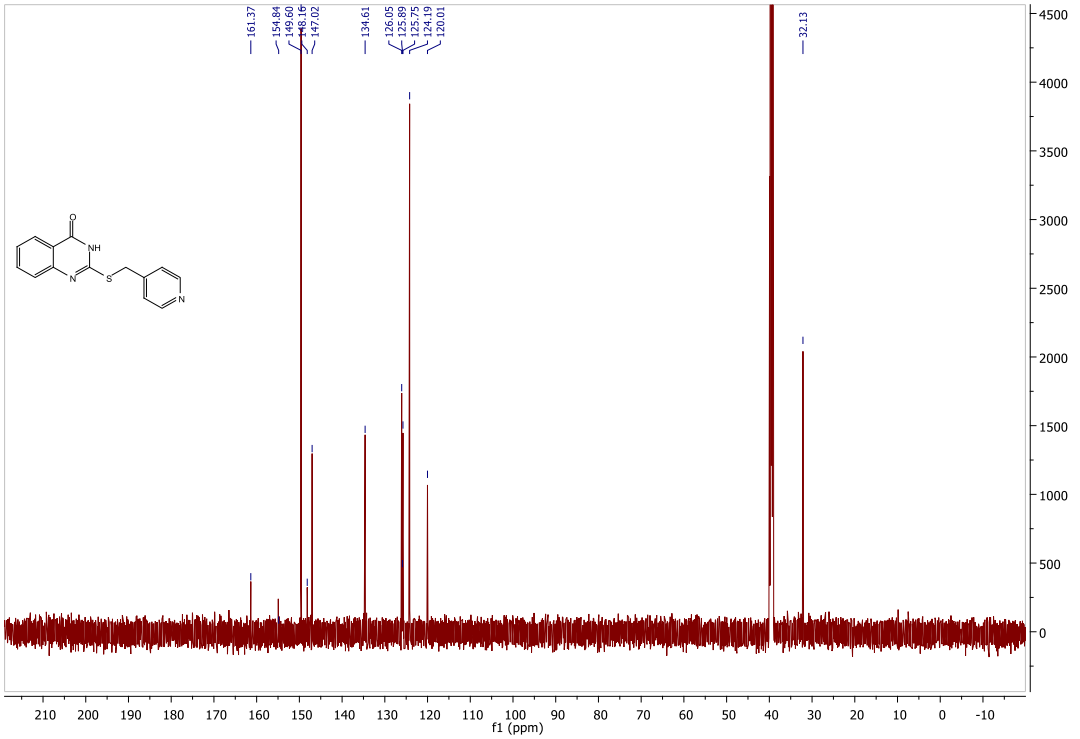

MS

Acquisition Parameter

Source Type	APCI	Ion Polarity	Positive	Set Nebulizer	1.6 Bar
Focus	Not active	Set Capillary	4500 V	Set Dry Heater	200 °C
Scan Begin	50 m/z	Set End Plate Offset	-500 V	Set Dry Gas	8.0 l/min
Scan End	1500 m/z	Set Collision Cell RF	100.0 Vpp	Set Divert Valve	Waste

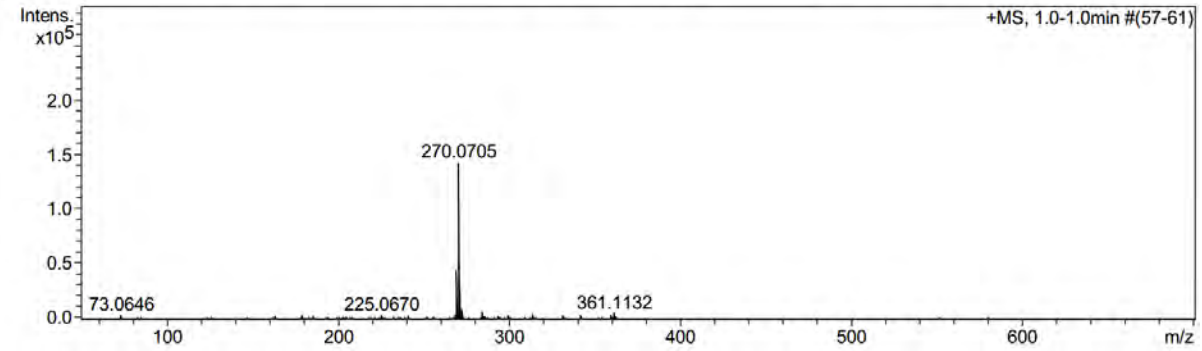

HPLC

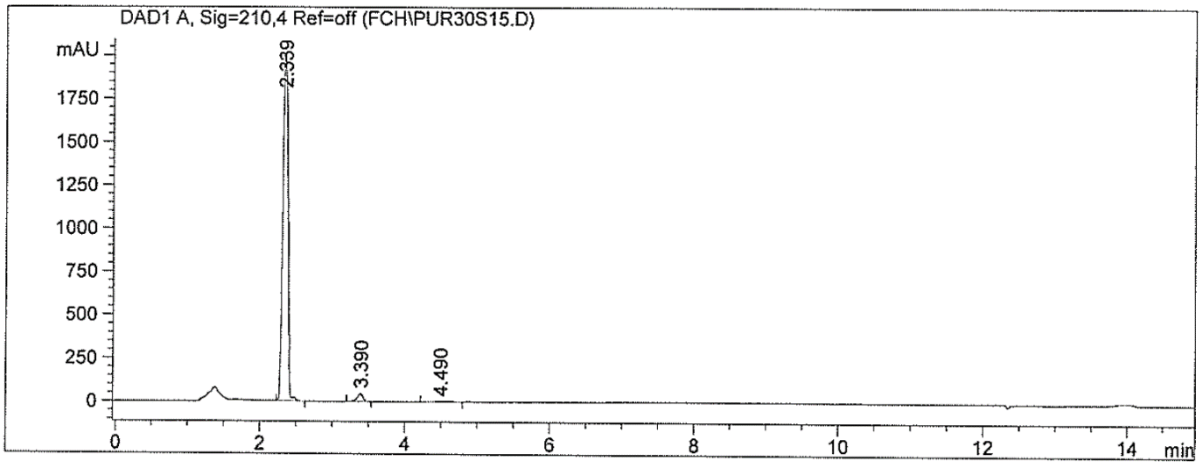

2-[(4-Fluorobenzyl)thio]quinazolin-4(3*H*)-one (3c)

^{1}H NMR

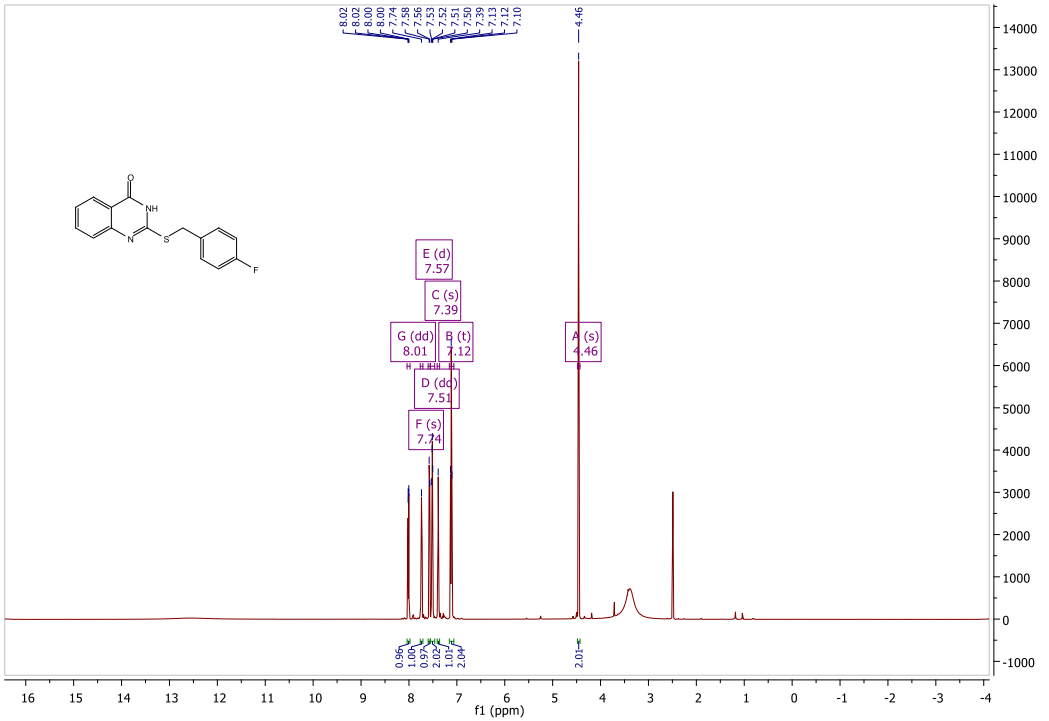

^{13}C NMR

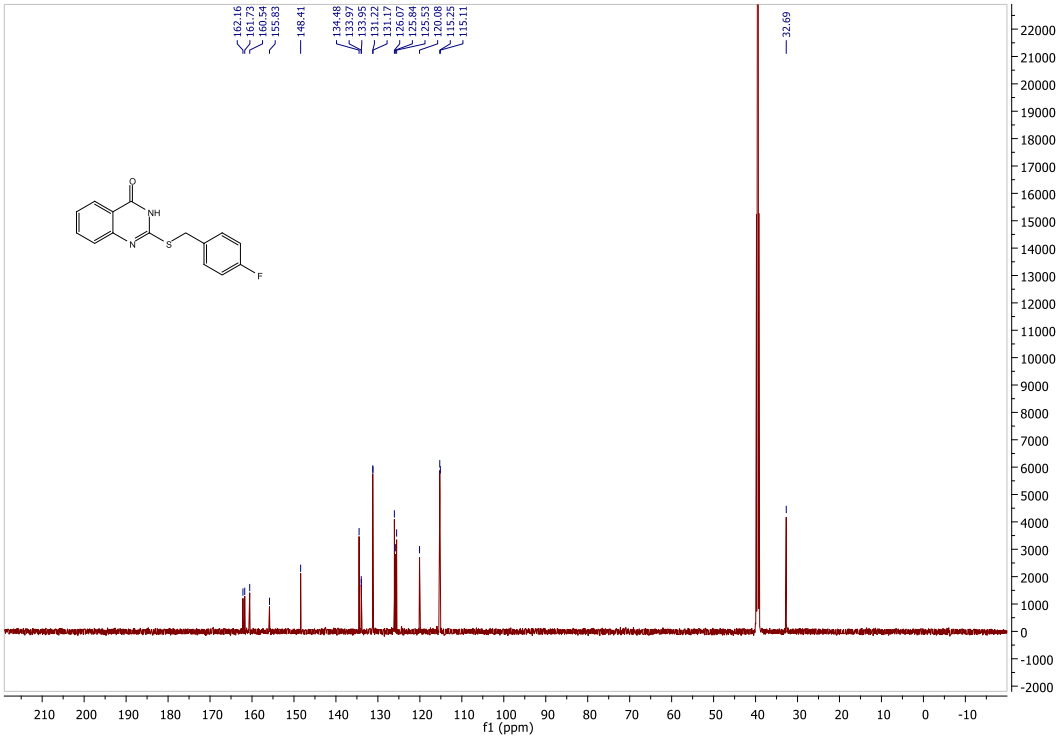

MS

Acquisition Parameter

Source Type	APCI	Ion Polarity	Positive	Set Nebulizer	1.6 Bar
Focus	Not active	Set Capillary	4500 V	Set Dry Heater	200 °C
Scan Begin	50 m/z	Set End Plate Offset	-500 V	Set Dry Gas	8.0 l/min
Scan End	1500 m/z	Set Collision Cell RF	100.0 Vpp	Set Divert Valve	Waste

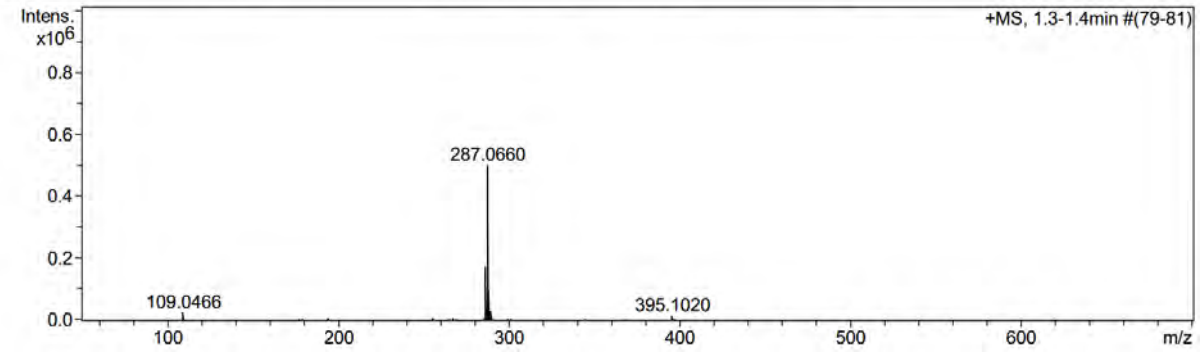

HPLC

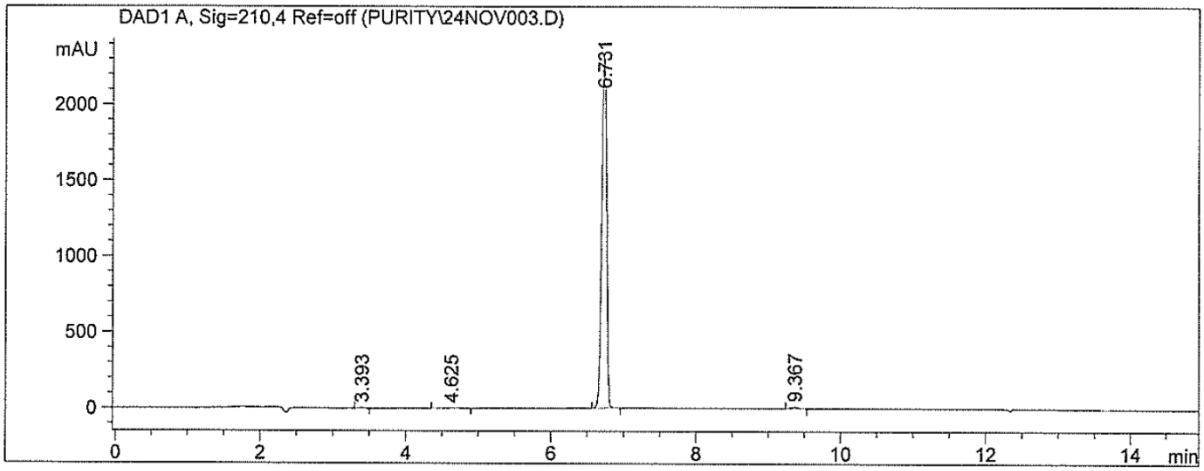

2-[(4-Chlorobenzyl)thio]quinazoline-4(3*H*)-one (3d)

^{1}H NMR

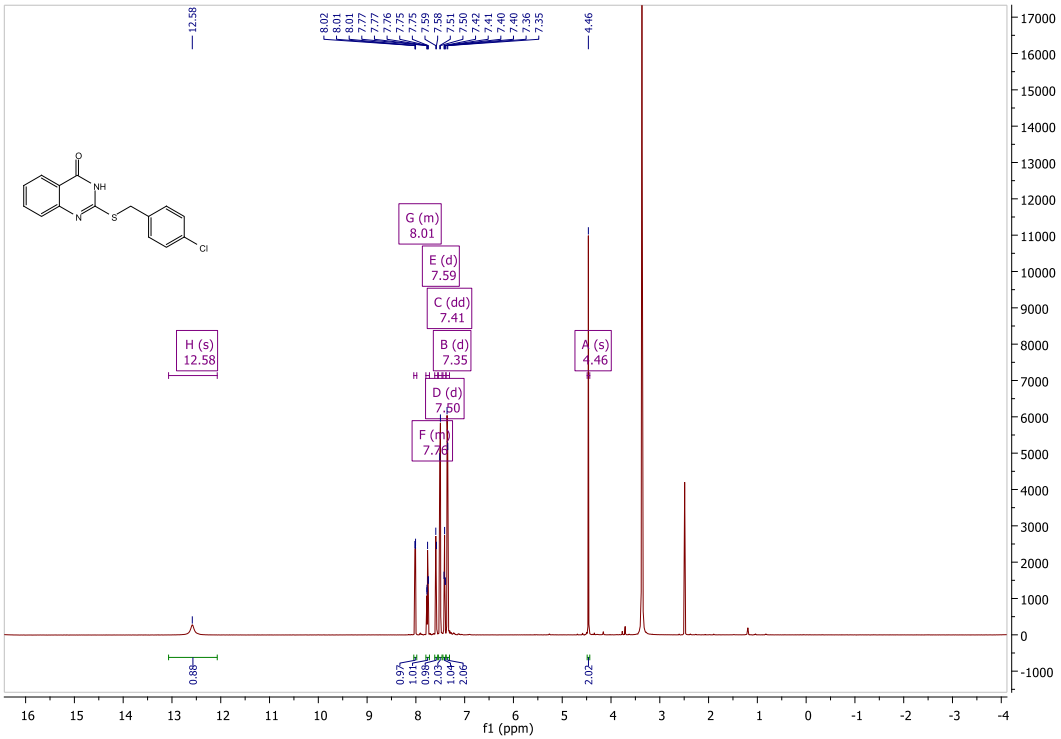

^{13}C NMR

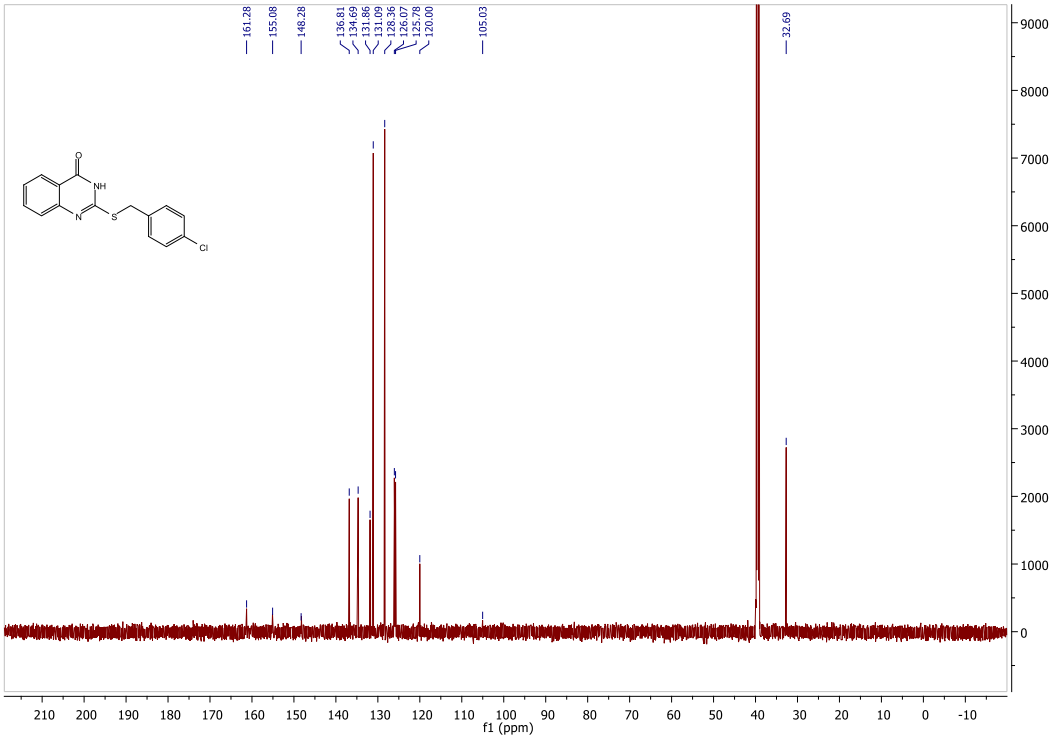

MS

Acquisition Parameter

Source Type	APCI	Ion Polarity	Positive	Set Nebulizer	1.6 Bar
Focus	Not active	Set Capillary	4500 V	Set Dry Heater	200 °C
Scan Begin	50 m/z	Set End Plate Offset	-500 V	Set Dry Gas	8.0 l/min
Scan End	1500 m/z	Set Collision Cell RF	100.0 Vpp	Set Divert Valve	Waste

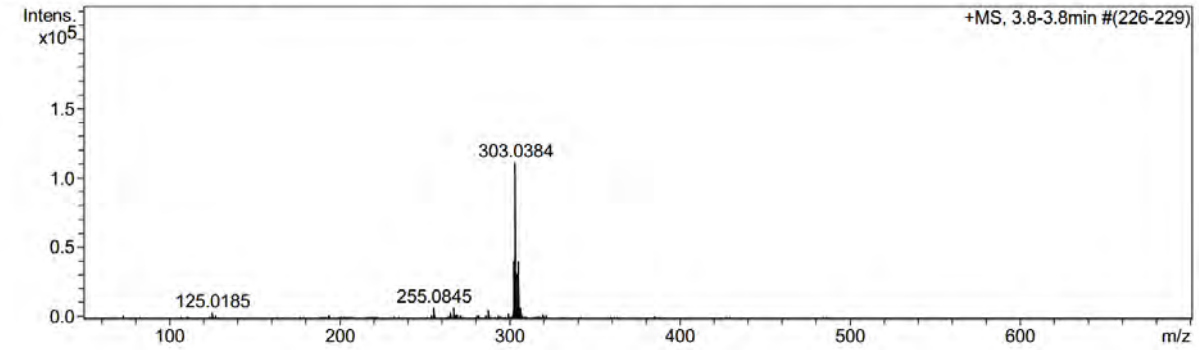

HPLC

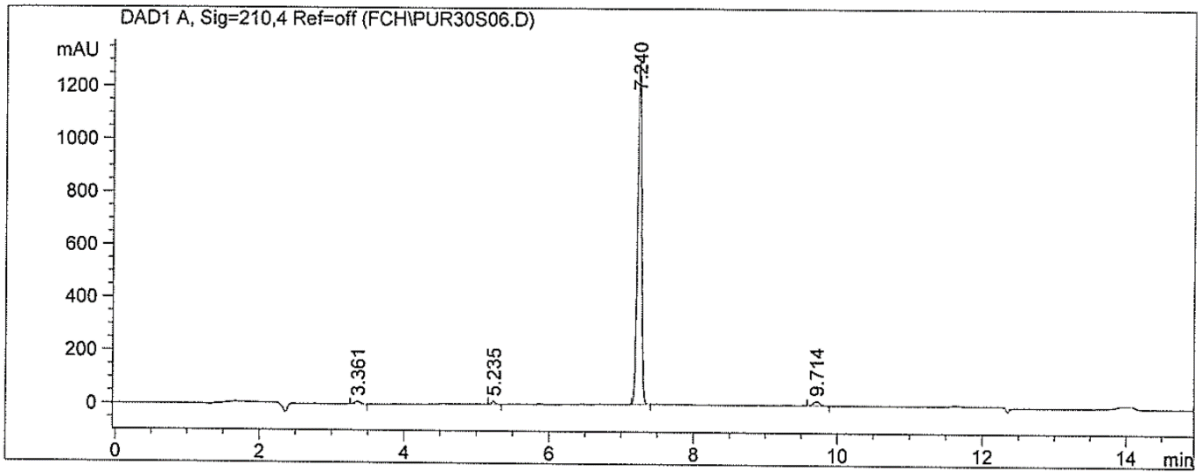

2-[(4-Bromobenzyl)thio]quinazoline-4(3*H*)-one (3e)

^{1}H NMR

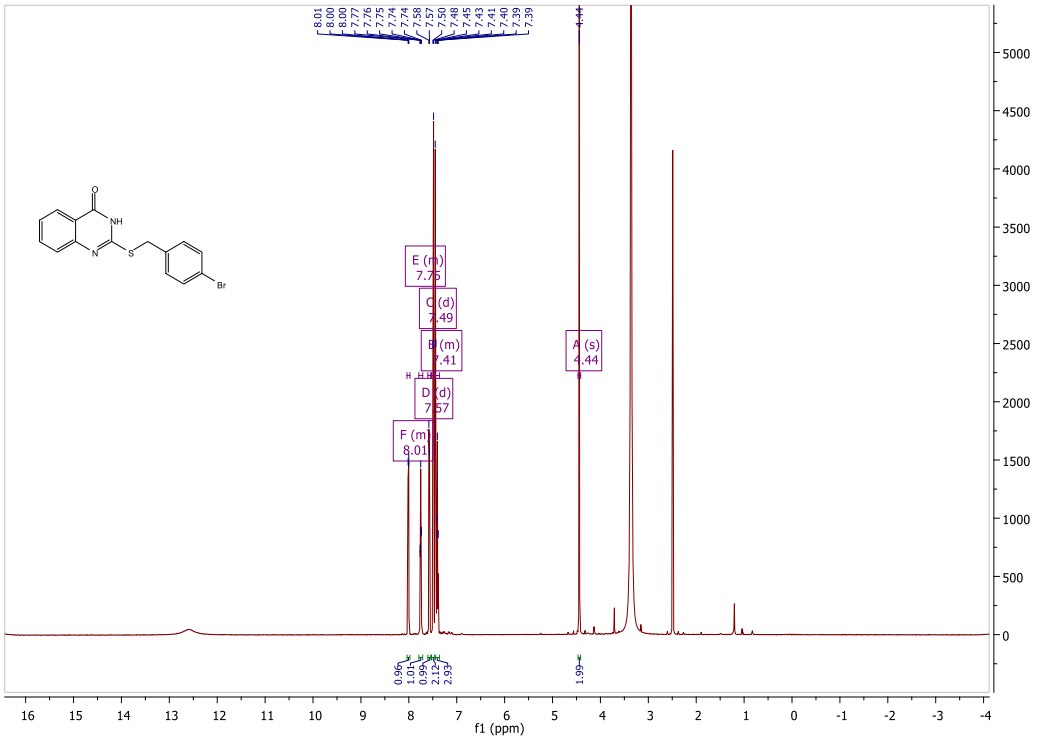

^{13}C NMR

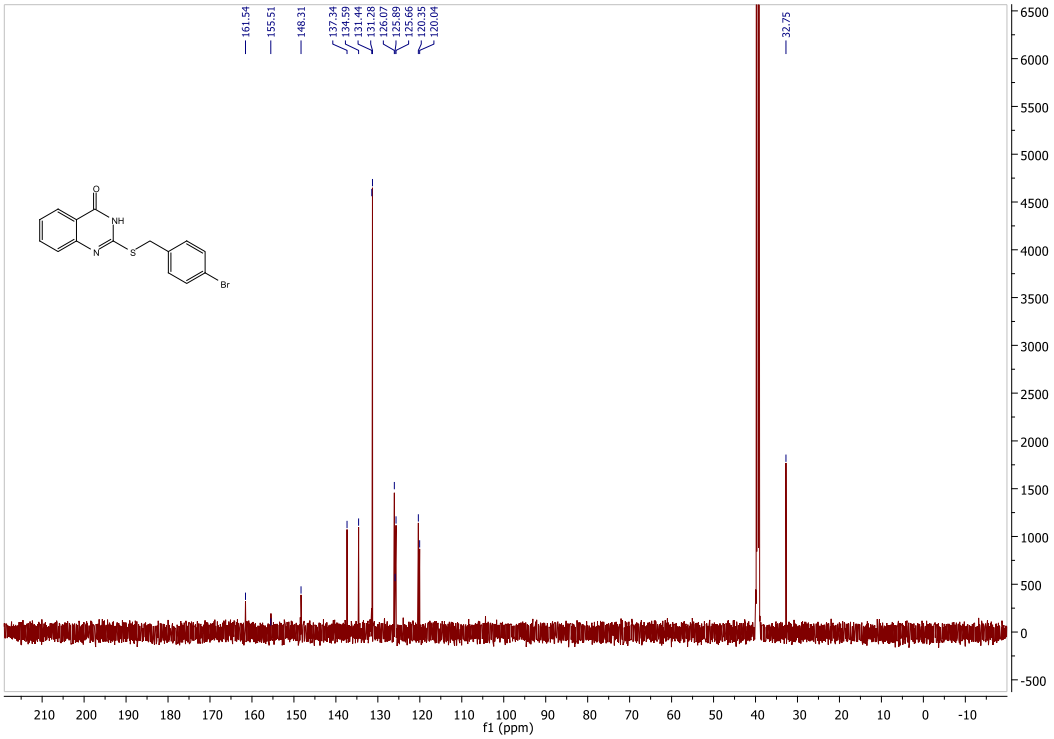

MS

Acquisition Parameter

Source Type	APCI	Ion Polarity	Positive	Set Nebulizer	1.6 Bar
Focus	Not active	Set Capillary	4500 V	Set Dry Heater	200 °C
Scan Begin	50 m/z	Set End Plate Offset	-500 V	Set Dry Gas	8.0 l/min
Scan End	1500 m/z	Set Collision Cell RF	100.0 Vpp	Set Divert Valve	Waste

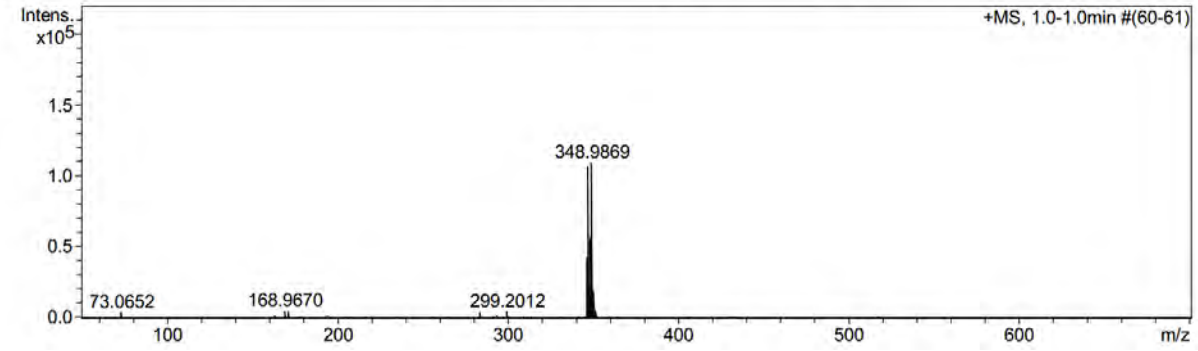

HPLC

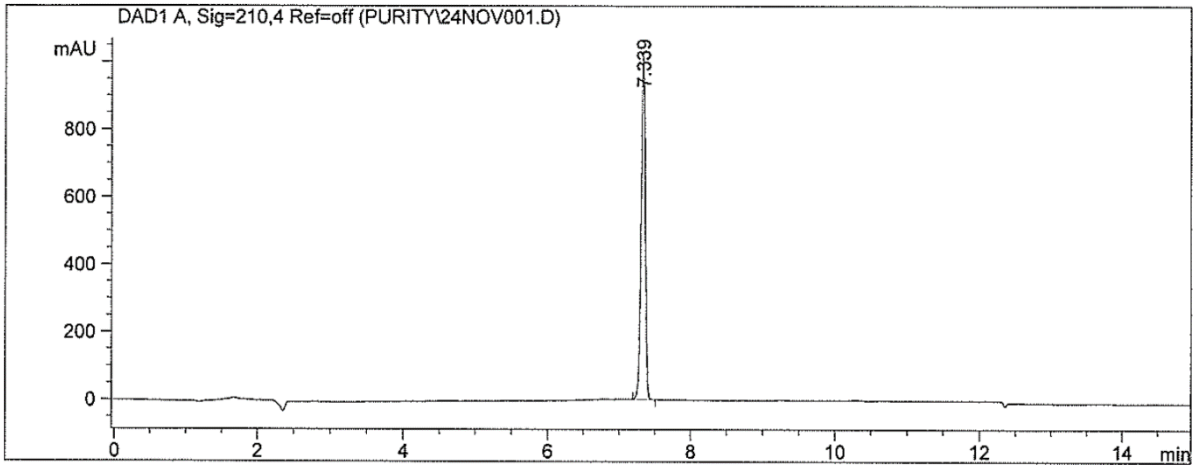

2-[(4-Iodobenzyl)thio]quinazoline-4(3*H*)-one (3f)

^{1}H NMR

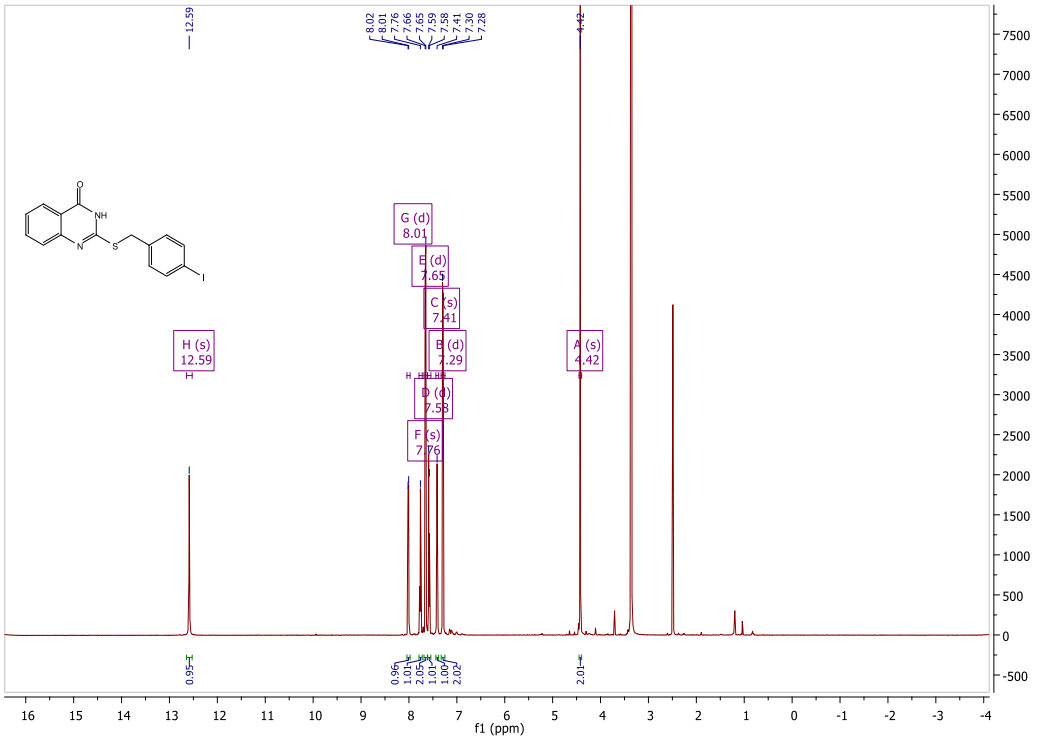

^{13}C NMR

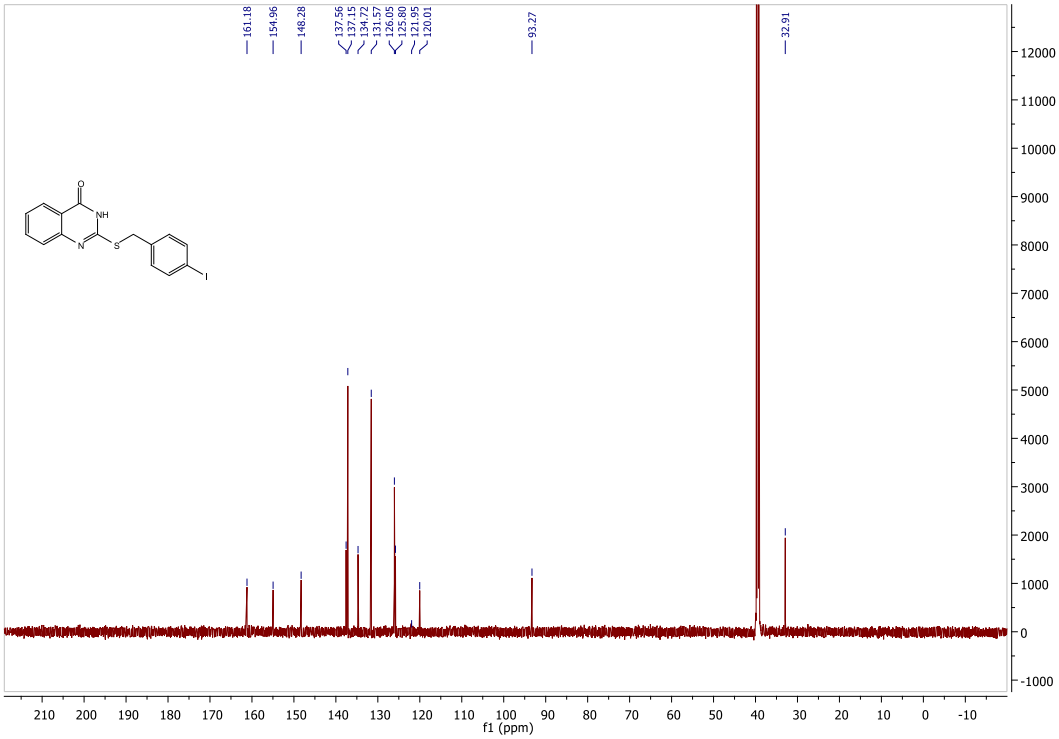

MS

Acquisition Parameter

Source Type	APCI	Ion Polarity	Positive	Set Nebulizer	1.6 Bar
Focus	Not active	Set Capillary	4500 V	Set Dry Heater	200 °C
Scan Begin	50 m/z	Set End Plate Offset	-500 V	Set Dry Gas	8.0 l/min
Scan End	1500 m/z	Set Collision Cell RF	100.0 Vpp	Set Divert Valve	Waste

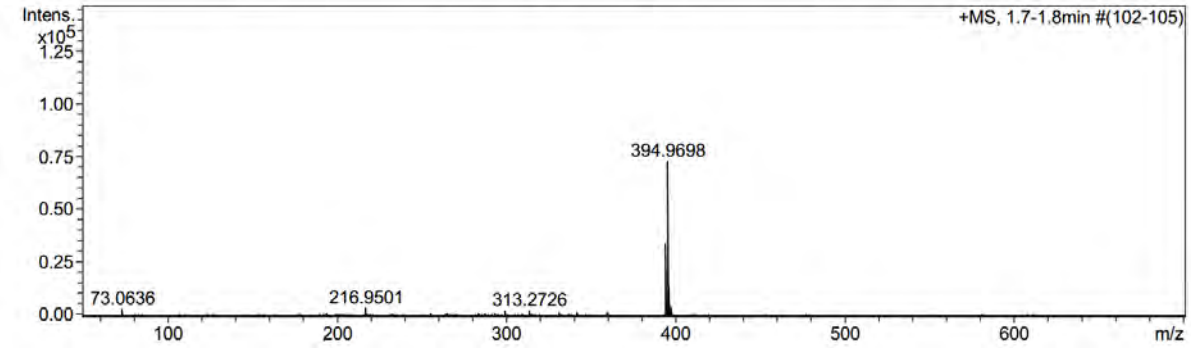

HPLC

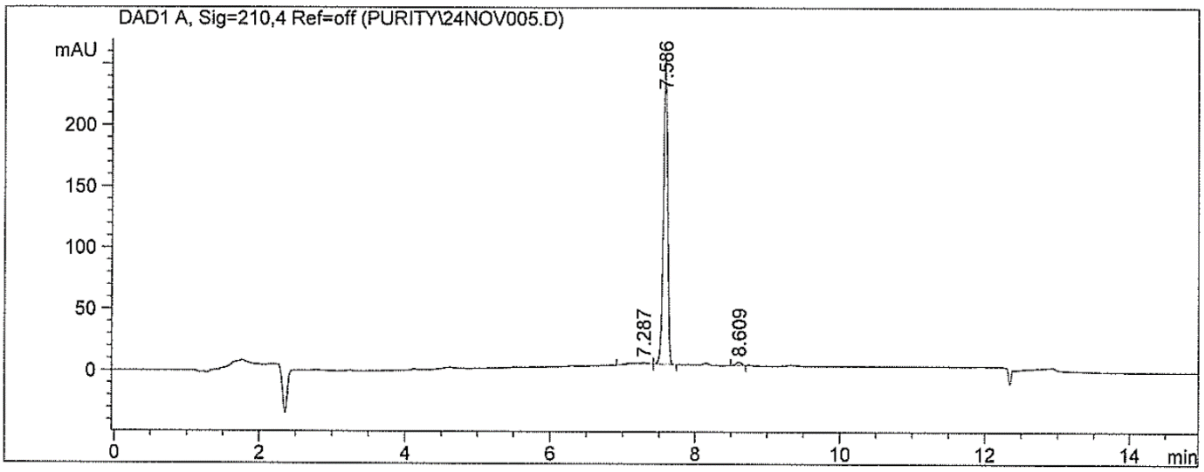

2-[(4-Trifluoromethyl)thio]quinazolin-4(3*H*)-one (3g)

^{1}H NMR

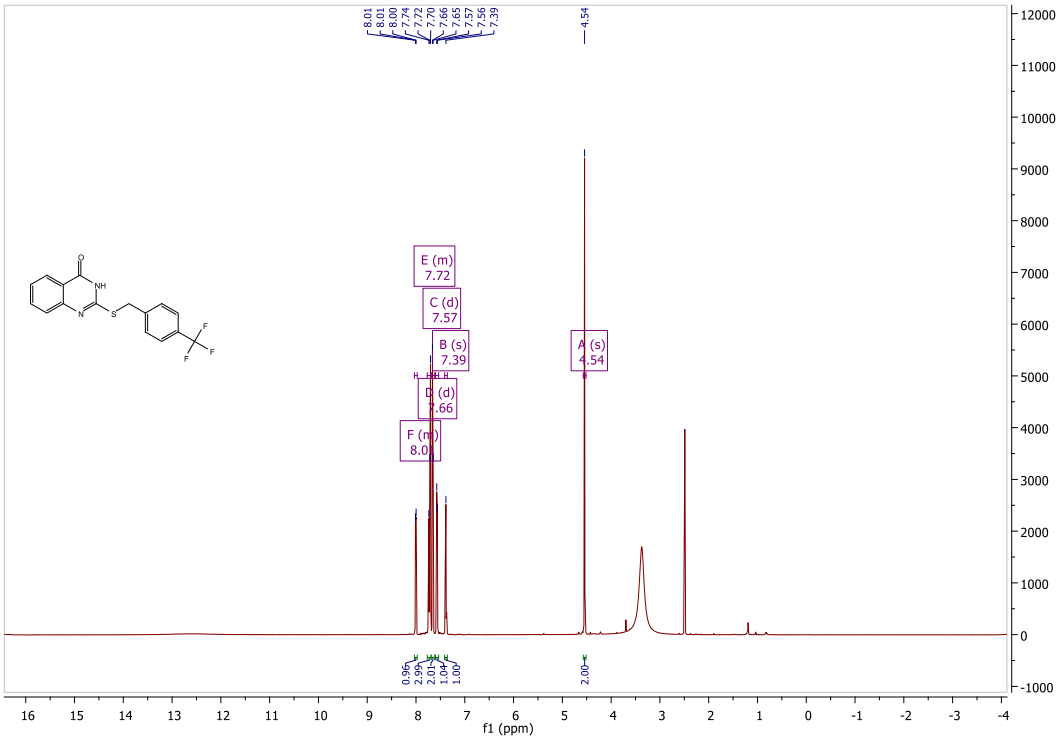

^{13}C NMR

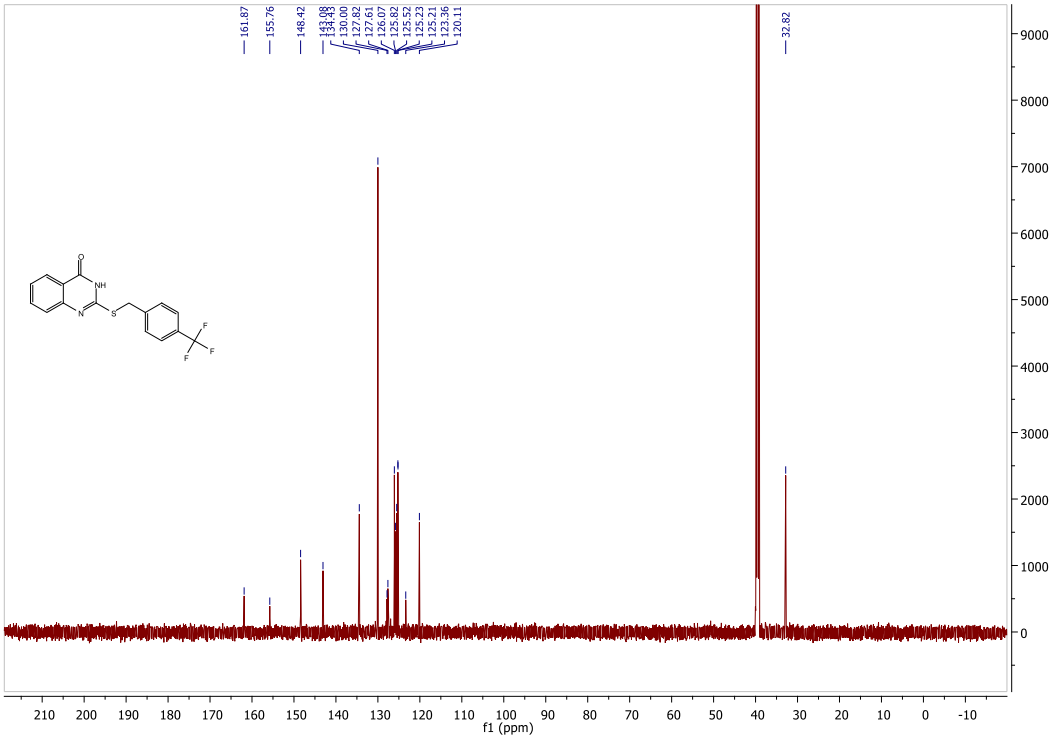

MS

Acquisition Parameter

Source Type	APCI	Ion Polarity	Positive	Set Nebulizer	1.6 Bar
Focus	Not active	Set Capillary	4500 V	Set Dry Heater	200 °C
Scan Begin	50 m/z	Set End Plate Offset	-500 V	Set Dry Gas	8.0 l/min
Scan End	1500 m/z	Set Collision Cell RF	100.0 Vpp	Set Divert Valve	Waste

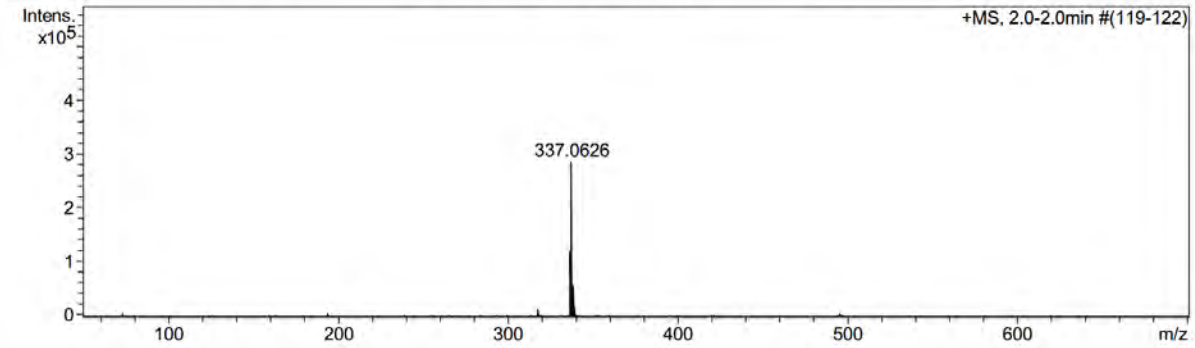

HPLC

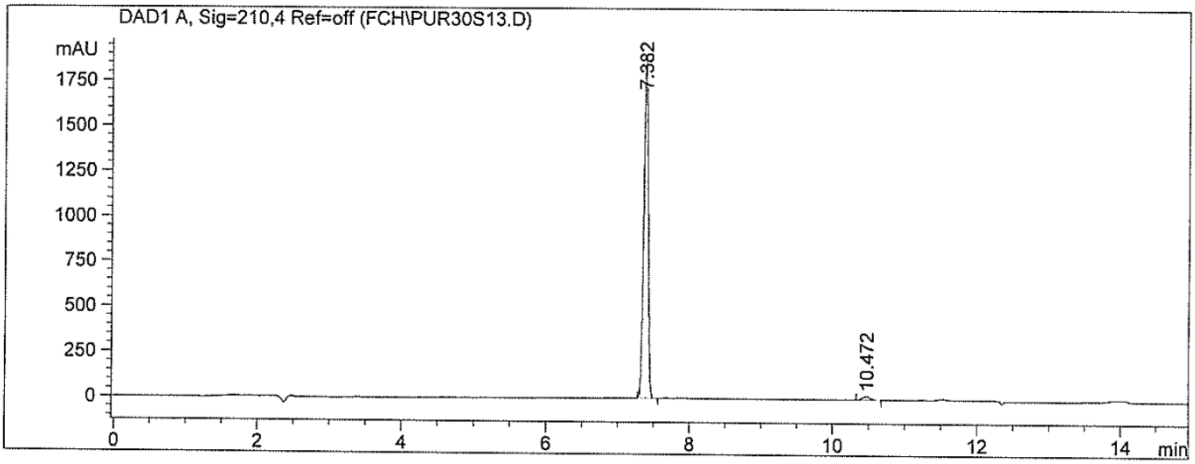

2-[(3-Fluorobenzyl)thio]quinazoline-4(3*H*)-one (3h)

^{1}H NMR

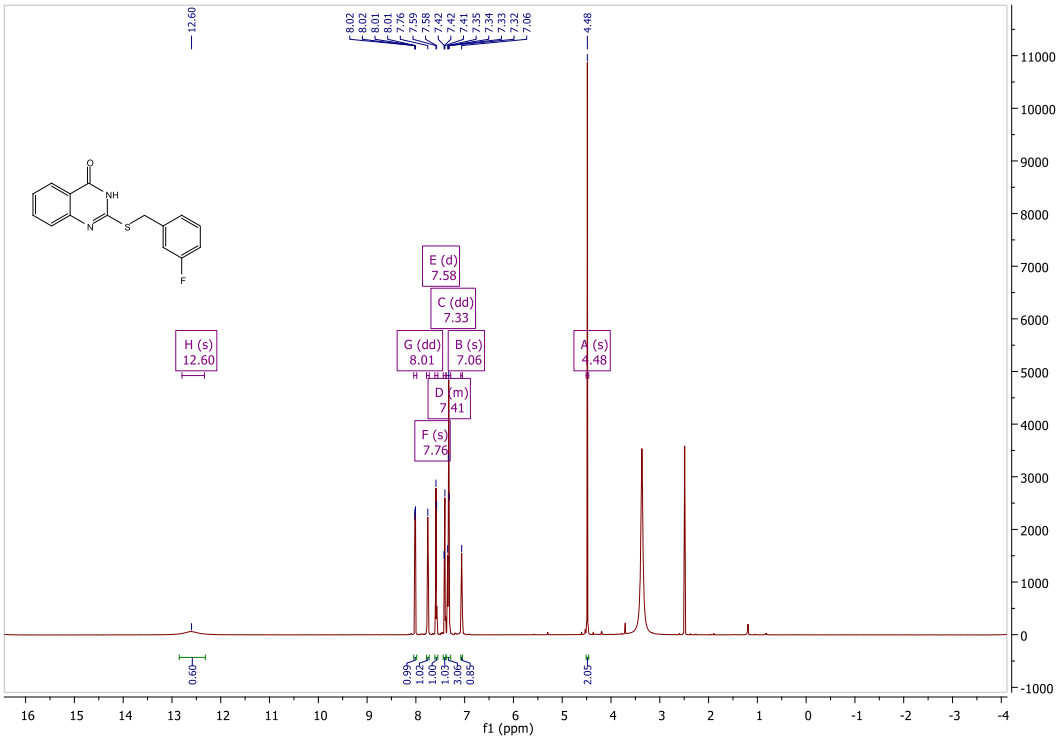

^{13}C NMR

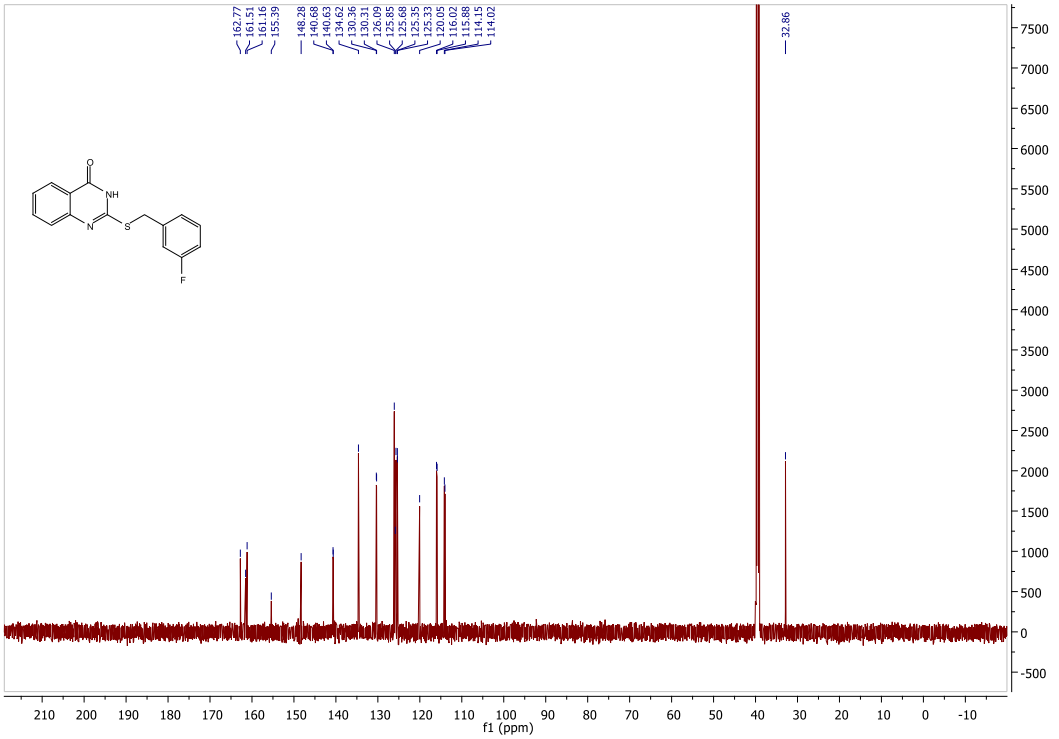

MS

Acquisition Parameter

Source Type	APCI	Ion Polarity	Positive	Set Nebulizer	1.6 Bar
Focus	Not active	Set Capillary	4500 V	Set Dry Heater	200 °C
Scan Begin	50 m/z	Set End Plate Offset	-500 V	Set Dry Gas	8.0 l/min
Scan End	1500 m/z	Set Collision Cell RF	100.0 Vpp	Set Divert Valve	Waste

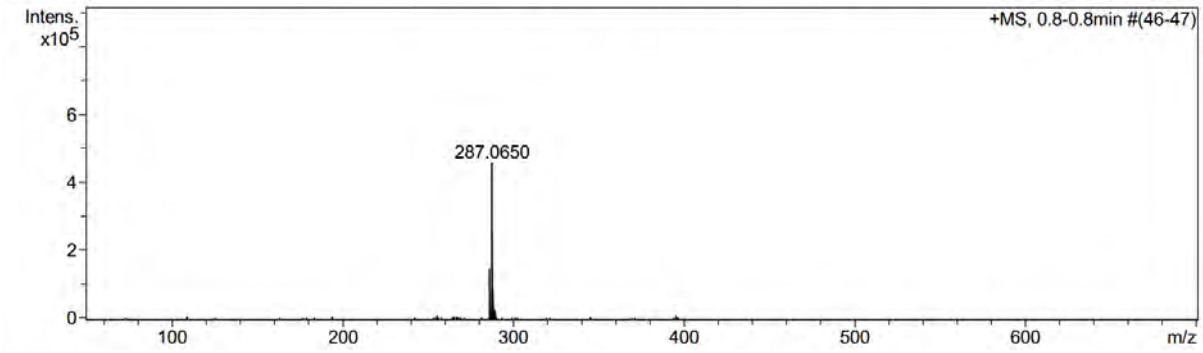

HPLC

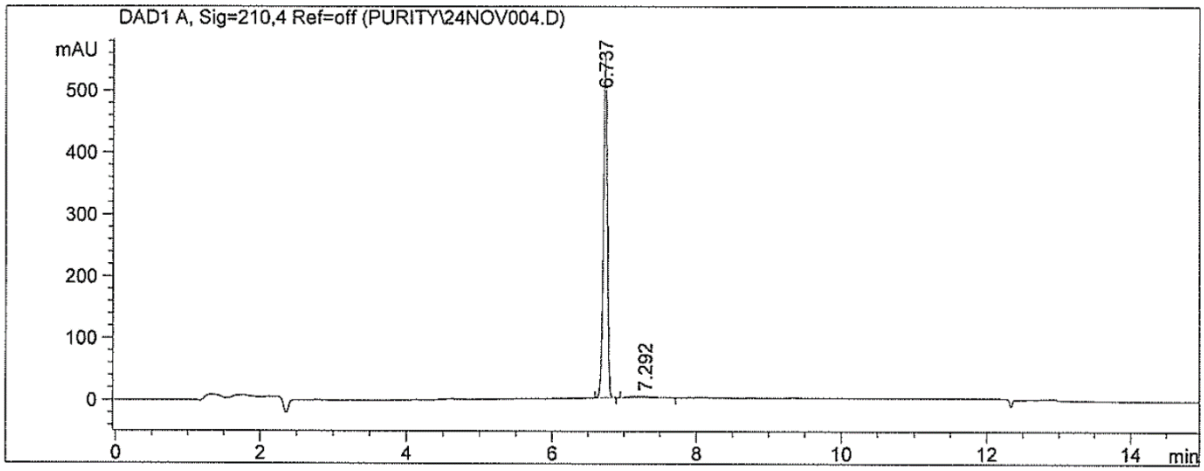

2-[(3-Chlorobenzyl)thio]quinazolin-4(3*H*)-one (3i)

^{1}H NMR

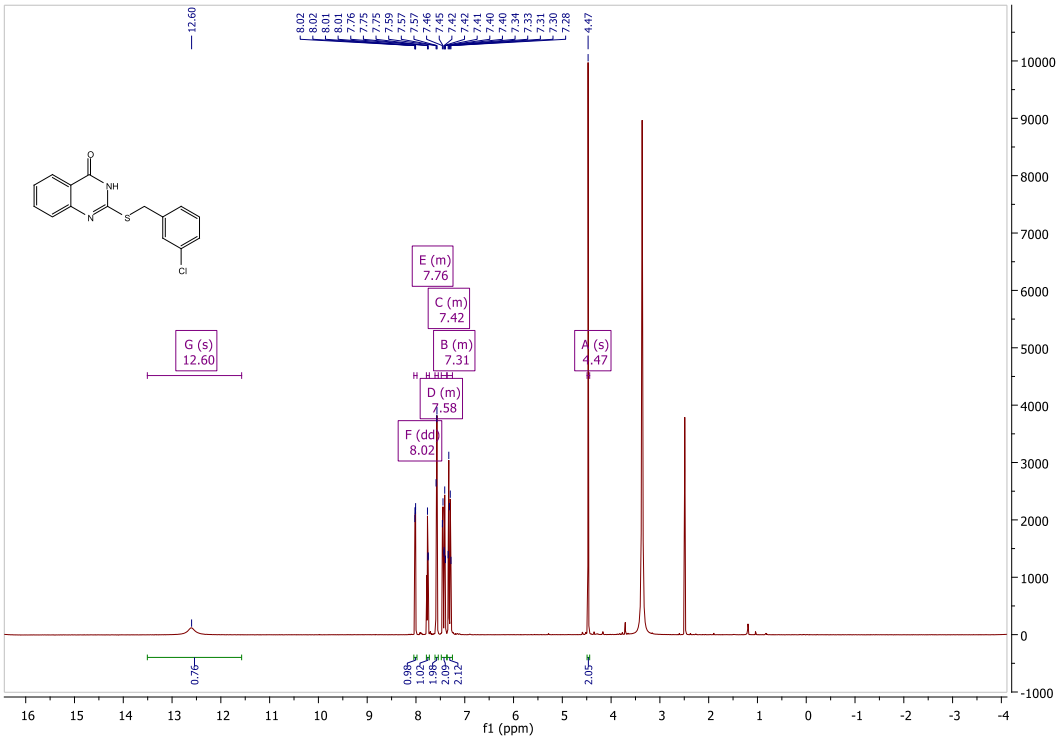

^{13}C NMR

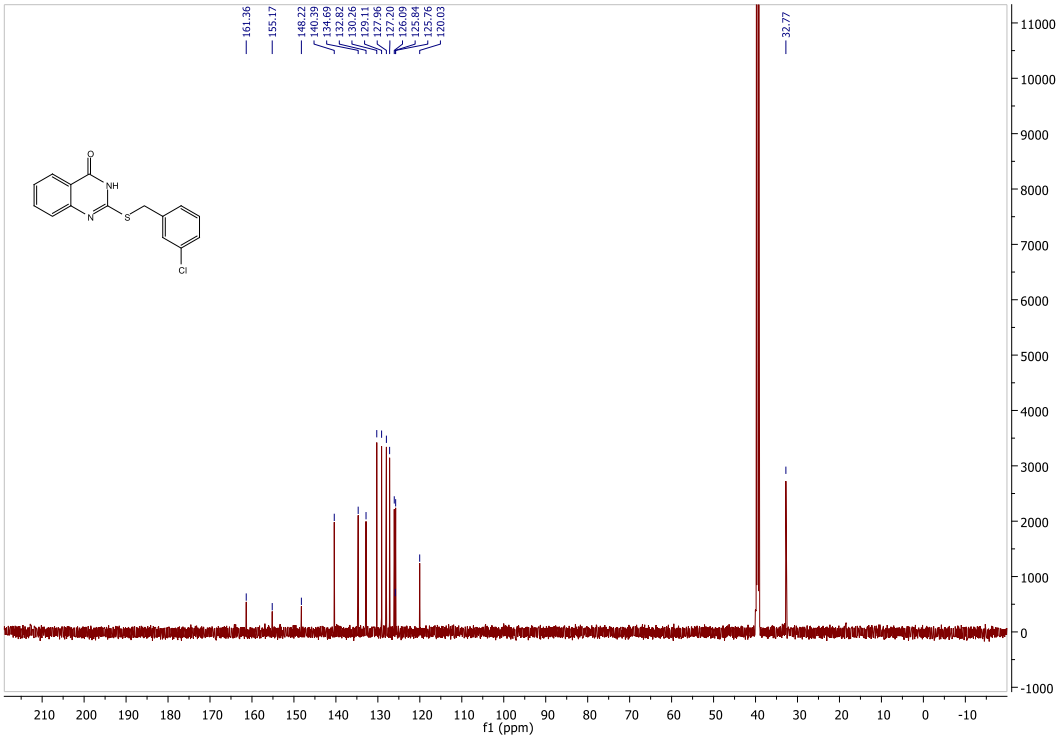

MS

Acquisition Parameter

Source Type	APCI	Ion Polarity	Positive	Set Nebulizer	1.6 Bar
Focus	Not active	Set Capillary	4500 V	Set Dry Heater	200 °C
Scan Begin	50 m/z	Set End Plate Offset	-500 V	Set Dry Gas	8.0 l/min
Scan End	1500 m/z	Set Collision Cell RF	100.0 Vpp	Set Divert Valve	Waste

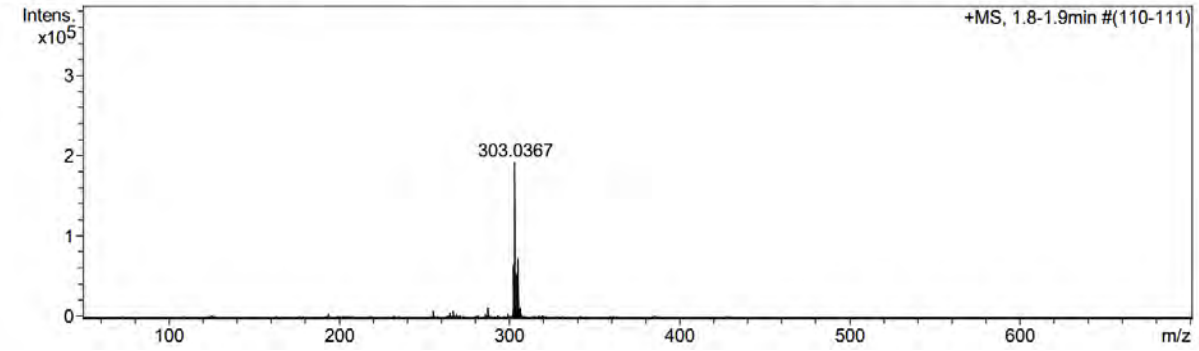

HPLC

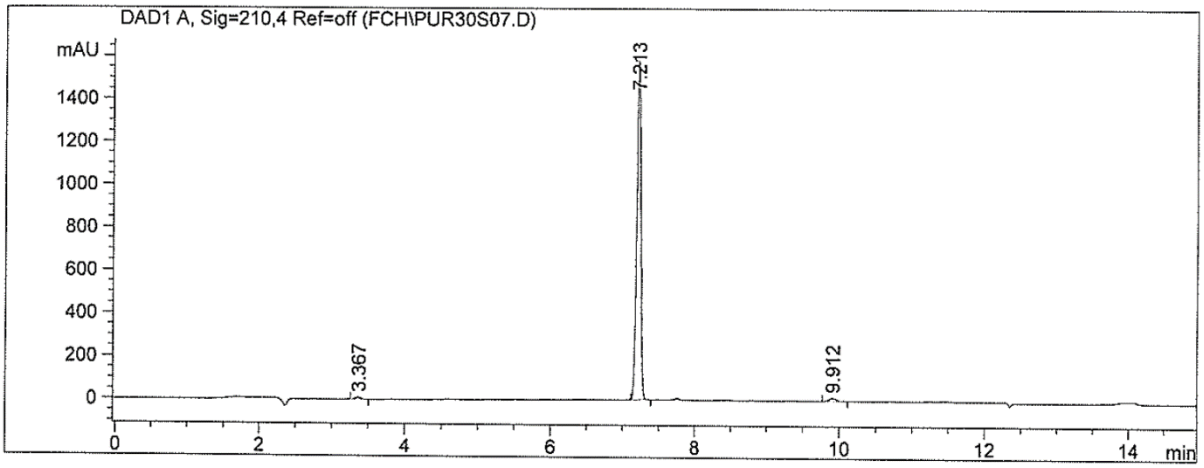

2-[(3-Bromobenzyl)thio]quinazoline-4(3*H*)-one (3j)

^{1}H NMR

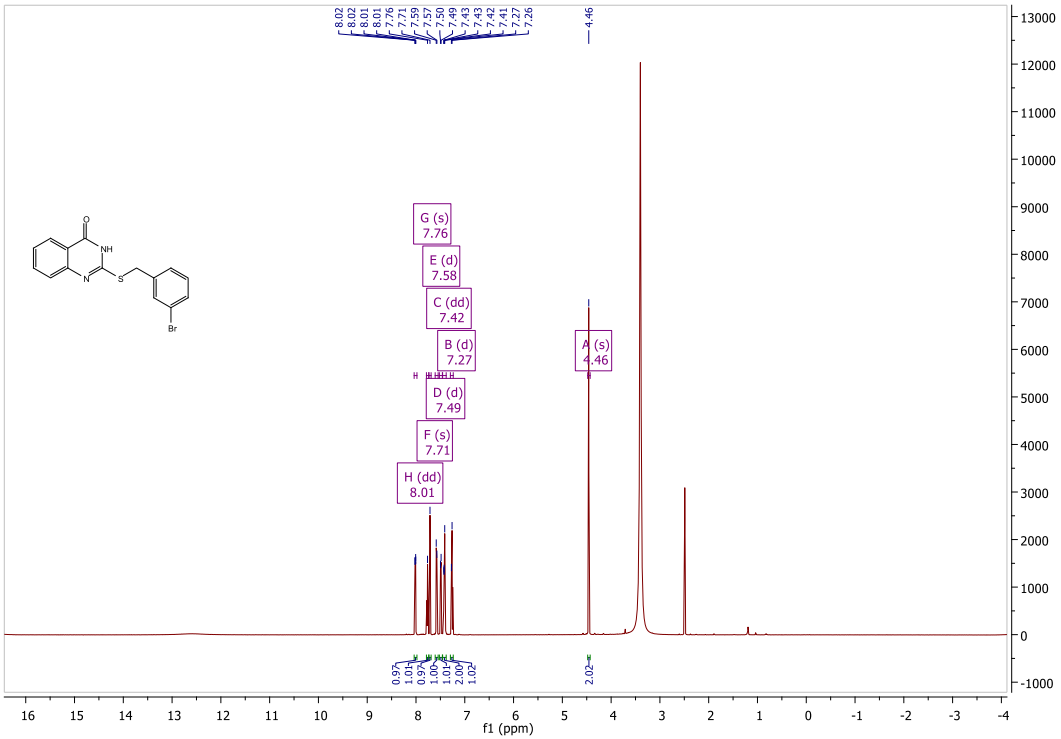

^{13}C NMR

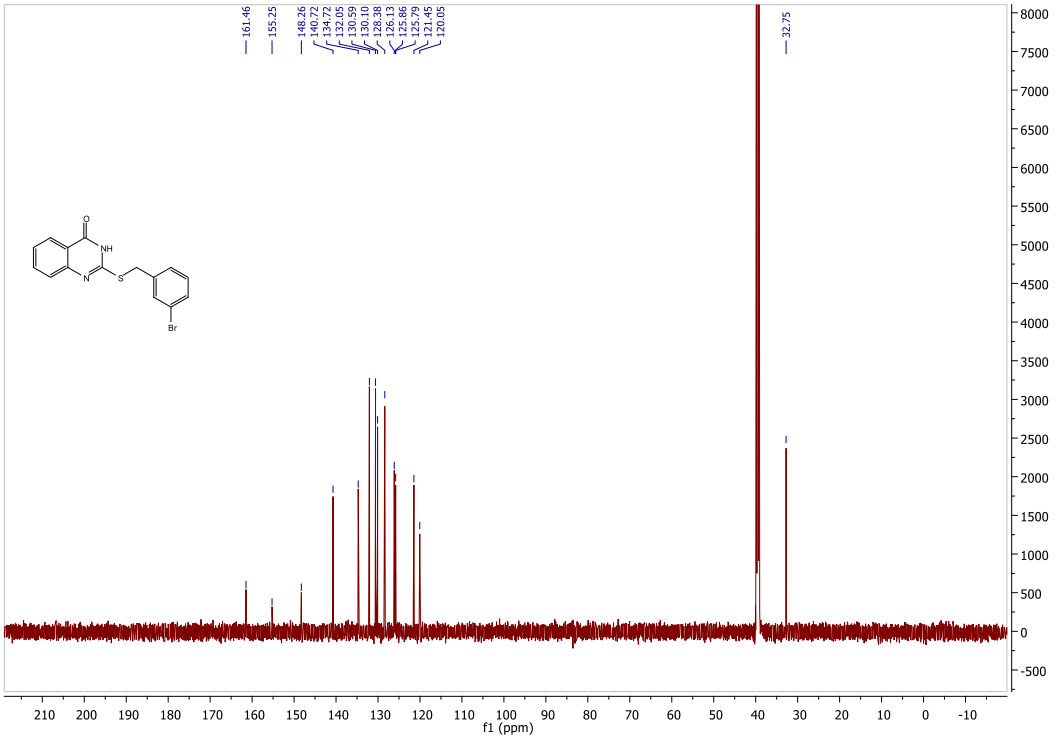

MS

Acquisition Parameter

Source Type	APCI	Ion Polarity	Positive	Set Nebulizer	1.6 Bar
Focus	Not active	Set Capillary	4500 V	Set Dry Heater	200 °C
Scan Begin	50 m/z	Set End Plate Offset	-500 V	Set Dry Gas	8.0 l/min
Scan End	1500 m/z	Set Collision Cell RF	100.0 Vpp	Set Divert Valve	Waste

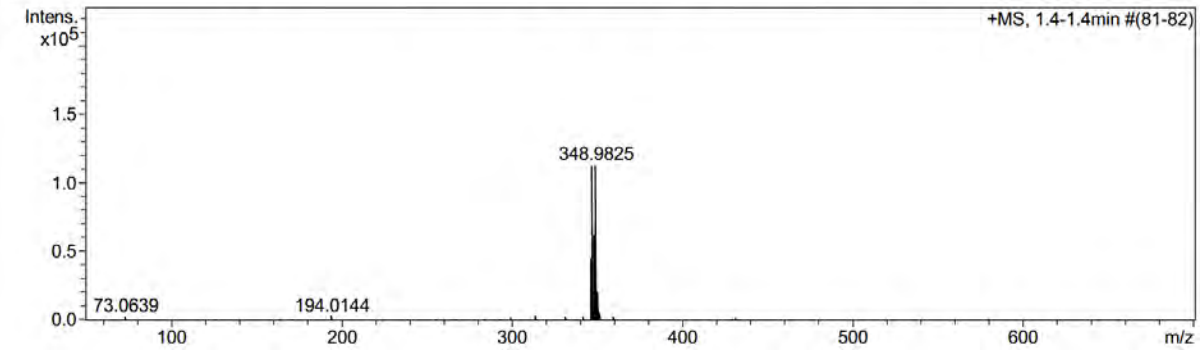

HPLC

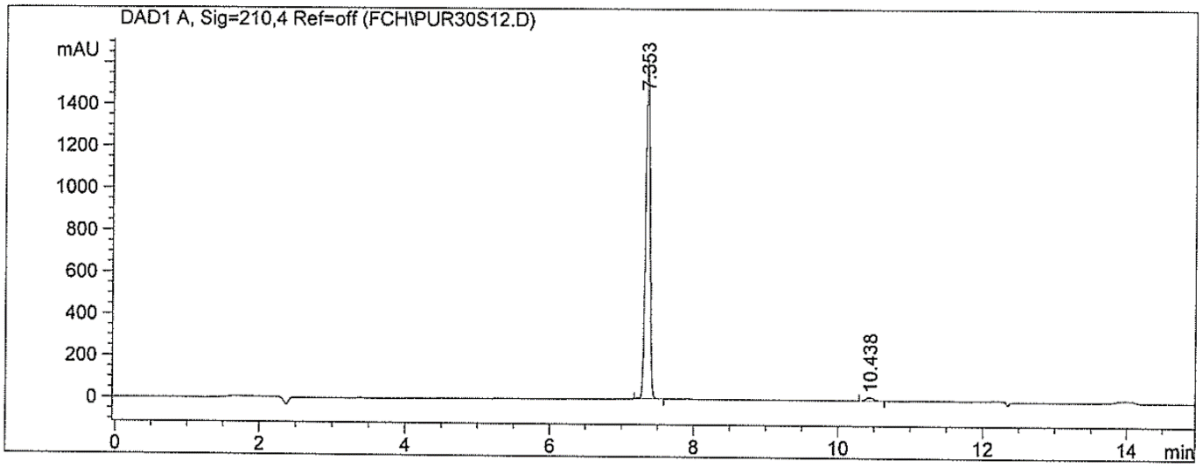

2-[(3-Iodobenzyl)thio]quinazoline-4(3*H*)-one (3k)

^{1}H NMR

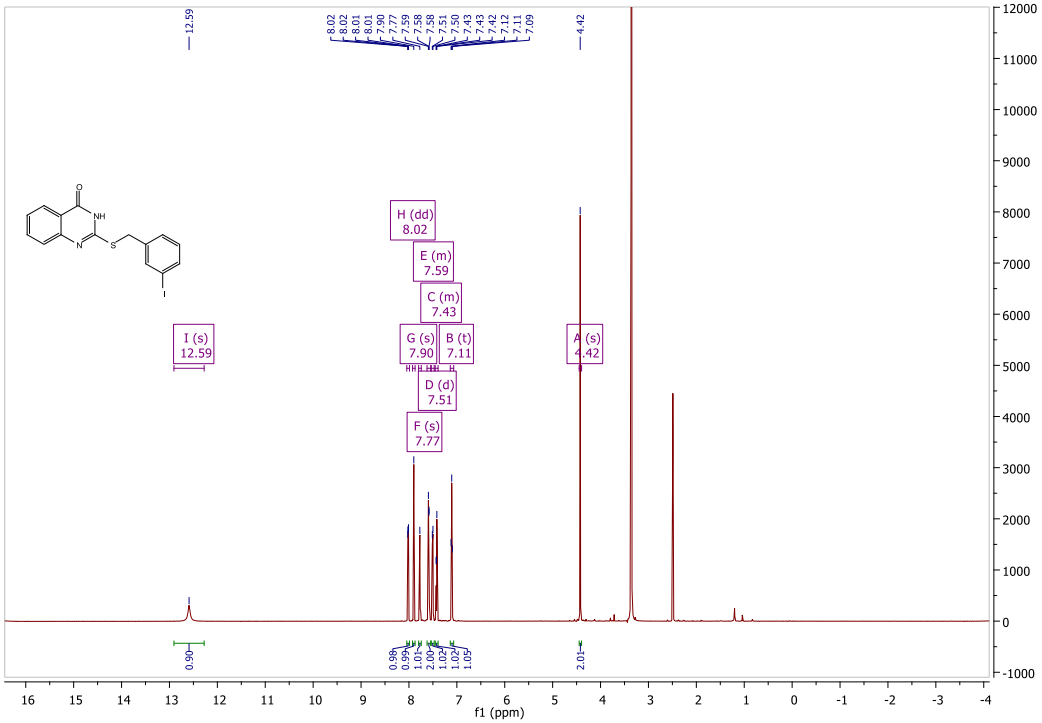

^{13}C NMR

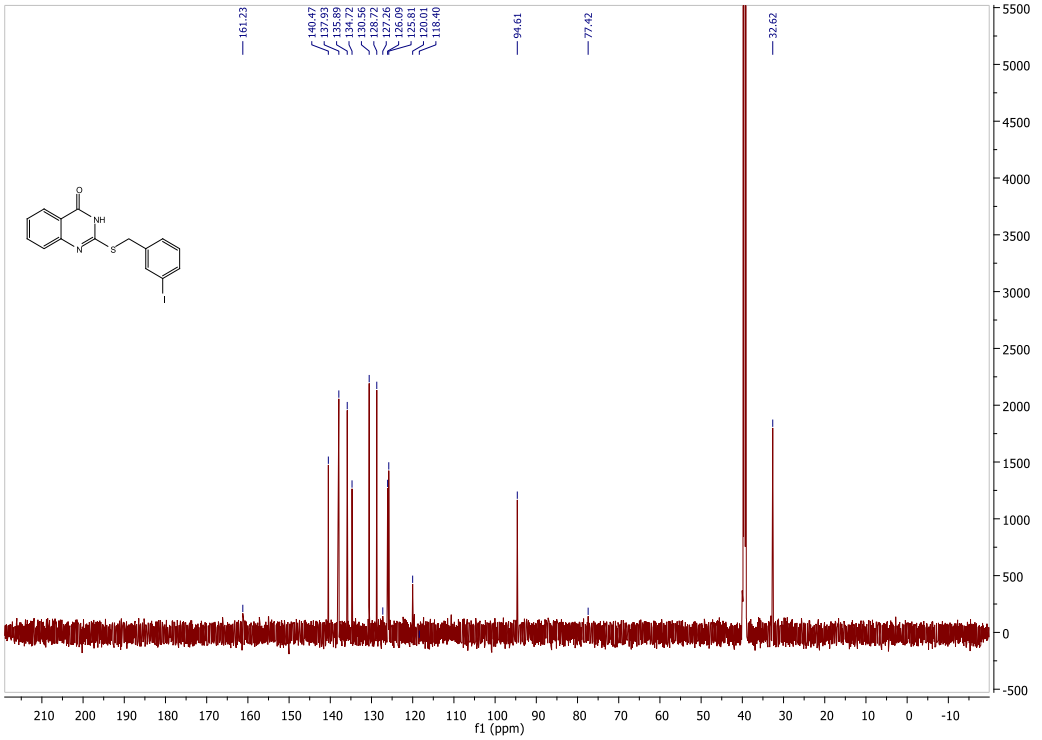

MS

Acquisition Parameter

Source Type	APCI	Ion Polarity	Positive	Set Nebulizer	1.6 Bar
Focus	Not active	Set Capillary	4500 V	Set Dry Heater	200 °C
Scan Begin	50 m/z	Set End Plate Offset	-500 V	Set Dry Gas	8.0 l/min
Scan End	1500 m/z	Set Collision Cell RF	100.0 Vpp	Set Divert Valve	Waste

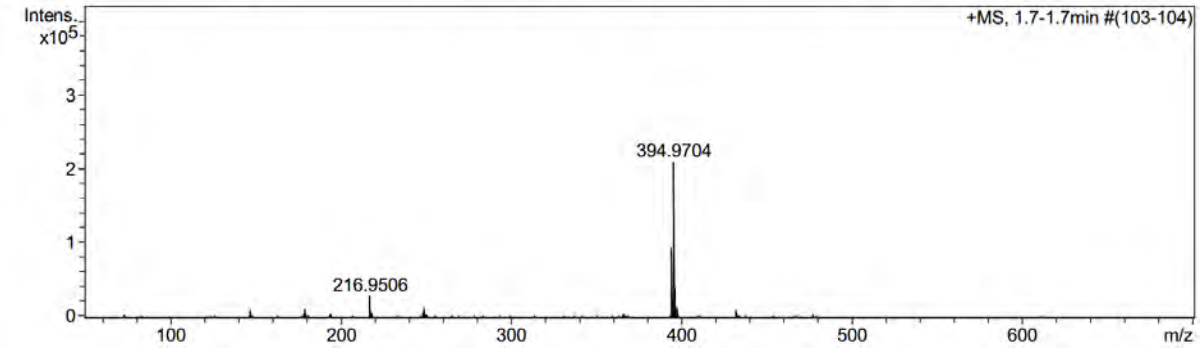

HPLC

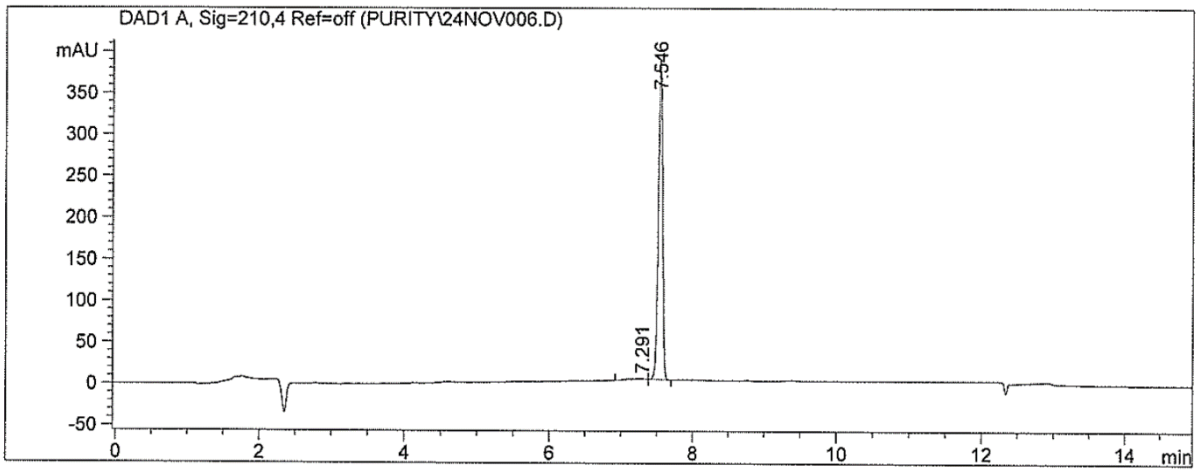

2-[(2-Oxo-2-phenylethyl)thio]quinazoline-4(3*H*)-one (3l)

^{1}H NMR

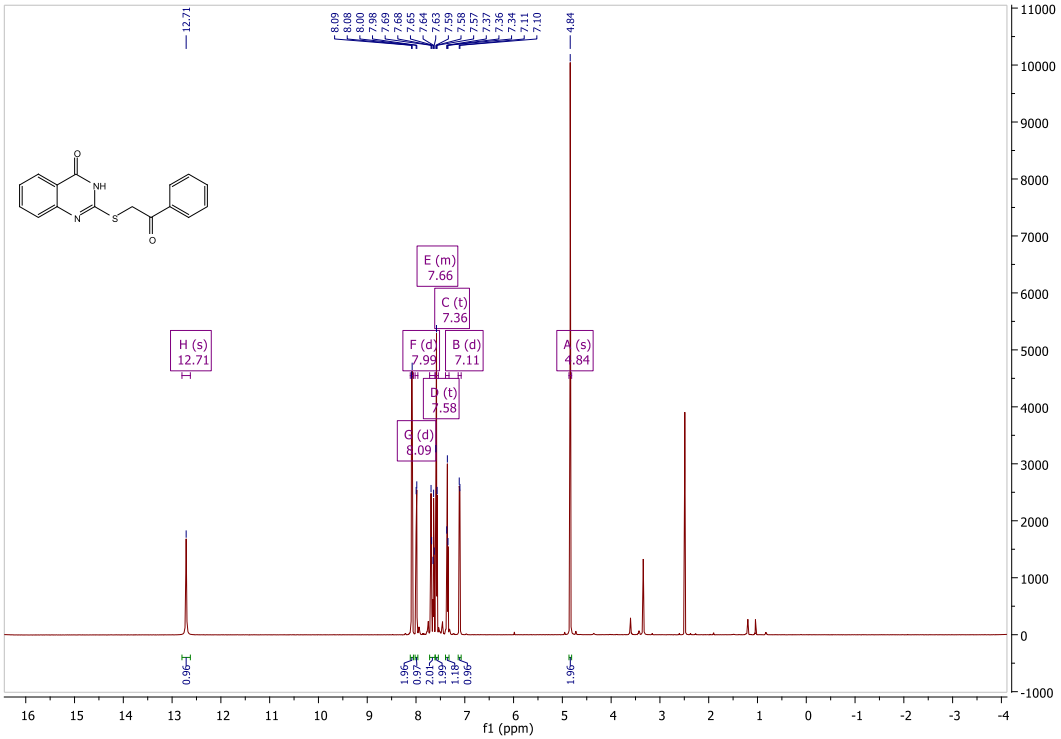

^{13}C NMR

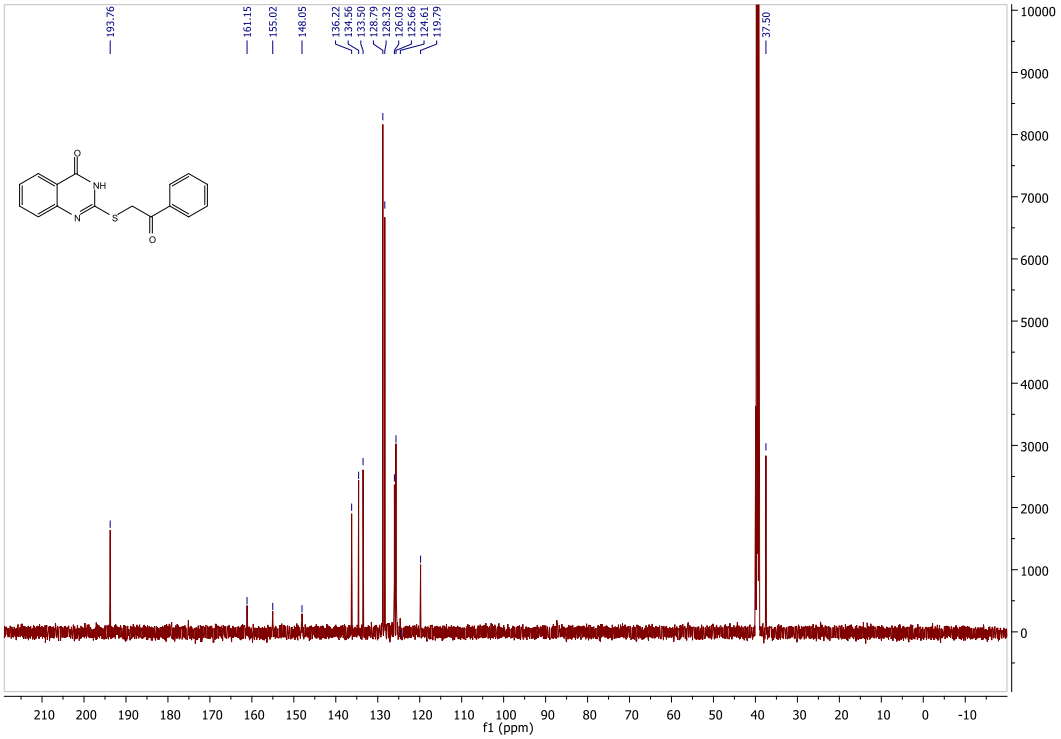

MS

Acquisition Parameter

Source Type	APCI	Ion Polarity	Positive	Set Nebulizer	1.6 Bar
Focus	Not active	Set Capillary	4500 V	Set Dry Heater	200 °C
Scan Begin	50 m/z	Set End Plate Offset	-500 V	Set Dry Gas	8.0 l/min
Scan End	1500 m/z	Set Collision Cell RF	100.0 Vpp	Set Divert Valve	Waste

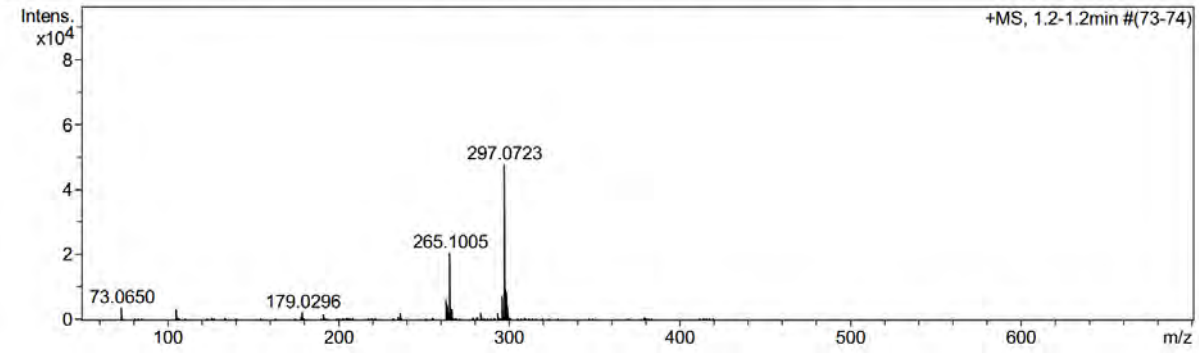

HPLC

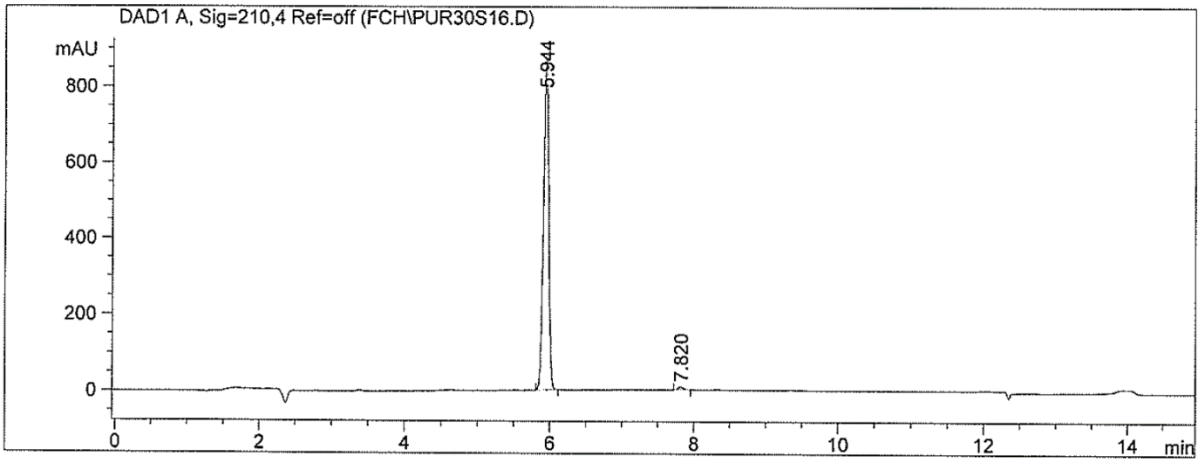

2-[(3-Phenylpropyl)thio]quinazoline-4(3*H*)-one (3m)

^{1}H NMR

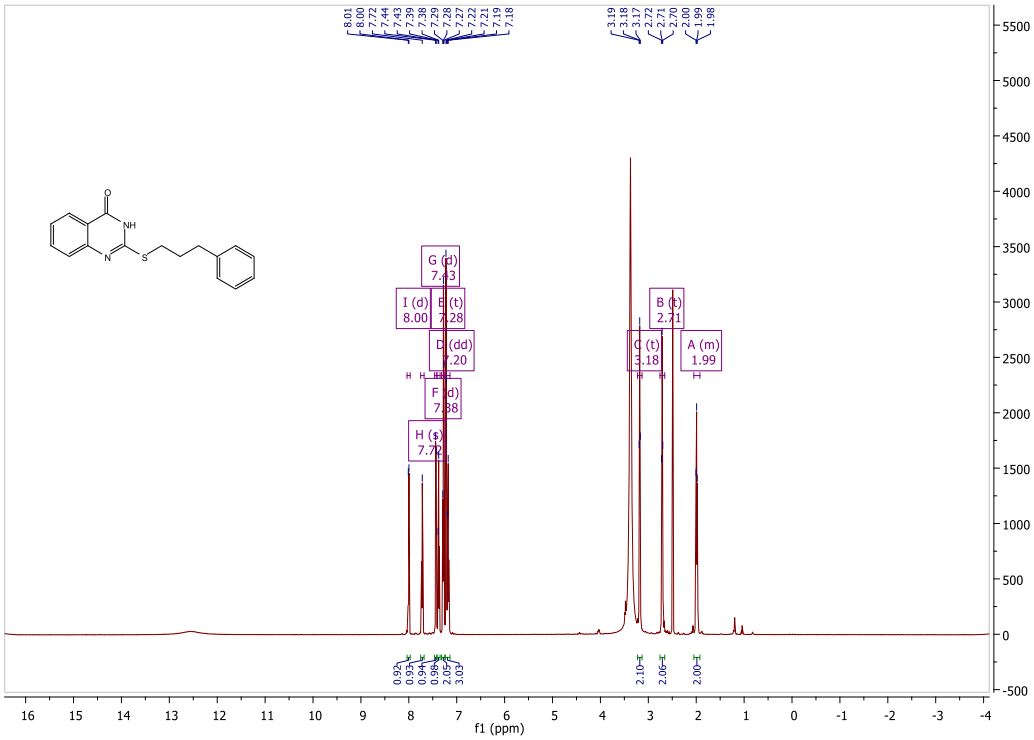

^{13}C NMR

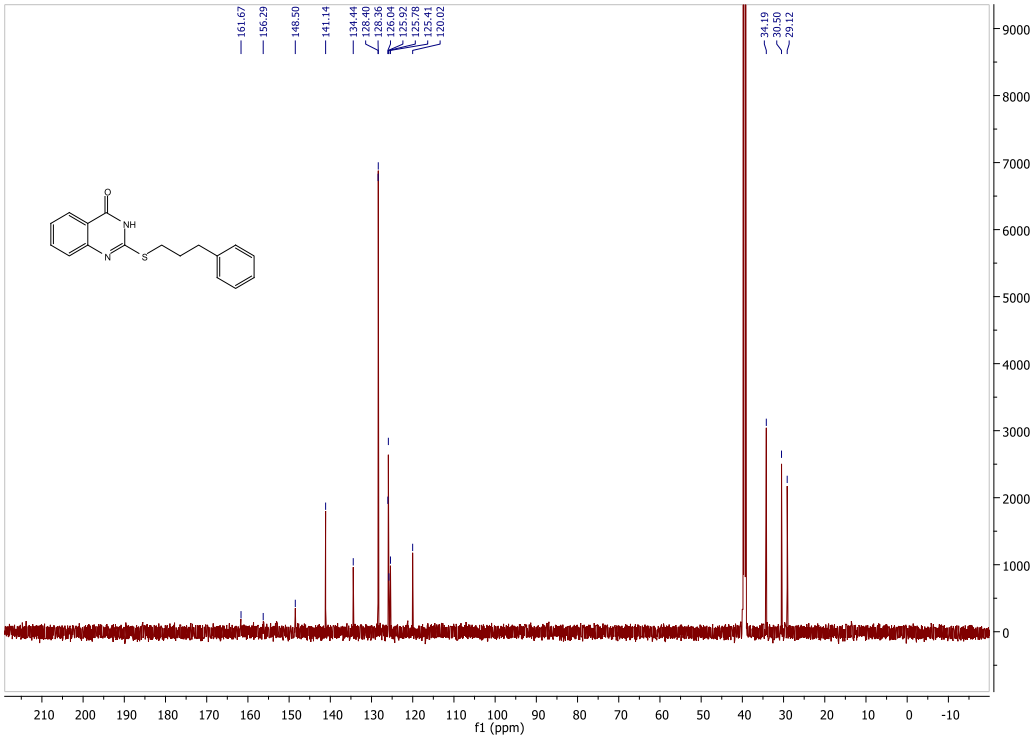

MS

Acquisition Parameter

Source Type	APCI	Ion Polarity	Positive	Set Nebulizer	1.6 Bar
Focus	Not active	Set Capillary	4500 V	Set Dry Heater	200 °C
Scan Begin	50 m/z	Set End Plate Offset	-500 V	Set Dry Gas	8.0 l/min
Scan End	1500 m/z	Set Collision Cell RF	100.0 Vpp	Set Divert Valve	Waste

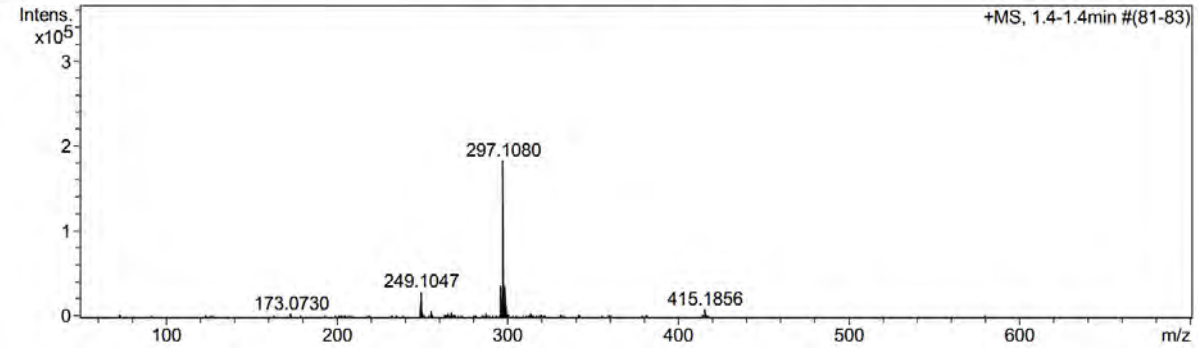

HPLC

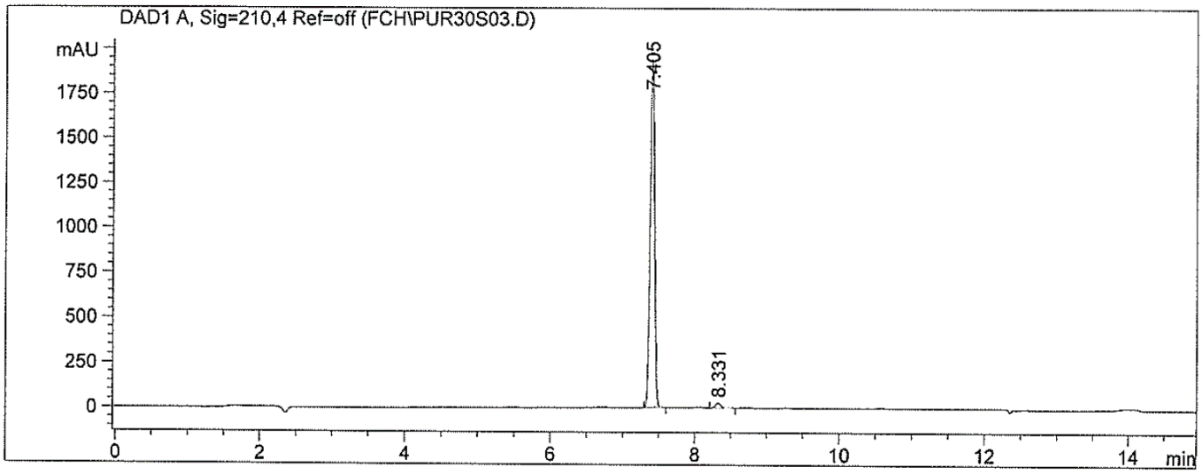

2-[(Phenoxyethyl)thio]quinazolin-4(3*H*)-one (3n)

^{1}H NMR

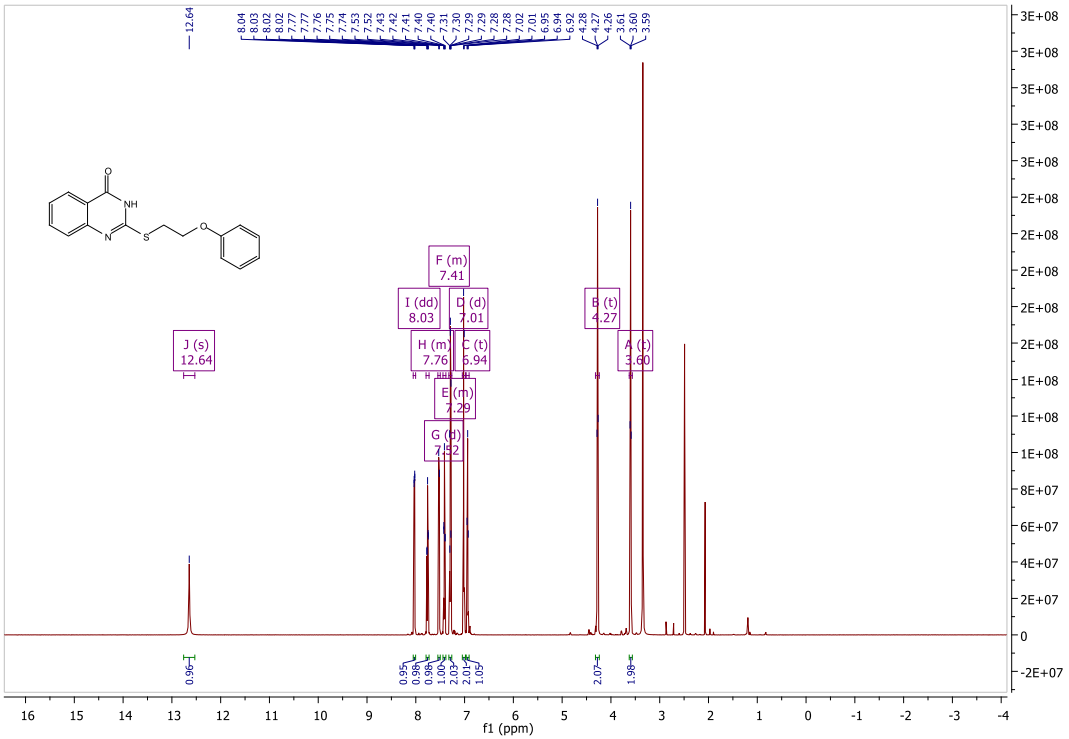

^{13}C NMR

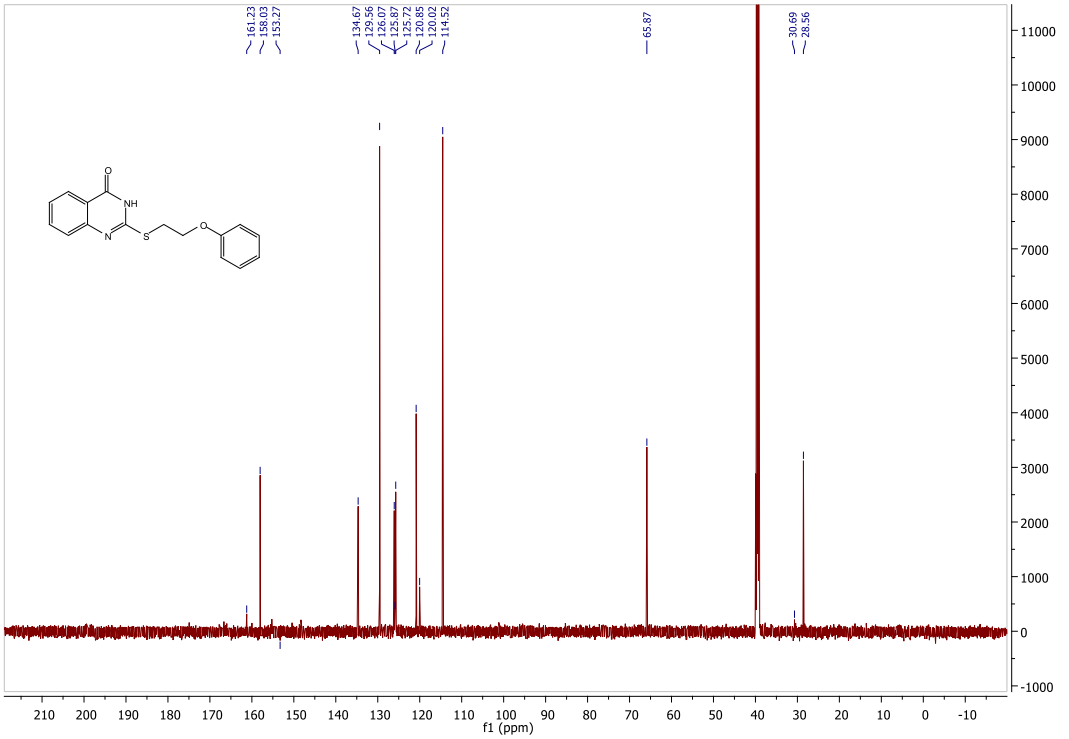

MS

Acquisition Parameter

Source Type	APCI	Ion Polarity	Positive	Set Nebulizer	1.6 Bar
Focus	Not active	Set Capillary	4500 V	Set Dry Heater	200 °C
Scan Begin	50 m/z	Set End Plate Offset	-500 V	Set Dry Gas	8.0 l/min
Scan End	1500 m/z	Set Collision Cell RF	100.0 Vpp	Set Divert Valve	Waste

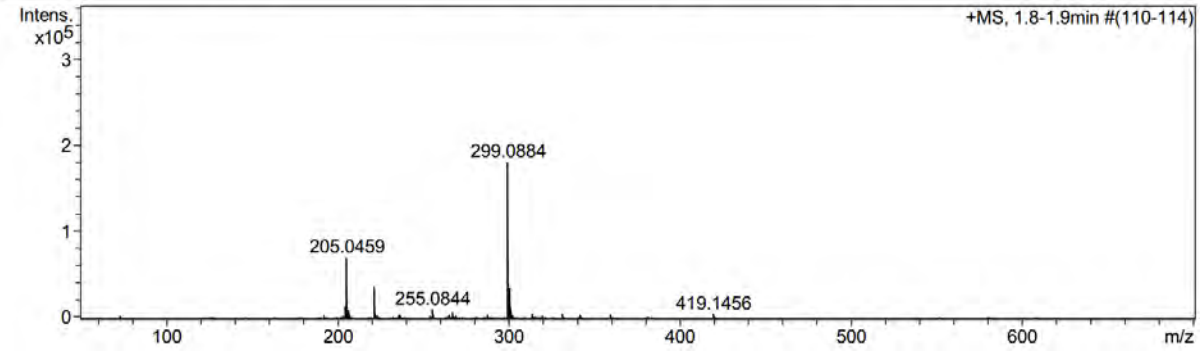

HPLC

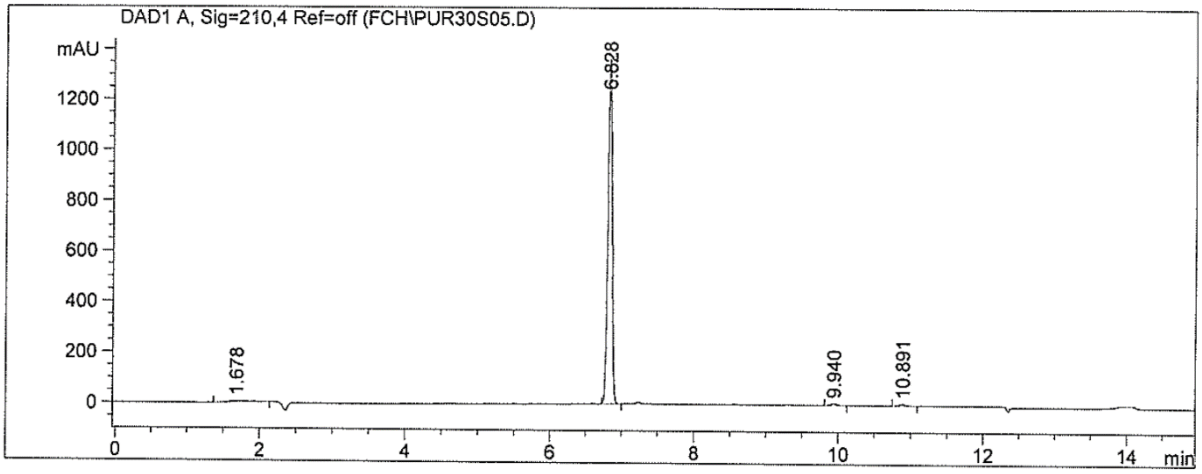

CHAPTER 4: ARTICLE 2

The monoamine oxidase inhibition properties of C6-mono- and N3/C6-disubstituted derivatives of 4(3*H*)-quinazolinone

Malikotsi A. Qhobosheane[1], Lesetja J. Legoabe[2,*], Jacobus P. Petzer[1,2], and Anél Petzer[1,2]

[1]*Pharmaceutical Chemistry, School of Pharmacy, North-West University, Private Bag X6001, Potchefstroom 2520, South Africa*

[2]*Centre of Excellence for Pharmaceutical Sciences, North-West University, Private Bag X6001, Potchefstroom 2520, South Africa*

Abstract

Parkinson's disease is a chronic progressive neurodegenerative disorder that is characterised by the death of the nigrostriatal neurons and depletion of striatal dopamine. The standard symptomatic therapy consists of dopamine replacement with L-dopa, the metabolic precursor of dopamine, which represents the most effective treatment. Since monoamine oxidase (MAO) B is a key dopamine metabolising enzyme in the brain, MAO-B inhibitors are often used as adjuvants to L-dopa. In addition to the symptomatic benefits offered by MAO-B inhibitors, these drugs have also been shown to delay the progression of Parkinson's disease when given in early stages of the disease. Based on the therapeutic use of MAO-B inhibitors, the present study evaluates a series of mono- and disubstituted derivatives of 4(3*H*)-quinazolinone as potential inhibitors of recombinant human MAO-A and MAO-B. Twelve C6-monosubstituted and nine N3/C6-disubstituted 4(3*H*)-quinazolinone derivatives were synthesised, which led to the discovery of novel quinazolinone derivatives with micromolar and submicromolar activities as inhibitors of MAO-B. The most potent mono- and disubstituted derivatives exhibited IC_{50} values of 6.354 μM (**1f**) and 0.685 μM (**2b**), respectively. This study identifies suitable substitution patterns for the design of 4(3*H*)-quinazolinone derivatives as MAO-B inhibitors.

Keywords: monoamine oxidase, MAO, quinazolinone, Parkinson's disease, inhibition.

Introduction

Parkinson's disease is caused by the death of the dopaminergic neurons that project from the substantia nigra to the striatum (Fernandez-Espejo, 2004). This leads to a deficiency of dopamine in the basal ganglia and extrapyramidal motor dysfunction including tremor, rigidity and bradykinesia (Du *et al.*, 2001). The signs and symptoms of Parkinson's disease can be effectively treated with drugs that enhance dopamine function in combination with

drugs that delay disease progression (Du *et al.*, 2001). L-Dopa has been the mainstay for the treatment of Parkinson's disease for over 30 years (Hely *et al.*, 2000), and is still the most effective symptomatic treatment to date. L-Dopa is known to improve the quality of life of Parkinson's disease patients and to reduce mortality when initiated in the early stages of the disease (Hely *et al.*, 2000; Martin & Wieler, 2003). However, when administered as monotherapy, L-dopa is converted into dopamine by intestinal and peripheral aromatic L-amino acid decarboxylase (AADC), which reduces the amount of the ingested dose that reaches the systemic circulation and brain (Aminoff, 1994). L-Dopa is thus routinely administered with a peripheral AADC inhibitor to prevent its extracerebral breakdown and reduce any side-effects that result from its peripheral activation (Aminoff, 1994; Martin & Wieler, 2003). L-Dopa is also frequently combined with selective MAO B inhibitors, which protect central dopamine from MAO-catalysed breakdown (Youdim *et al.*, 2006; Petzer *et al.*, 2013; Legoabe *et al.*, 2015). MAO-B inhibitors not only block dopamine metabolism but also reduce the production of neurotoxic by-products of the MAO catalytic cycle (Youdim & Bakhle, 2006; Youdim *et al.*, 2006). When given in the early stages of Parkinson's disease, MAO-B inhibitors delay the onset of more severe disability (Rossiter *et al.*, 2012), and also significantly delay the need to start L-dopa therapy (Legoabe *et al.*, 2015).

MAO are flavin adenine dinucleotide (FAD) containing enzymes which metabolise several bioactive amines including serotonin and catecholamines in both the central nervous system and peripheral organs (Nicotra *et al.*, 2004; Meiring *et al.*, 2013; Khattab *et al.*, 2015). MAO is not a single enzyme, but exists as two isoforms, MAO-A and MAO-B (Youdim & Weinstock, 2004), which are encoded by different genes and exhibit approximately 70% amino acid sequence identity (Shih *et al.*, 1999). MAO-A preferentially metabolises serotonin (5-hydroxytryptamine), while MAO-B preferentially oxidises the dietary amines, benzylamine and phenylethylamine. Certain amines such as dopamine and tyramine are substrates for both MAO isoforms (Youdim *et al.*, 2006; Petzer *et al.*, 2013; Legoabe *et al.*, 2015). In humans, MAO-A is the major isoform in the intestines, placenta and heart, while MAO-B is most abundant in platelets, glial cells in the brain and liver (Nel *et al.*, 2016). Because MAO-B activity increases in the human brain with age, elderly Parkinson's disease patients are expected to exhibit a higher MAO-catalysed metabolism of central dopamine and thus an increased production of by-products of the MAO catalytic cycle (Shih *et al.*, 1999). Age-related increases in brain MAO-B and its ability to produce reactive oxygen species as by-products of catalysis thus may contribute to the neurodegeneration associated with Parkinson's disease (Kumar *et al.*, 2003).

MAO inhibitors have been used clinically mainly for the treatment of depression and Parkinson's disease (Gaweska & Fitzpatrick, 2011). However, the clinical use of MAO

inhibitors declined because of their ability to induce a potentially life-threatening blood pressure elevation when combined with tyramine-containing food (Youdim & Bakhle, 2006; Youdim *et al.*, 2006; Legoabe *et al.*, 2014; Legoabe *et al.*, 2015). Under normal circumstances, dietary tyramine is extensively metabolised by MAO-A in the gut wall and in the liver (Youdim & Bakhle, 2006), and it is thus prevented from entering the systemic circulation. In the presence of a MAO-A inhibitor this protective system is abolished (Youdim & Bakhle, 2006), systemic tyramine levels increase and induce the release of norepinephrine from peripheral neurons (Legoabe *et al.*, 2015). The consequence of this release is severe hypertension which in some cases may be fatal (Youdim & Bakhle, 2006; Legoabe *et al.*, 2015). This adverse effect is associated with irreversible MAO-A inhibition. Reversible MAO-A inhibitors and selective MAO-B inhibitors do not provoke the tyramine-induced hypertensive response and are thus considered safe in this respect (Legoabe *et al.*, 2015).

Since selective and reversible MAO-B inhibitors are not associated with changes in blood pressure, they are preferred for the early treatment of Parkinson's disease (Carradori & Silvestri, 2015). Also since the by-products of MAO catalysis may damage neuronal cells if not adequately inactivated (Mostert *et al.*, 2015), MAO-B inhibitors may protect against these neurodegenerative processes by decreasing the levels of hydrogen peroxide and aldehydes resulting from MAO oxidation (Petzer *et al.*, 2013; Mostert *et al.*, 2015). As mentioned, MAO-B activity in the central nervous system increases with age, providing a further rationale for the use of MAO-B inhibitors in Parkinson's disease (Legoabe *et al.*, 2012). In pursuit of improved therapies for Parkinson's disease, several researchers are involved in the design and development of new MAO-B inhibitors.

Quinazolinones and their derivatives are building blocks for approximately 150 naturally occurring alkaloids (Arora *et al.*, 2011) and thus constitute a major class of biologically active molecules, both from natural and synthetic sources (Demeunynck & Baussanne, 2013). Because of their broad spectrum of biological and biochemical activities, quinazolinone derivatives have been developed as antitumor (Cao *et al.*, 2005), antibacterial and antifungal (Sharma *et al.*, 2011), anti-HIV (Asif, 2014) and antihypertensive agents (Sharma *et al.*, 2011), as well as dopamine agonists (Demeunynck & Baussanne, 2013). There are 2 structural isomers of quinazolinones, 2-quinazolinone and 4-quinazolinone, with the 4-isomer being the more common (Arora *et al.*, 2011; Chawla & Batra, 2013). The 4(3*H*)-quinazolinone scaffold serves as an important lead compound in search of new treatments for major diseases such as viral and bacterial infections, cancer and neurological pathologies including Alzheimer's and Parkinson's disease (Arora *et al.*, 2011; Demeunynck & Baussanne, 2013).

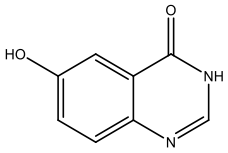

Figure 1: Structure of 6-hydroxy-4(3*H*)-quinazolinone

Among their wide range of biological properties, substituted quinazolinone derivatives also exhibit MAO and acetylcholinesterase inhibitory activities (Bahadur, 1983). In previous studies, quinazolinones substituted on position 6 exhibited good MAO inhibition (Bahadur, 1983). For example, quinazolinones bearing bromine on position 6 as well as a phenyl on position 2 are more potent MAO inhibitors than quinazolinones that bear 2-phenyl or 2-methyl, or compounds that are substituted on position 6 and/or position 8. In a study by Lata *et al.* (1982), it was observed that substitution of the quinazolinone moiety with a *o*- or *p*-tolyl yielded good MAO inhibitory activity, however, compounds bearing the phenyl, *meta*-fluorophenyl and *para*-methoxyphenyl moieties were more potent than the corresponding tolyl substituted derivatives. According to Srivastava *et al.* (1980), the MAO inhibitory activities of halogenated quinazolinone derivatives depend on the electronegativity of the halogen group, with more electronegative substituents leading to more potent inhibition. These observations indicate that the MAO inhibition activities of quinazolinone derivatives are dependent on the nature and position of substitution. The purpose of this study is to expand on the structure-activity relationships (SARs) of MAO inhibition by quinazolinone derivatives to enable the design of novel potent MAO inhibitors of this chemical class. In the current study 4(3*H*)-quinazolinone was used as lead and the effect of different substitution patterns on MAO inhibition was explored.

Results and discussions

Chemistry

As key reagent, 6-hydroxy-4(3*H*)-quinazolinone was synthesised by the Niementowski reaction (scheme 1). A mixture of 2-amino-5-hydroxybenzoic acid in formamide was refluxed at 190 °C for 1 h. The mixture was allowed to cool to room temperature, and thereafter, the excess solvent was decanted. The precipitate was washed with cyclohexane and then filtered and dried.

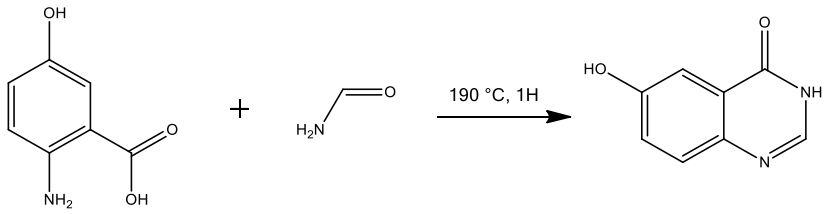

Scheme 1: Synthesis of 6-hydroxy-4(3*H*)-quinazolinone

The mono- and disubstituted 4(3*H*)-quinazolinone derivatives, **1a**–**l** and **2a**–**i**, were synthesised in poor to excellent yields (7-91%) as shown in scheme 2. A mixture of 6-hydroxy-4(3*H*)-quinazolinone and an appropriate arylkalkyl bromide or chloride were suspended in DMF and stirred in the presence of K_2CO_3 or NaOH at reduced temperatures (–10 °C to –20 °C) for 6 h. When one equivalent each of 6-hydroxy-4(3*H*)-quinazolinone and the arylalkyl halide was reacted, a mixture of mono- and disubstituted products was obtained.

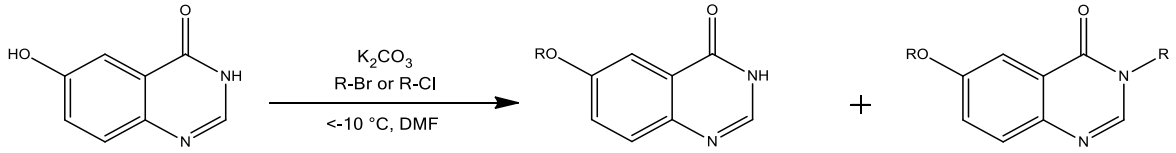

Scheme 2: Synthesis of 4(3*H*)-quinazolinone derivatives

However, when a 2-fold molar excess of the arylalkyl halide was used, the formation of the disubstituted product predominated (scheme 3). The target products were precipitated by the addition of ice-cold water, collected by filtration and dried. The mono- and disubstituted products were separated by heating the resultant precipitate in dichloromethane and hot-filtering the mixture. The crudes obtained were purified by recrystallisation. Water soluble products were extracted with ethyl acetate and recrystallised from appropriate solvents. The structures and purities of the target compounds were verified by ^{1}H NMR, ^{13}C NMR, mass spectrometry and HPLC analyses as cited in the experimental section.

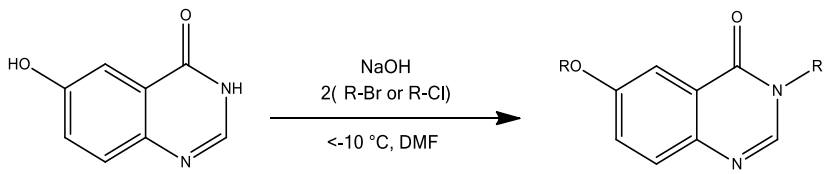

Scheme 3: Synthesis of disubstituted 4(3*H*)-quinazolinone derivatives

Biological activity

The MAO inhibitory properties of the 4(3*H*)-quinazolinone derivatives were investigated using the recombinant human MAO-A and MAO-B enzymes (Legoabe *et al.*, 2015; Mostert *et al.*, 2015; Nel *et al.*, 2016). The mixed MAO-A/B substrate kynuramine was used as

enzyme substrate and is oxidised by the MAOs to yield 4-hydroxyquinoline. 4-Hydroxyquinoline can be readily measured by fluorescence spectrophotometry (λ_{ex} = 310 nm; λ_{em} = 400 nm) since it fluoresces in alkaline media. This measuring technique reduces the possibility of interference from the test inhibitors and kynuramine since these compounds do not fluoresce under the specific assay conditions.

MAO inhibition potencies

The IC_{50} values for the inhibition of human MAO-A and MAO-B by the 4(3*H*)-quinazolinone derivatives (**1a**–**l** and **2a**–**i**) are reported in tables 1 and 2. While most of the 4(3*H*)-quinazolinone derivatives did not inhibit the MAOs, a number of derivatives (5 of 21) did exhibit selective inhibition of MAO-B. Among these, the disubstituted compounds **2b** and **2h**, are most notable as the most potent inhibitors of the series with IC_{50} values of 0.685 μM and 0.847 μM, respectively. Their corresponding monosubstituted derivatives, **1b** and **1i**, did not inhibit the MAOs, even at a maximal tested concentration of 100 μM. Since most of the compounds evaluated were not MAO inhibitors, meaningful SARs for the inhibition of the MAOs could not be derived. It is, however, noteworthy that nitrile substitution of the benzyl ring resulted in MAO-B inhibition for both the disubstituted and monosubstituted derivatives, **2h** (IC_{50} = 0.847 μM) and **1i** (IC_{50} = 15.783 μM). The disubstituted derivative is, however, 18-fold more potent than the monosubstituted compound. In general, disubstitution yields more potent MAO-B inhibition since the most potent inhibitors of the series are both disubstituted derivatives. Also, compound **2f**, bearing fluorine on the benzyloxy ring is a potent MAO-B inhibitor, while the corresponding chlorine (**2c**), bromine (**2e**) and iodine (**2g**) substituted derivatives are not inhibitors. Although speculative, this decrease in activity may be attributed to the steric effect, and increased steric hindrance reduces MAO-B inhibition. The observation that the unsubstituted derivative **2a** also is not a MAO inhibitor shows that steric considerations alone cannot explain the absence of MAO-B inhibition by **2c**, **2e** and **2g**. The key reagent for synthesis of the 4(3*H*)-quinazolinone derivatives, 6-hydroxy-4(3*H*)-quinazolinone, was also evaluated as a potential MAO inhibitor, but no activity was observed.

These data thus demonstrate that substitution with appropriate side chains is necessary for MAO-B inhibition by 4(3*H*)-quinazolinone derivatives, and in general disubstitution is more likely to yield good potency inhibition. Furthermore, the 4(3*H*)-quinazolinone derivatives investigated here are not MAO-A inhibitors, showing that selective inhibition of the MAO-B isoform may be attained with this class of compounds and appropriate substitution. As discussed above, compounds that show selectivity for MAO-B inhibition are suitable for design of Parkinson's disease therapy.

Table 1: The IC_{50} values for the inhibition of MAO-A and MAO-B by C6-monosubstituted 4(3*H*)-quinazolinone derivatives.

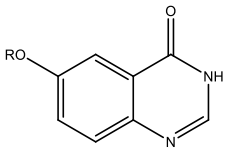

	R	IC_{50} (μM)[a]		SI[b]
		MAO-A	MAO-B	
	H	No inh[c]	No inh[c]	-
1a	$C_6H_5CH_2$-	No inh[c]	No inh[c]	-
1b	(4-FC_6H_4)CH_2-	No inh[c]	No inh[c]	-
1c	(4-ClC_6H_4)CH_2-	No inh[c]	No inh[c]	-
1d	(3-BrC_6H_4)CH_2-	No inh[c]	No inh[c]	-
1e	(4-BrC_6H_4)CH_2-	No inh[c]	No inh[c]	-
1f	(3-IC_6H_4)CH_2-	No inh[c]	6.354 ± 0.533	>16
1g	(4-IC_6H_4)CH_2-	No inh[c]	No inh[c]	-
1h	(4-$CF_3C_6H_4$)CH_2-	No inh[c]	No inh[c]	-
1i	(4-CNC_6H_4)CH_2-	No inh[c]	15.783 ± 1.615	>6
1j	4-pyridinyl-	No inh[c]	No inh[c]	-
1k	$C_6H_5(CH_2)_2$-	No inh[c]	No inh[c]	-
1l	$C_6H_5C(O)CH_2$-	No inh[c]	No inh[c]	-

Table 2: The IC_{50} values for the inhibition of MAO-A and MAO-B by N3/C6-disubstituted 4(3*H*)-quinazolinone derivatives.

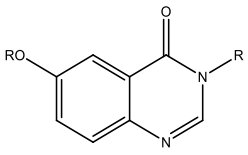

	R	IC_{50} (μM)[a]		SI[b]
		MAO-A	MAO-B	
	H	No inh[c]	No inh[c]	-
2a	$C_6H_5CH_2$-	No inh[c]	No inh[c]	-
2b	(4-FC_6H_4)CH_2-	No inh[c]	0.685 ± 0.013	>146
2c	(4-ClC_6H_4)CH_2-	No inh[c]	No inh[c]	-

2d	(3-BrC_6H_4)CH_2-	No inh[c]	No inh[c]	-
2e	(4-BrC_6H_4)CH_2-	No inh[c]	No inh[c]	-
2f	(3-IC_6H_4)CH_2-	No inh[c]	41.415 ± 1.888	>2
2g	(4-IC_6H_4)CH_2-	No inh[c]	No inh[c]	-
2h	(4-CNC_6H_4)CH_2-	No inh[c]	0.847 ± 0.078	>118
2i	$C_6H_5O(CH_2)_2$-	No inh[c]	No inh[c]	-

[a] All values are expressed as the mean ± standard deviation (SD) of triplicate determinations.

[b] Selectivity index (SI) = IC_{50}(MAO-A)/IC_{50}(MAO-B).

[c] No inhibition observed at a maximal tested concentration of 100 µM.

Reversibility of MAO-B inhibition

The reversibility of MAO inhibition by the 4(3*H*)-quinazolinone derivatives was determined by measuring the recoveries of enzymatic activities after dialysis of enzyme-inhibitor mixtures (Petzer *et al.*, 2013). For the purpose of this study, compound **2b** was selected as a representative inhibitor because it is the most potent inhibitor in this series (IC_{50} = 0.685 µM). Since none of the 4(3*H*)-quinazolinone derivatives were MAO-A inhibitors, only the reversibility of MAO-B inhibition was investigated. MAO-B was incubated with **2b** (at concentration 4 x IC_{50}) for 15 min and dialysed for 24 h. In addition, MAO-B was incubated and dialysed in the absence of inhibitor and in the presence of the irreversible MAO-B inhibitor, (R)-deprenyl, as negative and positive controls, respectively (Mostert *et al.*, 2015). The residual enzyme activities were subsequently measured and are reported in figure 2. Enzyme activity is expected to recover to 100% of the negative control value after dialysis of incubations containing reversible inhibitors, while enzyme activity is not expected to recover following dialysis of incubations containing irreversible inhibitors.

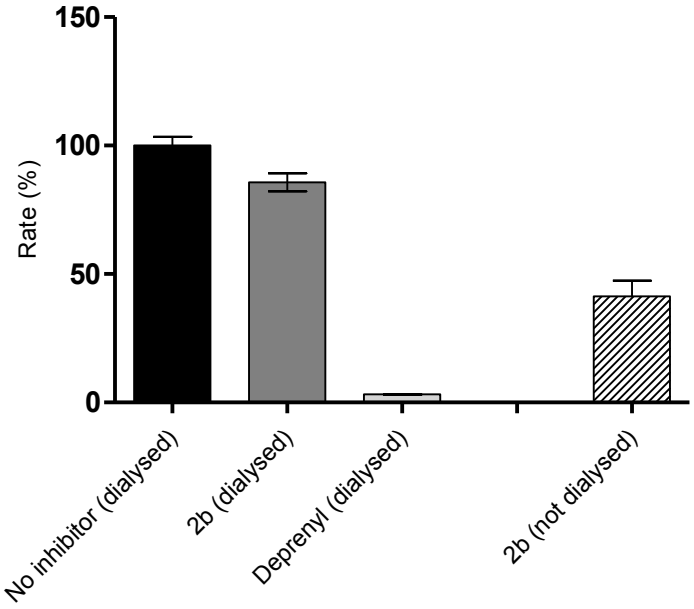

Figure 2: Reversibility of MAO-B inhibition by **2b**. MAO-B was pre-incubated with **2b** (at 4 x IC_{50}) for 15 min and then dialysed for 24 h. The enzyme was similarly pre-incubated in the absence of the inhibitor and in the presence of the irreversible MAO-B inhibitor, (R)-deprenyl. The mixtures were subsequently dialysed for 24 h and the residual enzyme activities were measured. For comparison, the residual activity of the undialysed mixture of MAO-B and **2b** are also shown (**2b** not dialysed).

After dialysis of mixtures of MAO-B and **2b**, MAO-B activity was recovered to 86% of the negative control value, while the enzyme activity of undialysed mixtures of MAO-B and **2b** is 41% of the control value. In contrast, enzyme activity was not recovered after 24 h of dialysis of mixtures of MAO-B and (R)-deprenyl, with only 3% enzyme activity remaining. This data suggests that **2b** interacts reversibly with MAO-B.

To investigate the mode of MAO-B inhibition by **2b**, a set of Lineweaver-Burk plots was constructed. The set consisted of six lines, each constructed by measuring MAO-B activity at eight different kynuramine concentrations (15–250 μM). The plots were constructed in the absence of inhibitor, and in the presence of five different concentrations of **2b**. The results show that the lines of the Lineweaver-Burk plots are linear and intersect at a single point, adjacent to the y-axis (Figure 3). This pattern resembles competitive inhibition and suggests that compound **2b** may be a competitive inhibitor of human MAO-B. From a replot of the slopes of the Lineweaver-Burk plots versus inhibitor concentration, a K_i value of 0.648 μM is estimated ($K_i = –x$ when $y = 0$).

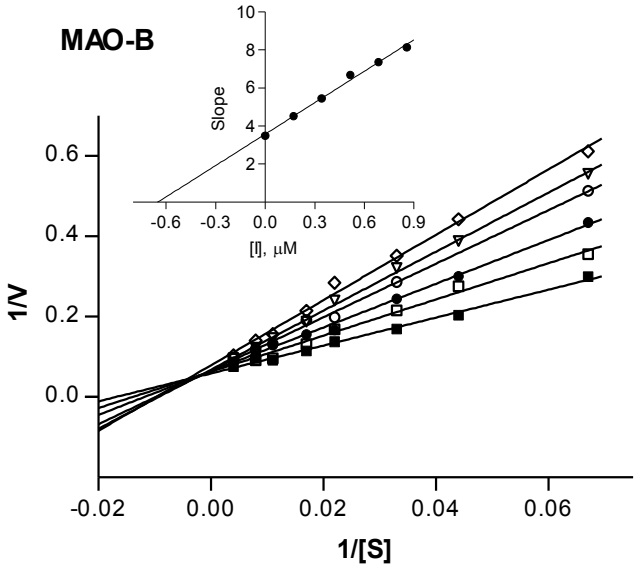

Figure 3: Lineweaver-Burke plots of the inhibition of human MAO-B by **2b** (IC_{50} = 0.685 μM). The graphs were constructed in the absence (filled squares) and presence of various concentrations of **2b**.

Conclusion

The present study shows that mono- and disubstituted 4(3*H*)-quinazolinone derivatives, with appropriate substitution, may act as selective inhibitors of human MAO-B. Five compounds (of 21) exhibited IC_{50} values in the micromolar to submicromolar range (0.685–41.415 μM). The most potent MAO-B inhibitor (**2b**) exhibits an IC_{50} value of 0.685 μM, and was found to be a reversible MAO-B inhibitor. Potent MAO-B inhibitors such as **2b** may act as leads for the future design of MAO-B inhibitors for the treatment of Parkinson's disease.

Acknowledgements

The NMR and MS spectra were recorded by André Joubert and Johan Jordaan of the SASOL Centre of Chemistry, North-West University. This work is based on the research supported by National Research Foundation of South Africa (Grant specific unique reference numbers (UID) 96135). The Grant holders acknowledge that opinions, findings and conclusions or recommendations expressed in any publication generated by the NRF supported research are that of the authors, and that the NRF accepts no liability whatsoever in this regard.

Experimental section

Chemicals and instrumentation

Unless otherwise noted, all starting materials and reagents, including microsomes from insect cells containing recombinant human MAO-A and MAO-B (5 mg protein/mL) and kynuramine dihydrobromide, were obtained from Sigma-Aldrich and were used without further purification. Fluorescence spectrophotometry was carried out with a Varian Cary Eclipse fluorescence spectrophotometer. Proton (^{1}H) and carbon (^{13}C) NMR spectra were recorded on a Bruker Avance III 600 spectrometer at frequencies of 600 MHz and 151 MHz respectively, with DMSO-*d*6 serving as NMR solvent. All chemical shifts are reported in parts per million (δ). Spin multiplicities are given as s (singlet), d (doublet), dd (doublet of doublets), ddd (doublet of doublet of doublets), dt (doublet of triplets), t (triplet), m (multiplet). High resolution mass spectra (HRMS) were recorded on a Bruker micrOTOF-Q II mass spectrometer in atmospheric-pressure chemical ionisation (APCI) mode. The melting points (mp) were determined with a Buchi B-545 melting point apparatus and are uncorrected. Thin layer chromatography (TLC) was carried out using silica gel 60 (Merck) with UV254 fluorescent indicator. Purities of the synthesised compounds were determined with HPLC analyses, which were carried out with an Agilent 1100 HPLC system equipped with a quaternary pump and a diode array detector. HPLC grade acetonitrile (Merck) and milli-Q water were used for the chromatography.

Synthesis of 6-hydroxy-4(3*H*)-quinazolinone

A mixture of 2-amino-5-hydroxybenzoic acid (4 g, 26.1 mmol) in formamide (34 mL) was stirred and heated to 190 °C for 1 h. The mixture was allowed to cool to room temperature, after which the excess solvent was decanted. The precipitate was washed 3 times with cyclohexane (20 mL), and then filtered and dried.

6-Hydroxyquinazolin-4(3*H*)-one

The title compound was prepared in a yield of 99%: mp 336.9-337.3 °C. ^{1}H NMR (600 MHz, DMSO) δ 11.05 (d, *J* = 1140.5 Hz, 2H), 7.89 (s, 1H), 7.52 (d, *J* = 8.8 Hz, 1H), 7.39 (d, *J* = 2.8 Hz, 1H), 7.24 (dd, *J* = 8.8, 2.9 Hz, 1H). ^{13}C NMR (151 MHz, DMSO) δ 162.95, 160.56, 156.14, 142.21, 141.95, 128.88, 123.67, 108.73. APCI-HRMS m/z: calcd for $C_8H_7N_2O_2$ (MH^+), 163.0502, found 163.0502. Purity (HPLC): 100.0%.

General procedure for synthesis of mono and disubstituted 4(3*H*)-quinazolinone derivatives

A mixture of 6-hydroxy-4(3*H*)-quinazolinone (0.3 g, 1.850 mmol), DMF (4 mL) and an appropriate arylalkyl bromide or chloride were stirred in the presence of K_2CO_3 (0.511 g, 3.70 mmol) or NaOH (0.164 g, 4.11 mmol) at reduced temperature (–10 °C to –20 °C) for 6

h. The progress of the reaction was monitored by silica gel TLC with ethyl acetate as mobile phase. The target products were precipitated with the addition of ice-cold water (15 mL), collected by filtration and dried. The mono- and disubstituted products were separated by heating the resultant precipitate for 10 min in dichloromethane (50 mL) and hot-filtering the mixture. The crudes obtained were purified by recrystallisation. Water soluble products were extracted with ethyl acetate (60 mL) and recrystallised from appropriate solvents.

6-(Benzyloxy)quinazolin-4(3*H*)-one (1a)

The title compound was prepared in a yield of 44%: mp 258.7-261.5 °C (ethanol). ^{1}H NMR (600 MHz, DMSO) δ 10.17 (s, 1H), 8.39 (s, 1H), 7.57 (d, *J* = 8.8 Hz, 1H), 7.44 (d, *J* = 2.8 Hz, 1H), 7.35 (d, *J* = 4.4 Hz, 4H), 7.28 (dd, *J* = 8.7, 2.8 Hz, 2H), 5.18 (s, 2H). ^{13}C NMR (151 MHz, DMSO) δ 160.33, 156.99, 145.38, 141.62, 137.51, 129.44, 129.10, 128.10, 124.28, 123.18, 119.61, 109.39, 49.19. APCI-HRMS m/z: calcd for $C_{15}H_{13}N_2O_2$ (MH^+), 253.0971, found 253.0972. Purity (HPLC):96.8%.

6-[(4-Fluorobenzyl)oxy]quinazolin-4(3*H*)-one (1b)

The title compound was prepared in a yield of 25%: mp 363.1-363.2 °C (ethanol). ^{1}H NMR (600 MHz, DMSO) δ 10.17 (s, 1H), 8.40 (s, 1H), 7.56 (d, *J* = 8.8 Hz, 1H), 7.47 – 7.37 (m, 3H), 7.28 (dd, *J* = 8.8, 2.8 Hz, 1H), 7.18 (t, *J* = 8.9 Hz, 2H), 5.15 (s, 2H). ^{13}C NMR (151 MHz, DMSO) δ 162.88, 161.26, 160.32, 157.00, 145.26, 141.60, 133.73, 133.71, 130.48, 130.43, 129.43, 124.30, 123.17, 115.94, 115.80, 109.37, 48.56. APCI-HRMS m/z: calcd for $C_{15}H_{12}FN_2O_2$ (MH^+), 271.0877, found 271.0892. Purity (HPLC): 97.8%.

6-[(4-Chlorobenzyl)oxy]quinazolin-4(3*H*)-one (1c)

The title compound was prepared in a yield of 73%: mp 51.4-51.5 °C. ^{1}H NMR (600 MHz, DMSO) δ 10.16 (s, 1H), 8.38 (s, 1H), 7.55 (d, *J* = 8.8 Hz, 1H), 7.39 (dt, *J* = 17.5, 5.7 Hz, 5H), 7.27 (dd, *J* = 8.8, 2.8 Hz, 1H), 5.14 (s, 2H). ^{13}C NMR (151 MHz, DMSO) δ 159.86, 156.55, 144.80, 141.13, 136.01, 132.27, 129.62, 128.98, 128.57, 123.85, 122.67, 108.89, 48.17. APCI-HRMS m/z: calcd for $C_{15}H_{12}ClN_2O_2$ (MH^+), 287.0582, found 287.0573. Purity (HPLC): 94.3%.

6-[(3-Bromobenzyl)oxy]quinazolin-4(3*H*)-one (1d)

The title compound was prepared in a yield of 49%: mp 51.3-51.4 °C (ethanol). ^{1}H NMR (600 MHz, DMSO) δ 10.17 (s, 1H), 8.39 (s, 1H), 7.59 – 7.53 (m, 2H), 7.48 (d, *J* = 7.9 Hz, 1H), 7.42 (d, *J* = 2.8 Hz, 1H), 7.35 – 7.25 (m, 3H), 5.14 (s, 2H). ^{13}C NMR (151 MHz, DMSO) δ 159.88, 156.57, 144.79, 141.11, 139.68, 130.82, 130.54, 130.51, 128.99, 126.77, 123.88, 122.64, 121.75, 108.90, 48.27. APCI-HRMS m/z: calcd for $C_{15}H_{12}BrN_2O_2$ (MH^+), 331.0077, found 331.0042. Purity (HPLC): 96.9%.

6-[(4-Bromobenzyl)oxy]quinazolin-4(3*H*)-one (1e)

The title compound was prepared in a yield of 9%: mp 298.8-300.9 °C. ^{1}H NMR (600 MHz, DMSO) δ 10.21 (s, 1H), 8.39 (s, 1H), 7.56 (dd, *J* = 14.9, 8.6 Hz, 3H), 7.43 (d, *J* = 2.8 Hz, 1H), 7.36 – 7.25 (m, 3H), 5.14 (s, 2H). ^{13}C NMR (151 MHz, DMSO) δ 160.33, 157.04, 145.27, 141.60, 136.91, 131.98, 130.42, 129.45, 124.34, 123.14, 121.27, 109.38, 48.72. APCI-HRMS m/z: calcd for $C_{15}H_{12}BrN_2O_2$ ($M+2H^+$), 331.0077, found 333.0049. Purity (HPLC):96.3%.

6-[(3-Iodobenzyl)oxy]quinazolin-4(3*H*)-one (1f)

The title compound was prepared in a yield of 47%: mp 234.4-239.7 °C. ^{1}H NMR (600 MHz, DMSO) δ 10.19 (s, 1H), 8.40 (s, 1H), 7.77 (s, 1H), 7.66 (d, *J* = 7.9 Hz, 1H), 7.57 (d, *J* = 8.8 Hz, 1H), 7.43 (d, *J* = 2.8 Hz, 1H), 7.36 (d, *J* = 7.8 Hz, 1H), 7.29 (dd, *J* = 8.8, 2.8 Hz, 1H), 7.15 (t, *J* = 7.8 Hz, 1H), 5.13 (s, 2H). ^{13}C NMR (151 MHz, DMSO) δ 160.34, 157.04, 145.28, 141.59, 140.02, 136.87, 136.78, 131.29, 129.48, 127.63, 124.36, 123.12, 109.38, 95.46, 48.63. APCI-HRMS m/z: calcd for $C_{15}H_{12}IN_2O_2$ (MH^+), 378.9938, found 378.9938. Purity (HPLC): 97.1%.

6-[(4-Iodobenzyl)oxy]quinazolin-4(3*H*)-one (1g)

The title compound was prepared in a yield of 39%: mp 51.3-51.4 °C. ^{1}H NMR (600 MHz, DMSO) δ 10.16 (s, 1H), 8.36 (s, 1H), 7.69 (d, *J* = 8.3 Hz, 2H), 7.55 (d, *J* = 8.8 Hz, 1H), 7.41 (d, *J* = 2.8 Hz, 1H), 7.27 (dd, *J* = 8.8, 2.8 Hz, 1H), 7.14 (d, *J* = 8.3 Hz, 2H), 5.11 (s, 2H). ^{13}C NMR (151 MHz, DMSO) δ 159.84, 156.54, 144.80, 141.12, 137.35, 136.80, 129.99, 128.97, 123.84, 122.65, 108.89, 93.73, 48.36. APCI-HRMS m/z: calcd for $C_{15}H_{12}IN_2O_2$ (MH^+), 378.9938, found 378.9922. Purity (HPLC): 98.0%.

6-{[4-(Trifluoromethyl)benzyl]oxy}quinazolin-4(3*H*)-one (1h)

The title compound was prepared in a yield of 11%: mp 51.3-51.4 °C. ^{1}H NMR (600 MHz, DMSO) δ 10.18 (s, 1H), 8.46 (s, 1H), 7.78 (s, 1H), 7.66 (dd, *J* = 14.6, 7.9 Hz, 2H), 7.59 (dd, *J* = 10.8, 8.3 Hz, 2H), 7.43 (d, *J* = 2.8 Hz, 1H), 7.29 (dd, *J* = 8.8, 2.9 Hz, 1H), 5.26 (s, 2H). ^{13}C NMR (151 MHz, DMSO) δ 160.41, 157.05, 145.29, 141.60, 138.85, 132.30, 130.24, 129.79, 129.58, 129.48, 125.47, 124.97, 124.94, 124.91, 124.36, 123.66, 123.11, 109.36, 48.99. APCI-HRMS m/z: calcd for $C_{16}H_{12}F_3N_2O_2$ (MH^+), 321.0845, found .321.0813. Purity (HPLC): 98.4%.

4-{[(4-Oxo-3,4-dihydroquinazolin-6-yl)oxy]methyl}benzonitrile (1i)

The title compound was prepared in a yield of 40%: mp 51.3-51.4 °C (methanol). ^{1}H NMR (600 MHz, DMSO) δ 10.20 (s, 1H), 8.40 (s, 1H), 7.82 (d, *J* = 8.4 Hz, 2H), 7.58 (d, *J* = 8.8 Hz, 1H), 7.51 (d, *J* = 8.3 Hz, 2H), 7.43 (d, *J* = 2.8 Hz, 1H), 7.29 (dd, *J* = 8.8, 2.9 Hz, 1H), 5.26 (s,

2H). ^{13}C NMR (151 MHz, DMSO) δ 160.39, 157.09, 145.29, 143.05, 141.62, 133.03, 129.50, 128.86, 124.40, 123.12, 119.14, 110.82, 109.38, 49.17. APCI-HRMS m/z: calcd for $C_{16}H_{12}N_3O_2$ (MH^+), 278.0924, found 278.0915. Purity (HPLC): 94.8%.

6-(Pyridin-4-ylmethoxy)quinazolin-4(3*H*)-one (1j)

The title compound was prepared in a yield of 8%: mp 51.4-51.5 ˚C. ^{1}H NMR (600 MHz, DMSO) δ 10.21 (s, 1H), 8.53 (d, *J* = 2.9 Hz, 2H), 8.38 (s, 1H), 7.60 (d, *J* = 8.8 Hz, 1H), 7.44 (d, *J* = 2.8 Hz, 1H), 7.34 – 7.24 (m, 3H), 5.22 (s, 2H). ^{13}C NMR (151 MHz, DMSO) δ 160.40, 157.08, 150.31, 146.30, 145.36, 141.67, 129.53, 124.40, 123.10, 122.61, 109.39, 48.53. APCI-HRMS m/z: calcd for $C_{14}H_{12}N_3O_2$ (MH^+), 254.0924, found 254.0930. Purity (HPLC): 100.0%.

6-(2-Phenylethoxy)quinazolin-4(3*H*)-one (1k)

The title compound was prepared in a yield of 9%: mp 218.0-218.2°C. ^{1}H NMR (600 MHz, DMSO) δ 10.14 (s, 1H), 7.98 (s, 1H), 7.51 (d, *J* = 8.8 Hz, 1H), 7.46 (d, *J* = 2.8 Hz, 1H), 7.26 (ddd, *J* = 23.7, 15.9, 6.9 Hz, 6H), 4.22 – 4.14 (m, 2H), 3.00 (t, *J* = 7.4 Hz, 2H). ^{13}C NMR (151 MHz, DMSO) δ 183.31, 160.33, 156.82, 145.24, 141.59, 138.46, 129.29, 128.96, 127.00, 124.12, 123.03, 109.27, 47.69, 34.79. APCI-HRMS m/z: calcd for $C_{16}H_{15}N_2O_2$ (MH^+), 267.1128, found 267.1117. Purity (HPLC): 98.0%.

6-(2-Oxo-2-phenylethoxy)quinazolin-4(3*H*)-one (1l)

The title compound was prepared in a yield of 15%: mp 236.2-239.9 °C. ^{1}H NMR (600 MHz, DMSO) δ 10.19 (s, 1H), 8.17 (s, 1H), 8.14 – 8.08 (m, 2H), 7.75 (d, *J* = 7.4 Hz, 1H), 7.67 – 7.59 (m, 3H), 7.44 (d, *J* = 2.8 Hz, 1H), 7.33 (dd, *J* = 8.8, 2.9 Hz, 1H), 5.61 (s, 2H). ^{13}C NMR (151 MHz, DMSO) δ 193.36, 160.39, 156.97, 145.67, 141.78, 134.83, 134.67, 129.52, 129.49, 128.55, 124.39, 122.95, 109.32, 52.55. APCI-HRMS m/z: calcd for $C_{16}H_{13}N_2O_3$ (MH^+), 281.0921, found 281.0943. Purity (HPLC): 93.7%.

3-Benzyl-6-(benzyloxy)quinazolin-4(3*H*)-one (2a)

The title compound was prepared in a yield of 43%: mp 129.5-131.9 °C (ethanol). ^{1}H NMR (600 MHz, DMSO) δ 8.48 (s, 1H), 7.65 (dd, *J* = 17.0, 5.9 Hz, 2H), 7.54 – 7.45 (m, 3H), 7.44 – 7.32 (m, 7H), 7.29 (d, *J* = 6.5 Hz, 1H), 5.24 (s, 2H), 5.20 (s, 2H). ^{13}C NMR (151 MHz, DMSO) δ 160.32, 157.59, 146.36, 142.97, 137.39, 137.05, 129.51, 129.11, 128.97, 128.44, 128.18, 128.15, 124.90, 122.97, 119.61 107.81, 70.18, 49.33. APCI-HRMS m/z: calcd for $C_{22}H_{19}N_2O_2$ (MH^+), 343.1441, found 343.1443. Purity (HPLC): 97.0%.

3-(4-Fluorobenzyl)-6-[(4-fluorobenzyl)oxy]quinazolin-4(3*H*)-one (2b)

The title compound was prepared in a yield of 13%: mp 154.5-177.3°C (ethanol). ^{1}H NMR (600 MHz, DMSO) δ 8.47 (s, 1H), 7.62 (dd, *J* = 21.1, 5.9 Hz, 2H), 7.50 (ddd, *J* = 11.9, 8.8,

4.3 Hz, 3H), 7.42 (dd, *J* = 8.7, 5.5 Hz, 2H), 7.18 (dt, *J* = 32.3, 8.9 Hz, 4H), 5.19 (s, 2H), 5.16 (s, 2H). ^{13}C NMR (151 MHz, DMSO) δ 163.11, 162.91, 161.49, 161.29, 160.30, 157.50, 146.28, 142.99, 133.60, 133.58, 133.29, 130.54, 130.49, 130.44, 129.51, 124.93, 122.94, 115.95, 115.86, 115.81, 115.71, 107.78, 69.47, 48.71, 25.96. APCI-HRMS m/z: calcd for $C_{22}H_{17}F_2N_2O_2$ (MH^+), 379.1253, found 379.1218. Purity (HPLC): 99.4%.

3-(4-Chlorobenzyl)-6-[(4-chlorobenzyl)oxy]quinazolin-4(3*H*)-one (2c)

The title compound was prepared in a yield of 16%: mp 51.3-51.4 °C (ethanol). ^{1}H NMR (600 MHz, DMSO) δ 8.47 (s, 1H), 7.65 (d, *J* = 8.9 Hz, 1H), 7.59 (d, *J* = 2.9 Hz, 1H), 7.52 – 7.43 (m, 5H), 7.41 – 7.34 (m, 5H), 5.23 (s, 2H), 5.17 (s, 2H). ^{13}C NMR (151 MHz, DMSO) δ 159.84, 156.96, 145.88, 142.57, 135.88, 135.66, 132.54, 132.34, 129.69, 129.52, 129.11, 128.61, 128.52, 124.50, 122.46, 107.37, 68.86, 48.33. APCI-HRMS m/z: calcd for $C_{22}H_{17}Cl_2N_2O_2$ (MH^+), 411.0662, found 411.0666. Purity (HPLC): 97.1%.

3-(3-Bromobenzyl)-6-[(3-bromobenzyl)oxy]quinazolin-4(3*H*)-one (2d)

The title compound was prepared in a yield of 11%: mp 151.4-152.5 °C. ^{1}H NMR (600 MHz, DMSO) δ 8.51 (s, 1H), 7.68 (dd, *J* = 14.5, 5.2 Hz, 2H), 7.62 (dd, *J* = 3.8, 2.3 Hz, 2H), 7.60 – 7.47 (m, 4H), 7.37 (dd, *J* = 10.6, 4.8 Hz, 2H), 7.32 (d, *J* = 7.8 Hz, 1H), 5.26 (s, 2H), 5.19 (s, 2H). ^{13}C NMR (151 MHz, DMSO) δ 160.33, 157.39, 146.33, 143.07, 140.00, 139.89, 131.30, 131.25, 131.18, 131.08, 131.07, 130.68, 129.58, 127.32, 127.06, 124.98, 122.91, 122.23, 122.20, 107.82, 69.18, 48.89. APCI-HRMS m/z: calcd for $C_{22}H_{17}Br_2N_2O_2$ ($M+2H^+$), 498.9651, found 500.9557. Purity (HPLC): 99.3%.

3-(4-Bromobenzyl)-6-[(4-bromobenzyl)oxy]quinazolin-4(3*H*)-one (2e)

The title compound was prepared in a yield of 18%: mp 182.2-228.2 °C (ethanol). ^{1}H NMR (600 MHz, DMSO) δ 8.48 (s, 1H), 7.66 (d, *J* = 8.9 Hz, 1H), 7.63 – 7.58 (m, 3H), 7.57 – 7.49 (m, 3H), 7.45 (d, *J* = 8.4 Hz, 2H), 7.33 (d, *J* = 8.4 Hz, 2H), 5.23 (s, 2H), 5.17 (s, 2H). ^{13}C NMR (151 MHz, DMSO) δ 160.30, 157.40, 146.33, 143.05, 136.76, 136.55, 131.99, 131.90, 130.47, 130.27, 129.57, 124.94, 122.93, 121.55, 121.34, 107.87, 69.37, 48.86. APCI-HRMS m/z: calcd for $C_{22}H_{17}Br_2N_2O_2$ ($M+2H^+$), 498.9651, found 500.9632. Purity (HPLC): 100.0%.

3-(3-Iodobenzyl)-6-[(3-iodobenzyl)oxy]quinazolin-4(3*H*)-one (2f)

The title compound was prepared in a yield of 22%: mp 152.7-158.1 °C (ethanol). ^{1}H NMR (600 MHz, DMSO) δ 8.50 (s, 1H), 7.87 (s, 1H), 7.79 (s, 1H), 7.69 (dd, *J* = 26.4, 8.4 Hz, 3H), 7.62 (d, *J* = 2.9 Hz, 1H), 7.56 – 7.48 (m, 2H), 7.38 (d, *J* = 7.8 Hz, 1H), 7.22 (t, *J* = 7.8 Hz, 1H), 7.16 (t, *J* = 7.8 Hz, 1H), 5.22 (s, 2H), 5.15 (s, 2H). ^{13}C NMR (151 MHz, DMSO) δ 160.32, 157.43, 146.34, 143.05, 139.87, 139.72, 137.12, 136.92, 136.88, 136.56, 131.29,

131.17, 129.58, 127.69, 127.50, 125.00, 122.91, 107.81, 95.46, 95.35, 69.15, 48.78. APCI-HRMS m/z: calcd for $C_{22}H_{17}I_2N_2O_2$ (MH^+), 594.9374, found 594.9347. Purity (HPLC): 99.1%.

3-(4-Iodobenzyl)-6-[(4-iodobenzyl)oxy]quinazolin-4(3*H*)-one (2g)

The title compound was prepared in a yield of 7%: mp 51.3-51.4 °C. ^{1}H NMR (600 MHz, DMSO) δ 8.45 (s, 1H), 7.75 (d, *J* = 8.3 Hz, 2H), 7.69 (d, *J* = 8.4 Hz, 2H), 7.64 (d, *J* = 8.9 Hz, 1H), 7.57 (d, *J* = 2.9 Hz, 1H), 7.52 – 7.47 (m, 1H), 7.27 (d, *J* = 8.3 Hz, 2H), 7.15 (d, *J* = 8.4 Hz, 2H), 5.19 (s, 2H), 5.13 (s, 2H). ^{13}C NMR (151 MHz, DMSO) δ 159.79, 156.91, 145.84, 142.54, 137.35, 137.26, 136.65, 136.42, 130.03, 129.83, 129.07, 124.45, 122.42, 107.37, 94.06, 93.80, 68.99, 48.48. APCI-HRMS m/z: calcd for $C_{22}H_{17}I_2N_2O_2$ (MH^+), 594.9374, found 594.9333. Purity (HPLC): 100.0%.

4-({[3-(4-Cyanobenzyl)-4-oxo-3,4-dihydroquinazolin-6-yl]oxy}methyl)benzonitrile (2h)

The title compound was prepared in a yield of 91%: mp 51.5-51.6 °C. ^{1}H NMR (600 MHz, DMSO) δ 8.50 (s, 1H), 7.89 (d, *J* = 8.2 Hz, 2H), 7.82 (d, *J* = 8.3 Hz, 2H), 7.69 (t, *J* = 8.5 Hz, 3H), 7.63 – 7.49 (m, 4H), 5.37 (s, 2H), 5.28 (s, 2H). ^{13}C NMR (151 MHz, DMSO) δ 160.34, 157.27, 146.46, 143.19, 142.89, 133.04, 132.96, 129.75, 129.68, 128.91, 128.53, 125.00, 122.91, 119.21, 119.13, 111.06, 110.86, 107.90, 69.21, 49.32. APCI-HRMS m/z: calcd for $C_{24}H_{17}N_4O_2$ (MH^+), 393.1346, found 393.1342. Purity (HPLC): 97.9%.

6-(2-Phenoxyethoxy)-3-(2-phenoxyethyl)quinazolin-4(3*H*)-one (2i)

The title compound was prepared in a yield of 51%: mp 51.3-51.4 °C. ^{1}H NMR (600 MHz, DMSO) δ 8.32 (s, 1H), 7.63 (dd, *J* = 19.4, 5.9 Hz, 2H), 7.49 (dd, *J* = 8.9, 2.9 Hz, 1H), 7.35 – 7.21 (m, 4H), 7.04 – 6.88 (m, 7H), 4.49 – 4.40 (m, 3H), 4.40 – 4.31 (m, 4H), 4.29 (t, *J* = 5.3 Hz, 2H). ^{13}C NMR (151 MHz, DMSO) δ 160.50, 158.73, 158.42, 157.55, 146.75, 142.99, 130.04, 130.03, 129.48, 124.78, 123.81, 122.80, 121.45, 121.27, 114.96, 114.92, 107.26, 67.49, 66.55, 65.33, 45.90. APCI-HRMS m/z: calcd for $C_{25}H_{25}N_2O_4$ (MH^+), 403.1652, found 403.1624. Purity (HPLC): 96.8%.

Protocol for the measurement of IC_{50} values

The IC_{50} values for MAO inhibition were measured according to the method reported in literature (Mostert *et al.*, 2016). For this purpose, recombinant human MAO-A and MAO-B were used as enzyme sources. The enzyme reactions were carried out in white 96-well microtiter plates (Eppendorf) and potassium phosphate buffer (100 mM, made isotonic with KCl) at pH 7.4 served as reaction medium. The final volume of the reactions was 200 µL and contained the test inhibitors at different concentrations (0.003–100 µM) and the non-selective MAO substrate kynuramine (50 µM). Stock solutions of the test inhibitors were prepared in DMSO and added to the reactions to yield a final concentration of 4% DMSO.

The enzyme reactions were initiated with MAO-A (0.0075 g protein/mL) and MAO-B (0.015 g protein/mL), incubated for 20 min at 37 ºC in a convection oven, and terminated with 80 µL NaOH (2 N). The rate of formation of 4-hydroxyquinoline, the product of kynuramine oxidation, was measured by fluorescence spectrometry (λ_{ex} = 310 nm; λ_{em} = 400 nm). A linear calibration curve containing authentic 4-hydroxyquinoline (0.047–1.56 µM) was constructed and used for these measurements. The inhibition data were fitted to the one site competition model incorporated into the Prism 5 software package (GraphPad) and the IC_{50} values were determined from the resulting sigmoidal plots (rate versus the logarithm of inhibitor concentration). IC_{50} values are expressed as mean ± standard deviation (SD) of triplicate measurements.

Dialysis of enzyme reactions

Reversibility of MAO-B inhibition by **2b** was investigated by dialysis. Slide-A-Lyzer® dialysis cassettes (Thermo Scientific) with a molecular weight cut-off of 10 000 and sample volume capacity of 0.3–5 mL were employed for the purpose of this study (Petzer *et al.*, 2013; Mostert *et al.*, 2016). The test inhibitor (**2b** at concentration equal to 4 x IC_{50}) and MAO-B (0.03 mg/mL) were pre-incubated for 15 min at 37 ºC in potassium phosphate buffer (100 mM, pH 7.4, 5% sucrose) to a final volume of 0.8 mL. The incubations contained 4% DMSO as co-solvent. As controls, MAO-B was similarly pre-incubated in the absence of the inhibitor and in the presence of the irreversible MAO-B inhibitor, (R)-deprenyl. The concentration of (R)-deprenyl used was equal to 4-fold its reported IC_{50} value for the inhibition of MAO-B. The enzyme-inhibitor incubations were subsequently dialysed at 4 ºC in 80 mL dialysis buffer (100 mM potassium phosphate, pH 7.4, 5% sucrose). The dialysis buffer was replaced with fresh buffer at 3 h and 7 h after the start of dialysis. After 24 h, the reactions were diluted 2-fold with addition of kynuramine to yield a final concentration of kynuramine and **2b** of 50 µM and 2 x IC_{50}, respectively. The reactions were further incubated at 37 ºC for 20 min and then terminated with the addition of NaOH (400 µL of 2 N) and water (1000 µL). The concentrations of MAO-generated 4-hydroxyquinoline were measured by fluorescence spectrometry (λ_{ex} = 310 nm; λ_{em} = 400 nm) as described for the IC_{50} value determination above. For comparison, undialysed mixtures of MAO-B and **2b** were maintained at 4 ºC over a period of 24 h. All reactions were carried out in triplicate and the residual enzyme catalytic rates were expressed as mean ± SD.

Construction of Lineweaver-Burk plots and K_i value estimation

To examine the mode of MAO-B inhibition by **2b**, a set of Lineweaver-Burke plots was constructed (Legoabe *et al.*, 2014; Mostert *et al.*, 2016). For this purpose, the first plot was constructed in the absence of the inhibitor, while the remaining 5 plots were constructed in

the presence of various concentrations of the test inhibitor (¼ x IC_{50}, ½ x IC_{50}, ¾ x IC_{50}, 1 x IC_{50}, 1¼ x IC_{50}). Kynuramine, at concentrations of 15–250 µM served as substrate, and MAO-B was used at a concentration of 0.015 mg/mL. The rate of formation of 4-hydroxyquinoline was measured by fluorescence spectrometry as described for the IC_{50} value determination (Mostert *et al.*, 2015). K_i values were estimated from plots of the slopes of the Lineweaver-Burke plots versus inhibitor concentration, where the x-intercept equals – K_i.

REFERENCES

Aminoff, M.J. 1994. Treatment of Parkinson's disease. *Western journal of medicine*, 161(3):303.

Arora, R., Kapoor, A., Gill, N. & Rana, A. 2011. Quinazolinone: an overview. *International research journal of pharmacy*, 2:21-28.

Bahadur, S. 1983. Syntheses and biological activities of some new 4 (3*H*)-quinazolinones. *Archiv der pharmazie*, 316(11):964-968.

Cao, S.-L., Feng, Y.-P., Jiang, Y.-Y., Liu, S.-Y., Ding, G.-Y. & Li, R.-T. 2005. Synthesis and in vitro antitumor activity of 4(3*H*)-quinazolinone derivatives with dithiocarbamate side chains. *Bioorganic & medicinal chemistry letters*, 15(7):1915-1917.

Carradori, S. & Silvestri, R. 2015. New frontiers in selective human MAO-B inhibitors: miniperspective. *Journal of medicinal chemistry*, 58(17):6717-6732.

Chawla, A. & Batra, C. 2013. Recent advances of quinazolinone derivatives as marker for various biological activities. *International research journal of pharmacy*, 4(3):49-58.

Demeunynck, M. & Baussanne, I. 2013. Survey of recent literature related to the biologically active 4 (3*H*)-quinazolinones containing fused heterocycles. *Current medicinal chemistry*, 20(6):794-814.

Du, Y., Ma, Z., Lin, S., Dodel, R.C., Gao, F., Bales, K.R., Triarhou, L.C., Chernet, E., Perry, K.W., Nelson, D.L., Luecke, S., Phebus, L.A., Bymaster, F.P. & Paul, S.M. 2001. Minocycline prevents nigrostriatal dopaminergic neurodegeneration in the MPTP model of Parkinson's disease. *Proceedings of the national academy of sciences*, 98(25):14669-14674.

Fernandez-Espejo, E. 2004. Pathogenesis of Parkinson’s disease. *Molecular neurobiology*, 29(1):15-30.

Gaweska, H. & Fitzpatrick, P.F. 2011. Structures and mechanism of the monoamine oxidase family. *Biomolecular concepts*, 2(5):365-377.

Hely, M.A., Fung, V.S. & Morris, J.G. 2000. Treatment of Parkinson's disease. *Journal of clinical neuroscience*, 7(6):484-494.

Khattab, S.N., Haiba, N.S., Asal, A.M., Bekhit, A.A., Amer, A., Abdel-Rahman, H.M. & El-Faham, A. 2015. Synthesis and evaluation of quinazoline amino acid derivatives as monoamine oxidase (MAO) inhibitors. *Bioorganic & medicinal chemistry*, 23(13):3574-3585.

Kumar, M.J., Nicholls, D.G. & Andersen, J.K. 2003. Oxidative alpha-ketoglutarate dehydrogenase inhibition via subtle elevations in monoamine oxidase B levels results in loss of spare respiratory capacity: implications for Parkinson's disease. *Journal of biological chemistry*, 278(47):46432-46439.

Lata, A., Satsangi, R.K., Srivastava, V.K. & Kishor, K. 1982. Monoamine oxidase inhibitory and CNS activities of some quinazolinones. *Arzneimittelforschung*, 32(1):24-27.

Legoabe, L.J., Petzer, A. & Petzer, J.P. 2012. Inhibition of monoamine oxidase by selected C6-substituted chromone derivatives. *European journal of medicinal chemistry*, 49:343-353.

Legoabe, L.J., Petzer, A. & Petzer, J.P. 2014. α-Tetralone derivatives as inhibitors of monoamine oxidase. *Bioorganic & medicinal chemistry letters*, 24(12):2758-2763.

Legoabe, L.J., Petzer, A. & Petzer, J.P. 2015. The synthesis and evaluation of C7-substituted α-tetralone derivatives as inhibitors of monoamine oxidase. *Chemical biology & drug design*, 86(4):895-904.

Martin, W.W. & Wieler, M. 2003. Treatment of Parkinson's disease. *Canadian journal of neurological sciences*, 30(S1):S27-S33.

Meiring, L., Petzer, J.P. & Petzer, A. 2013. Inhibition of monoamine oxidase by 3, 4-dihydro-2 (1*H*)-quinolinone derivatives. *Bioorganic & medicinal chemistry letters*, 23(20):5498-5502.

Mostert, S., Petzer, A. & Petzer, J.P. 2015. Indanones as high-potency reversible inhibitors of monoamine oxidase. *ChemMedChem*, 10(5):862-873.

Mostert, S., Petzer, A. & Petzer, J.P. 2016. Inhibition of monoamine oxidase by benzoxathiolone analogues. *Bioorganic & medicinal chemistry letters*, 26(4):1200-1204.

Nel, M.S., Petzer, A., Petzer, J.P. & Legoabe, L.J. 2016. 2-Benzylidene-1-indanone derivatives as inhibitors of monoamine oxidase. *Bioorganic & medicinal chemistry letters*, 26(19):4599-4605.

Nicotra, A., Pierucci, F., Parvez, H. & Senatori, O. 2004. Monoamine oxidase expression during development and aging. *Neurotoxicology*, 25(1-2):155-165.

Petzer, A., Pienaar, A. & Petzer, J.P. 2013. The inhibition of monoamine oxidase by esomeprazole. *Drug research*, 63:462-467.

Rossiter, D., Blockman, M., Barnes, K.I., Cohen, K., Decloedt, E., Waal, R., Maartens, G., McIlleron, H. & Sixanda, P.Z. 2012. South African medicines formulary. 10th ed. Cape Town: Health and Medical Publishing Group.

Sharma, C.P., Kaur, G., Pahwa, R., Sharma, A. & Rajak, H. 2011. Quinazolinone analogs as potential therapeutic agents. *Current medicinal chemistry*, 18(31):4786-4812.

Shih, J.C., Chen, K. & Ridd, M.J. 1999. Monoamine oxidase: from genes to behavior. *Annual review of neuroscience*, 22:197-217.

Srivastava, V.K., Satsangi, R.K., Kumar, P. & Kishor, K. 1980. Monoamine oxidase inhibitory activity of 2-aryl-3-(5'-chlorobenzophenon-2'-yl)-quinazolin-4-(3*H*)-ones. *Indian journal of physiology and pharmacology*, 24(4):361-363.

Youdim, M.B. & Bakhle, Y. 2006. Monoamine oxidase: isoforms and inhibitors in Parkinson's disease and depressive illness. *British journal of pharmacology*, 147(S1):S287-S296.

Youdim, M.B., Edmondson, D. & Tipton, K.F. 2006. The therapeutic potential of monoamine oxidase inhibitors. *Nature reviews neuroscience*, 7(4):295-309.

Youdim, M.B. & Weinstock, M. 2004. Therapeutic applications of selective and non-selective inhibitors of monoamine oxidase A and B that do not cause significant tyramine potentiation. *Neurotoxicology*, 25(1-2):243-250.

APPENDIX B: SPECTRA

^{1}H NMR, ^{13}C NMR, MS and HPLC

Malikotsi A. Qhobosheane[1], Lesetja J. Legoabe[2,*], Jacobus P. Petzer[1,2], and Anél Petzer[1,2]

[1]Pharmaceutical Chemistry, School of Pharmacy, North-West University, Private Bag X6001, Potchefstroom 2520, South Africa

[2]Centre of Excellence for Pharmaceutical Sciences, North-West University, Private Bag X6001, Potchefstroom 2520, South Africa

6-(Benzyloxy)quinazolin-4(3*H*)-one (1a)

^{1}H NMR

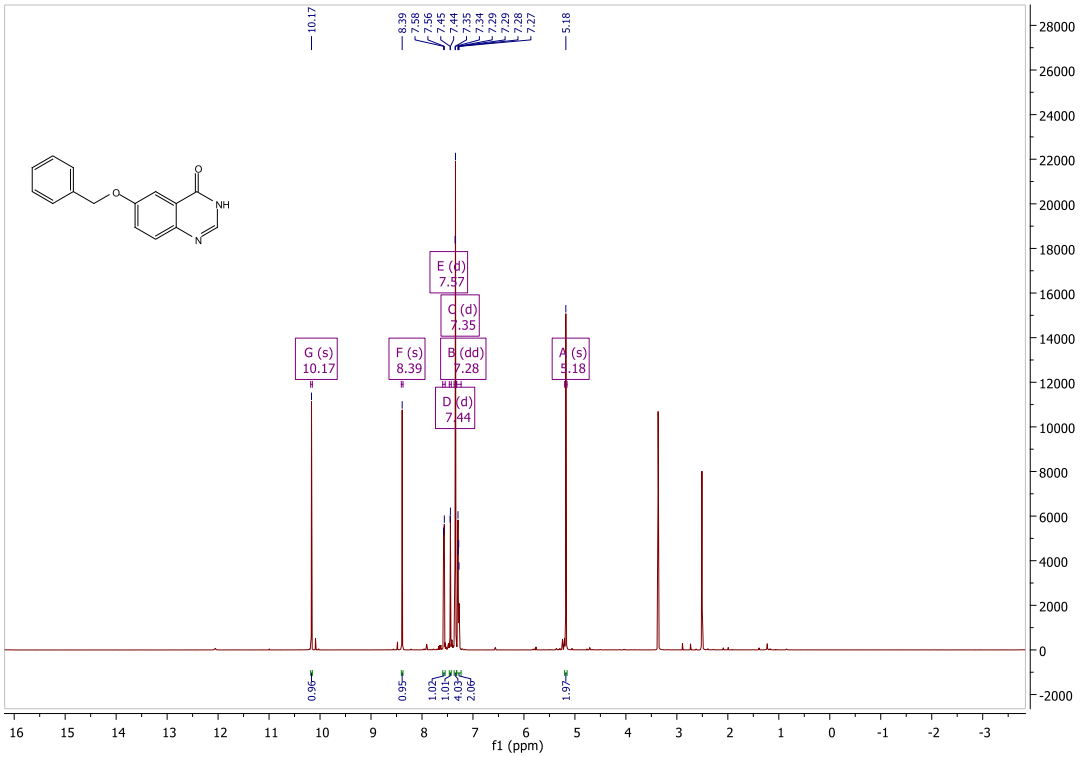

^{13}C NMR

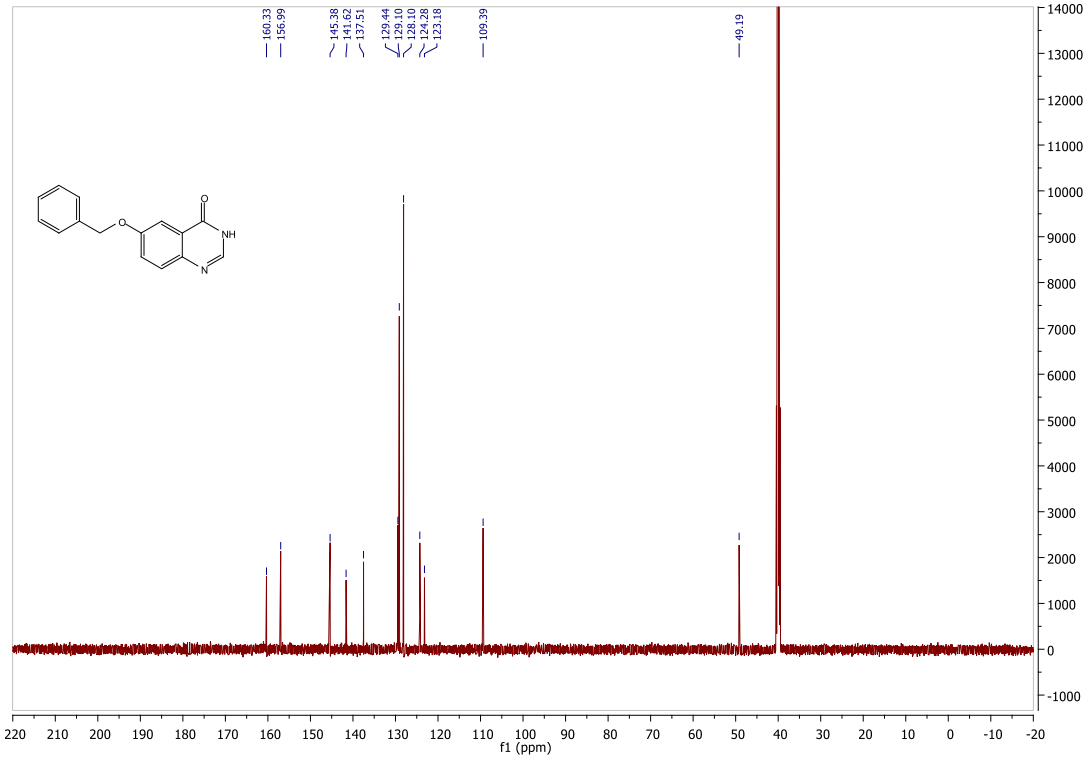

MS

Acquisition Parameter

Source Type	APCI	Ion Polarity	Positive	Set Nebulizer	1.6 Bar
Focus	Not active	Set Capillary	4500 V	Set Dry Heater	200 °C
Scan Begin	50 m/z	Set End Plate Offset	-500 V	Set Dry Gas	8.0 l/min
Scan End	1500 m/z	Set Collision Cell RF	100.0 Vpp	Set Divert Valve	Waste

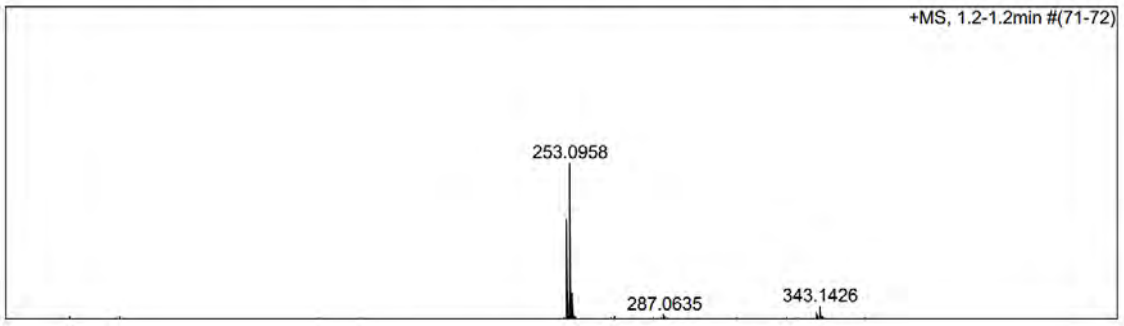

HPLC

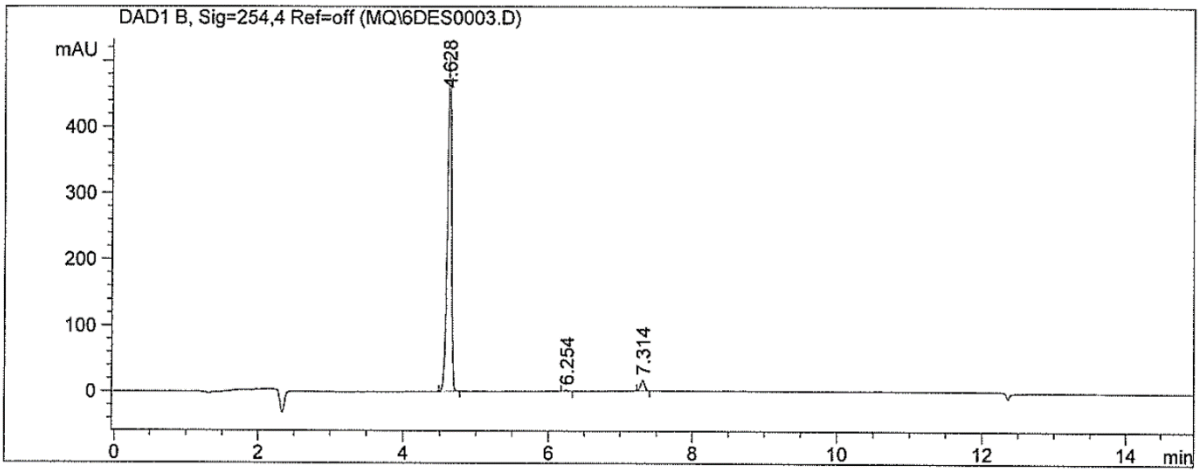

6-[(4-Fluorobenzyl)oxy]quinazoline-4(3*H*)-one (1b)

^{1}H NMR

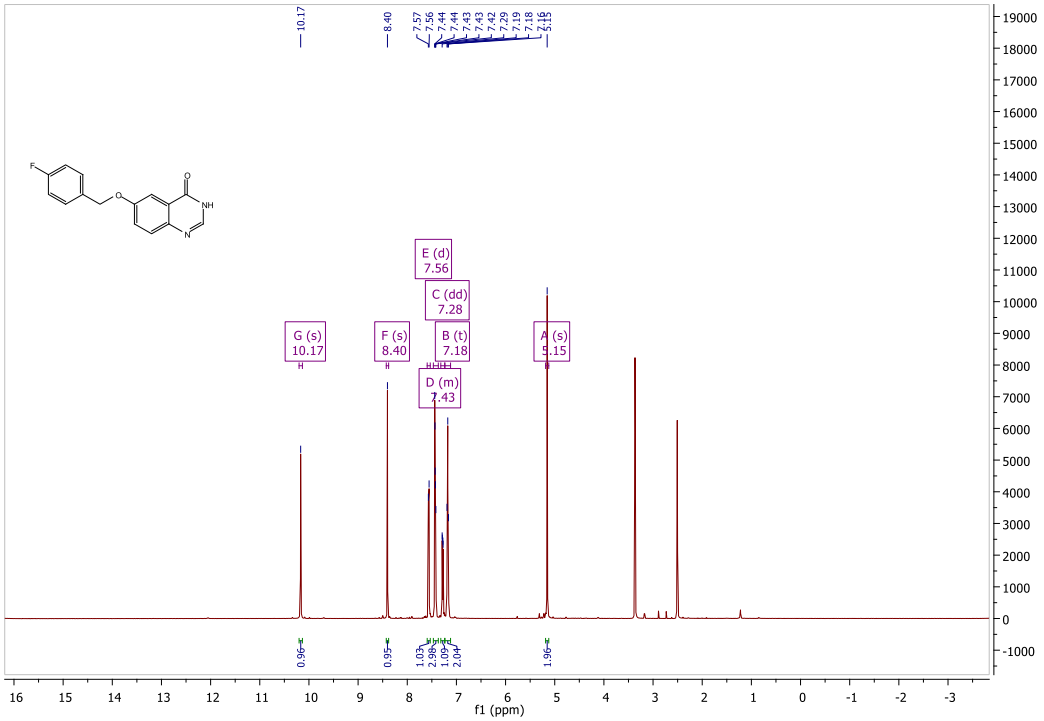

^{13}C NMR

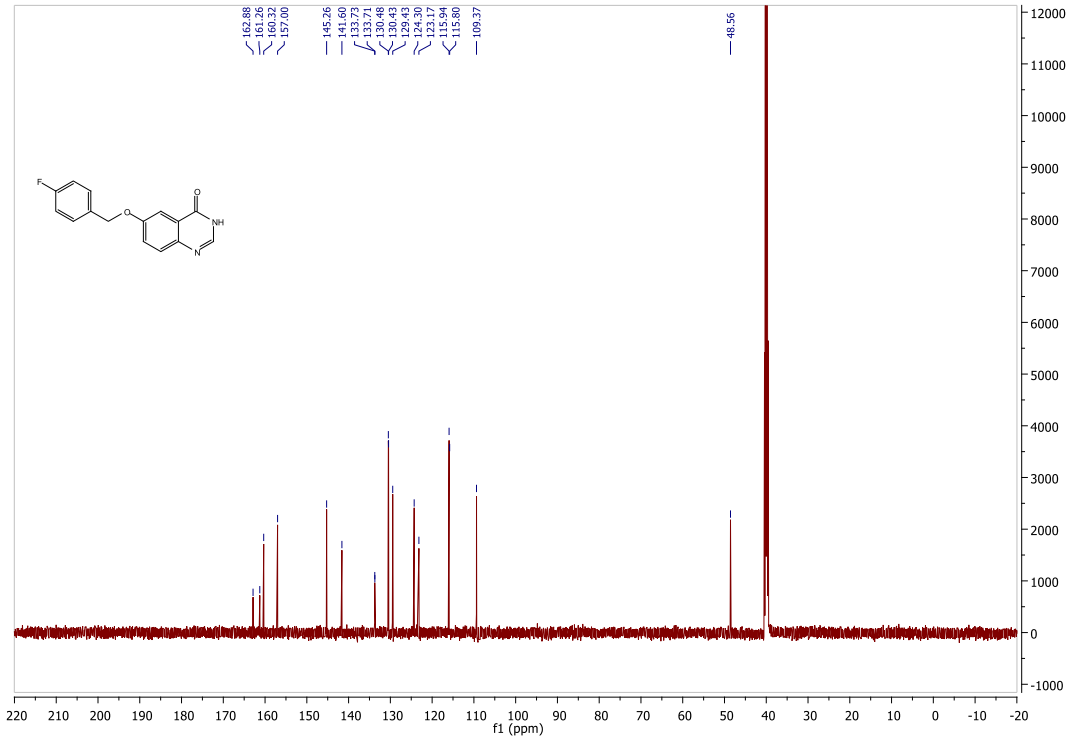

MS

Acquisition Parameter

Source Type	APCI	Ion Polarity	Positive	Set Nebulizer	1.6 Bar
Focus	Not active	Set Capillary	4500 V	Set Dry Heater	200 °C
Scan Begin	50 m/z	Set End Plate Offset	-500 V	Set Dry Gas	8.0 l/min
Scan End	1500 m/z	Set Collision Cell RF	100.0 Vpp	Set Divert Valve	Waste

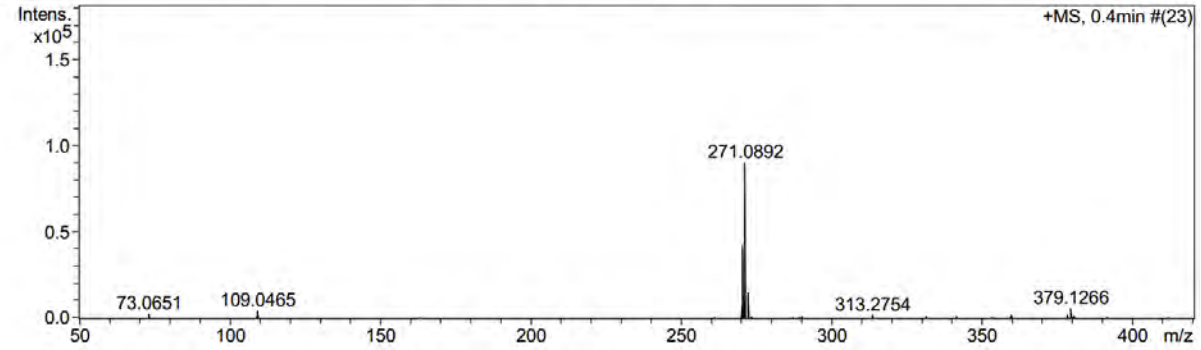

HPLC

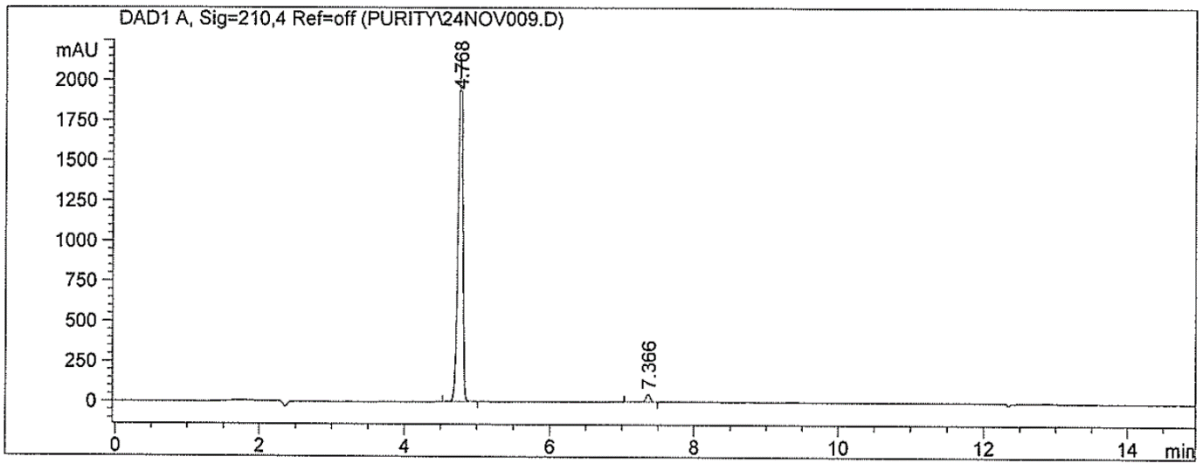

6-[(4-Chlorobenzyl)oxy]quinazoline-4(3*H*)-one (1c)

^{1}H NMR

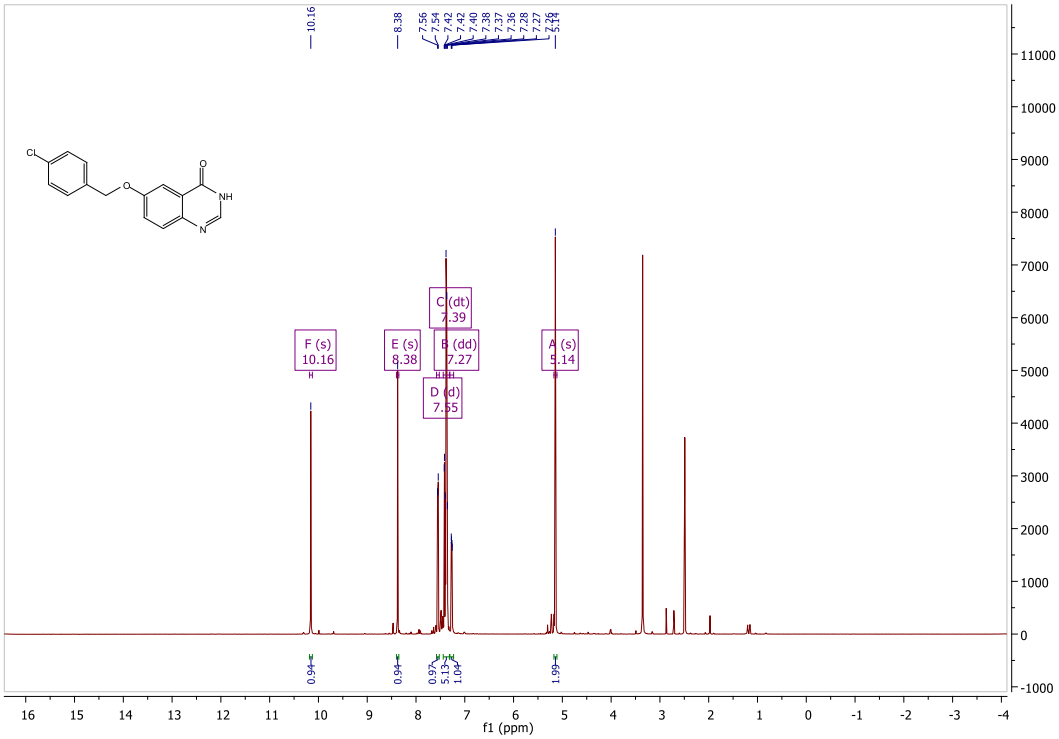

^{13}C NMR

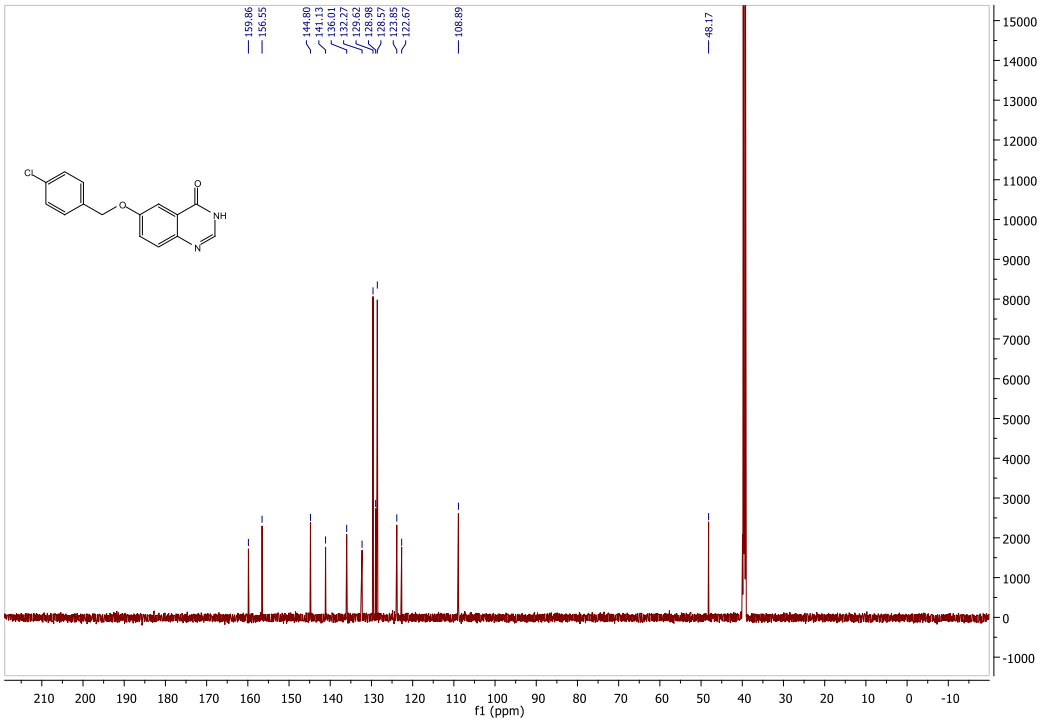

MS

Acquisition Parameter

Source Type	APCI	Ion Polarity	Positive	Set Nebulizer	1.6 Bar
Focus	Not active	Set Capillary	4500 V	Set Dry Heater	200 °C
Scan Begin	50 m/z	Set End Plate Offset	-500 V	Set Dry Gas	8.0 l/min
Scan End	1500 m/z	Set Collision Cell RF	100.0 Vpp	Set Divert Valve	Waste

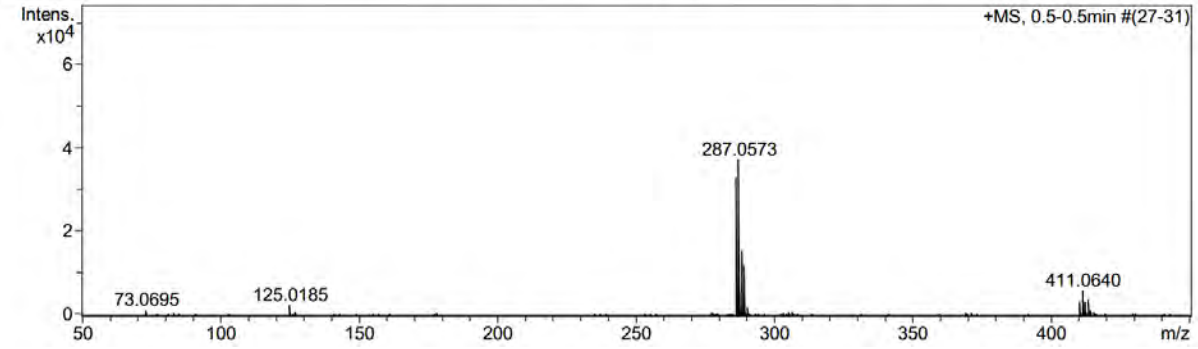

HPLC

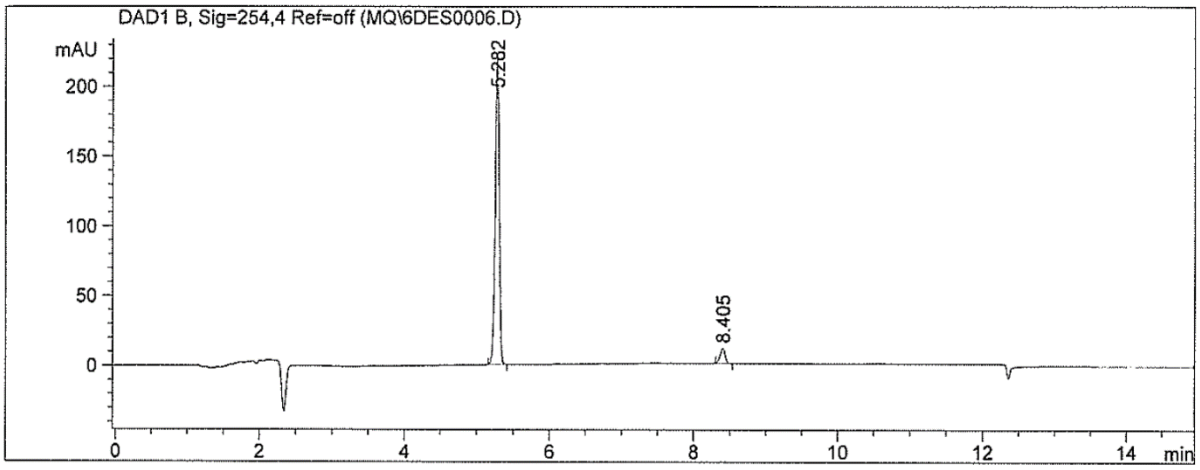

6-[(3-Bromobenzyl)oxy]quinazoline-4(3*H*)-one (1d)

^{1}H NMR

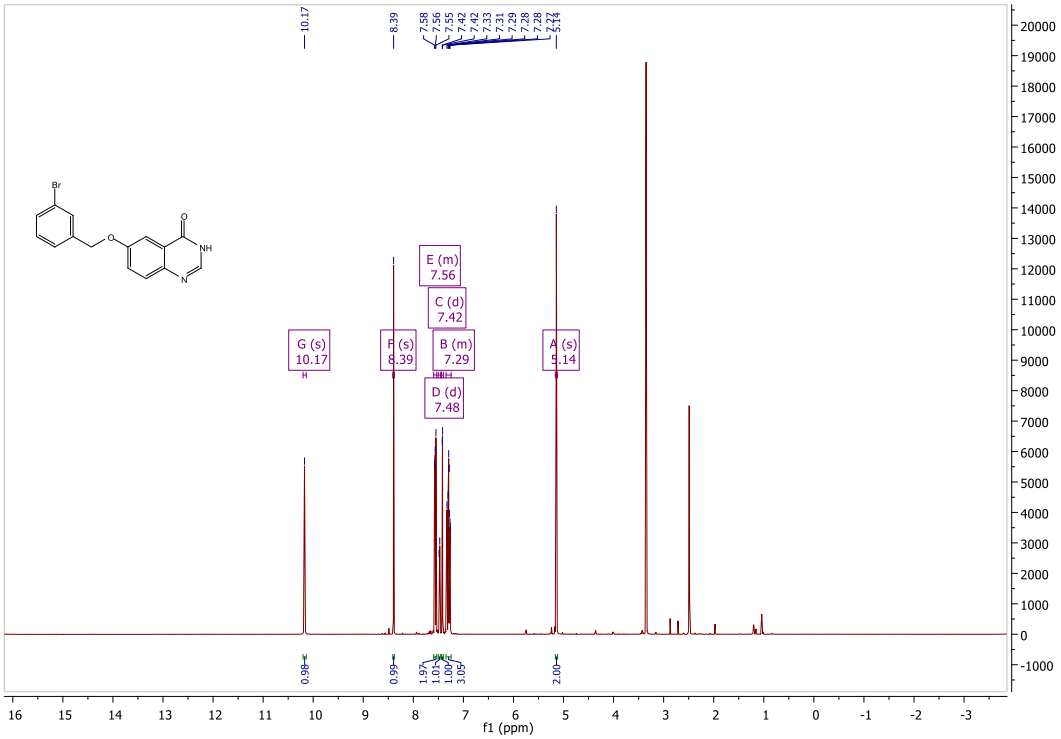

^{13}C NMR

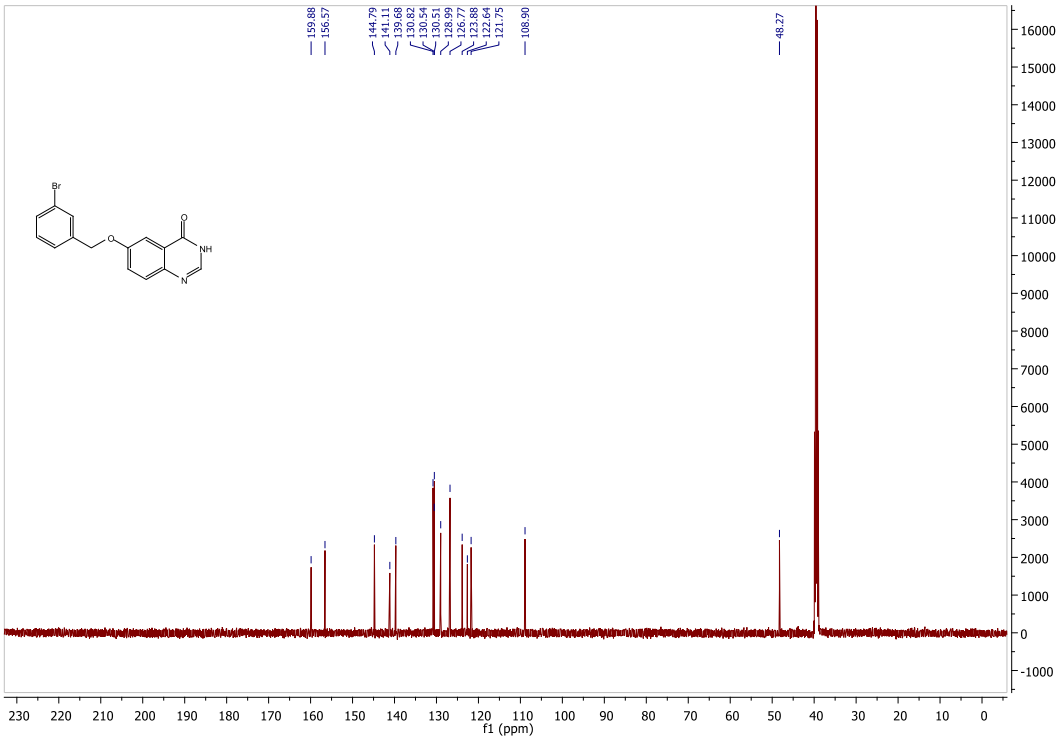

MS

Acquisition Parameter

Source Type	APCI	Ion Polarity	Positive	Set Nebulizer	1.6 Bar
Focus	Not active	Set Capillary	4500 V	Set Dry Heater	200 °C
Scan Begin	50 m/z	Set End Plate Offset	-500 V	Set Dry Gas	8.0 l/min
Scan End	1500 m/z	Set Collision Cell RF	100.0 Vpp	Set Divert Valve	Waste

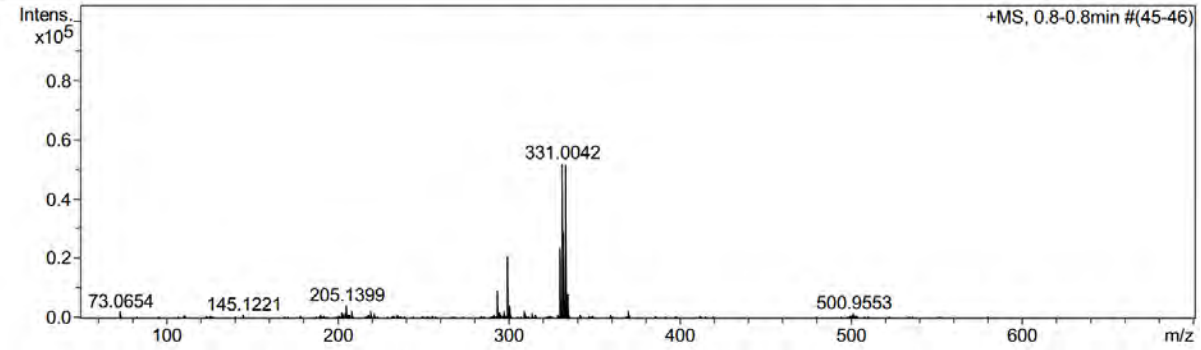

HPLC

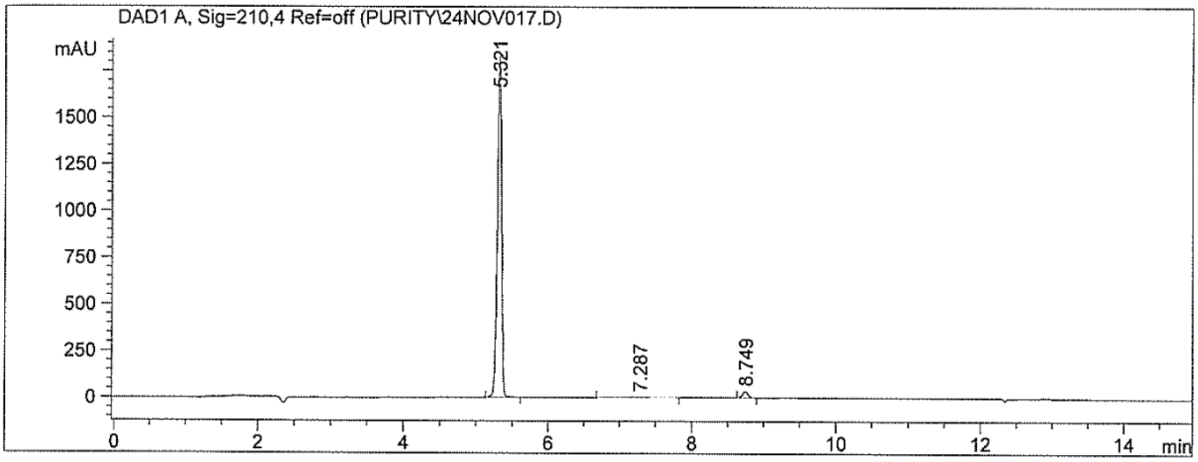

6-[(4-Bromobenzyl)oxy]quinazoline-4(3*H*)-one (1e)

^{1}H NMR

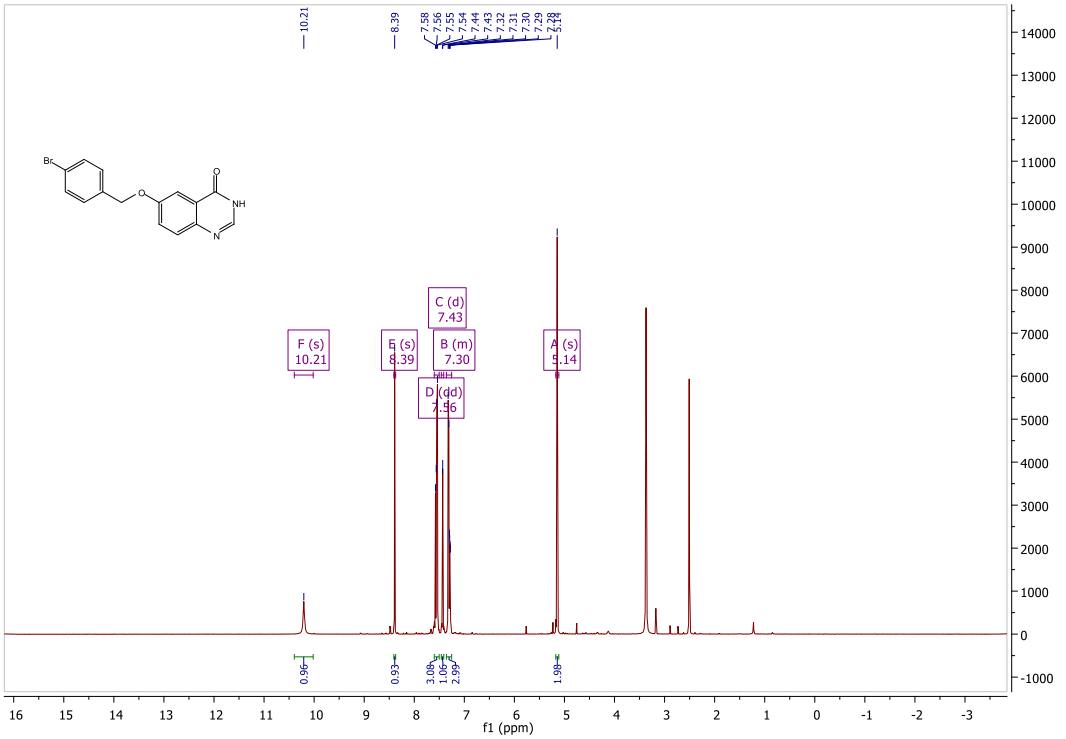

^{13}C NMR

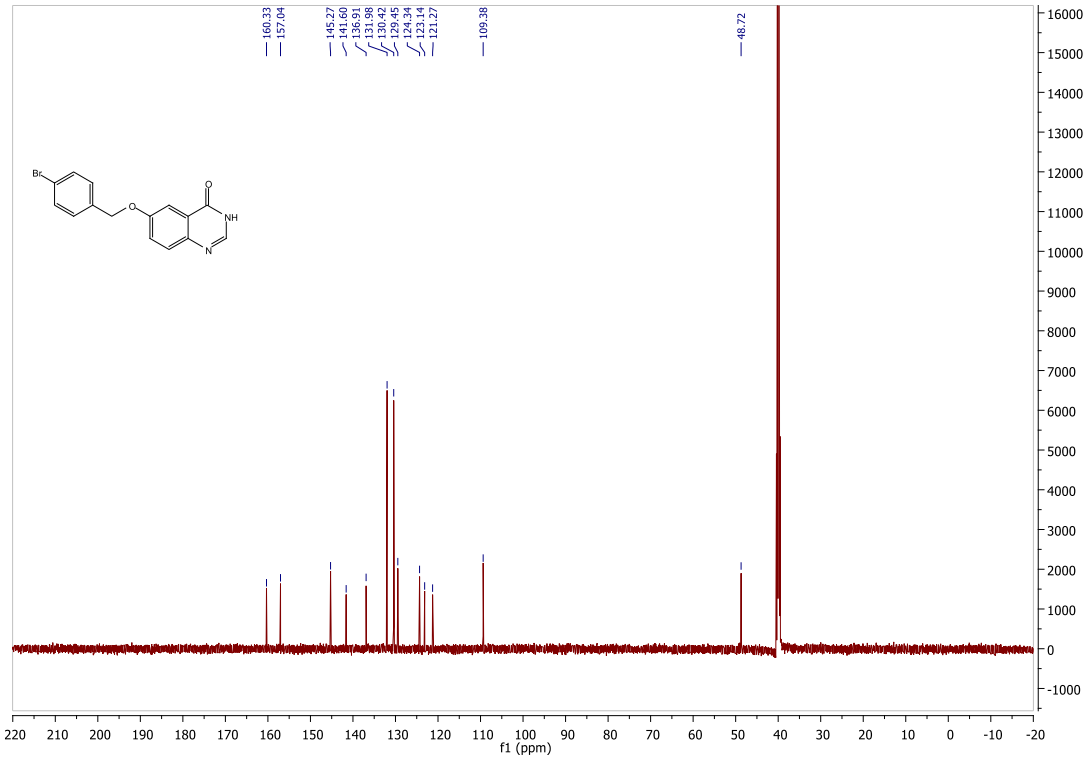

MS

Acquisition Parameter

Source Type	APCI	Ion Polarity	Positive	Set Nebulizer	1.6 Bar
Focus	Not active	Set Capillary	4500 V	Set Dry Heater	200 °C
Scan Begin	50 m/z	Set End Plate Offset	-500 V	Set Dry Gas	8.0 l/min
Scan End	1500 m/z	Set Collision Cell RF	100.0 Vpp	Set Divert Valve	Waste

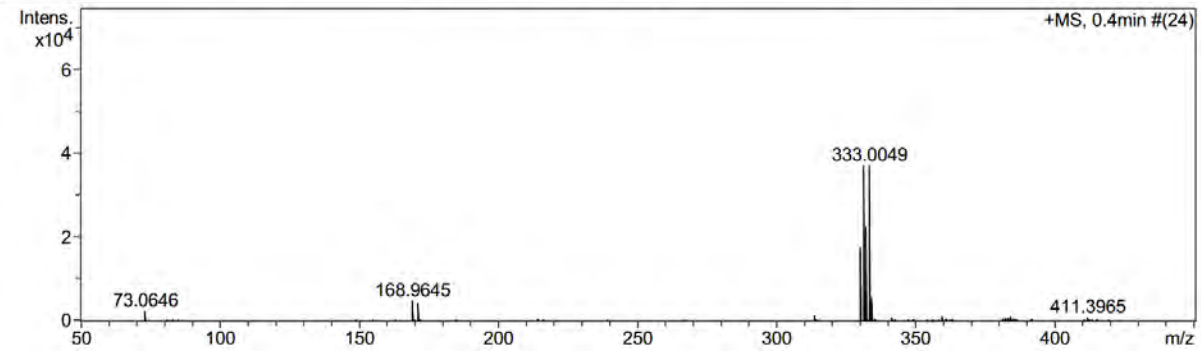

HPLC

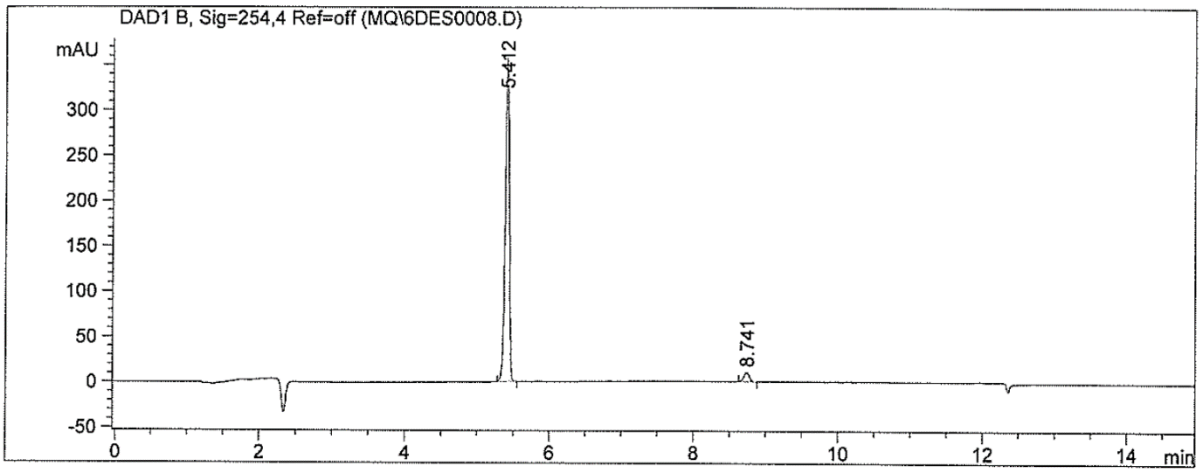

6-[(3-Iodobenzyl)oxy]quinazoline-4(3*H*)-one (1f)

^{1}H MNR

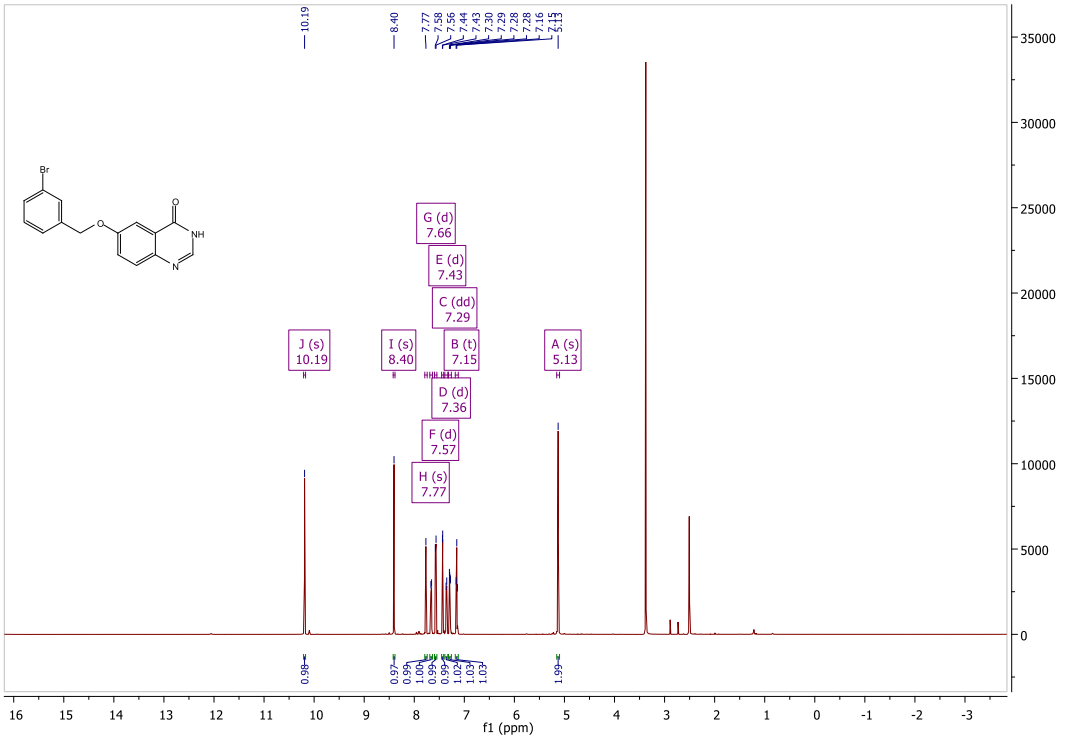

^{13}C NMR

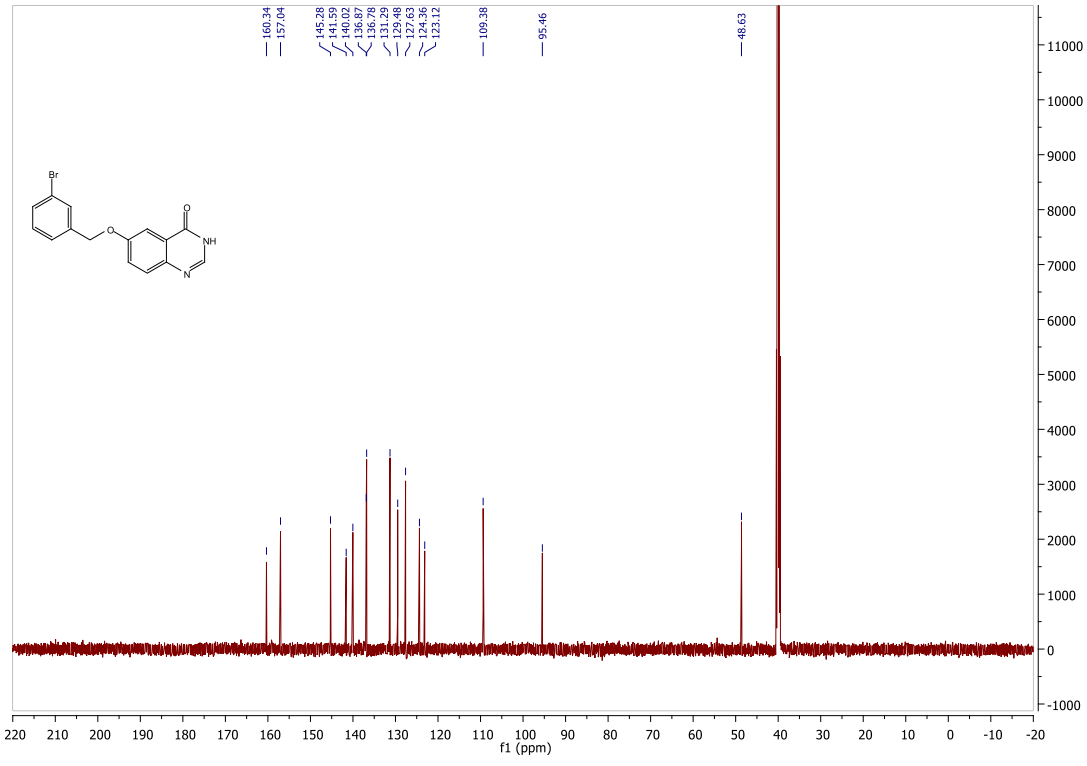

MS

Acquisition Parameter

Source Type	APCI	Ion Polarity	Positive	Set Nebulizer	1.6 Bar
Focus	Not active	Set Capillary	4500 V	Set Dry Heater	200 °C
Scan Begin	50 m/z	Set End Plate Offset	-500 V	Set Dry Gas	8.0 l/min
Scan End	1500 m/z	Set Collision Cell RF	100.0 Vpp	Set Divert Valve	Waste

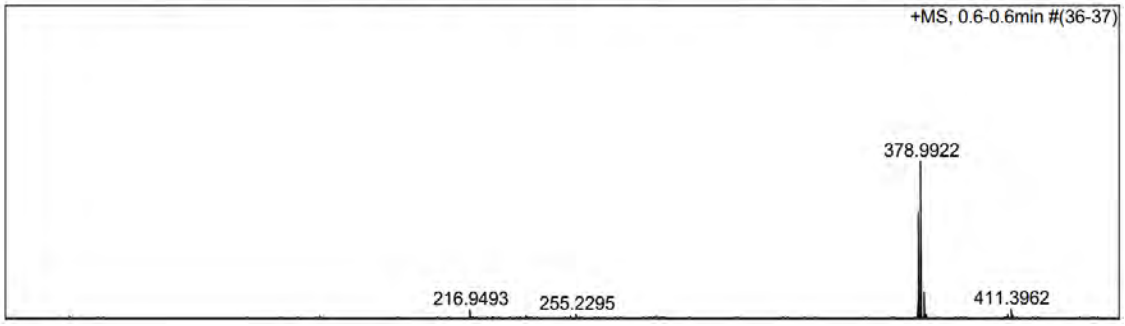

HPLC

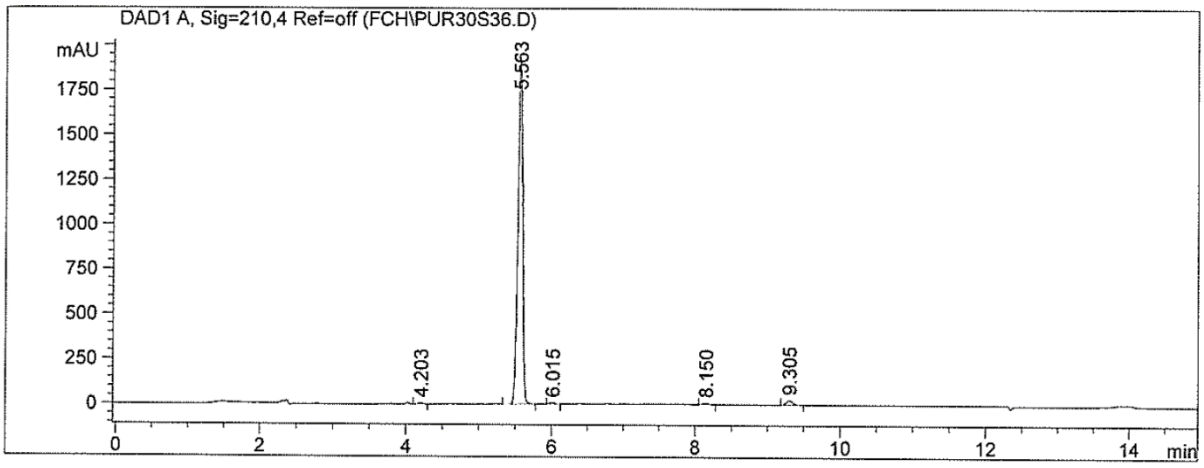

6-[(4-Iodobenzyl)oxy]quinazoline-4(3*H*)-one (1g)

^{1}H NMR

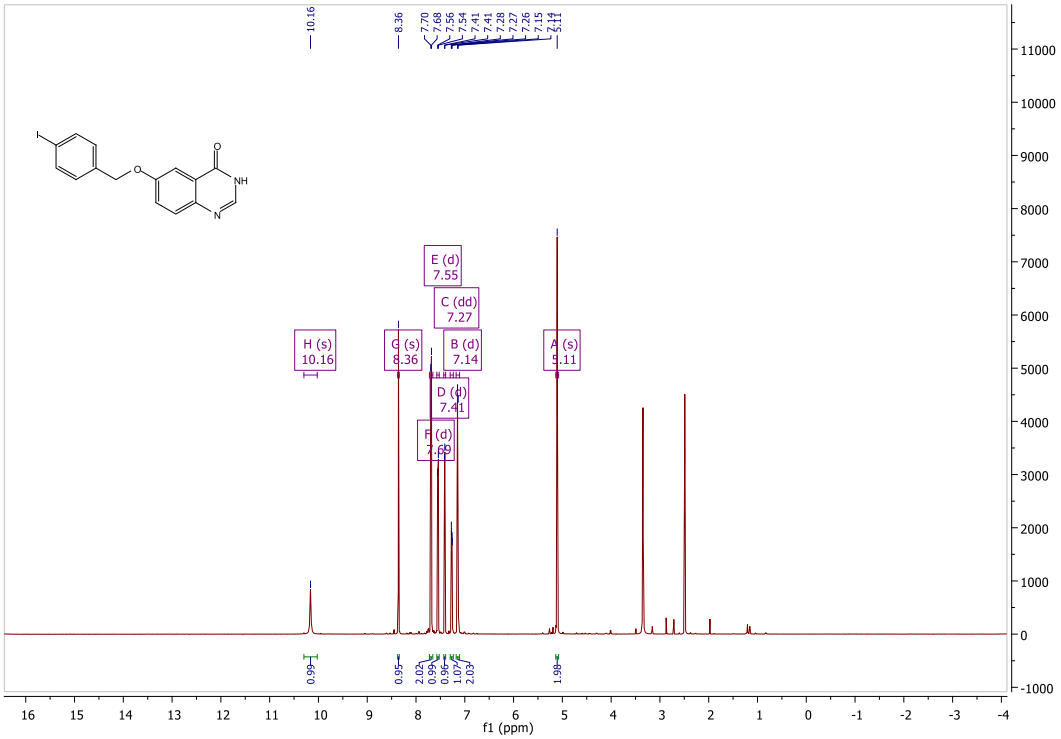

^{13}C NMR

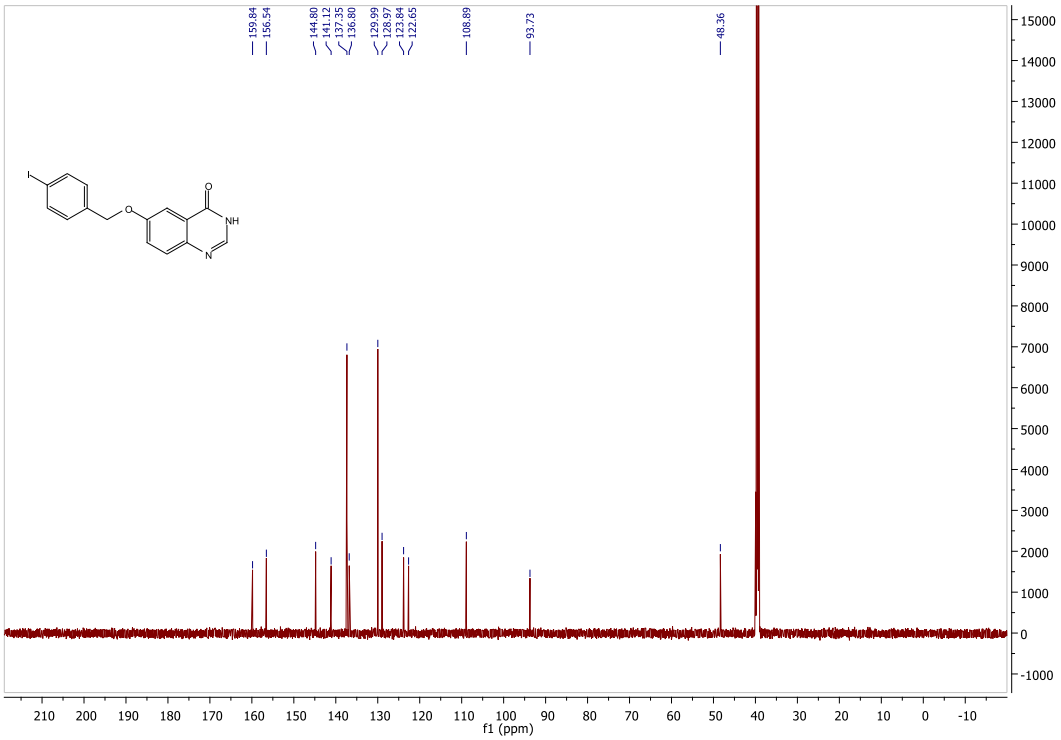

MS

Acquisition Parameter

Source Type	APCI	Ion Polarity	Positive	Set Nebulizer	1.6 Bar
Focus	Not active	Set Capillary	4500 V	Set Dry Heater	200 °C
Scan Begin	50 m/z	Set End Plate Offset	-500 V	Set Dry Gas	8.0 l/min
Scan End	1500 m/z	Set Collision Cell RF	100.0 Vpp	Set Divert Valve	Waste

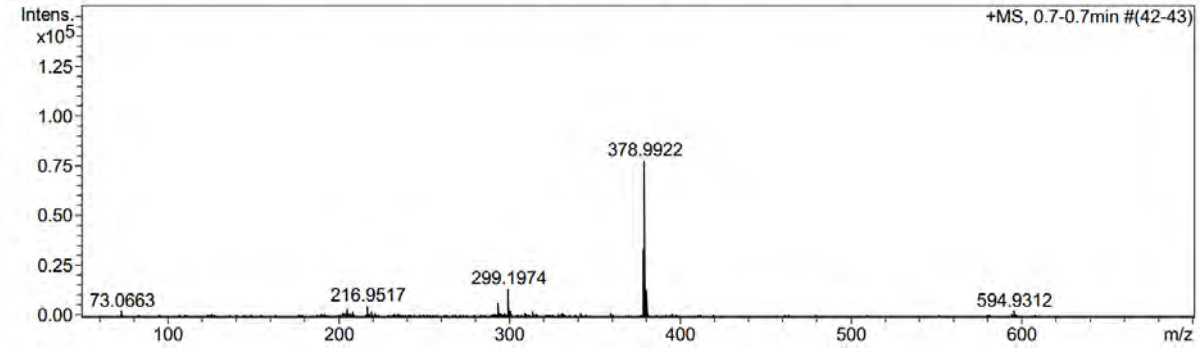

HPLC

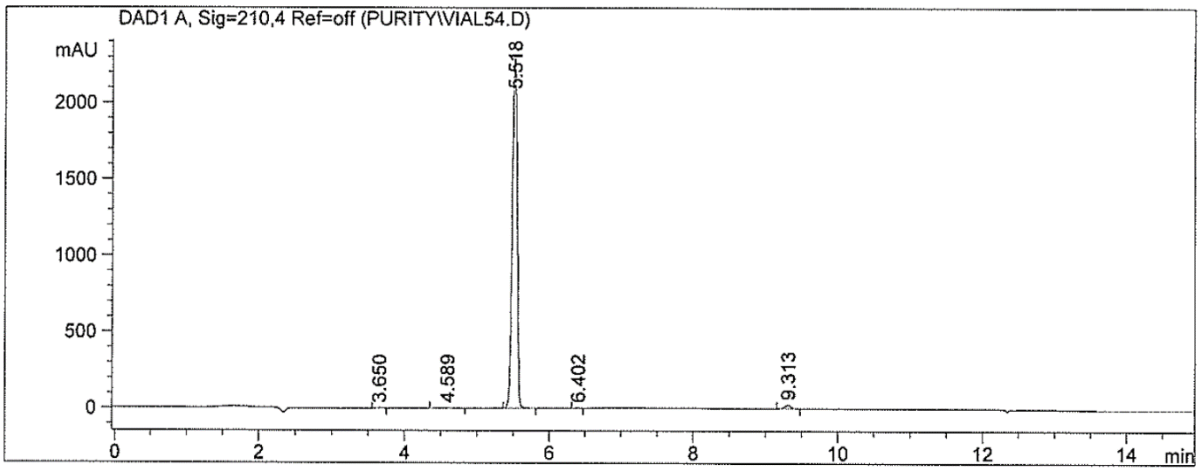

6-{[4-(Trifluoromethyl)benzyl]oxy}quinazoline-4(3*H*)-one (1h)

^{1}H NMR

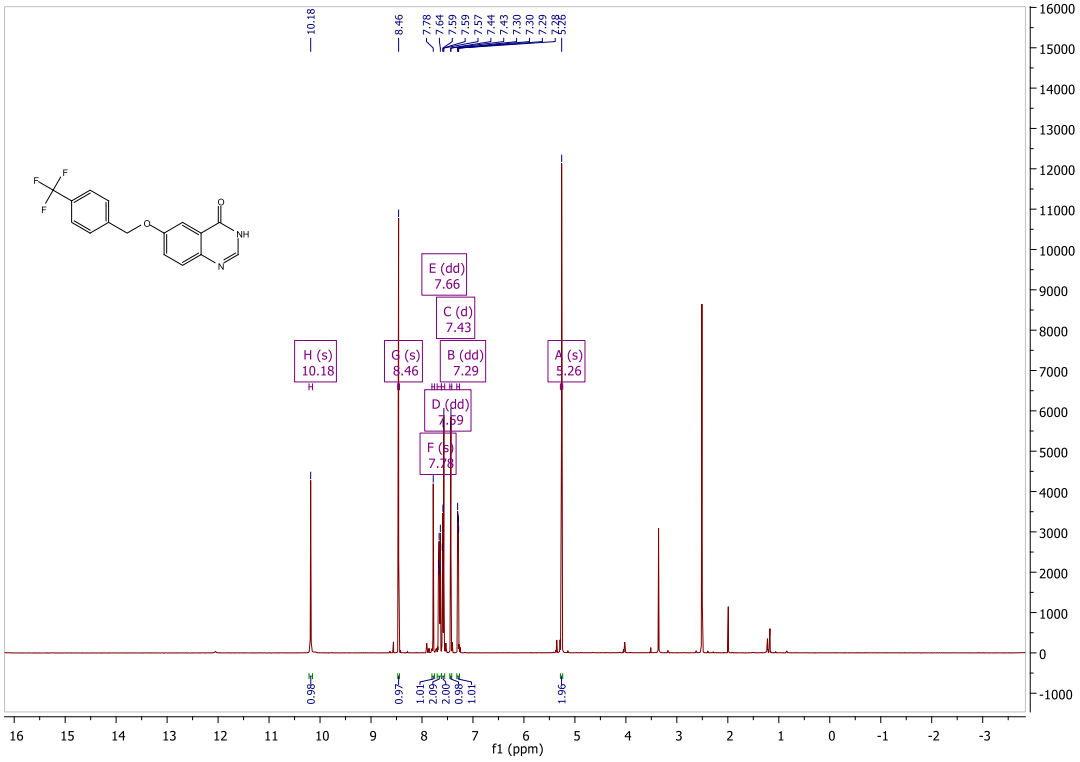

^{13}C NMR

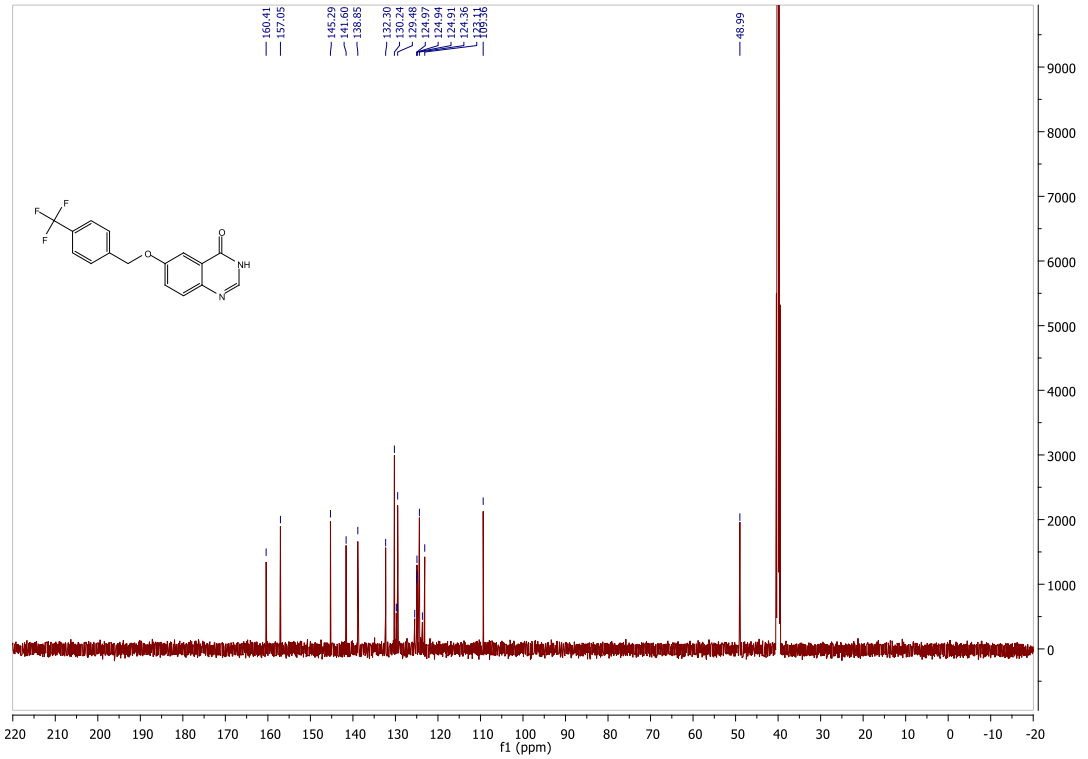

MS

Acquisition Parameter

Source Type	APCI	Ion Polarity	Positive	Set Nebulizer	1.6 Bar
Focus	Not active	Set Capillary	4500 V	Set Dry Heater	200 °C
Scan Begin	50 m/z	Set End Plate Offset	-500 V	Set Dry Gas	8.0 l/min
Scan End	1500 m/z	Set Collision Cell RF	100.0 Vpp	Set Divert Valve	Waste

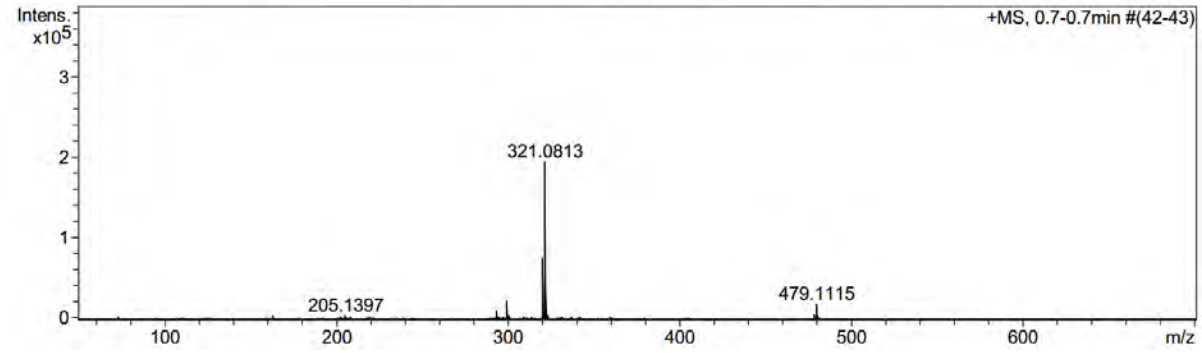

HPLC

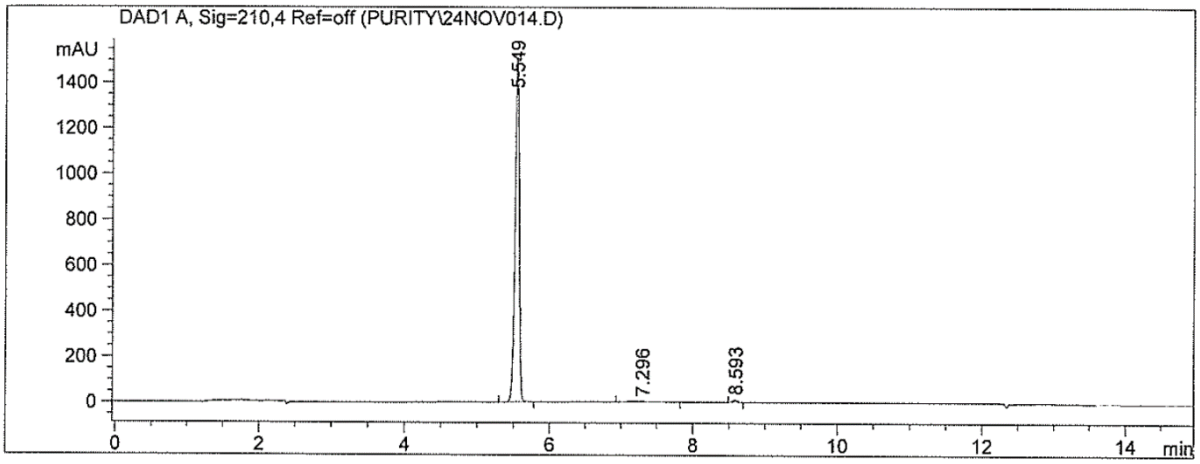

4-{[(4-Oxo-3,4-dihydroquinazolin-6-yl)oxy]methyl}benzonitrile (1i)

^{1}H NMR

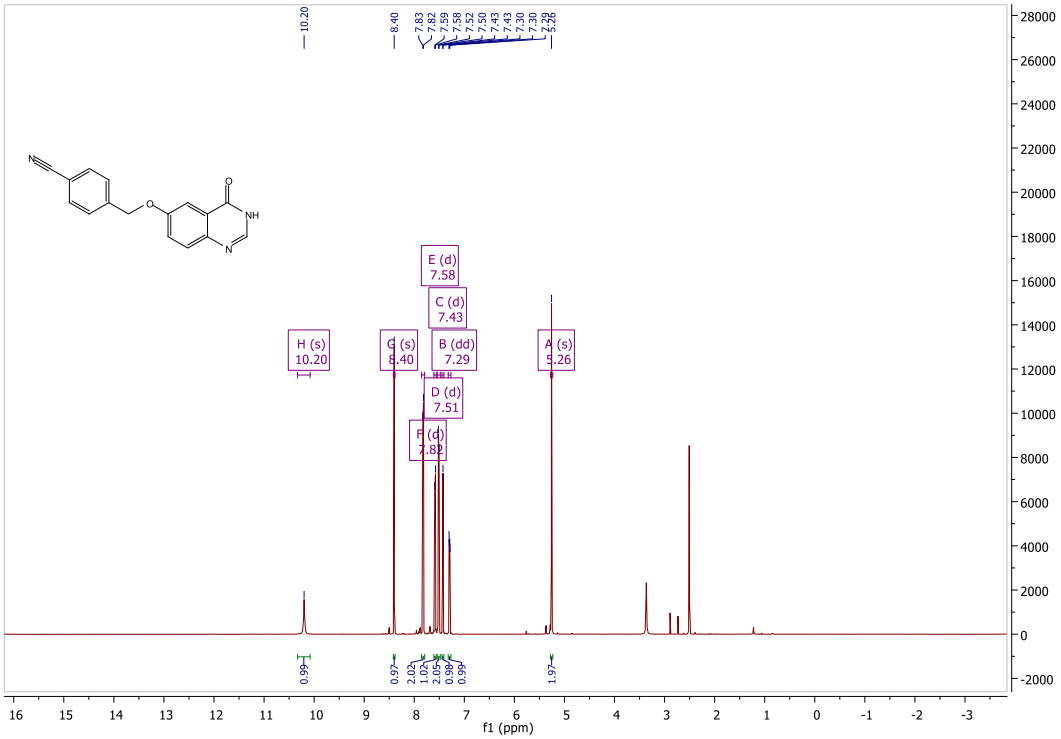

^{13}C NMR

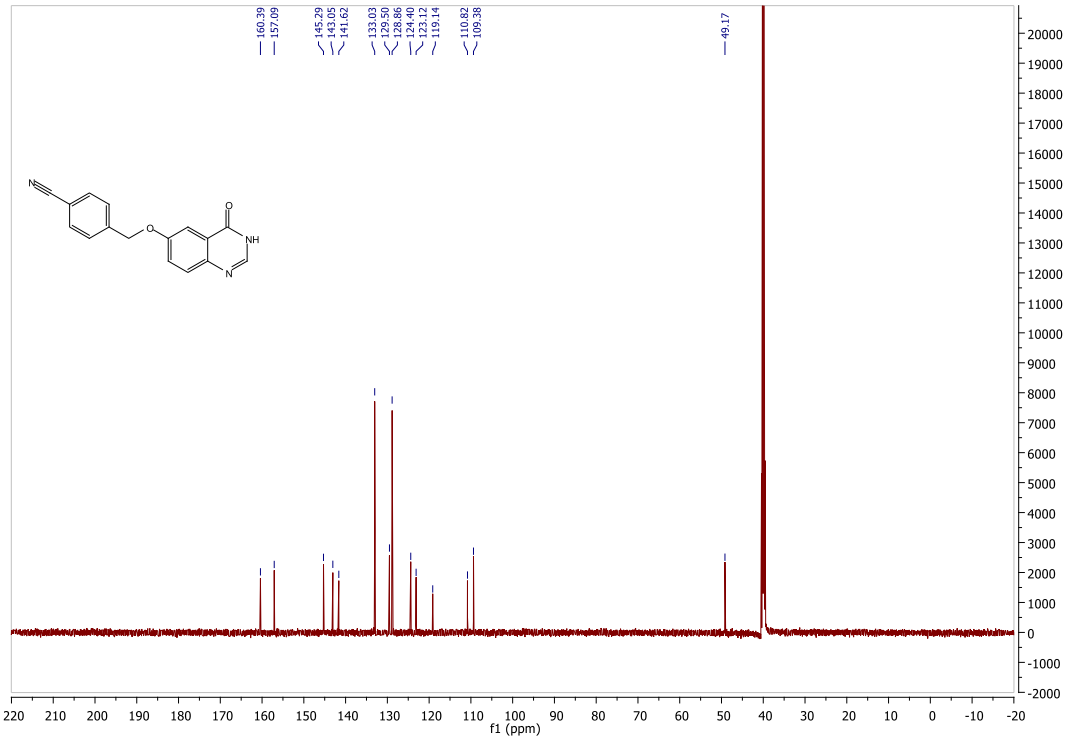

MS

Acquisition Parameter

Source Type	APCI	Ion Polarity	Positive	Set Nebulizer	1.6 Bar
Focus	Not active	Set Capillary	4500 V	Set Dry Heater	200 °C
Scan Begin	50 m/z	Set End Plate Offset	-500 V	Set Dry Gas	8.0 l/min
Scan End	1500 m/z	Set Collision Cell RF	100.0 Vpp	Set Divert Valve	Waste

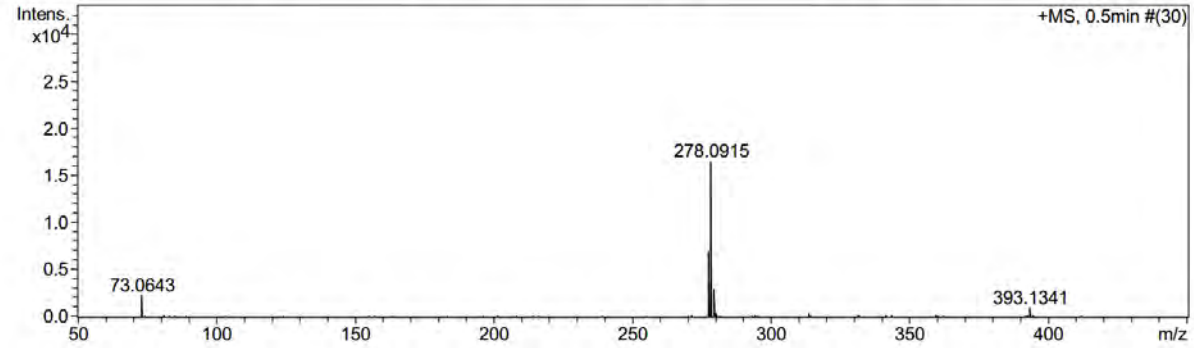

HPLC

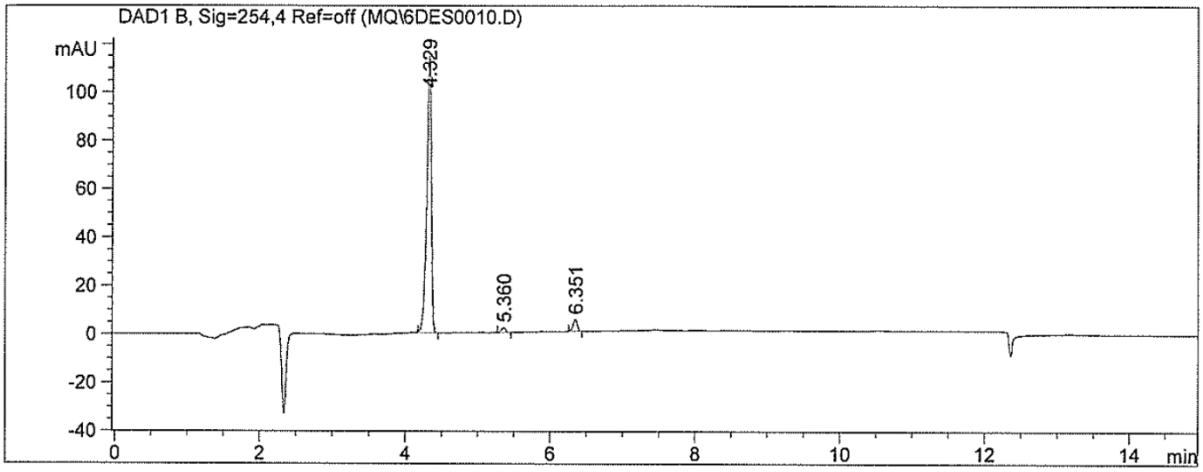

6-(Pyridin-4-ylmethoxy)quinazoline-4(3*H*)-one (1j)

^{1}H NMR

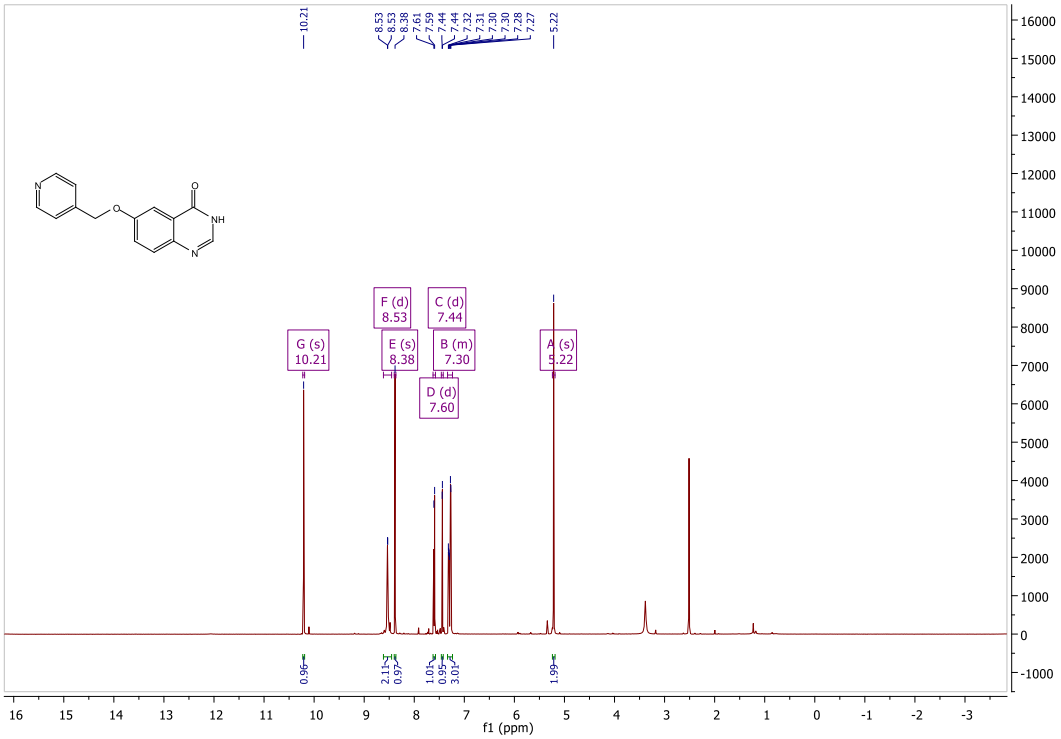

^{13}C NMR

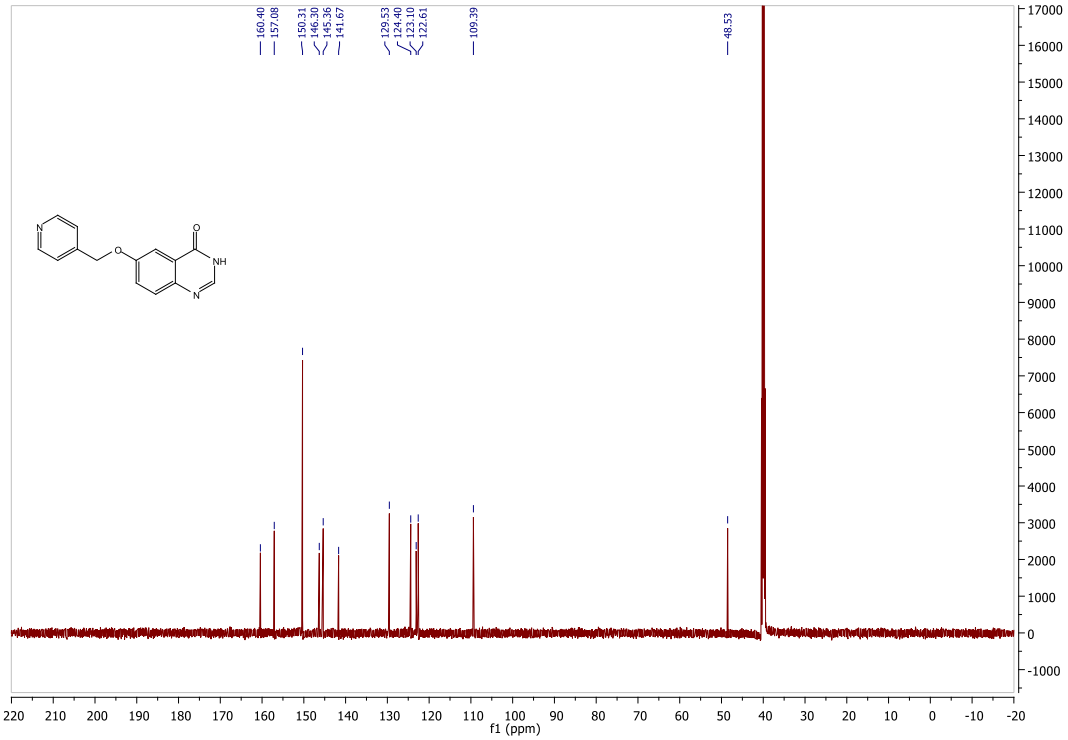

MS

Acquisition Parameter

Source Type	APCI	Ion Polarity	Positive	Set Nebulizer	1.6 Bar
Focus	Not active	Set Capillary	4500 V	Set Dry Heater	200 °C
Scan Begin	50 m/z	Set End Plate Offset	-500 V	Set Dry Gas	8.0 l/min
Scan End	1500 m/z	Set Collision Cell RF	100.0 Vpp	Set Divert Valve	Waste

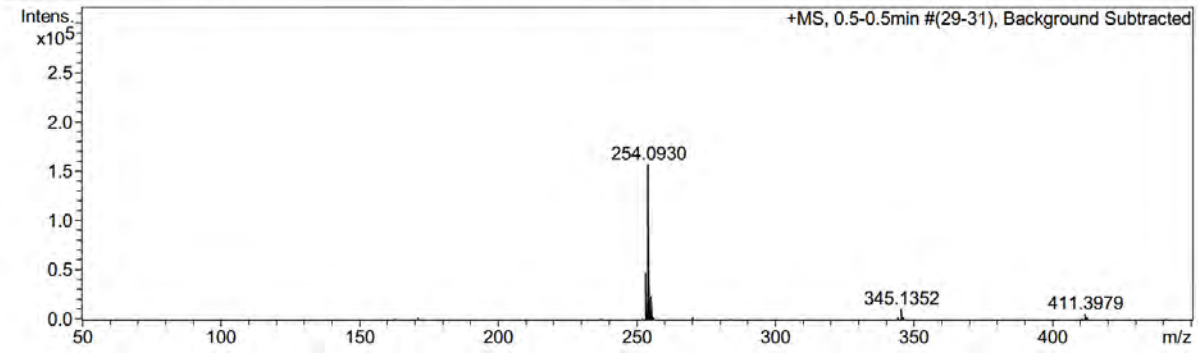

HPLC

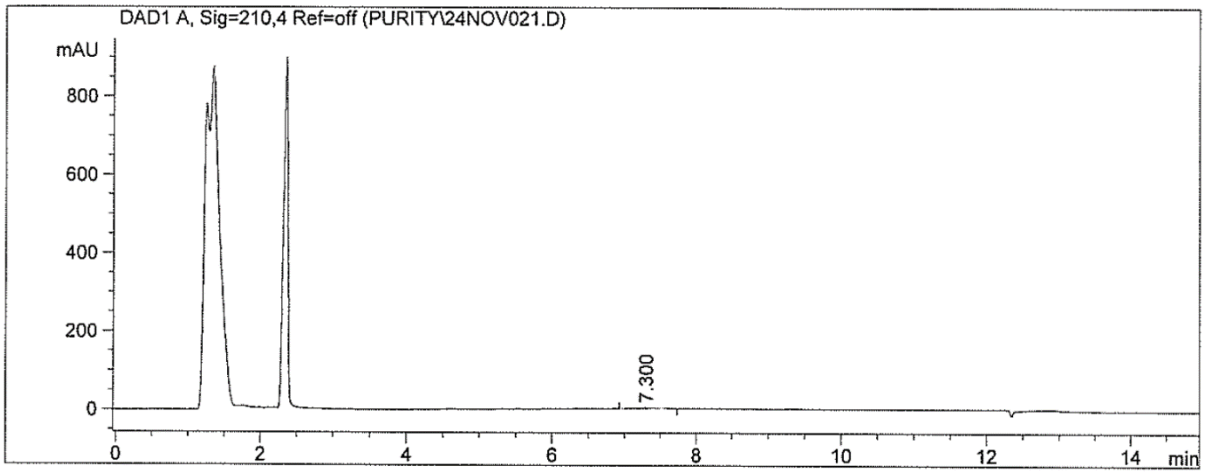

6-(2-Phenylethoxy)quinazoline-4(3*H*)-one (1k)

^{1}H NMR

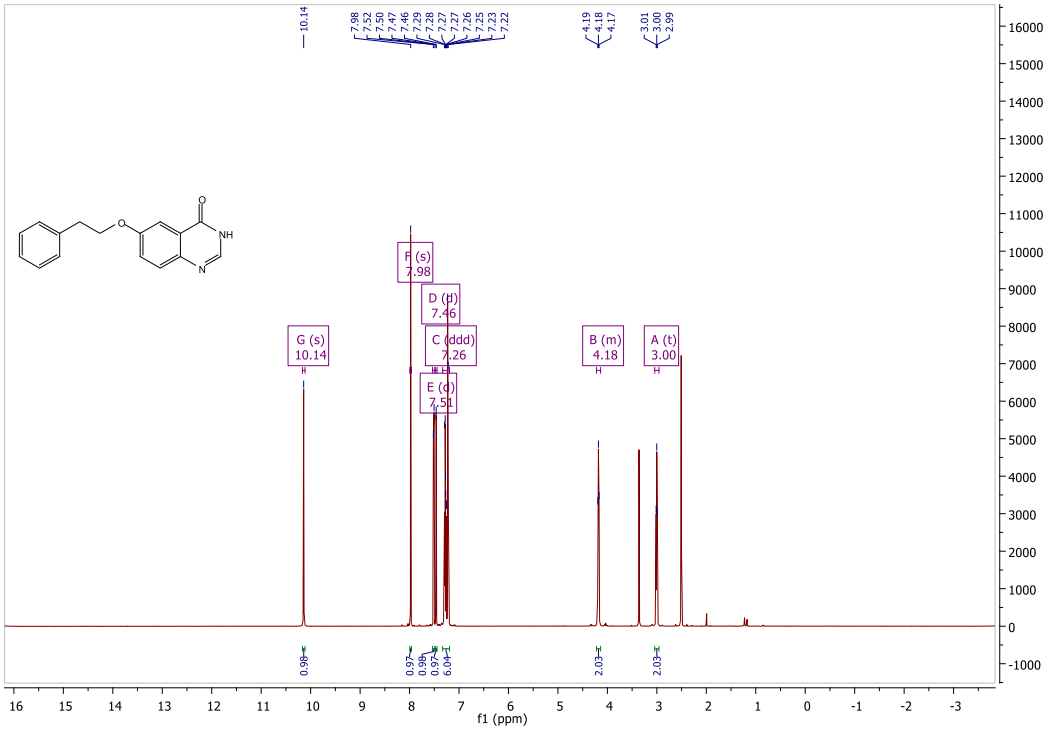

^{13}C NMR

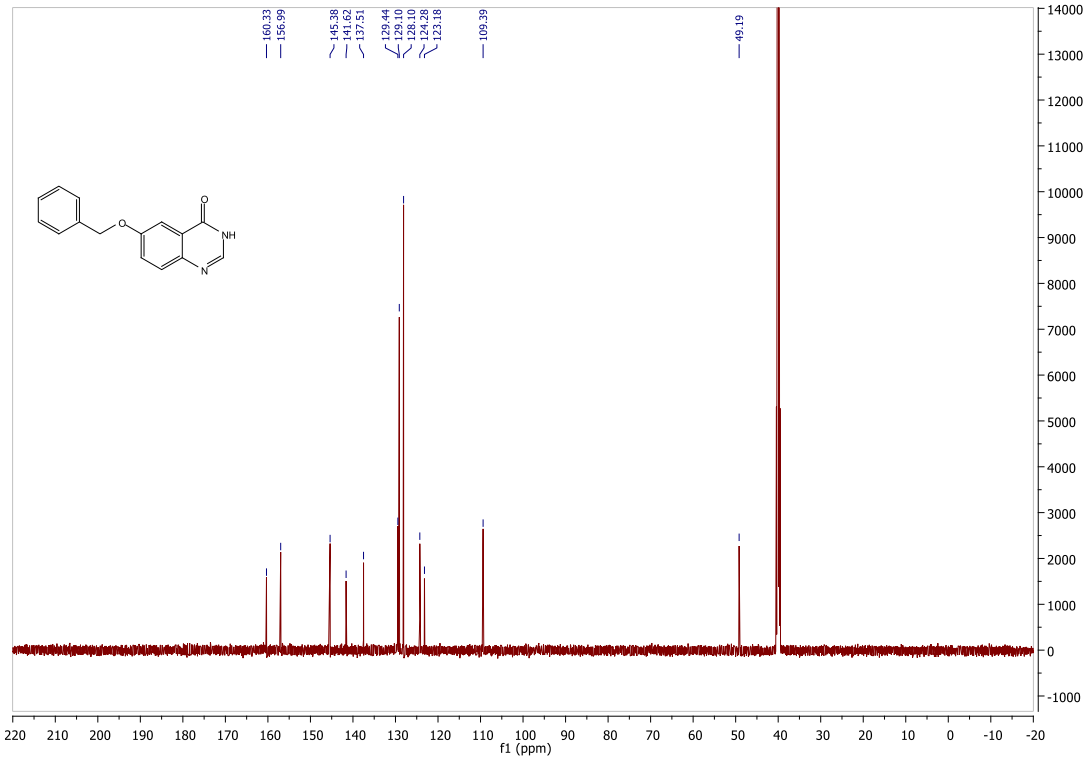

MS

Acquisition Parameter

Source Type	APCI	Ion Polarity	Positive	Set Nebulizer	1.6 Bar
Focus	Not active	Set Capillary	4500 V	Set Dry Heater	200 °C
Scan Begin	50 m/z	Set End Plate Offset	-500 V	Set Dry Gas	8.0 l/min
Scan End	1500 m/z	Set Collision Cell RF	100.0 Vpp	Set Divert Valve	Waste

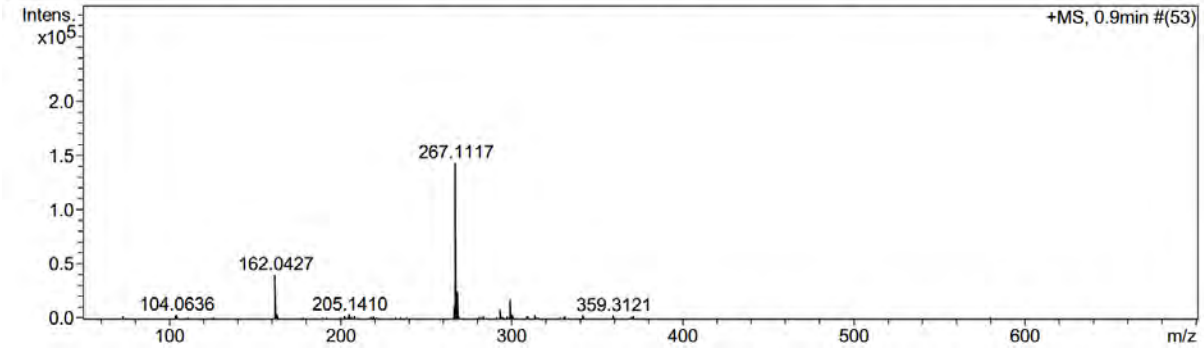

HPLC

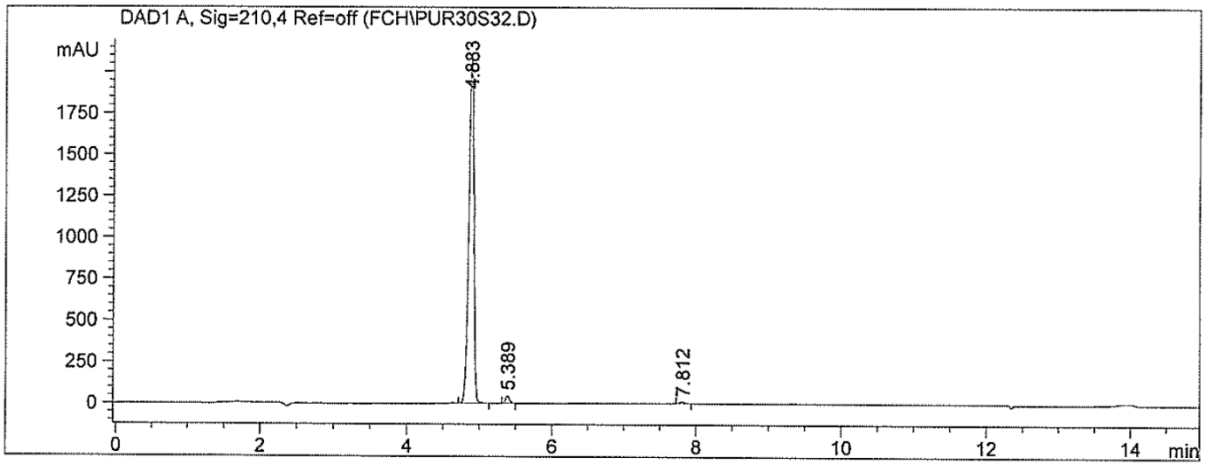

6-(2-Oxo-2-phenylethoxy)quinazoline-4(3*H*)-one (1l)

^{1}H NMR

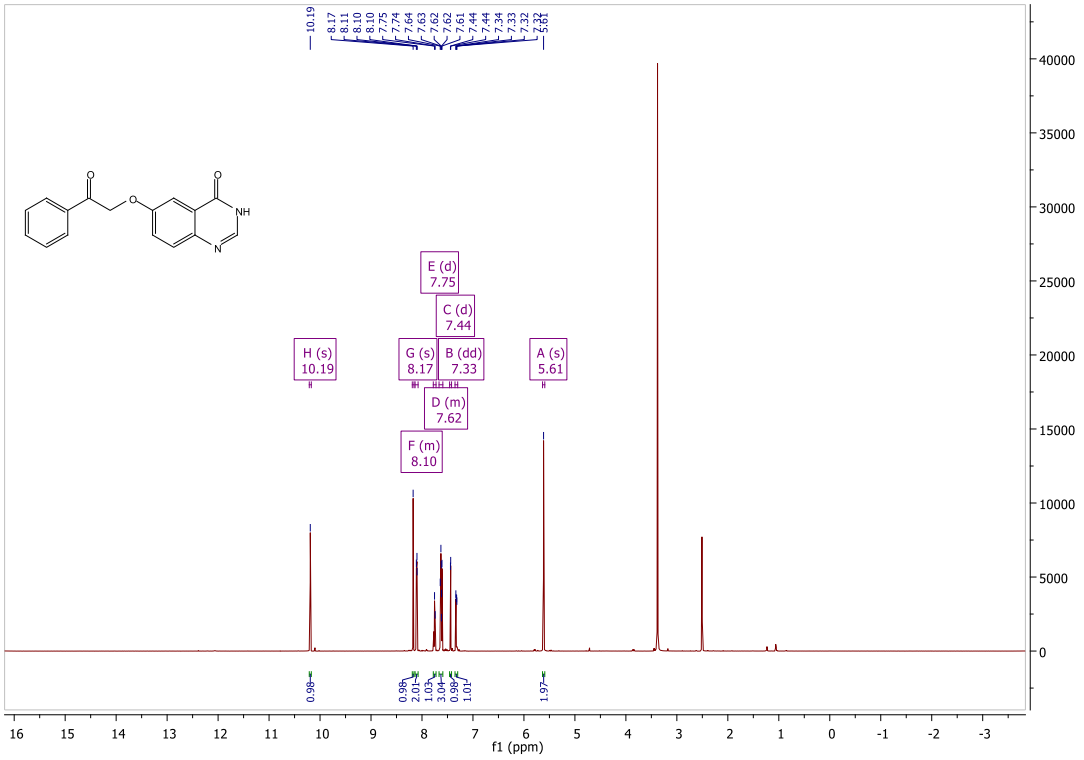

^{13}C NMR

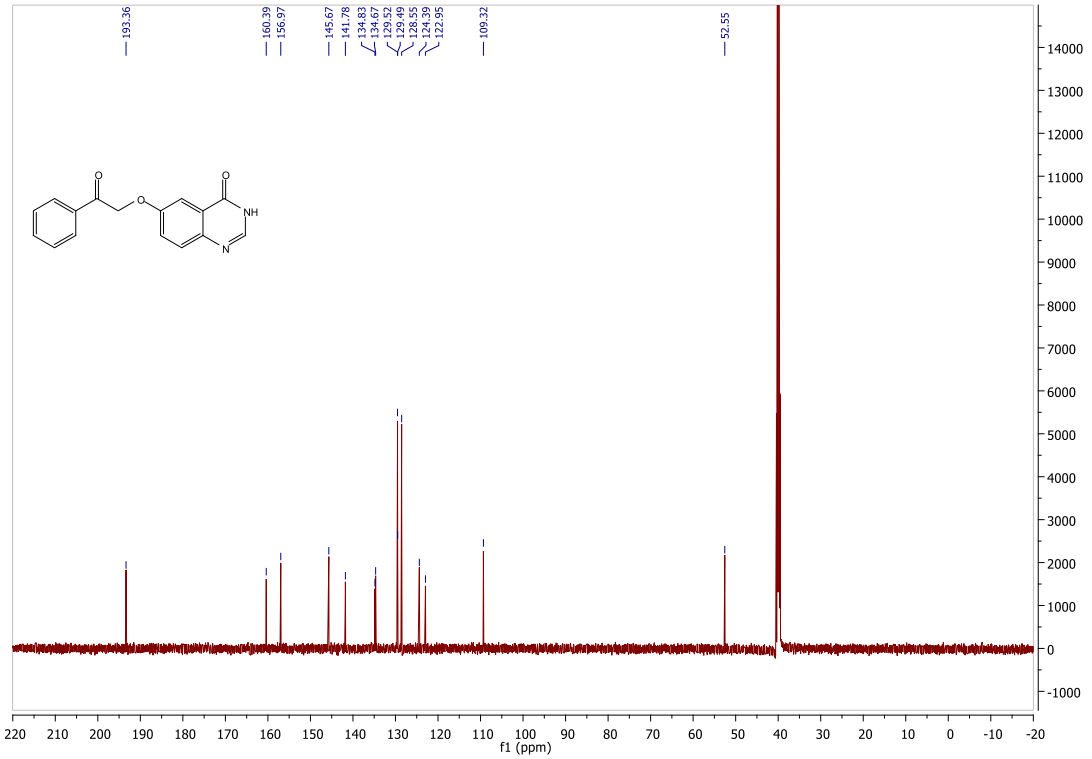

MS

Acquisition Parameter

Source Type	APCI	Ion Polarity	Positive	Set Nebulizer	1.6 Bar
Focus	Not active	Set Capillary	4500 V	Set Dry Heater	200 °C
Scan Begin	50 m/z	Set End Plate Offset	-500 V	Set Dry Gas	8.0 l/min
Scan End	1500 m/z	Set Collision Cell RF	100.0 Vpp	Set Divert Valve	Waste

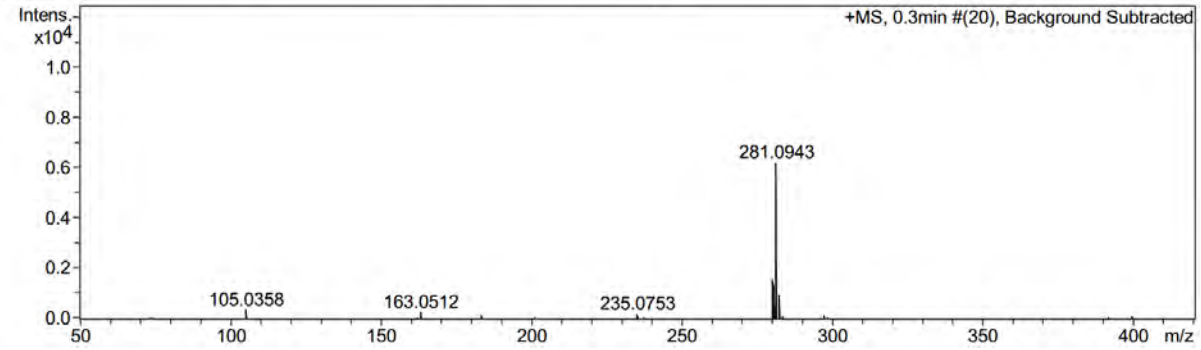

HPLC

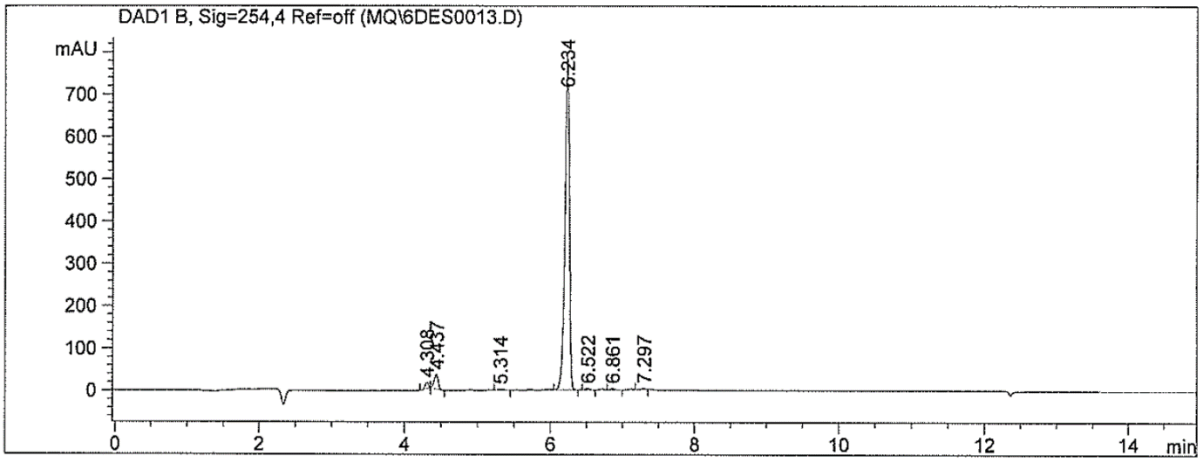

3-Benzyl-6-(benzyloxy)quinazolin-4(3*H*)-one (2a)

^{1}H NMR

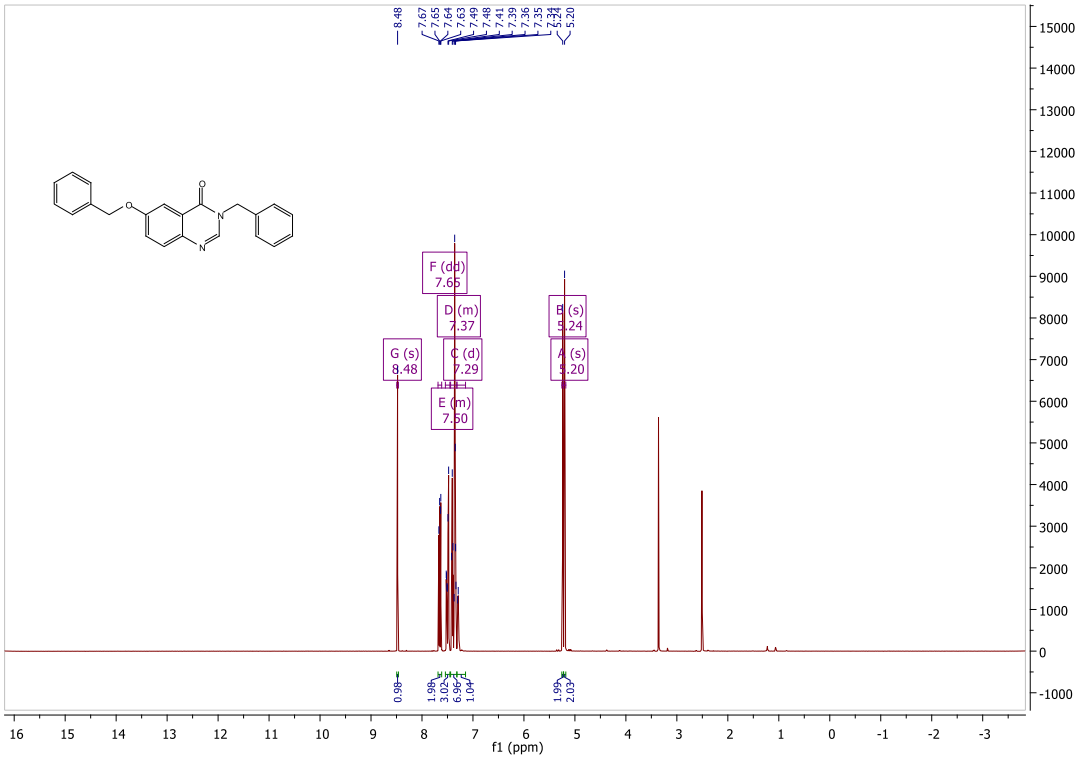

^{13}C NMR

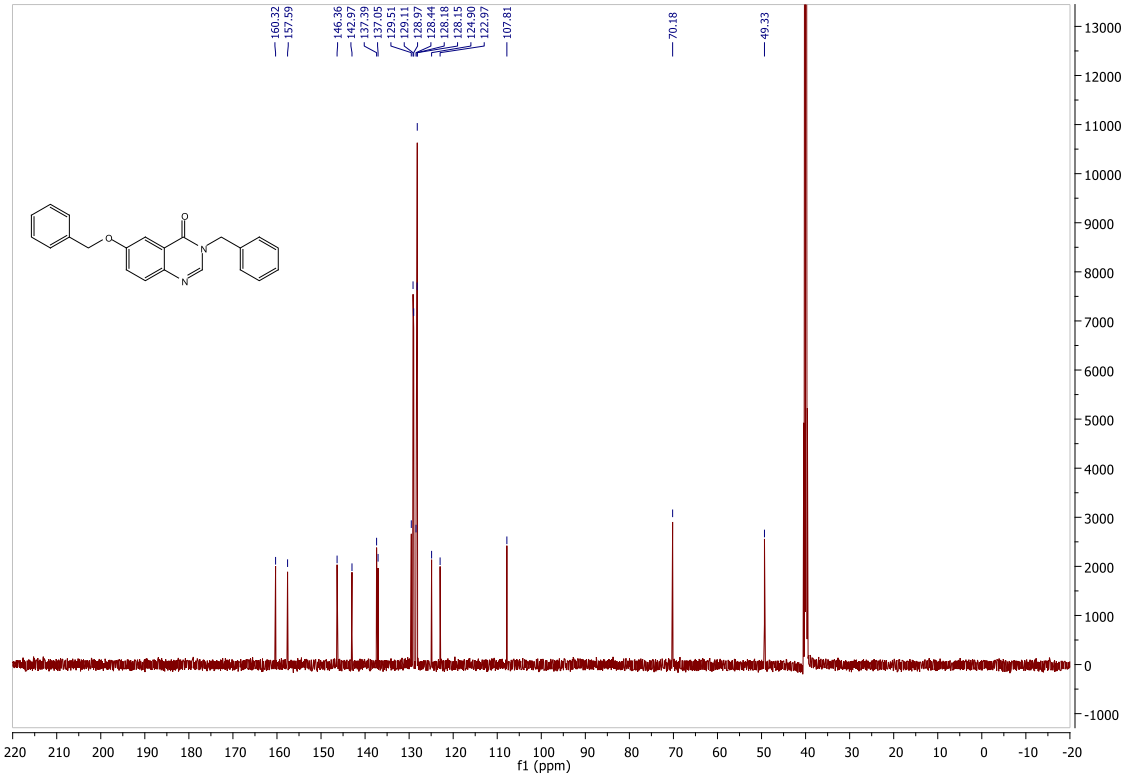

MS

Acquisition Parameter

Source Type	APCI	Ion Polarity	Positive	Set Nebulizer	1.6 Bar
Focus	Not active	Set Capillary	4500 V	Set Dry Heater	200 °C
Scan Begin	50 m/z	Set End Plate Offset	-500 V	Set Dry Gas	8.0 l/min
Scan End	1500 m/z	Set Collision Cell RF	100.0 Vpp	Set Divert Valve	Waste

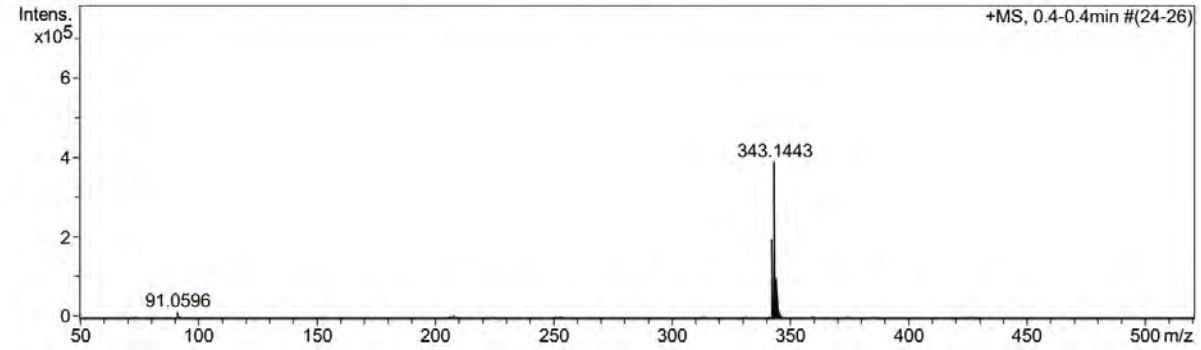

HPLC

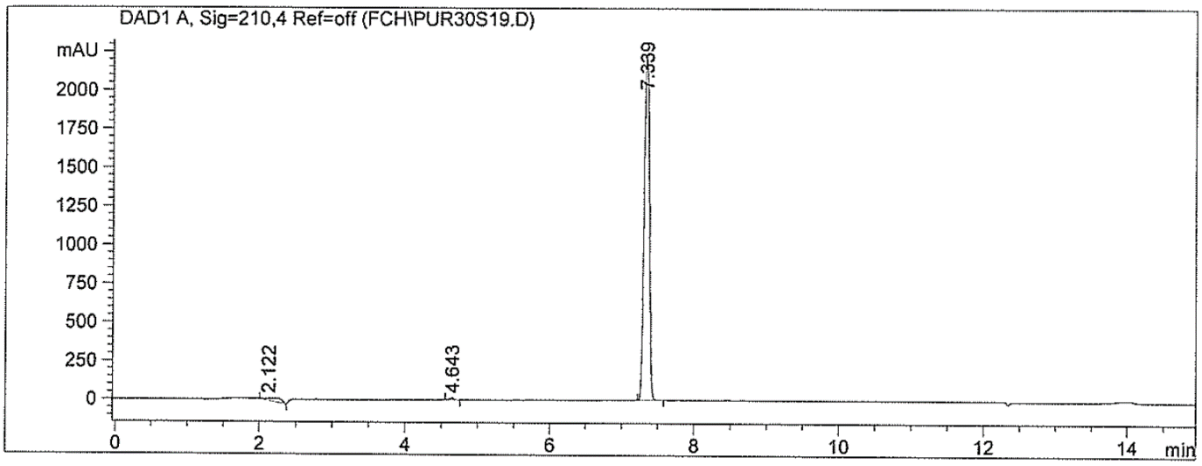

3-(4-Fluorobenzyl)-6-[(4-fluorobenzyl)oxy]quinazolin-4(3*H*)-one (2b)

^{1}H NMR

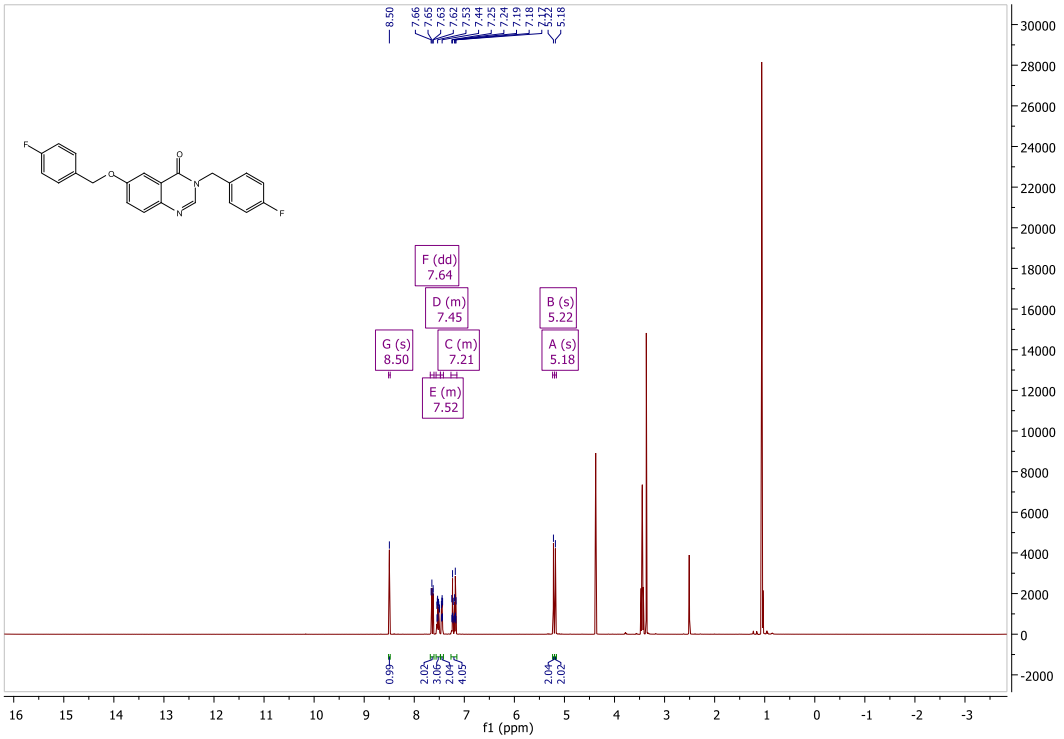

^{13}C NMR

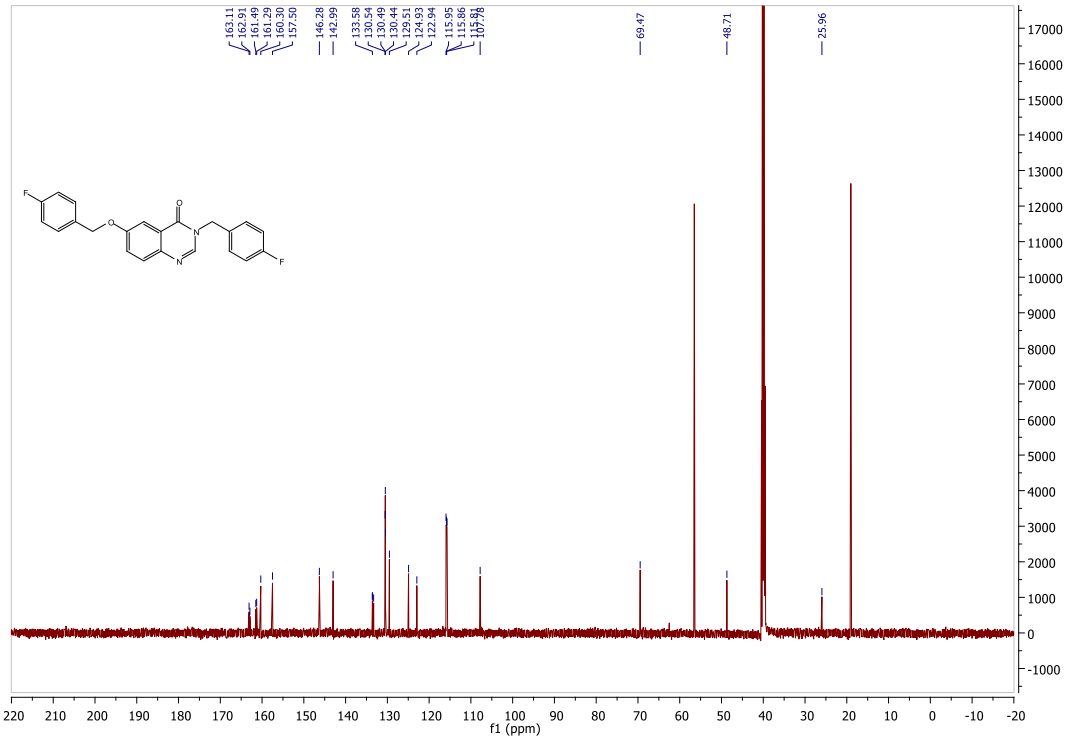

MS

Acquisition Parameter

Source Type	APCI	Ion Polarity	Positive	Set Nebulizer	1.6 Bar
Focus	Not active	Set Capillary	4500 V	Set Dry Heater	200 °C
Scan Begin	50 m/z	Set End Plate Offset	-500 V	Set Dry Gas	8.0 l/min
Scan End	1500 m/z	Set Collision Cell RF	100.0 Vpp	Set Divert Valve	Waste

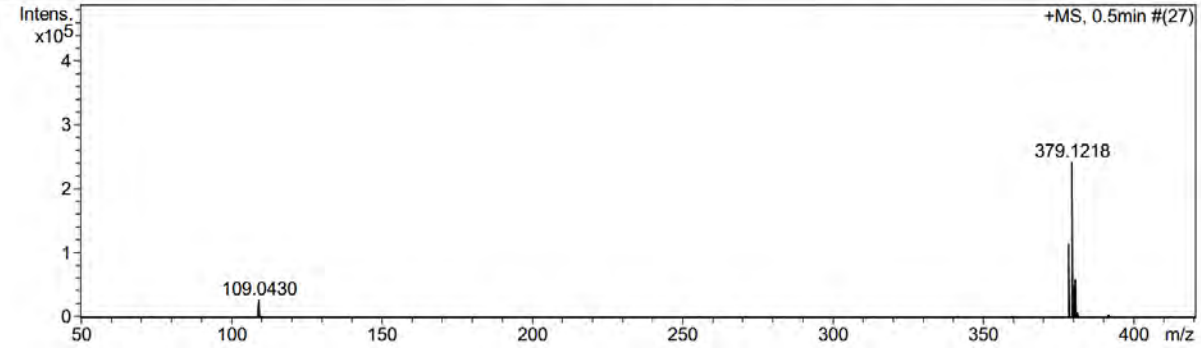

HPLC

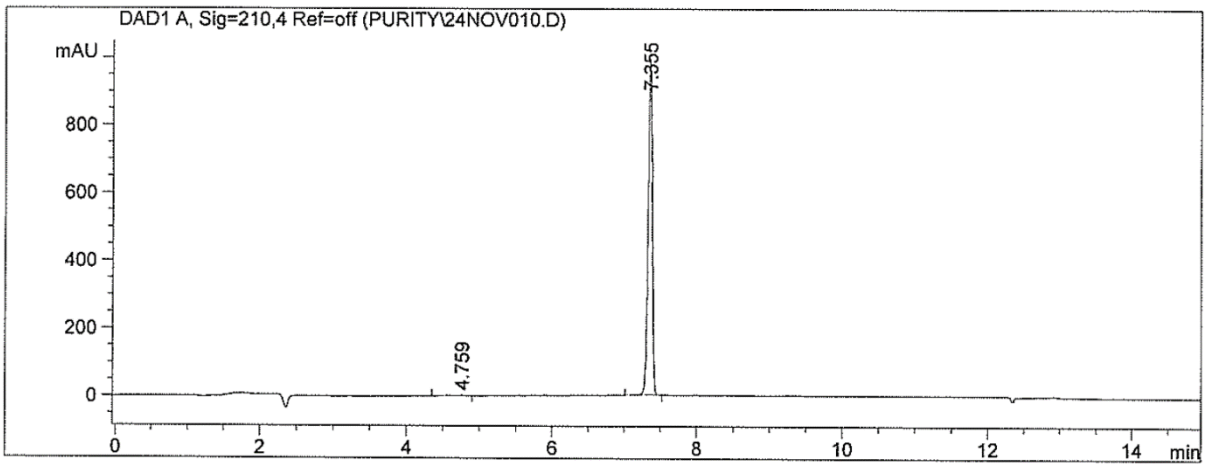

3-(4-Chlorobenzyl)-6-[(4-chlorobenzyl)oxy]quinazoline-4(3*H*)-one (2c)

^{1}H NMR

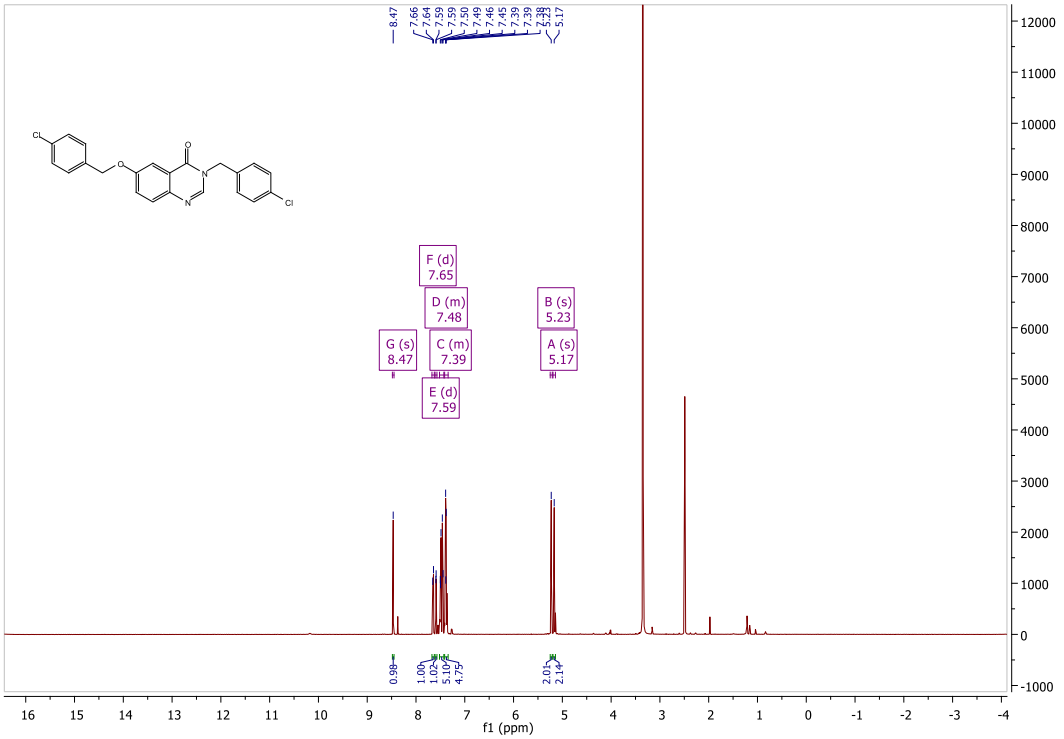

^{13}C NMR

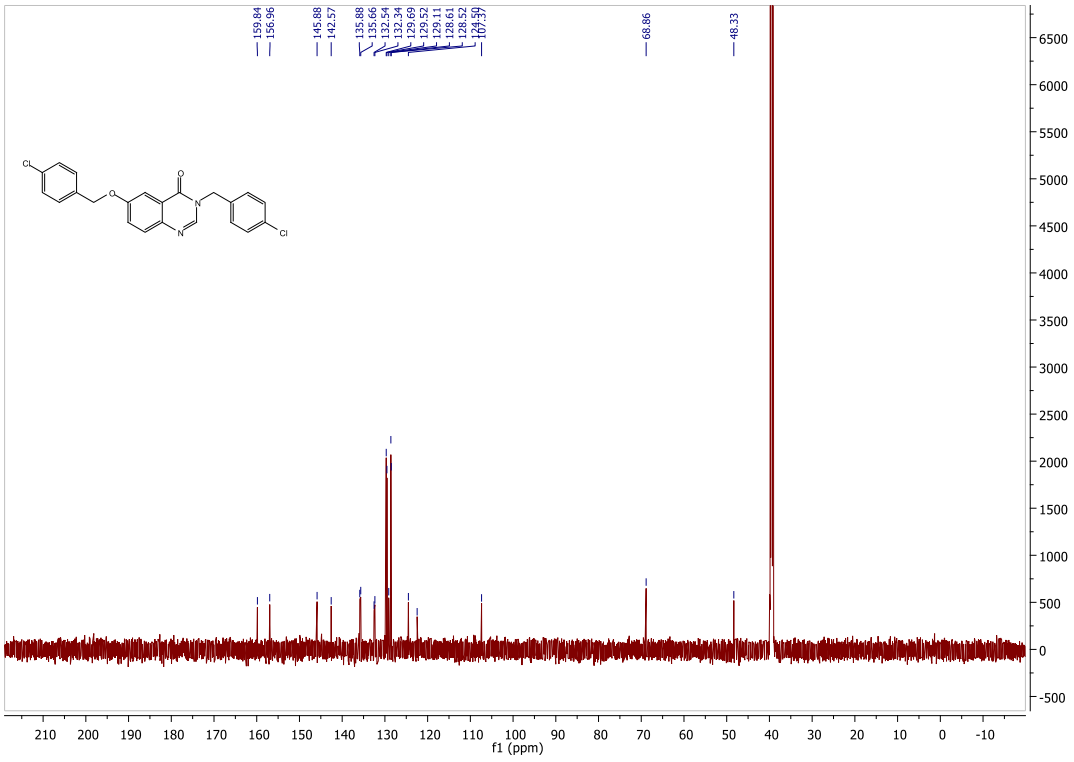

MS

Acquisition Parameter

Source Type	APCI	Ion Polarity	Positive	Set Nebulizer	1.6 Bar
Focus	Not active	Set Capillary	4500 V	Set Dry Heater	200 °C
Scan Begin	50 m/z	Set End Plate Offset	-500 V	Set Dry Gas	8.0 l/min
Scan End	1500 m/z	Set Collision Cell RF	100.0 Vpp	Set Divert Valve	Waste

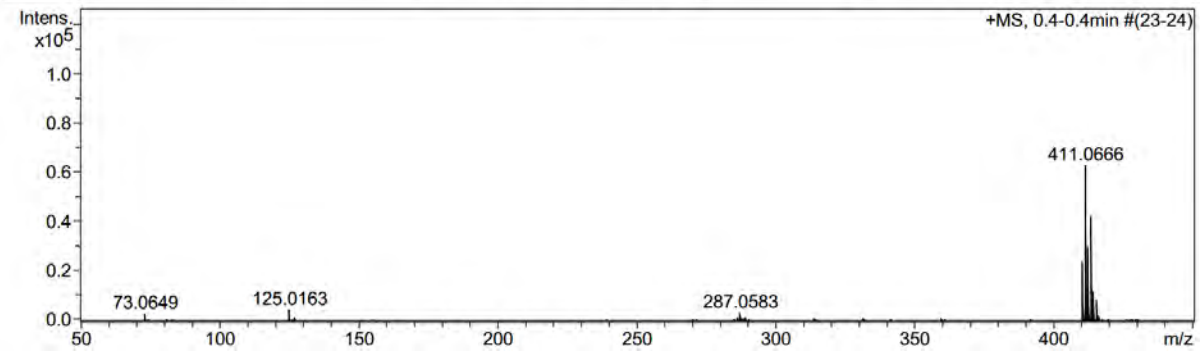

HPLC

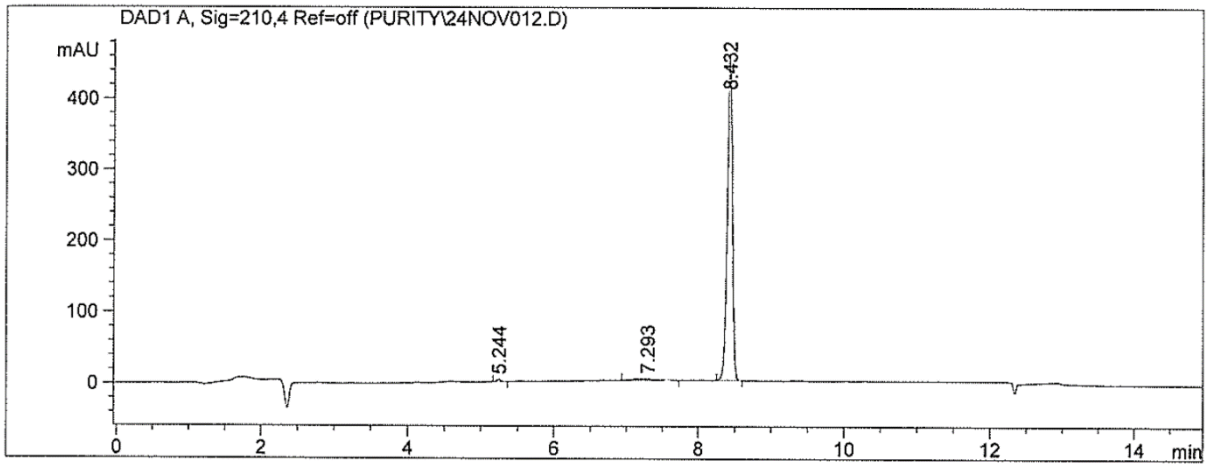

3-(3-Bromobenzyl)-6-[(3-bromobenzyl)oxy]quinazoline-4(3*H*)-one (2d)

^{1}H NMR

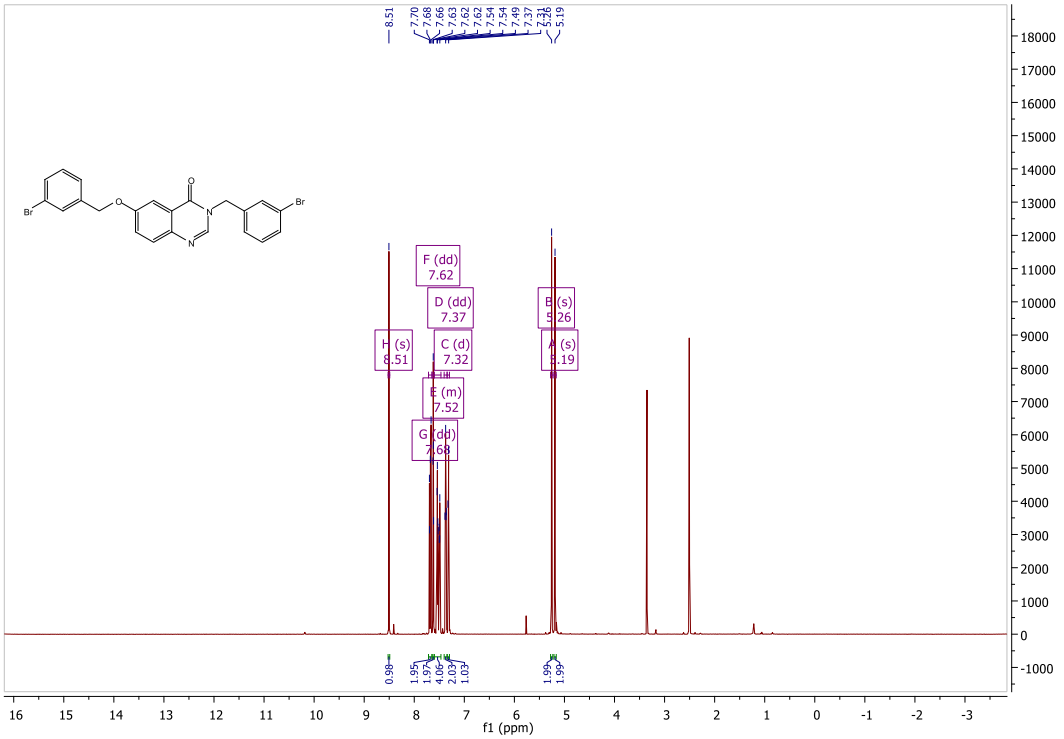

^{13}C NMR

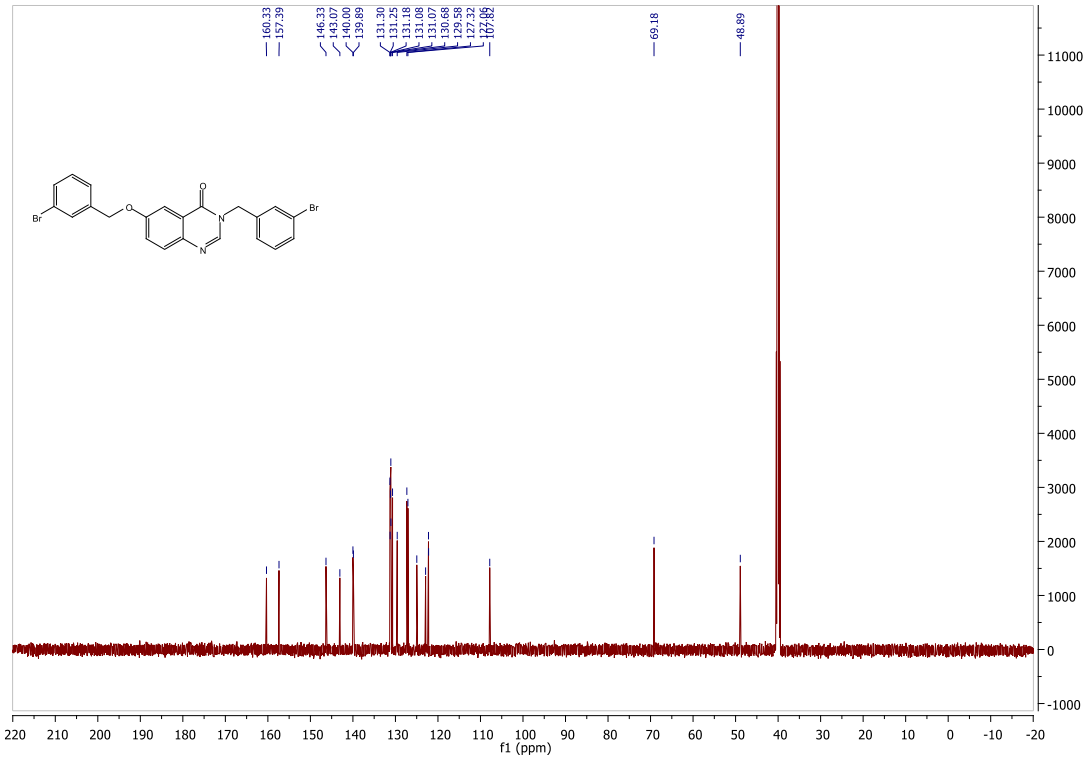

MS

Acquisition Parameter

Source Type	APCI	Ion Polarity	Positive	Set Nebulizer	1.6 Bar
Focus	Not active	Set Capillary	4500 V	Set Dry Heater	200 °C
Scan Begin	50 m/z	Set End Plate Offset	-500 V	Set Dry Gas	8.0 l/min
Scan End	1500 m/z	Set Collision Cell RF	100.0 Vpp	Set Divert Valve	Waste

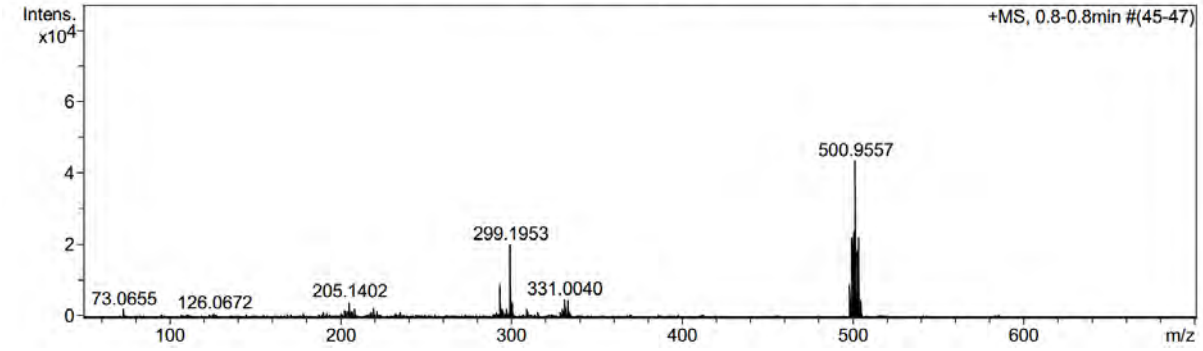

HPLC

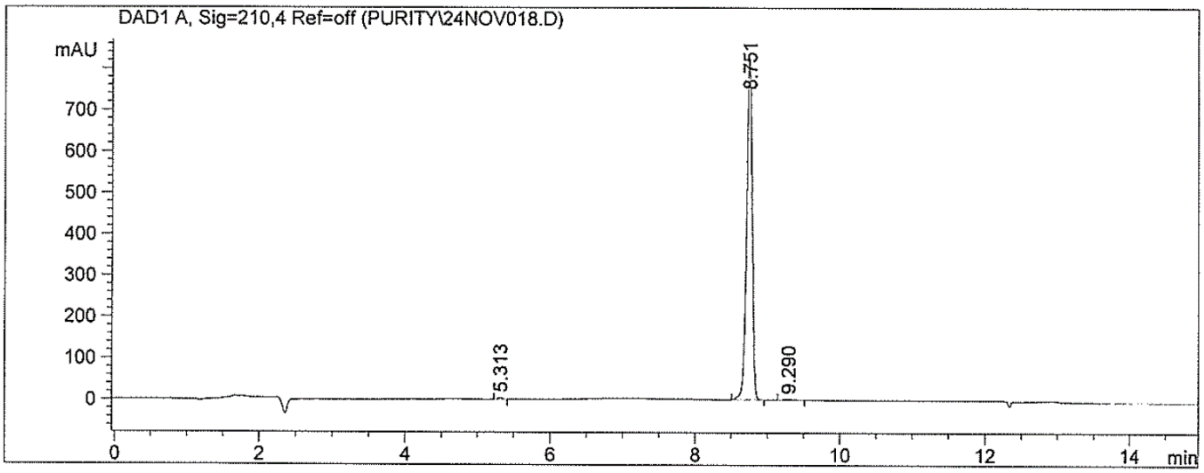

3-(4-Bromobenzyl)-6-[(4-bromobenzyl)oxy]quinazoline-4(3*H*)-one (2e)

^{1}H NMR

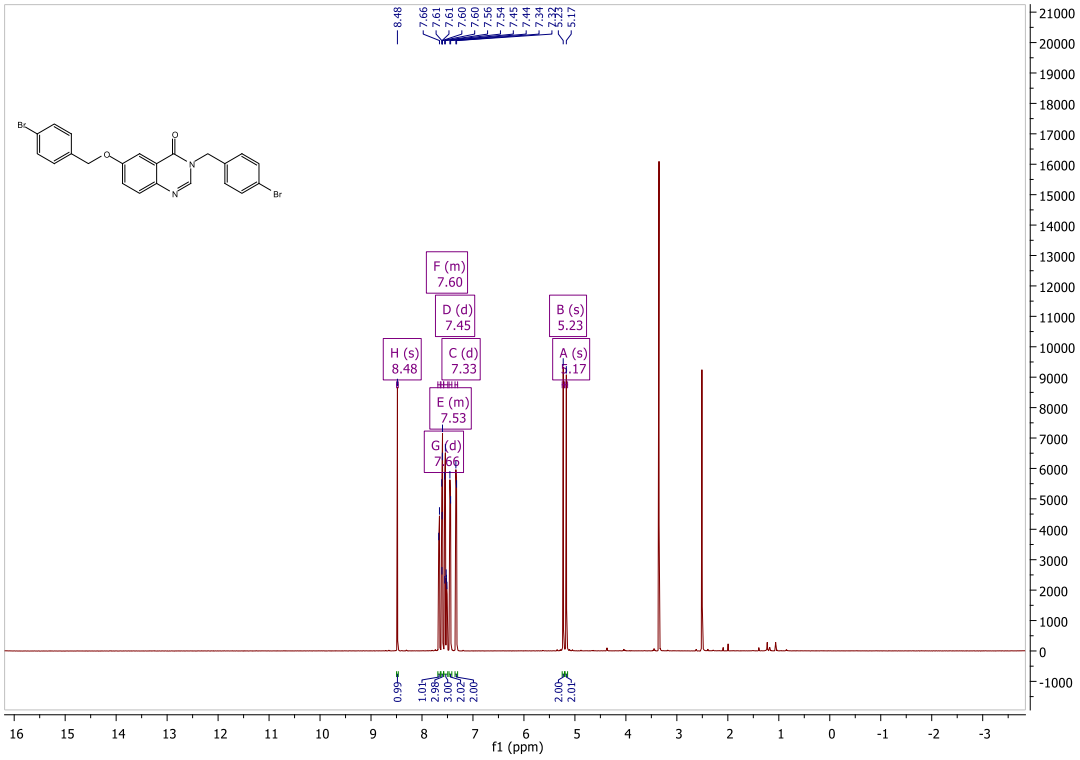

^{13}C NMR

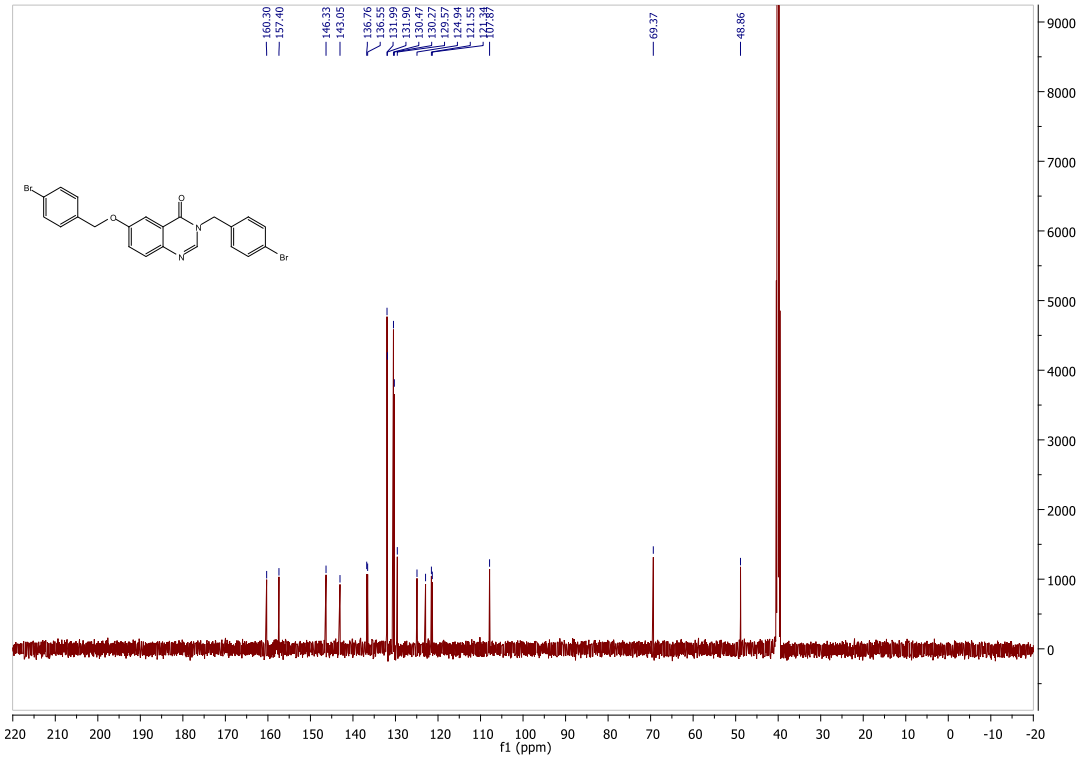

MS

Acquisition Parameter

Source Type	APCI	Ion Polarity	Positive	Set Nebulizer	1.6 Bar
Focus	Not active	Set Capillary	4500 V	Set Dry Heater	200 °C
Scan Begin	50 m/z	Set End Plate Offset	-500 V	Set Dry Gas	8.0 l/min
Scan End	1500 m/z	Set Collision Cell RF	100.0 Vpp	Set Divert Valve	Waste

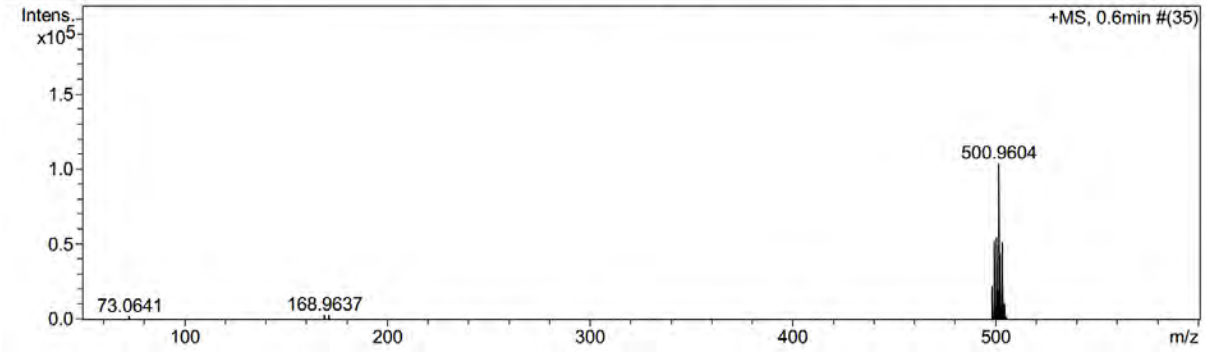

HPLC

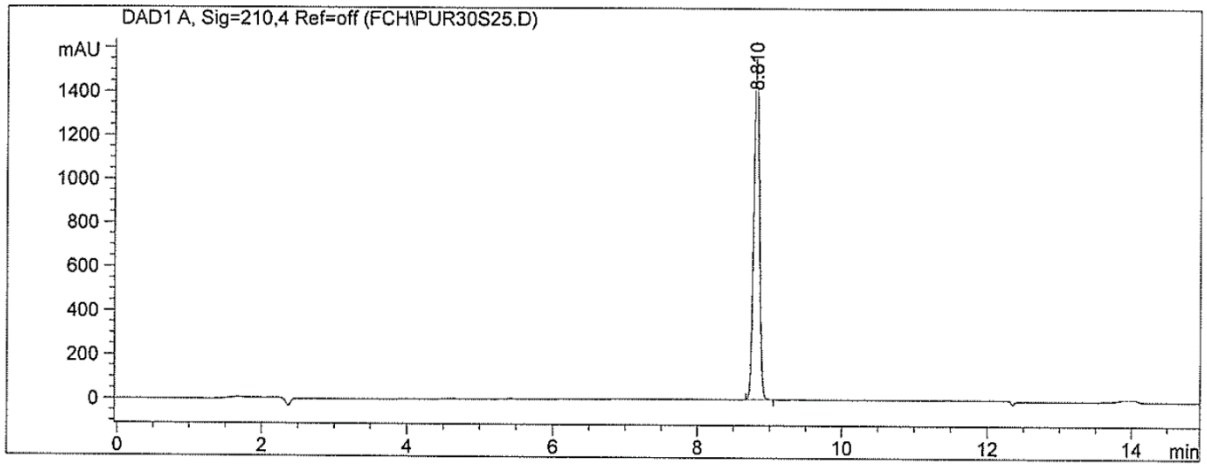

3-(3-Iodobenzyl)-6-[(3-iodobenzyl)oxy]quinazoline-4(3*H*)-one (2f)

^{1}H NMR

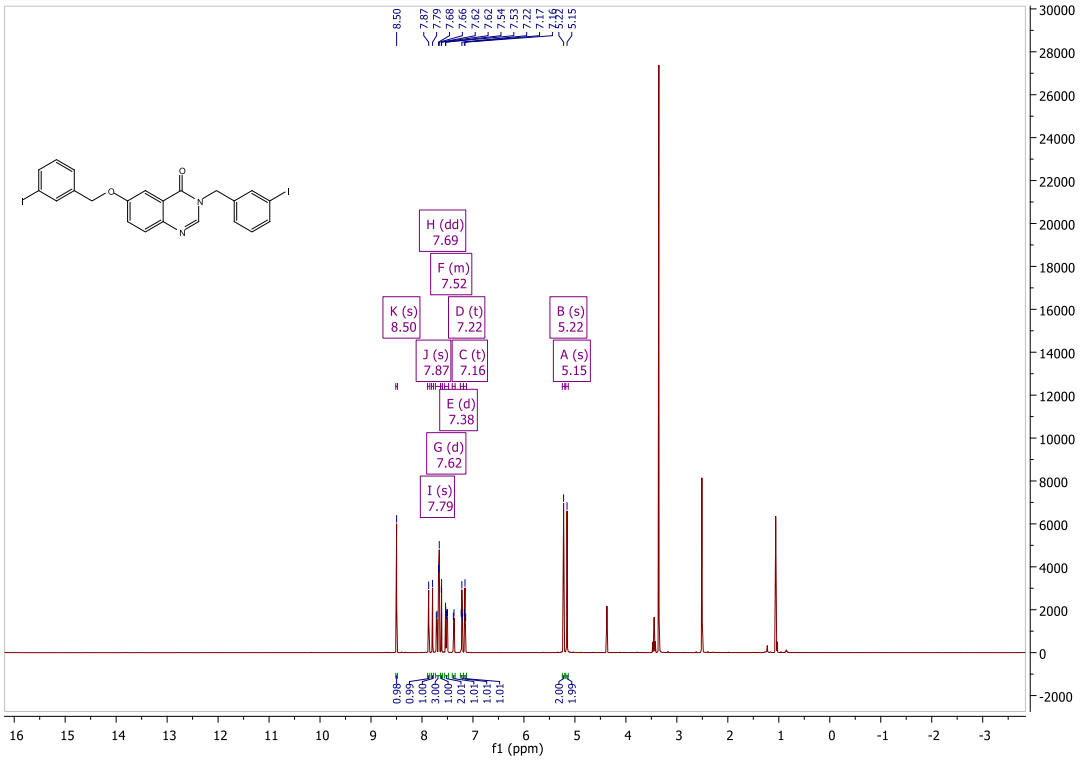

^{13}C NMR

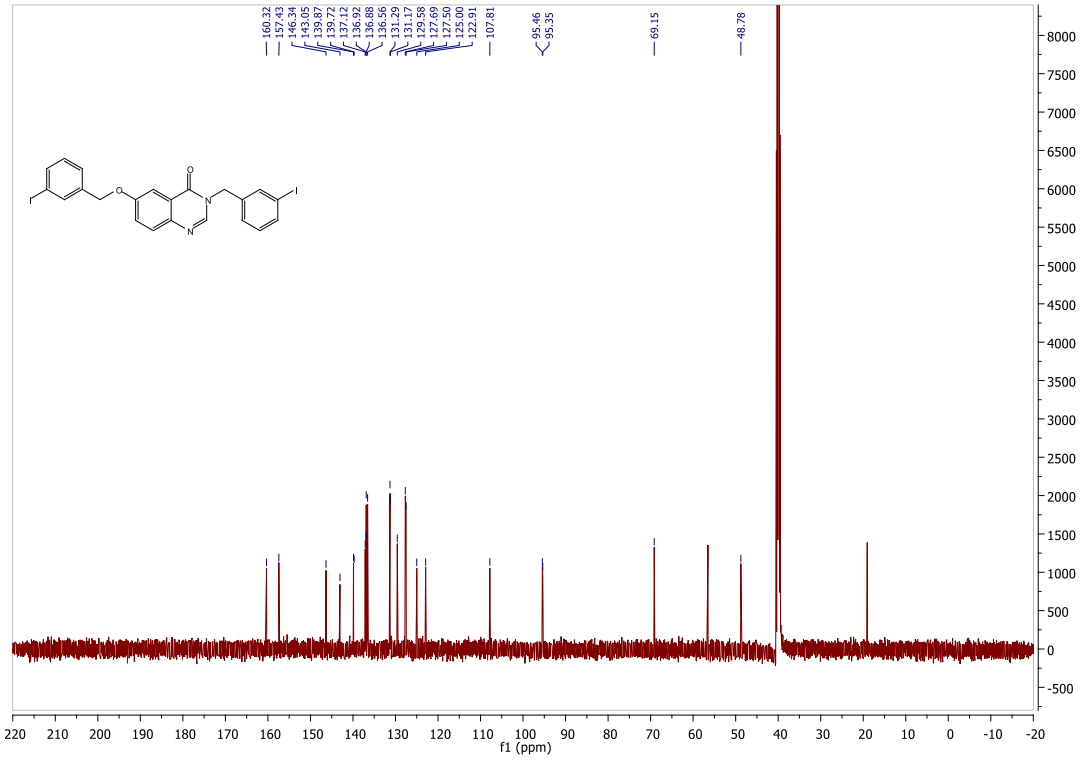

MS

Acquisition Parameter

Source Type	APCI	Ion Polarity	Positive	Set Nebulizer	1.6 Bar
Focus	Not active	Set Capillary	4500 V	Set Dry Heater	200 °C
Scan Begin	50 m/z	Set End Plate Offset	-500 V	Set Dry Gas	8.0 l/min
Scan End	1500 m/z	Set Collision Cell RF	100.0 Vpp	Set Divert Valve	Waste

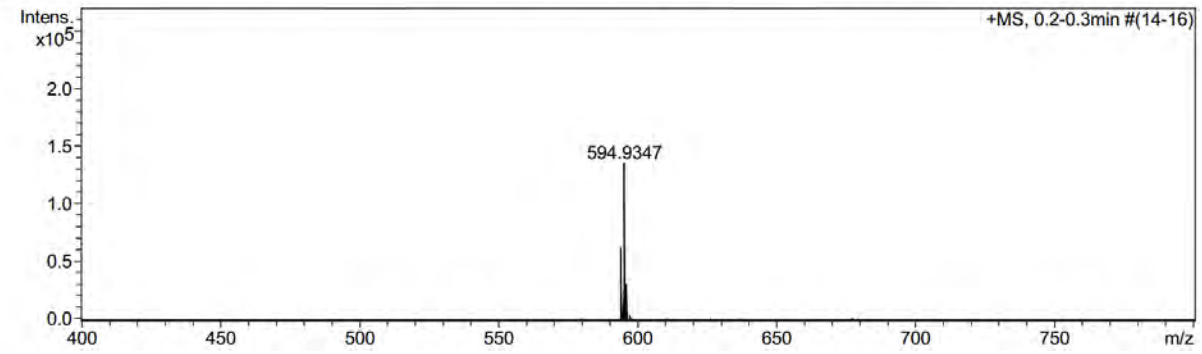

HPLC

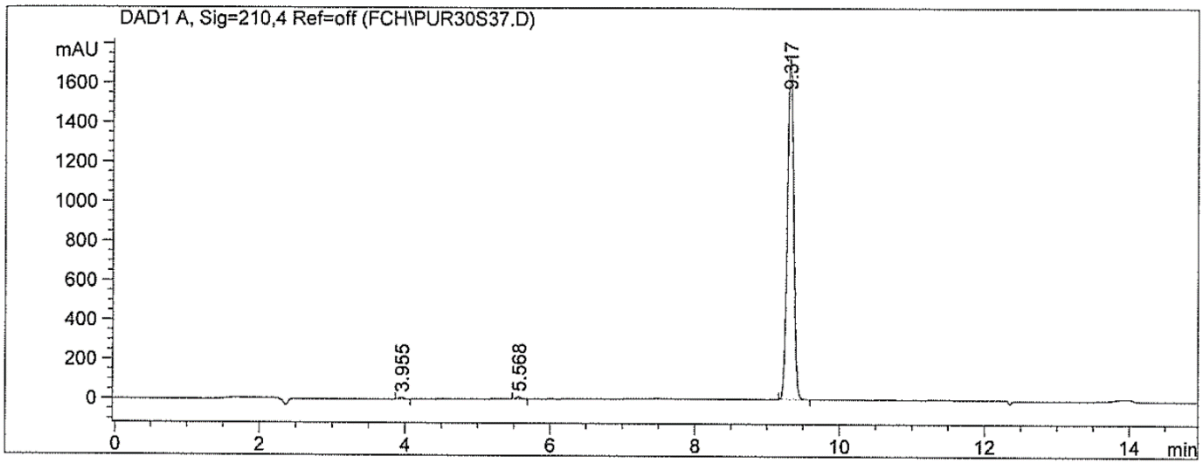

3-(4-Iodobenzyl)-6-[(4-iodobenzyl)oxy]quinazoline-4(3*H*)-one (2g)

^{1}H NMR

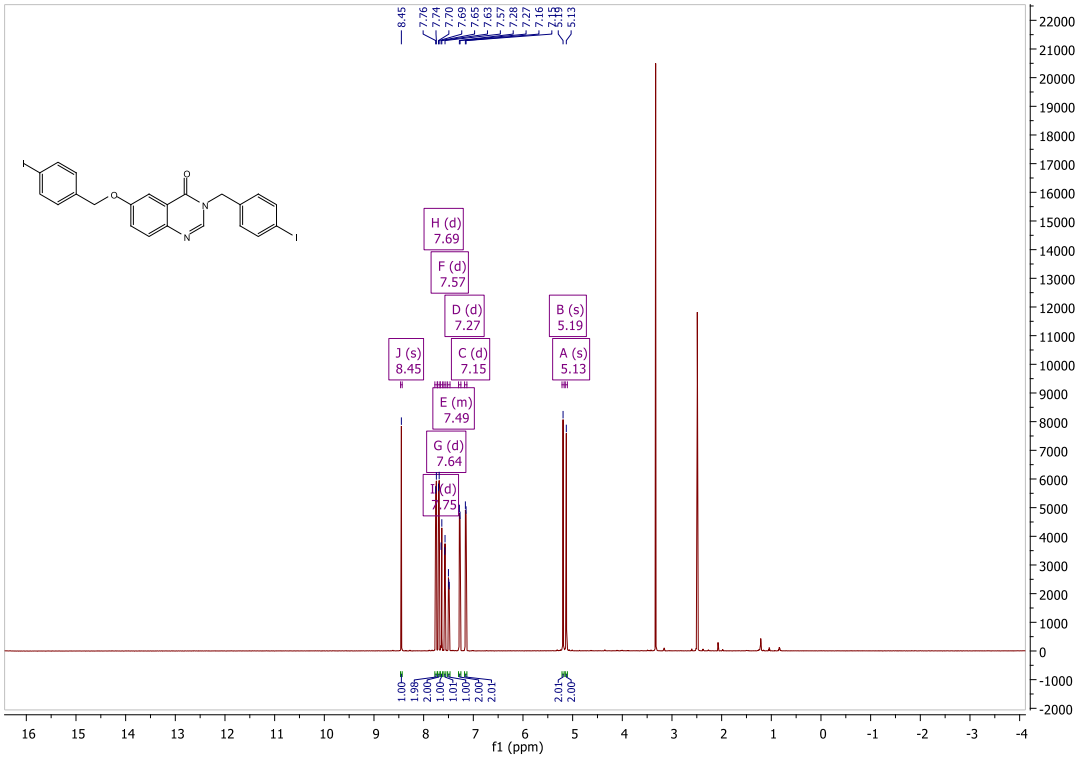

^{13}C NMR

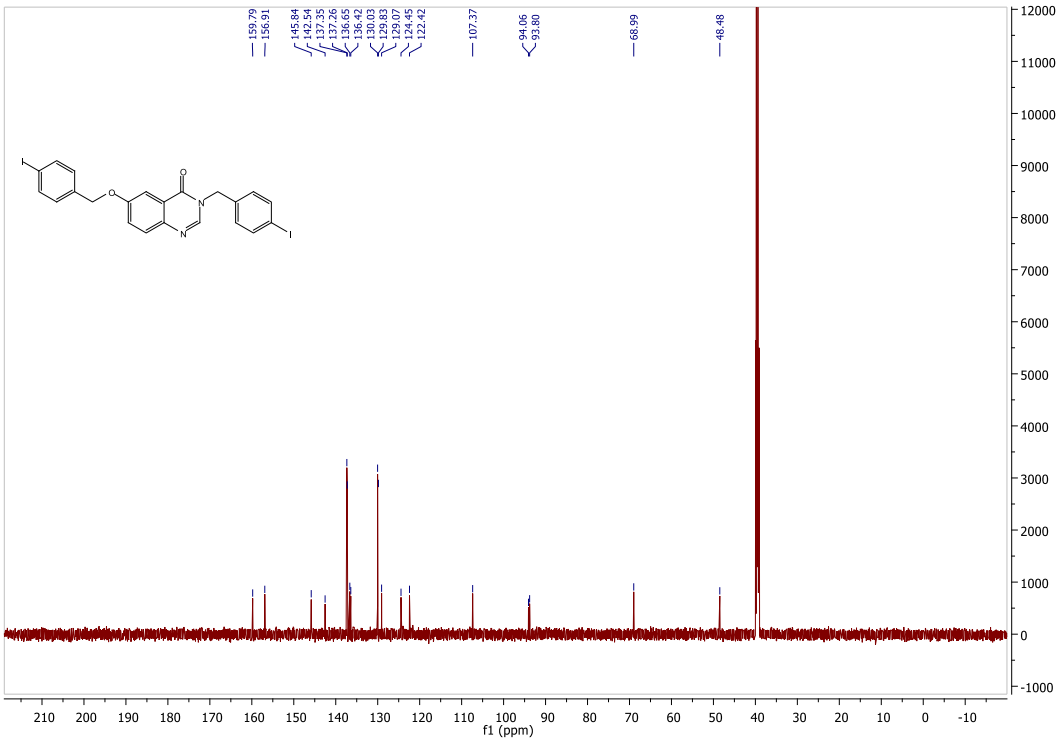

MS

Acquisition Parameter

Source Type	APCI	Ion Polarity	Positive	Set Nebulizer	1.6 Bar
Focus	Not active	Set Capillary	4500 V	Set Dry Heater	200 °C
Scan Begin	50 m/z	Set End Plate Offset	-500 V	Set Dry Gas	8.0 l/min
Scan End	1500 m/z	Set Collision Cell RF	100.0 Vpp	Set Divert Valve	Waste

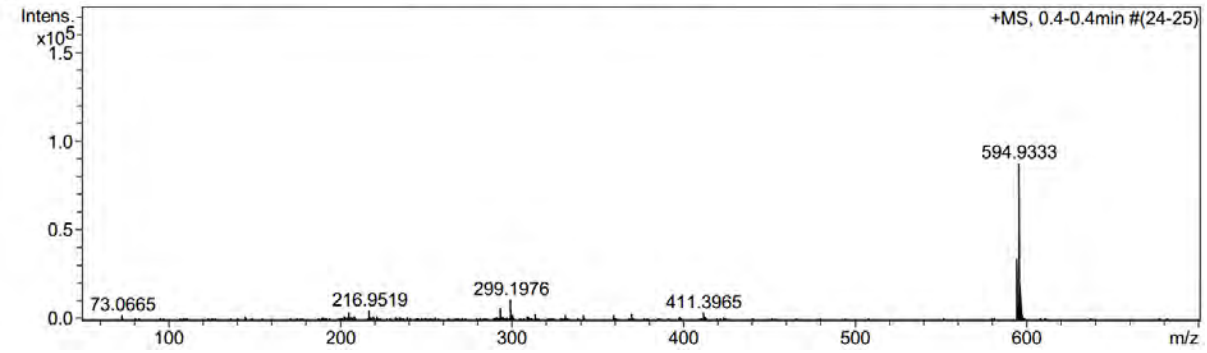

HPLC

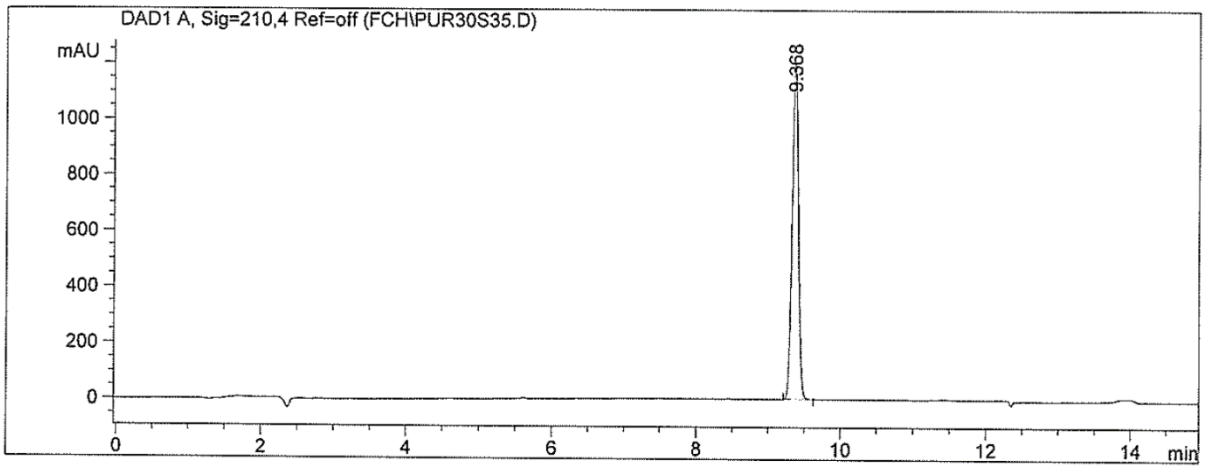

4-({[3-(4-Cyanobenzyl)-4-oxo-3,4-dihydroquinazolin-6-yl]oxy}methyl)benzonitrile (2h)

^{1}H NMR

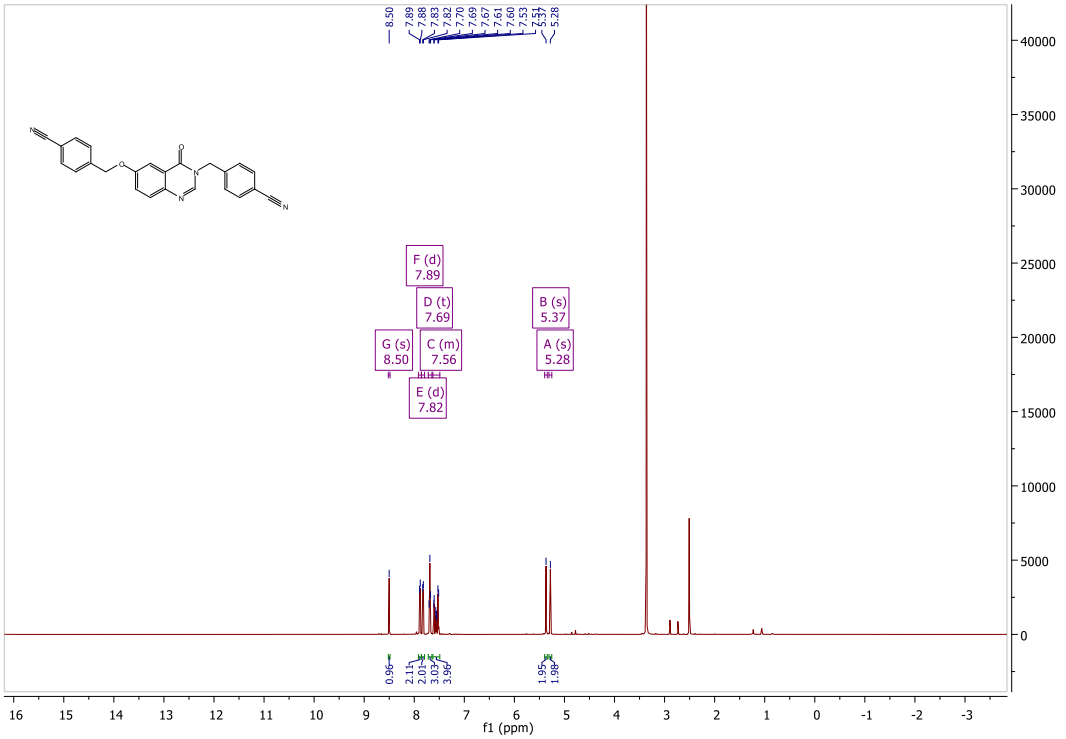

^{13}C NMR

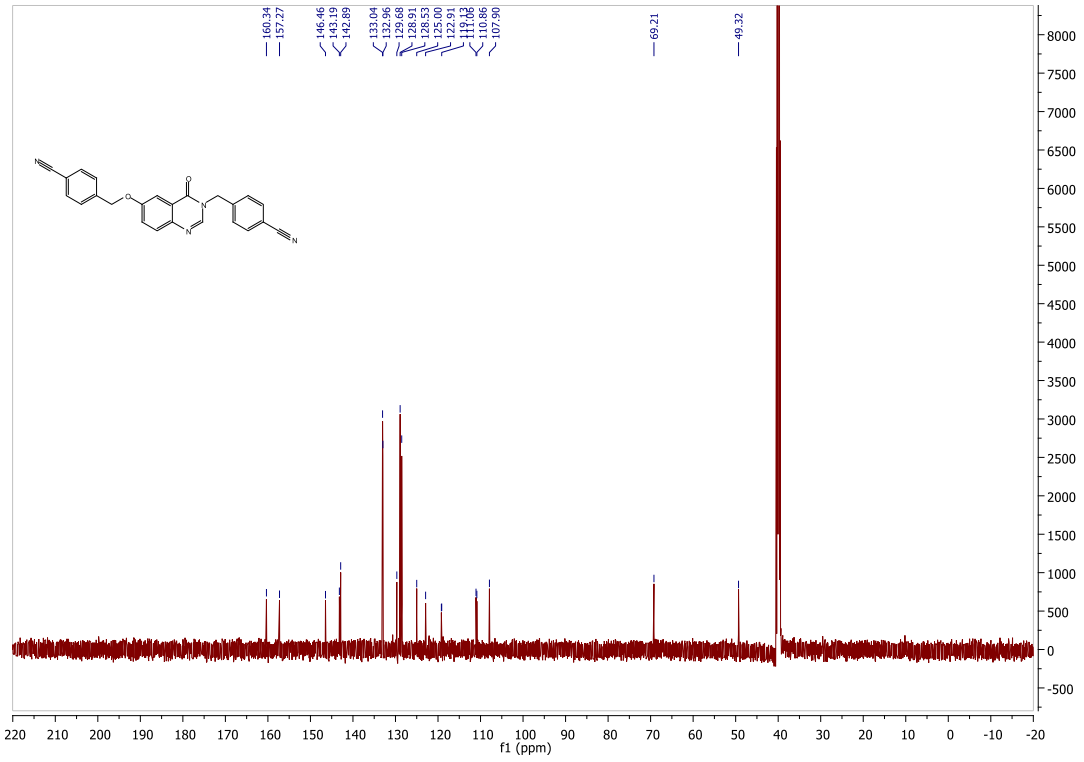

MS

Acquisition Parameter

Source Type	APCI	Ion Polarity	Positive	Set Nebulizer	1.6 Bar
Focus	Not active	Set Capillary	4500 V	Set Dry Heater	200 °C
Scan Begin	50 m/z	Set End Plate Offset	-500 V	Set Dry Gas	8.0 l/min
Scan End	1500 m/z	Set Collision Cell RF	100.0 Vpp	Set Divert Valve	Waste

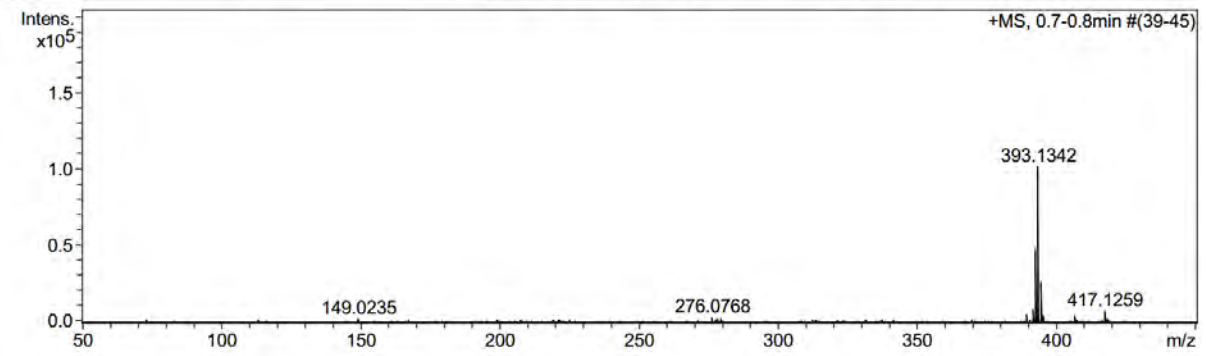

HPLC

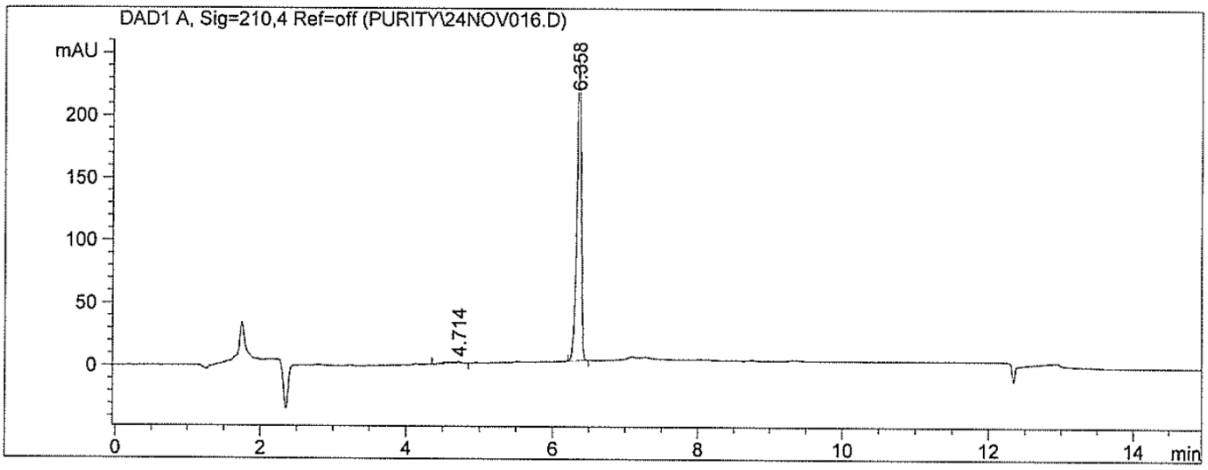

6-(2-Phenoxyethoxy)-3-(2-phenoxyethyl)quinazoline-4(3*H*)-one (2i)

^{1}H NMR

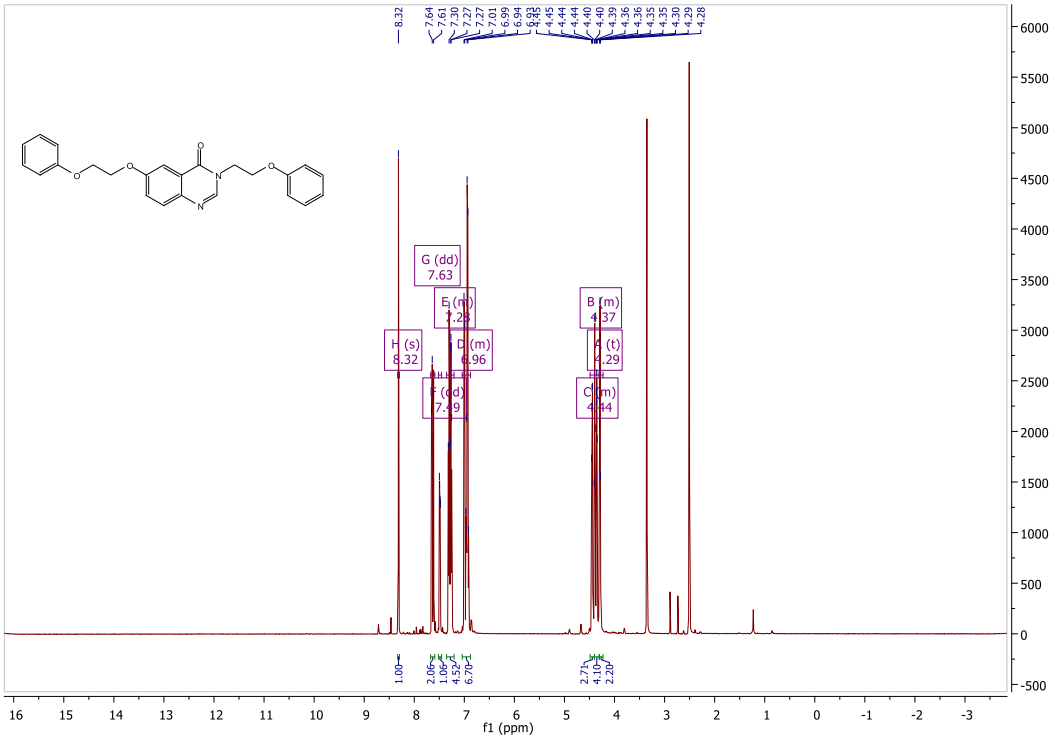

^{13}C NMR

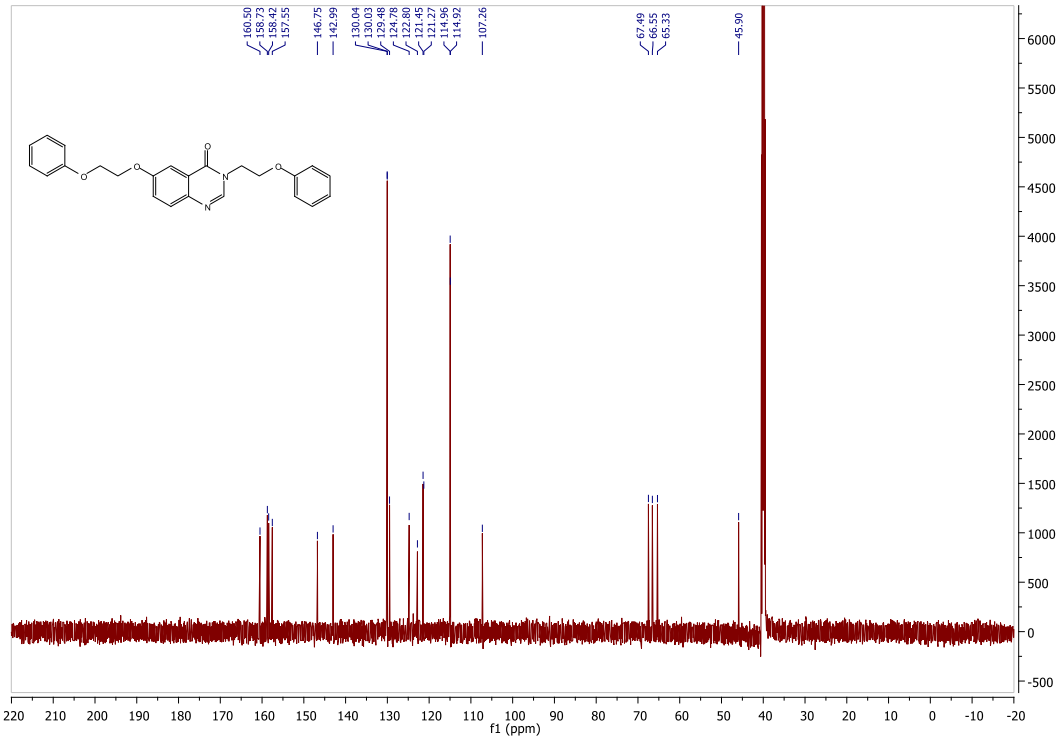

MS

Acquisition Parameter

Source Type	APCI	Ion Polarity	Positive	Set Nebulizer	1.6 Bar
Focus	Not active	Set Capillary	4500 V	Set Dry Heater	200 °C
Scan Begin	50 m/z	Set End Plate Offset	-500 V	Set Dry Gas	8.0 l/min
Scan End	1500 m/z	Set Collision Cell RF	100.0 Vpp	Set Divert Valve	Waste

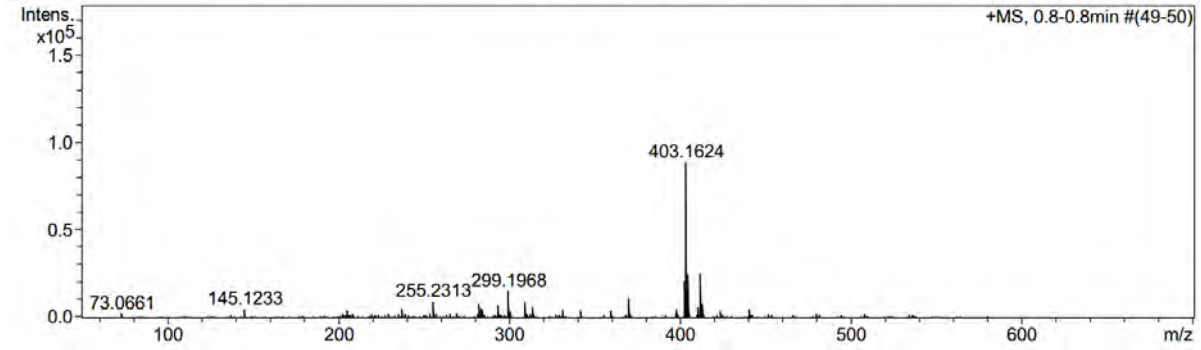

HPLC

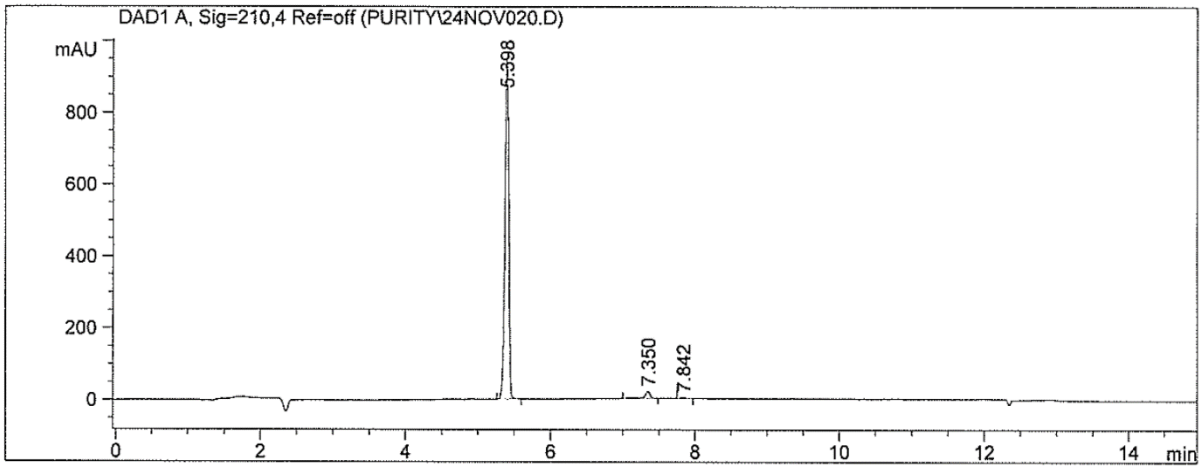

CHAPTER 5
CONCLUSION

As discussed earlier, PD is a progressive neurodegenerative disorder characterised by motor and non-motor signs and symptoms, which include resting tremor, rigidity, akinesia, sleep disturbances, depression and anxiety (Jankovic, 2008; Fil *et al.*, 2013). PD is characterised by the loss of the nigrostriatal dopaminergic pathway that leads from the SNpc to the striatum (Przedborski, 2005; McNamara *et al.*, 2010). The pathological hallmark of PD is the presence of LBs in the remaining dopaminergic neurons of the substantia nigra (Przedborski, 2005; Gibrat *et al.*, 2009). Although there are many aspects of the pathogenesis of the disorder (Reeve *et al.*, 2014), age is the major risk factor of PD (Lees *et al.*, 2009). Some forms of genetic mutations have been reported as underlying causes of PD, however, in the majority of PD cases the cause is unknown (Gibrat *et al.*, 2009). There is no cure for PD and the current treatment can neither reverse nor stop the disease progression. However, several drugs may be used to manage the symptoms (Singh *et al.*, 2007). The main goals of treatment of PD are to boost levels of DA in the brain in order to reduce the symptoms while minimising motor and non-motor complications, and thus to improve the patient's overall quality of life (Rao *et al.*, 2006; DeMaagd & Philip, 2015). For over 40 years, L-dopa in combination with a peripheral decarboxylase inhibitor has been the primary treatment of PD (Rao *et al.*, 2006; Davie, 2008). MAO inhibitors have also been used in the treatment of PD because MAO is implicated in the depletion of DA along the nigrostriatal pathway (Fernandez & Chen, 2007). The role of MAO inhibitors in PD is to enhance striatal dopaminergic activity by inhibiting DA metabolism, thus improving the motor symptoms of the disease (Fernandez & Chen, 2007).

The MAOs are mitochondrial outer membrane-bound flavoproteins that catalyse the oxidative deamination of monoamine neurotransmitters (e.g. DA, epinephrine, norepinephrine etc.), and occur as two isoforms, MAO-A and MAO-B (Edmondson *et al.*, 2004; Robakis & Fahn, 2015). The MAOs are located in different regions of the human body, with MAO-A dominating in the intestines, placenta and heart, while MAO-B is most abundant in platelets, glial cells in the brain and liver (Nel *et al.*, 2016). The MAOs have been identified as therapeutic targets for the management of neurodegenerative disorders (Ademosun & Oboh, 2014). The use of MAO inhibitors in the management of depression and other neurodegenerative conditions such as PD and Alzheimer's disease has thus been established (Ademosun & Oboh, 2014). Certain MAO inhibitors may, however, cause potentially fatal adverse effects ("the cheese reaction") as a result of their irreversibility and non-selectivity (Youdim *et al.*, 2006). Selective reversible inhibitors of MAO-A and MAO-B

have thus been developed to avoid this problem. Therapeutically, MAO-A inhibitors are used for the treatment of depression, while MAO-B inhibitors are used for the treatment of PD (Youdim & Bakhle, 2006; Youdim *et al.*, 2006). MAO-B inhibitors potentiate striatal neuronal responses to DA, and therefore alleviate the symptoms of PD (Robakis & Fahn, 2015).

The aim of the present study was to design potent, reversible MAO inhibitors with selectivity towards MAO-B. The lead compound for this study was 4(3*H*)-quinazolinone, which has previously been used as a scaffold for the design of potent MAO inhibitors (Srivastava *et al.*, 1980). In the present study, two series of 4(3*H*)-quinazolinone derivatives were synthesised and evaluated as potential MAO inhibitors. In the first series, 4(3*H*)-quinazolinone thioether derivatives were synthesised, with substitution with halogens at the *meta* and *para* positions of the side chain phenyl ring. In the second study, a series of C6-mono- and N3/C6-disubstituted derivatives of 4(3*H*)-quinazolinone was synthesised. For this series, further substitution with halogens and alkyl groups on the side chain phenyl rings were considered.

Thus, fourteen 4(3*H*)-quinazolinone thioether derivatives, twelve C6 mono- and nine N3/C6 disubstituted 4(3*H*)-quinazolinone derivatives were successfully synthesised by reacting 2-mercapto-4(3*H*)-quinazolinone or 6-hydroxy-4(3*H*)-quinazolinone with an appropriate arylalkyl halide in the presence of a base (K_2CO_3 or NaOH). The crudes obtained were purified by recrystallisation, and the structures and purities of the target compounds were verified by NMR, MS and HPLC analyses.

The 4(3*H*)-quinazolinone derivatives were evaluated as inhibitors of recombinant human MAO-A and MAO-B. To measure MAO activities, the MAO-A/B mixed substrate kynuramine was employed. The catalytic activities of the MAO enzymes were measured based on the rate of production of 4-hydroxyquinoline, the product of kynuramine deamination by MAO. Since 4-hydroxyquinoline is fluorescent, its concentrations were measured by fluorescence spectrophotometry (λ_{ex} = 310 nm; λ_{em} = 400 nm). The test inhibitors did not fluoresce under similar assay conditions, and thus did not interfere with the fluorescence measurements. The rates of oxidation of kynuramine by MAO in the presence of various concentrations of the test inhibitor were measured, and sigmoidal dose-response curves were constructed. The results indicated that the 4(3*H*)-quinazolinone thioether derivatives and C6 mono- and N3/C6 disubstituted 4(3*H*)-quinazolinone derivatives are in general good MAO inhibitors, with the majority of compounds exhibiting selectivity for MAO-B. However, the test compounds did not inhibit MAO-A, even at maximal tested concentrations of 100 µM. The N3/C6 disubstituted 4(3*H*)-quinazolinone derivatives showed superior MAO-B inhibition activity compared to the C6 monosubstituted derivatives. The most potent inhibitor among the two series was 2-[(3-iodobenzyl)thio]quinazolin-4(3*H*)-one (**3k**), with an IC_{50} value of 0.142 µM.

From the inhibition data it may also be concluded that the 4(3*H*)-quinazolinone thioether derivatives were generally more potent MAO-B inhibitors than the C6 mono- and N3/C6 disubstituted 4(3*H*)-quinazolinone derivatives.

To evaluate whether the 4(3*H*)-quinazolinone derivatives bind reversibly or irreversibly to MAO-B, the enzymatic activity was examined after dialysis of enzyme-inhibitor complexes. Compounds **3k** and **2b** were selected as representative inhibitors because they were the most potent MAO-B inhibitors in series 1 and 2, respectively. The results suggested that both compounds are reversible inhibitors of MAO-B. Further studies were conducted to determine the mode of inhibition of **3k** and **2b**. A set of Lineweaver-Burke plots was constructed and it revealed that these representative compounds inhibit MAO-B in a competitive manner. It may thus be concluded that 4(3*H*)-quinazolinone derivatives are reversible and competitive inhibitors of MAO-B.

This study has shown that halogen substitution on the phenyl ring side chains of the 4(3*H*)-quinazolinone derivatives gives rise to potent MAO-B inhibitors. Based on the above discussions, it may also be concluded that the objectives of this study have been achieved, and that the hypothesis has been proved; 4(3*H*)-quinazolinone is a suitable scaffold for the design of MAO-B inhibitors, and appropriate substitution yields potent MAO-B inhibitors. Such compounds are promising leads in the design of therapies for neurodegenerative disorders such as PD.

REFERENCES

Ademosun, A.O. & Oboh, G. 2014. Comparison of the inhibition of monoamine oxidase and butyrylcholinesterase activities by infusions from green tea and some citrus peels. *International journal of Alzheimer's disease*, 2014:5.

Davie, C.A. 2008. A review of Parkinson's disease. *British medical bulletin*, 86:109-127.

DeMaagd, G. & Philip, A. 2015. Parkinson's disease and its management: Part 1: disease entity, risk factors, pathophysiology, clinical presentation, and diagnosis. *Pharmacy and therapeutics*, 40(8):504.

Edmondson, D.E., Binda, C. & Mattevi, A. 2004. The FAD binding sites of human monoamine oxidases A and B. *Neurotoxicology*, 25(1-2):63-72.

Fil, A., Cano-de-la-Cuerda, R., Muñoz-Hellín, E., Vela, L., Ramiro-González, M. & Fernández-de-las-Peñas, C. 2013. Pain in Parkinson disease: a review of the literature. *Parkinsonism & related disorders*, 19(3):285-294.

Gibrat, C., Saint-Pierre, M., Bousquet, M., Lévesque, D., Rouillard, C. & Cicchetti, F. 2009. Differences between subacute and chronic MPTP mice models: investigation of dopaminergic neuronal degeneration and α-synuclein inclusions. *Journal of neurochemistry*, 109(5):1469-1482.

Jankovic, J. 2008. Parkinson's disease: clinical features and diagnosis. *Journal of neurology, neurosurgery & psychiatry*, 79(4):368-376.

Lees, A.J., Hardy, J. & Revesz, T. 2009. Parkinson's disease. *Lancet*, 373(9680):2055-2066.

McNamara, P., Stavitsky, K., Harris, E., Szent-Imrey, O. & Durso, R. 2010. Mood, side of motor symptom onset and pain complaints in Parkinson's disease. *International journal of geriatric psychiatry*, 25(5):519-524.

Nel, M.S., Petzer, A., Petzer, J.P. & Legoabe, L.J. 2016. 2-Benzylidene-1-indanone derivatives as inhibitors of monoamine oxidase. *Bioorganic & medicinal chemistry letters*, 26(19):4599-4605.

Przedborski, S. 2005. Pathogenesis of nigral cell death in Parkinson's disease. *Parkinsonism & related disorders*, 11:S3-S7.

Rao, S.S., Hofmann, L.A. & Shakil, A. 2006. Parkinson's disease: diagnosis and treatment. *American family physician*, 74(12):2046-2054.

Reeve, A., Simcox, E. & Turnbull, D. 2014. Ageing and Parkinson's disease: why is advancing age the biggest risk factor? *Ageing research reviews*, 14(100):19-30.

Robakis, D. & Fahn, S. 2015. Defining the role of the monoamine oxidase-B inhibitors for Parkinson's disease. *CNS drugs*, 29(6):433-441.

Singh, N., Pillay, V. & Choonara, Y.E. 2007. Advances in the treatment of Parkinson's disease. *Progress in Neurobiology*, 81(1):29-44.

Srivastava, V.K., Satsangi, R.K., Kumar, P. & Kishor, K. 1980. Monoamine oxidase inhibitory activity of 2-aryl-3-(5'-chlorobenzophenon-2'-yl)-quinazolin-4-(3*H*)-ones. *Indian journal of physiology and pharmacology*, 24(4):361-363.

Youdim, M.B. & Bakhle, Y. 2006. Monoamine oxidase: isoforms and inhibitors in Parkinson's disease and depressive illness. *British journal of pharmacology*, 147(S1):S287-S296.

Youdim, M.B., Edmondson, D. & Tipton, K.F. 2006. The therapeutic potential of monoamine oxidase inhibitors. *Nature reviews neuroscience*, 7(4):295-309.

APPENDIX C:

AUTHOR GUIDELINES

ELSEVIER

BIOORGANIC & MEDICINAL CHEMISTRY

The Tetrahedron Journal for Research at the Interface of Chemistry and Biology

AUTHOR INFORMATION PACK

TABLE OF CONTENTS

ISSN: 0968-0896

DESCRIPTION

Bioorganic & Medicinal Chemistry publishes complete accounts of research of outstanding significance and timeliness on all aspects of molecular interactions at the interface of chemistry and biology, together with critical review articles. The journal publishes reports of experimental results in medicinal chemistry, chemical biology and drug discovery and design, emphasizing new and emerging advances and concepts in these fields. The aim of the journal is to promote a better understanding at the molecular level of life processes, and living organisms, as well as the interaction of these with chemical agents.

The Journal welcomes papers on: the medicinal chemistry and associated biology (including target identification and validation) of established or new disease targets the reporting of the discovery, design or optimization of potent new compounds or biological agents the analysis and discussion of structure-activity relationships and pharmacological issues relevant to drug design and action using in vitro and in vivo models, including the use of computational techniques when closely linked to experimental data the reporting of "first-in-class" new therapeutic compounds the chemical biology or bioorganic/bioinorganic chemistry that significantly advances knowledge of a biological mechanism methodological advances that are chemistry-based and which significantly impact on medicine or biology the preparation and examination of biotherapeutics for the treatment of pathophysiological disease states the development of materials for specific therapeutic targeting

All manuscripts will be rigorously peer-reviewed by independent experts following an initial assessment by the Editors. Please note that BMC is not suitable for straightforward reports of incremental advances. Above all the presentation of a rational basis and a sound underlying hypothesis for the work is of particular importance, whatever its exact field.

AUDIENCE

Chemists, Medicinal Chemists, Pharmacologists, Biochemists, Molecular Biologists.

IMPACT FACTOR

2016: 2.930 © Thomson Reuters Journal Citation Reports 2017

ABSTRACTING AND INDEXING

BIOSIS
Reaxys
Biochemistry and Biophysics Citation Index
Cancerlit
Chemical Abstracts
Chemical Citation Index
Current Contents
Current Contents/Life Sciences
MEDLINE®
EMBASE
Pascal
Research Alert
SCISEARCH
Science Citation Index
Excerpta Medica
Elsevier BIOBASE/Current Awareness in Biological Sciences
TOXFILE
Scopus

EDITORIAL BOARD

GUIDE FOR AUTHORS

INTRODUCTION

Bioorganic & Medicinal Chemistry seeks to publish research results of outstanding significance and timeliness and review articles in the fields of medicinal chemistry, chemical biology, bioorganic chemistry, bioinorganic chemistry, and related disciplines.

Articles should describe original research of high quality and timeliness.

Reviews of topical importance and current relevance are specially commissioned in appropriate fields. Authors wishing to submit a non-solicited review article are requested to first contact the Europe Editor, Professor H. Waldmann bmc@mpi-dortmund.mpg.de.

Perspectives briefly review (in 1-4 printed pages) specific subjects that already have or are likely to have major impact in areas related to chemical biology and drug discovery. Authors of perspectives are those who have made the original contribution or have extended the original research to new breakthroughs. Perspectives are generally specially commissioned by the editors; however, suggestions for topics and authors are welcomed. Individuals interested in contributing should contact the Europe Editor, Professor H. Waldmann bmc@mpi-dortmund.mpg.de.

Symposia-in-Print comprise collections of original research papers (including experimental sections) covering specific topics. Topics for forthcoming symposia are announced in the journal from time to time. A guest editor will invite authors active in the field to submit papers, which are then reviewed and processed for publication by the guest editor under the usual refereeing system. Opportunity is also provided for other active investigators to submit contributions.

Submission checklist

You can use this list to carry out a final check of your submission before you send it to the journal for review. Please check the relevant section in this Guide for Authors for more details.

Ensure that the following items are present:

One author has been designated as the corresponding author with contact details:
- E-mail address
- Full postal address

All necessary files have been uploaded:
Manuscript:
- Include keywords
- All figures (include relevant captions)
- All tables (including titles, description, footnotes)
- Ensure all figure and table citations in the text match the files provided
- Indicate clearly if color should be used for any figures in print

Graphical Abstracts / Highlights files (where applicable)
Supplemental files (where applicable)

Further considerations
- Manuscript has been 'spell checked' and 'grammar checked'
- All references mentioned in the Reference List are cited in the text, and vice versa
- Permission has been obtained for use of copyrighted material from other sources (including the Internet)
- A competing interests statement is provided, even if the authors have no competing interests to declare
- Journal policies detailed in this guide have been reviewed
- Referee suggestions and contact details provided, based on journal requirements

For further information, visit our Support Center.

BEFORE YOU BEGIN

Ethics in publishing
Please see our information pages on Ethics in publishing and Ethical guidelines for journal publication.

Declaration of interest
All authors must disclose any financial and personal relationships with other people or organizations that could inappropriately influence (bias) their work. Examples of potential conflicts of interest include employment, consultancies, stock ownership, honoraria, paid expert testimony, patent applications/ registrations, and grants or other funding. If there are no conflicts of interest then please state this: 'Conflicts of interest: none'. More information.

Submission declaration and verification
Submission of an article implies that the work described has not been published previously (except in the form of an abstract or as part of a published lecture or academic thesis or as an electronic preprint, see 'Multiple, redundant or concurrent publication' section of our ethics policy for more information), that it is not under consideration for publication elsewhere, that its publication is approved by all authors and tacitly or explicitly by the responsible authorities where the work was carried out, and that, if accepted, it will not be published elsewhere in the same form, in English or in any other language, including electronically without the written consent of the copyright-holder. To verify originality, your article may be checked by the originality detection service CrossCheck.

Changes to authorship
Authors are expected to consider carefully the list and order of authors **before** submitting their manuscript and provide the definitive list of authors at the time of the original submission. Any addition, deletion or rearrangement of author names in the authorship list should be made only **before** the manuscript has been accepted and only if approved by the journal Editor. To request such a change, the Editor must receive the following from the **corresponding author**: (a) the reason for the change in author list and (b) written confirmation (e-mail, letter) from all authors that they agree with the addition, removal or rearrangement. In the case of addition or removal of authors, this includes confirmation from the author being added or removed.
Only in exceptional circumstances will the Editor consider the addition, deletion or rearrangement of authors **after** the manuscript has been accepted. While the Editor considers the request, publication of the manuscript will be suspended. If the manuscript has already been published in an online issue, any requests approved by the Editor will result in a corrigendum.

Article transfer service
This journal is part of our Article Transfer Service. This means that if the Editor feels your article is more suitable in one of our other participating journals, then you may be asked to consider transferring the article to one of those. If you agree, your article will be transferred automatically on your behalf with no need to reformat. Please note that your article will be reviewed again by the new journal. More information.

Copyright
Upon acceptance of an article, authors will be asked to complete a 'Journal Publishing Agreement' (see more information on this). An e-mail will be sent to the corresponding author confirming receipt of the manuscript together with a 'Journal Publishing Agreement' form or a link to the online version of this agreement.

Subscribers may reproduce tables of contents or prepare lists of articles including abstracts for internal circulation within their institutions. Permission of the Publisher is required for resale or distribution outside the institution and for all other derivative works, including compilations and translations. If excerpts from other copyrighted works are included, the author(s) must obtain written permission from the copyright owners and credit the source(s) in the article. Elsevier has prepinted forms for use by authors in these cases.

For open access articles: Upon acceptance of an article, authors will be asked to complete an 'Exclusive License Agreement' (more information). Permitted third party reuse of open access articles is determined by the author's choice of user license.

Author rights
As an author you (or your employer or institution) have certain rights to reuse your work. More information.

Elsevier supports responsible sharing
Find out how you can share your research published in Elsevier journals.

Role of the funding source

You are requested to identify who provided financial support for the conduct of the research and/or preparation of the article and to briefly describe the role of the sponsor(s), if any, in study design; in the collection, analysis and interpretation of data; in the writing of the report; and in the decision to submit the article for publication. If the funding source(s) had no such involvement then this should be stated.

Funding body agreements and policies
Elsevier has established a number of agreements with funding bodies which allow authors to comply with their funder's open access policies. Some funding bodies will reimburse the author for the Open Access Publication Fee. Details of existing agreements are available online.

Open access

This journal offers authors a choice in publishing their research:

Subscription
• Articles are made available to subscribers as well as developing countries and patient groups through our universal access programs.
• No open access publication fee payable by authors.
Open access
• Articles are freely available to both subscribers and the wider public with permitted reuse.
• An open access publication fee is payable by authors or on their behalf, e.g. by their research funder or institution.

Regardless of how you choose to publish your article, the journal will apply the same peer review criteria and acceptance standards.

For open access articles, permitted third party (re)use is defined by the following Creative Commons user licenses:

Creative Commons Attribution (CC BY)
Lets others distribute and copy the article, create extracts, abstracts, and other revised versions, adaptations or derivative works of or from an article (such as a translation), include in a collective work (such as an anthology), text or data mine the article, even for commercial purposes, as long as they credit the author(s), do not represent the author as endorsing their adaptation of the article, and do not modify the article in such a way as to damage the author's honor or reputation.

Creative Commons Attribution-NonCommercial-NoDerivs (CC BY-NC-ND)
For non-commercial purposes, lets others distribute and copy the article, and to include in a collective work (such as an anthology), as long as they credit the author(s) and provided they do not alter or modify the article.

The open access publication fee for this journal is **USD 2200**, excluding taxes. Learn more about Elsevier's pricing policy: http://www.elsevier.com/openaccesspricing.

Green open access
Authors can share their research in a variety of different ways and Elsevier has a number of green open access options available. We recommend authors see our green open access page for further information. Authors can also self-archive their manuscripts immediately and enable public access from their institution's repository after an embargo period. This is the version that has been accepted for publication and which typically includes author-incorporated changes suggested during submission, peer review and in editor-author communications. Embargo period: For subscription articles, an appropriate amount of time is needed for journals to deliver value to subscribing customers before an article becomes freely available to the public. This is the embargo period and it begins from the date the article is formally published online in its final and fully citable form. Find out more.

This journal has an embargo period of 24 months.

Elsevier Publishing Campus
The Elsevier Publishing Campus (www.publishingcampus.com) is an online platform offering free lectures, interactive training and professional advice to support you in publishing your research. The College of Skills training offers modules on how to prepare, write and structure your article and explains how editors will look at your paper when it is submitted for publication. Use these resources, and more, to ensure that your submission will be the best that you can make it.

Language (usage and editing services)
Please write your text in good English (American or British usage is accepted, but not a mixture of these). Authors who feel their English language manuscript may require editing to eliminate possible grammatical or spelling errors and to conform to correct scientific English may wish to use the English Language Editing service available from Elsevier's WebShop.

Submission

Our online submission system guides you stepwise through the process of entering your article details and uploading your files. The system converts your article files to a single PDF file used in the peer-review process. Editable files (e.g., Word, LaTeX) are required to typeset your article for final publication. All correspondence, including notification of the Editor's decision and requests for revision, is sent by e-mail.

Manuscripts should be addressed to the appropriate regional editor:

Submissions from Japan and other Asian countries:
Professor Yuichi Hashimoto, Institute of Molecular & Cellular Biosciences, The University of Tokyo, Japan

Submissions from Europe:
Professor H. Waldmann, Department of Chemical Biology, Max-Planck-Institut fur Molekulare Physiologie, Dortmund, Germany

Submissions from USA, Canada, and all others:
Professor K. Janda, Department of Chemistry, The Scripps Research Institute, Maildrop: BCC 582, 10550 North Torrey Pines Road, La Jolla, CA, 92037, USA

All manuscripts will be centrally handled by the journal editorial office, which will forward manuscripts to the regional editors:

E-mail: bmc-eo@elsevier.com

Submit your article

Please submit your article via https://www.evise.com/profile/api/navigate/BMC

Compound characterization checklist
Characterization of new compounds: All new compounds should be fully characterized with relevant spectroscopic data. Microanalyses should be included whenever possible. Under appropriate circumstances, mass spectra may serve in lieu of microanalysis, if accompanied by suitable NMR criteria for sample homogeneity.
CHARACTERIZATION OF ALL NEW COMPOUNDS HAS TO BE SPECIFIED (GIVEN) IN A COMPOUND CHARACTERIZATION CHECKLIST.

PREPARATION

X-ray crystallographic data: All crystallographic data must be deposited with the appropriate database and an accession number must be given in the manuscript in order for final acceptance of a manuscript. Small-molecule crystal structures are to be deposited with the Cambridge Crystallographic Data Centre (http://www.ccdc.cam.ac.uk) and macromolecular structures with the Protein Data Bank (http://www.rcsb.org). Full details on deposition procedures are available directly from these data bases.

Peer review

This journal operates a single blind review process. All contributions will be initially assessed by the editor for suitability for the journal. Papers deemed suitable are then typically sent to a minimum of two independent expert reviewers to assess the scientific quality of the paper. The Editor is responsible for the final decision regarding acceptance or rejection of articles. The Editor's decision is final. More information on types of peer review.

Use of word processing software

It is important that the file be saved in the native format of the word processor used. The text should be in single-column format. Keep the layout of the text as simple as possible. Most formatting codes will be removed and replaced on processing the article. In particular, do not use the word processor's options to justify text or to hyphenate words. However, do use bold face, italics, subscripts, superscripts etc. When preparing tables, if you are using a table grid, use only one grid for each individual table and not a grid for each row. If no grid is used, use tabs, not spaces, to align columns. The electronic text should be prepared in a way very similar to that of conventional manuscripts (see also the Guide to Publishing with Elsevier). Note that source files of figures, tables and text graphics will be required whether or not you embed your figures in the text. See also the section on Electronic artwork.

To avoid unnecessary errors you are strongly advised to use the 'spell-check' and 'grammar-check' functions of your word processor.

Figures, schemes and tables

Please note that all figures, schemes and tables should be embedded in the relevant positions within the manuscript file for ease of reference by the Editor and reviewers. Figures, schemes and tables may also be supplied as separate source files, but must always be included within the manuscript file as well.

Templates

Templates are provided to allow authors to view their paper in a style close to the final printed form. Their use is optional. All manuscripts will be fully typeset from the author's electronic files. It should be noted that due to defined typesetting standards and the complex requirements of electronic publishing, the publisher will not always be able to exactly match the layout the author has submitted. In particular, in the finished journal article, figures and tables are usually placed at the top or bottom of pages. The template is only intended to be used in assisting with the preparation and submission of manuscripts.

It should be noted that use of the journal templates is not a requirement and their adoption will neither speed nor delay publication. Elsevier can handle most major word processing packages and in general most formatting applied by authors for style and layout is replaced when the article is being typeset.

These templates contain a large number of macros. To ensure successful PDF conversion during online submission, it is important that the author save a new document based on the template, rather than saving the template itself. To use the template, the author should save the final document as a Word file with a '.doc' extension (rather than the '.dot' extension).

The templates can be found at http://www.elsevier.com/bmc-templates.

Article structure

Subdivision - numbered sections

Divide your article into clearly defined and numbered sections. Subsections should be numbered 1.1 (then 1.1.1, 1.1.2, ...), 1.2, etc. (the abstract is not included in section numbering). Use this numbering also for internal cross-referencing: do not just refer to 'the text'. Any subsection may be given a brief heading. Each heading should appear on its own separate line.

Introduction

State the objectives of the work and provide an adequate background, avoiding a detailed literature survey or a summary of the results.

Material and methods

Provide sufficient detail to allow the work to be reproduced. Methods already published should be indicated by a reference: only relevant modifications should be described.

Theory/calculation
A Theory section should extend, not repeat, the background to the article already dealt with in the Introduction and lay the foundation for further work. In contrast, a Calculation section represents a practical development from a theoretical basis.

Results
Results should be clear and concise.

Discussion
This should explore the significance of the results of the work, not repeat them. A combined Results and Discussion section is often appropriate. Avoid extensive citations and discussion of published literature.

Conclusions
The main conclusions of the study may be presented in a short Conclusions section, which may stand alone or form a subsection of a Discussion or Results and Discussion section.

Appendices
If there is more than one appendix, they should be identified as A, B, etc. Formulae and equations in appendices should be given separate numbering: Eq. (A.1), Eq. (A.2), etc.; in a subsequent appendix, Eq. (B.1) and so on. Similarly for tables and figures: Table A.1; Fig. A.1, etc.

Vitae
When submitting a review article, authors should include biographical information for each author as well as a black-and-white photograph. Each biography should be one paragraph (approximately 150-200 words) and should include date and place of birth, universities attended, degrees obtained, principal professional posts held, present title, a line or two about the major research interests, and anything else professionally relevant that is of special interest.

Essential title page information

• ***Title.*** Concise and informative. Titles are often used in information-retrieval systems. Avoid abbreviations and formulae where possible.
• ***Author names and affiliations.*** Please clearly indicate the given name(s) and family name(s) of each author and check that all names are accurately spelled. Present the authors' affiliation addresses (where the actual work was done) below the names. Indicate all affiliations with a lower-case superscript letter immediately after the author's name and in front of the appropriate address. Provide the full postal address of each affiliation, including the country name and, if available, the e-mail address of each author.
• ***Corresponding author.*** Clearly indicate who will handle correspondence at all stages of refereeing and publication, also post-publication. **Ensure that the e-mail address is given and that contact details are kept up to date by the corresponding author.**
• ***Present/permanent address.*** If an author has moved since the work described in the article was done, or was visiting at the time, a 'Present address' (or 'Permanent address') may be indicated as a footnote to that author's name. The address at which the author actually did the work must be retained as the main, affiliation address. Superscript Arabic numerals are used for such footnotes.

Abstract

A concise and factual abstract is required. The abstract should state briefly the purpose of the research, the principal results and major conclusions. An abstract is often presented separately from the article, so it must be able to stand alone. For this reason, References should be avoided, but if essential, then cite the author(s) and year(s). Also, non-standard or uncommon abbreviations should be avoided, but if essential they must be defined at their first mention in the abstract itself.

Graphical abstract
A graphical abstract is mandatory for this journal. It should summarize the contents of the article in a concise, pictorial form designed to capture the attention of a wide readership online. Authors must provide images that clearly represent the work described in the article. Graphical abstracts should be submitted as a separate file in the online submission system. Image size: please provide an image with a minimum of 531 × 1328 pixels (h × w) or proportionally more. The image should be readable at a size of 5 × 13 cm using a regular screen resolution of 96 dpi. Preferred file types: TIFF, EPS, PDF or MS Office files. You can view Example Graphical Abstracts on our information site.
Authors can make use of Elsevier's Illustration Services to ensure the best presentation of their images also in accordance with all technical requirements.

Highlights
Highlights are a short collection of bullet points that convey the core findings of the article. Highlights are optional and should be submitted in a separate editable file in the online submission system. Please use 'Highlights' in the file name and include 3 to 5 bullet points (maximum 85 characters, including spaces, per bullet point). You can view example Highlights on our information site.

Abbreviations
Define abbreviations that are not standard in this field in a footnote to be placed on the first page of the article. Such abbreviations that are unavoidable in the abstract must be defined at their first mention there, as well as in the footnote. Ensure consistency of abbreviations throughout the article.

Acknowledgements
Collate acknowledgements in a separate section at the end of the article before the references and do not, therefore, include them on the title page, as a footnote to the title or otherwise. List here those individuals who provided help during the research (e.g., providing language help, writing assistance or proof reading the article, etc.).

Formatting of funding sources
List funding sources in this standard way to facilitate compliance to funder's requirements:

Funding: This work was supported by the National Institutes of Health [grant numbers xxxx, yyyy]; the Bill & Melinda Gates Foundation, Seattle, WA [grant number zzzz]; and the United States Institutes of Peace [grant number aaaa].

It is not necessary to include detailed descriptions on the program or type of grants and awards. When funding is from a block grant or other resources available to a university, college, or other research institution, submit the name of the institute or organization that provided the funding.

If no funding has been provided for the research, please include the following sentence:

This research did not receive any specific grant from funding agencies in the public, commercial, or not-for-profit sectors.

Footnotes
Footnotes should be used sparingly. Number them consecutively throughout the article. Many word processors can build footnotes into the text, and this feature may be used. Otherwise, please indicate the position of footnotes in the text and list the footnotes themselves separately at the end of the article. Do not include footnotes in the Reference list.

Electronic artwork
General points
• Make sure you use uniform lettering and sizing of your original artwork.
• Embed the used fonts if the application provides that option.
• Aim to use the following fonts in your illustrations: Arial, Courier, Times New Roman, Symbol, or use fonts that look similar.
• Number the illustrations according to their sequence in the text.
• Use a logical naming convention for your artwork files.
• Provide captions to illustrations separately.
• Size the illustrations close to the desired dimensions of the published version.
• Submit each illustration as a separate file.
A detailed guide on electronic artwork is available.
You are urged to visit this site; some excerpts from the detailed information are given here.
Formats
If your electronic artwork is created in a Microsoft Office application (Word, PowerPoint, Excel) then please supply 'as is' in the native document format.
Regardless of the application used other than Microsoft Office, when your electronic artwork is finalized, please 'Save as' or convert the images to one of the following formats (note the resolution requirements for line drawings, halftones, and line/halftone combinations given below):
EPS (or PDF): Vector drawings, embed all used fonts.
TIFF (or JPEG): Color or grayscale photographs (halftones), keep to a minimum of 300 dpi.
TIFF (or JPEG): Bitmapped (pure black & white pixels) line drawings, keep to a minimum of 1000 dpi.
TIFF (or JPEG): Combinations bitmapped line/half-tone (color or grayscale), keep to a minimum of 500 dpi.

Please do not:
• Supply files that are optimized for screen use (e.g., GIF, BMP, PICT, WPG); these typically have a low number of pixels and limited set of colors;
• Supply files that are too low in resolution;
• Submit graphics that are disproportionately large for the content.

Color artwork
Please make sure that artwork files are in an acceptable format (TIFF (or JPEG), EPS (or PDF), or MS Office files) and with the correct resolution. If, together with your accepted article, you submit usable color figures then Elsevier will ensure, at no additional charge, that these figures will appear in color online (e.g., ScienceDirect and other sites) regardless of whether or not these illustrations are reproduced in color in the printed version. **For color reproduction in print, you will receive information regarding the costs from Elsevier after receipt of your accepted article**. Please indicate your preference for color: in print or online only. Further information on the preparation of electronic artwork.

Figure captions
Ensure that each illustration has a caption. Supply captions separately, not attached to the figure. A caption should comprise a brief title (**not** on the figure itself) and a description of the illustration. Keep text in the illustrations themselves to a minimum but explain all symbols and abbreviations used.

Tables
Please submit tables as editable text and not as images. Tables can be placed either next to the relevant text in the article, or on separate page(s) at the end. Number tables consecutively in accordance with their appearance in the text and place any table notes below the table body. Be sparing in the use of tables and ensure that the data presented in them do not duplicate results described elsewhere in the article. Please avoid using vertical rules and shading in table cells.

References
Citation in text
Please ensure that every reference cited in the text is also present in the reference list (and vice versa). Any references cited in the abstract must be given in full. Unpublished results and personal communications are not recommended in the reference list, but may be mentioned in the text. If these references are included in the reference list they should follow the standard reference style of the journal and should include a substitution of the publication date with either 'Unpublished results' or 'Personal communication'. Citation of a reference as 'in press' implies that the item has been accepted for publication.

Web references
As a minimum, the full URL should be given and the date when the reference was last accessed. Any further information, if known (DOI, author names, dates, reference to a source publication, etc.), should also be given. Web references can be listed separately (e.g., after the reference list) under a different heading if desired, or can be included in the reference list.

Data references
This journal encourages you to cite underlying or relevant datasets in your manuscript by citing them in your text and including a data reference in your Reference List. Data references should include the following elements: author name(s), dataset title, data repository, version (where available), year, and global persistent identifier. Add [dataset] immediately before the reference so we can properly identify it as a data reference. The [dataset] identifier will not appear in your published article.

References in a special issue
Please ensure that the words 'this issue' are added to any references in the list (and any citations in the text) to other articles in the same Special Issue.

Reference style
Text: Indicate references by (consecutive) superscript arabic numerals in the order in which they appear in the text. The numerals are to be used *outside* periods and commas, *inside* colons and semicolons. For further detail and examples you are referred to the AMA Manual of Style, A Guide for Authors and Editors, Tenth Edition, ISBN 0-978-0-19-517633-9.
List: Number the references in the list in the order in which they appear in the text.
Examples:
Reference to a journal publication:

1. Van der Geer J, Hanraads JAJ, Lupton RA. The art of writing a scientific article. *J Sci Commun.* 2010;163:51–59.
Reference to a book:
2. Strunk W Jr, White EB. *The Elements of Style.* 4th ed. New York, NY: Longman; 2000.
Reference to a chapter in an edited book:
3. Mettam GR, Adams LB. How to prepare an electronic version of your article. In: Jones BS, Smith RZ, eds. *Introduction to the Electronic Age.* New York, NY: E-Publishing Inc; 2009:281–304.
Reference to a website:
4. Cancer Research UK. Cancer statistics reports for the UK. http://www.cancerresearchuk.org/aboutcancer/statistics/cancerstatsreport/; 2003 Accessed 13 March 2003.
Reference to a dataset:
[dataset] 5. Oguro, M, Imahiro, S, Saito, S, Nakashizuka, T. Mortality data for Japanese oak wilt disease and surrounding forest compositions, Mendeley Data, v1; 2015. https://doi.org/10.17632/xwj98nb39r.1.

Journal abbreviations source
Journal names should be abbreviated according to the List of Title Word Abbreviations.

Supplementary material

Supplementary material such as applications, images and sound clips, can be published with your article to enhance it. Submitted supplementary items are published exactly as they are received (Excel or PowerPoint files will appear as such online). Please submit your material together with the article and supply a concise, descriptive caption for each supplementary file. If you wish to make changes to supplementary material during any stage of the process, please make sure to provide an updated file. Do not annotate any corrections on a previous version. Please switch off the 'Track Changes' option in Microsoft Office files as these will appear in the published version.

Note that supplementary material is published online exactly as supplied (i.e. it is not typeset). The typesetter is unable to implement corrections to supplementary material. Should any corrections be necessary, authors should supply a revised supplementary material file.

RESEARCH DATA

This journal encourages and enables you to share data that supports your research publication where appropriate, and enables you to interlink the data with your published articles. Research data refers to the results of observations or experimentation that validate research findings. To facilitate reproducibility and data reuse, this journal also encourages you to share your software, code, models, algorithms, protocols, methods and other useful materials related to the project.

Below are a number of ways in which you can associate data with your article or make a statement about the availability of your data when submitting your manuscript. If you are sharing data in one of these ways, you are encouraged to cite the data in your manuscript and reference list. Please refer to the "References" section for more information about data citation. For more information on depositing, sharing and using research data and other relevant research materials, visit the research data page.

Data linking
If you have made your research data available in a data repository, you can link your article directly to the dataset. Elsevier collaborates with a number of repositories to link articles on ScienceDirect with relevant repositories, giving readers access to underlying data that gives them a better understanding of the research described.

There are different ways to link your datasets to your article. When available, you can directly link your dataset to your article by providing the relevant information in the submission system. For more information, visit the database linking page.

For supported data repositories a repository banner will automatically appear next to your published article on ScienceDirect.

In addition, you can link to relevant data or entities through identifiers within the text of your manuscript, using the following format: Database: xxxx (e.g., TAIR: AT1G01020; CCDC: 734053; PDB: 1XFN).

Mendeley Data
This journal supports Mendeley Data, enabling you to deposit any research data (including raw and processed data, video, code, software, algorithms, protocols, and methods) associated with your manuscript in a free-to-use, open access repository. During the submission process, after uploading your manuscript, you will have the opportunity to upload your relevant datasets directly to *Mendeley Data*. The datasets will be listed and directly accessible to readers next to your published article online.

For more information, visit the Mendeley Data for journals page.

Data statement
To foster transparency, we encourage you to state the availability of your data in your submission. This may be a requirement of your funding body or institution. If your data is unavailable to access or unsuitable to post, you will have the opportunity to indicate why during the submission process, for example by stating that the research data is confidential. The statement will appear with your published article on ScienceDirect. For more information, visit the Data Statement page.

ARTICLE ENRICHMENTS

AudioSlides
The journal encourages authors to create an AudioSlides presentation with their published article. AudioSlides are brief, webinar-style presentations that are shown next to the online article on ScienceDirect. This gives authors the opportunity to summarize their research in their own words and to help readers understand what the paper is about. More information and examples are available. Authors of this journal will automatically receive an invitation e-mail to create an AudioSlides presentation after acceptance of their paper.

Chemical Compound Viewer (Reaxys)
You can enrich your article with visual representations, links and details for those chemical structures that you define as the main chemical compounds described. Please follow the instructions to learn how to do this.

3D molecular models
You can enrich your online articles by providing 3D molecular models (optional) in PDB, PSE or MOL/MOL2 format, which will be visualized using the interactive viewer embedded within the article. Using the viewer, it will be possible to zoom into the model, rotate and pan the model, and change display settings. Submitted models will also be available for downloading from your online article on ScienceDirect. Each molecular model will have to be uploaded to the online submission system separately, via the '3D molecular models' submission category. More information.

Interactive plots
This journal enables you to show an Interactive Plot with your article by simply submitting a data file. Full instructions.

AFTER ACCEPTANCE

Online proof correction
Corresponding authors will receive an e-mail with a link to our online proofing system, allowing annotation and correction of proofs online. The environment is similar to MS Word: in addition to editing text, you can also comment on figures/tables and answer questions from the Copy Editor. Web-based proofing provides a faster and less error-prone process by allowing you to directly type your corrections, eliminating the potential introduction of errors.
If preferred, you can still choose to annotate and upload your edits on the PDF version. All instructions for proofing will be given in the e-mail we send to authors, including alternative methods to the online version and PDF.
We will do everything possible to get your article published quickly and accurately. Please use this proof only for checking the typesetting, editing, completeness and correctness of the text, tables and figures. Significant changes to the article as accepted for publication will only be considered at this stage with permission from the Editor. It is important to ensure that all corrections are sent back to us in one communication. Please check carefully before replying, as inclusion of any subsequent corrections cannot be guaranteed. Proofreading is solely your responsibility.

Offprints
The corresponding author will, at no cost, receive a customized Share Link providing 50 days free access to the final published version of the article on ScienceDirect. The Share Link can be used for sharing the article via any communication channel, including email and social media. For an

extra charge, paper offprints can be ordered via the offprint order form which is sent once the article is accepted for publication. Both corresponding and co-authors may order offprints at any time via Elsevier's Webshop. Corresponding authors who have published their article open access do not receive a Share Link as their final published version of the article is available open access on ScienceDirect and can be shared through the article DOI link.

AUTHOR INQUIRIES

Visit the Elsevier Support Center to find the answers you need. Here you will find everything from Frequently Asked Questions to ways to get in touch.
You can also check the status of your submitted article or find out when your accepted article will be published.

APPENDIX D:

COPYRIGHT LICENCES

JOHN WILEY AND SONS LICENSE TERMS AND CONDITIONS

Sep 05, 2017

This Agreement between Malikotsi Qhobosheane ("You") and John Wiley and Sons ("John Wiley and Sons") consists of your license details and the terms and conditions provided by John Wiley and Sons and Copyright Clearance Center.

License Number	4152390895254
License date	Jul 19, 2017
Licensed Content Publisher	John Wiley and Sons
Licensed Content Publication	Archiv der Pharmazie
Licensed Content Title	Syntheses and Biological Activities of Some New 4(3H)-Quinazolinones
Licensed Content Author	Surendra Bahadur,Mukta Saxena (Miss)
Licensed Content Date	Sep 23, 2006
Licensed Content Pages	5
Type of use	Dissertation/Thesis
Requestor type	University/Academic
Format	Print and electronic
Portion	Figure/table
Number of figures/tables	1
Original Wiley figure/table number(s)	Table 1
Will you be translating?	No
Title of your thesis / dissertation	Design, synthesis and evaluation of quinazolinone analogues as Monoamine Oxidase inhibitors
Expected completion date	Oct 2017
Expected size (number of pages)	200
Requestor Location	Malikotsi Qhobosheane 93 Albert Luthuli Street Potchefstroom Potchefstroom, North-West 2531 South Africa Attn: Malikotsi Qhobosheane
Publisher Tax ID	EU826007151
Billing Type	Invoice
Billing Address	Malikotsi Qhobosheane 93 Albert Luthuli Street Potchefstroom Potchefstroom, South Africa 2531 Attn: Malikotsi Qhobosheane
Total	0.00 USD

Terms and Conditions

TERMS AND CONDITIONS

This copyrighted material is owned by or exclusively licensed to John Wiley & Sons, Inc. or one of its group companies (each a"Wiley Company") or handled on behalf of a society with

ELSEVIER LICENSE
TERMS AND CONDITIONS

Sep 05, 2017

This Agreement between Malikotsi Qhobosheane ("You") and Elsevier ("Elsevier") consists of your license details and the terms and conditions provided by Elsevier and Copyright Clearance Center.

License Number	4152391190817
License date	Jul 19, 2017
Licensed Content Publisher	Elsevier
Licensed Content Publication	Bioorganic & Medicinal Chemistry
Licensed Content Title	Synthesis and evaluation of quinazoline amino acid derivatives as mono amine oxidase (MAO) inhibitors
Licensed Content Author	Sherine Nabil Khattab,Nesreen Saied Haiba,Ahmed Mosaad Asal,Adnan A. Bekhit,Adel Amer,Hamdy M. Abdel-Rahman,Ayman El-Faham
Licensed Content Date	Jul 1, 2015
Licensed Content Volume	23
Licensed Content Issue	13
Licensed Content Pages	12
Start Page	3574
End Page	3585
Type of Use	reuse in a thesis/dissertation
Intended publisher of new work	other
Portion	figures/tables/illustrations
Number of figures/tables/illustrations	1
Format	both print and electronic
Are you the author of this Elsevier article?	No
Will you be translating?	No
Original figure numbers	Scheme 2
Title of your thesis/dissertation	Design, synthesis and evaluation of quinazolinone analogues as Monoamine Oxidase inhibitors
Expected completion date	Oct 2017
Estimated size (number of pages)	200
Requestor Location	Malikotsi Qhobosheane 93 Albert Luthuli Street Potchefstroom Potchefstroom, North-West 2531 South Africa Attn: Malikotsi Qhobosheane
Publisher Tax ID	ZA 4110266048
Total	0.00 USD
Terms and Conditions	

ELSEVIER LICENSE
TERMS AND CONDITIONS

May 16, 2017

This Agreement between Malikotsi Qhobosheane ("You") and Elsevier ("Elsevier") consists of your license details and the terms and conditions provided by Elsevier and Copyright Clearance Center.

License Number	4110681001458
License date	
Licensed Content Publisher	Elsevier
Licensed Content Publication	Neuron
Licensed Content Title	Parkinson's Disease Mechanisms and Models
Licensed Content Author	William Dauer,Serge Przedborski
Licensed Content Date	11 September 2003
Licensed Content Volume	39
Licensed Content Issue	6
Licensed Content Pages	21
Start Page	889
End Page	909
Type of Use	reuse in a thesis/dissertation
Portion	figures/tables/illustrations
Number of figures/tables/illustrations	1
Format	both print and electronic
Are you the author of this Elsevier article?	No
Will you be translating?	No
Order reference number	
Original figure numbers	figure 1
Title of your thesis/dissertation	Design, synthesis and evaluation of quinazolinone analogues as Monoamine Oxidase inhibitors
Expected completion date	Oct 2017
Estimated size (number of pages)	200
Elsevier VAT number	GB 494 6272 12
Requestor Location	Malikotsi Qhobosheane 93 Albert Luthuli Street Potchefstroom Potchefstroom, North-West 2531 South Africa Attn: Malikotsi Qhobosheane
Publisher Tax ID	ZA 4110266048
Total	0.00 USD
Terms and Conditions	

INTRODUCTION

NATURE PUBLISHING GROUP LICENSE TERMS AND CONDITIONS

Sep 05, 2017

This Agreement between Malikotsi Qhobosheane ("You") and Nature Publishing Group ("Nature Publishing Group") consists of your license details and the terms and conditions provided by Nature Publishing Group and Copyright Clearance Center.

License Number	4136370968199
License date	Jun 26, 2017
Licensed Content Publisher	Nature Publishing Group
Licensed Content Publication	Nature Medicine
Licensed Content Title	Genetic clues to the pathogenesis of Parkinson's disease
Licensed Content Author	Miquel VilaandSerge Przedborski
Licensed Content Date	Jul 1, 2004
Licensed Content Volume	10
Type of Use	reuse in a dissertation / thesis
Requestor type	academic/educational
Format	print and electronic
Portion	figures/tables/illustrations
Number of figures/tables/illustrations	1
High-res required	no
Figures	Figure 1
Author of this NPG article	no
Your reference number	
Title of your thesis / dissertation	Design, synthesis and evaluation of quinazolinone analogues as Monoamine Oxidase inhibitors
Expected completion date	Oct 2017
Estimated size (number of pages)	200
Requestor Location	Malikotsi Qhobosheane 93 Albert Luthuli Street Potchefstroom Potchefstroom, North-West 2531 South Africa Attn: Malikotsi Qhobosheane
Billing Type	Invoice
Billing Address	Malikotsi Qhobosheane 93 Albert Luthuli Street Potchefstroom Potchefstroom, South Africa 2531 Attn: Malikotsi Qhobosheane
Total	0.00 USD
Terms and Conditions	

Terms and Conditions for Permissions

Nature Publishing Group hereby grants you a non-exclusive license to reproduce this material for this purpose, and for no other use,subject to the conditions below:

ELSEVIER LICENSE
TERMS AND CONDITIONS

Sep 05, 2017

This Agreement between Malikotsi Qhobosheane ("You") and Elsevier ("Elsevier") consists of your license details and the terms and conditions provided by Elsevier and Copyright Clearance Center.

License Number	4182540578077
License date	Sep 05, 2017
Licensed Content Publisher	Elsevier
Licensed Content Publication	Parkinsonism & Related Disorders
Licensed Content Title	MAO-B inhibitors: multiple roles in the therapy of neurodegenerative disorders?
Licensed Content Author	P. Foley,M. Gerlach,M.B.H. Youdim,P. Riederer
Licensed Content Date	Jan 1, 2000
Licensed Content Volume	6
Licensed Content Issue	1
Licensed Content Pages	23
Start Page	25
End Page	47
Type of Use	reuse in a thesis/dissertation
Intended publisher of new work	other
Portion	figures/tables/illustrations
Number of figures/tables/illustrations	1
Format	both print and electronic
Are you the author of this Elsevier article?	No
Will you be translating?	No
Original figure numbers	Table 2
Title of your thesis/dissertation	Design, synthesis and evaluation of quinazolinone analogues as Monoamine Oxidase inhibitors
Expected completion date	Oct 2017
Estimated size (number of pages)	200
Requestor Location	Malikotsi Qhobosheane 93 Albert Luthuli Street Potchefstroom Potchefstroom, North-West 2531 South Africa Attn: Malikotsi Qhobosheane
Publisher Tax ID	ZA 4110266048
Total	0.00 USD
Terms and Conditions	

INTRODUCTION

NATURE PUBLISHING GROUP LICENSE TERMS AND CONDITIONS

Sep 05, 2017

This Agreement between Malikotsi Qhobosheane ("You") and Nature Publishing Group ("Nature Publishing Group") consists of your license details and the terms and conditions provided by Nature Publishing Group and Copyright Clearance Center.

License Number	4110751468234
License date	May 16, 2017
Licensed Content Publisher	Nature Publishing Group
Licensed Content Publication	Nature Reviews Neuroscience
Licensed Content Title	The therapeutic potential of monoamine oxidase inhibitors
Licensed Content Author	Moussa B. H. Youdim, Dale Edmondson and Keith F. Tipton
Licensed Content Date	Apr 1, 2006
Licensed Content Volume	7
Licensed Content Issue	4
Type of Use	reuse in a dissertation / thesis
Requestor type	academic/educational
Format	electronic
Portion	figures/tables/illustrations
Number of figures/tables/illustrations	1
High-res required	no
Figures	Table 1
Author of this NPG article	no
Your reference number	
Title of your thesis / dissertation	Design, synthesis and evaluation of quinazolinone analogues as Monoamine Oxidase inhibitors
Expected completion date	Oct 2017
Estimated size (number of pages)	200
Requestor Location	Malikotsi Qhobosheane 93 Albert Luthuli Street Potchefstroom Potchefstroom, North-West 2531 South Africa Attn: Malikotsi Qhobosheane
Billing Type	Invoice
Billing Address	Malikotsi Qhobosheane 93 Albert Luthuli Street Potchefstroom Potchefstroom, South Africa 2531 Attn: Malikotsi Qhobosheane
Total	0.00 USD
Terms and Conditions	

Terms and Conditions for Permissions

ELSEVIER LICENSE
TERMS AND CONDITIONS

May 16, 2017

This Agreement between Malikotsi Qhobosheane ("You") and Elsevier ("Elsevier") consists of your license details and the terms and conditions provided by Elsevier and Copyright Clearance Center.

License Number	4110740030953
License date	
Licensed Content Publisher	Elsevier
Licensed Content Publication	Archives of Biochemistry and Biophysics
Licensed Content Title	Structural insights into the mechanism of amine oxidation by monoamine oxidases A and B
Licensed Content Author	Dale E. Edmondson,Claudia Binda,Andrea Mattevi
Licensed Content Date	15 August 2007
Licensed Content Volume	464
Licensed Content Issue	2
Licensed Content Pages	8
Start Page	269
End Page	276
Type of Use	reuse in a thesis/dissertation
Intended publisher of new work	other
Portion	figures/tables/illustrations
Number of figures/tables/illustrations	4
Format	electronic
Are you the author of this Elsevier article?	No
Will you be translating?	No
Order reference number	
Original figure numbers	figures 1, 3, 7 and 9
Title of your thesis/dissertation	Design, synthesis and evaluation of quinazolinone analogues as Monoamine Oxidase inhibitors
Expected completion date	Oct 2017
Estimated size (number of pages)	200
Elsevier VAT number	GB 494 6272 12
Requestor Location	Malikotsi Qhobosheane 93 Albert Luthuli Street Potchefstroom Potchefstroom, North-West 2531 South Africa Attn: Malikotsi Qhobosheane
Publisher Tax ID	ZA 4110266048
Total	0.00 USD

JOHN WILEY AND SONS LICENSE TERMS AND CONDITIONS

Sep 05, 2017

This Agreement between Malikotsi Qhobosheane ("You") and John Wiley and Sons ("John Wiley and Sons") consists of your license details and the terms and conditions provided by John Wiley and Sons and Copyright Clearance Center.

License Number	4141311361161
License date	Jul 03, 2017
Licensed Content Publisher	John Wiley and Sons
Licensed Content Publication	Rapid Communications in Mass Spectrometry
Licensed Content Title	A high-throughput monoamine oxidase inhibition assay using liquid chromatography with tandem mass spectrometry
Licensed Content Author	Zhengyin Yan,Gary W. Caldwell,Boyu Zhao,Allen B. Reitz
Licensed Content Date	Mar 10, 2004
Licensed Content Pages	7
Type of use	Dissertation/Thesis
Requestor type	University/Academic
Format	Print and electronic
Portion	Figure/table
Number of figures/tables	1
Original Wiley figure/table number(s)	Figure 1
Will you be translating?	No
Title of your thesis / dissertation	Design, synthesis and evaluation of quinazolinone analogues as Monoamine Oxidase inhibitors
Expected completion date	Oct 2017
Expected size (number of pages)	200
Requestor Location	Malikotsi Qhobosheane 93 Albert Luthuli Street Potchefstroom Potchefstroom, North-West 2531 South Africa Attn: Malikotsi Qhobosheane
Publisher Tax ID	EU826007151
Billing Type	Invoice
Billing Address	Malikotsi Qhobosheane 93 Albert Luthuli Street Potchefstroom Potchefstroom, South Africa 2531 Attn: Malikotsi Qhobosheane
Total	0.00 USD
Terms and Conditions	

TERMS AND CONDITIONS

This copyrighted material is owned by or exclusively licensed to John Wiley & Sons, Inc. or one of its group companies (each a"Wiley Company") or handled on behalf of a society with

JOHN WILEY AND SONS LICENSE TERMS AND CONDITIONS

Sep 05, 2017

This Agreement between Malikotsi Qhobosheane ("You") and John Wiley and Sons ("John Wiley and Sons") consists of your license details and the terms and conditions provided by John Wiley and Sons and Copyright Clearance Center.

License Number	4171280894660
License date	Aug 17, 2017
Licensed Content Publisher	John Wiley and Sons
Licensed Content Publication	BioEssays
Licensed Content Title	Animal models of Parkinson\'s disease
Licensed Content Author	Ranjita Betarbet,Todd B. Sherer,J. Timothy Greenamyre
Licensed Content Date	Mar 29, 2002
Licensed Content Pages	11
Type of use	Dissertation/Thesis
Requestor type	University/Academic
Format	Print and electronic
Portion	Figure/table
Number of figures/tables	1
Original Wiley figure/table number(s)	Figure 4
Will you be translating?	No
Title of your thesis / dissertation	Design, synthesis and evaluation of quinazolinone analogues as Monoamine Oxidase inhibitors
Expected completion date	Oct 2017
Expected size (number of pages)	200
Requestor Location	Malikotsi Qhobosheane 93 Albert Luthuli Street Potchefstroom Potchefstroom, North-West 2531 South Africa Attn: Malikotsi Qhobosheane
Publisher Tax ID	EU826007151
Billing Type	Invoice
Billing Address	Malikotsi Qhobosheane 93 Albert Luthuli Street Potchefstroom Potchefstroom, South Africa 2531 Attn: Malikotsi Qhobosheane
Total	0.00 USD
Terms and Conditions	

TERMS AND CONDITIONS

This copyrighted material is owned by or exclusively licensed to John Wiley & Sons, Inc. or one of its group companies (each a"Wiley Company") or handled on behalf of a society with which a Wiley Company has exclusive publishing rights in relation to a particular work

(https://www.omicsonline.org/chemical-biology-therapeutics.php)

ISSN: 2572-0406

Journal of Chemical Biology & Therapeutics

Review Article Open Access

Implication of Quinazoline-4(3H)-ones in Medicinal Chemistry: A Brief Review

Bipransh Kumar Tiwary[1], Kiran Pradhan[2], Ashis Kumar Nanda[3]* and Ranadhir Chakraborty[1]*

[1]Omics Laboratory, Department of Biotechnology, University of North Bengal, Darjeeling, West Bengal, India

[2]Department of Chemistry, St. Joseph's College, PO-North Point, Darjeeling, India

[3]Department of Chemistry, University of North Bengal, Darjeeling, West Bengal, India

***Corresponding Author:**
Ranadhir Chakraborty
Department of Biotechnology
University of North Bengal, Siliguri-734013, West Bengal, India
Tel: 0353-2776354
Fax: 0353-2699001
E-mail: rcnbusiliguri@gmail.com

***Corresponding Author:**
Ashis Kumar Nanda
Department of Chemistry
University of North Bengal
Siliguri-734013, West Bengal, India
Tel: 09474329191
E-mail: ashis_nanda@ hotmail.com

Received date: October 16, 2015;**Accepted date:** November 15, 2015; **Published date:** November 22, 2015

Citation: Tiwary BK, Pradhan K, Nanda AK, Chakraborty R (2015) Implication of Quinazoline-4(3H)-ones in Medicinal Chemistry: A Brief Review. J Chem Biol Ther 1:104. doi: 10.4172/2572-0406.1000104

Abstract

Quinazoline (https://www.omicsonline.org/open-access/implication-of-quinazoline43hones-in-medicinal-chemistry-a-briefreview-jcbt-1000104.php?aid=64607), a heterocyclic compound, has been extensively studied and used in certain specific biological activities. The quinazoline-4(3H)-one and its derivatives constitute an important class of fused heterocycles that are found in more than 200 naturally occurring alkaloids. With passage of time, newer and more complex variants of the quinazolinone structures are being discovered. The stability of the quinazolinone nucleus has inspired researchers to introduce many bioactive moieties to this nucleus to create new potential medicinal agents. With a view to explore the versatile lead molecule 4(3H)-quinazolinones, a series of novel 2-methyl-3-(1′3′4-thiadiazole-2- yl)-4-(3H) quinazolinones have been synthesized by reacting 2-amino-5-aryl/alkyl-1′3′4′-thiadiazoyl with 2-substituted benzoxazin-2-one. The designed compounds have shown antibacterial activity on Staphylococcus aureus (https://www.omicsonline.org/open-access/mice-infection-by-methicillinresistant-staphylococcus-aureus-from-different-colonization-sites-in-humans-resulting-in-difusion-to-2161-0681-1000283.php?aid=76229), **Bacillus subtilis** (https://www.omicsonline.org/open-access/administration-of-three-autochthonous-bacillus-subtilis-strains-induceearly-appearance-of-gastric-glands-and-vestiges-of-pylorus-i-2155-9821-1000271.php?aid=70328) and **Escherichia coli** (https://www.omicsonline.org/open-access/evaluation-germicidal-of-disinfectants-on-staphylococcus-aureus-and-escherichia-coli-2155-9597-1000232.php?aid=78945). In the journey of a compound to be established as a lead and finally to a drug, the problem of solubility is a major challenge for medicinal chemists and formulation scientists. The present review has touched all these issues with a hope that some of the quinazoline derivative with sufficient bioavailability (https://www.omicsonline.org/bioequivalence-bioavailability.php)could help us to counter the menace of **antibiotic resistance** (https://www.omicsonline.org/open-access/irrational-use-of-antibiotics-in-different-age-groups-of-karachi-a-wakeupcall-for-antibiotic-resistance-and-future-infections-jbb-1000302.php?aid=79061).

Keywords

Quinazoline-4-(3H)-ones; Heterocycles; Antibiotic resistant; ADMET

Introduction

In the early 1900s, Paul Ehrlich, the legendary German chemist, initiated the use of drugs for infectious diseases. He developed methods for screening a series of chemicals for their potential activity against diseases. The term ''chemotherapy (https://www.omicsonline.org/chemotherapy-open-access.php)'', which means the use of chemicals to treat disease, was also coined by him [1]. The synthetic drugs were hugely used in early twentieth century (1900-1930s). But the use of synthetic drugs for treating microbial diseases reduced after the discovery and development of **antibiotics** (https://www.omicsonline.org/bioequivalence-bioavailability.php). A paradigm shift in **therapeutics** (https://www.omicsonline.org/open-access/cyclic-dependent-kinase-cdk-role-in-cancer-pathogenesis-and-as-drugtarget-in-cancer-therapeutics-1948-5956-1000408.php?aid=75466) for treating bacterial diseases took place after the industrial production of **penicillin** (https://www.rroij.com/open-access/antibiotic-resistance-profile-and-genetic-traits-of-soil-isolated-bacteriaand-their-subsistence-on-penicillin-or-tetracycline-.php?aid=72598) and succeeding development of other antibiotics. There was extraordinary decline in encumber of disease due to large-scale use of these antibiotics [2]. Hence, a general opinion was generated among citizens and policy-makers that **infectious diseases** (https://www.omicsonline.org/open-access/toll-like-receptor-in-infectious-diseases-2329-8731-1000e123.php?aid=78818) would not produce significant problem in the future. But to everyone's surprise, in the last few decades the historical statement, made by the surgeon-general William H. Stewart in the US Congress (1969)- "It is time to close the book on infectious diseases", has not only been reversed but left least possibility of the closure of the said book [3]. With progress in time, the effect of antibiotics is getting drastically reduced in treatment of bacterial infection. A great constraint arose with the emergence of antibiotic resistant variants of the earlier sensitive bacteria and the emergence vis-à-vis development of new infectious diseases. A timeline representing the discovery and development of antibiotics and the emergence of antibiotic resistant bacteria is shown in **Figure 1.** It is true that the pressure currently imposed on pharmaceutical companies to deliver novel antimicrobials more rapidly and at lower cost will coerce innovation and discovery to enable many new methods. To tackle the problem of emergence of resistant bacteria against the newly discovered antibiotics, happening in a very short period of time from the date of release in the market, it has now become imperative to return back to the classical approach of drug design where substrate analogues gain inspiration from existing natural ligands. In this context, heterocycles are good targets and are,found abundantly in natural products. Heterocyclic compounds have already provided a platform for the rapid swap of research in the areas of organic, pharmaceutical, analytical, and medicinal chemistry. In the pharmaceutical industry, among the top two hundred branded drugs, more than 75% have heterocyclic fragments in their structures [4]. Most importantly, we find in the literature that 4(3H)-quinazolinones with 3-substitution has been associated with antimicrobial properties [5]. Hence we have attempted to review the implications of **heterocycles** (https://www.omicsonline.org/open-access/heterocycles-for-alzheimer-disease-4-and-5substituted-benzothiophenesas-starting-scaffold-in-the-construction-of-potential-new-inh-2161-0444-1000373.php?aid=74570) with special emphasis on quinazoline-4-(3H)-ones in medicinal chemistry and also hint upon the prospect of developing antibacterial compounds (https://www.omicsonline.org/open-access/antibacterial-compounds-in-predominant-trees-in-finland-review-2155-9821-1000167.php?aid=27852).